Application of microfluidics for the development of intensified aminotransferase (ATA) processes

Heintz, Søren

Publication date:
2015

Document Version
Publisher's PDF, also known as Version of record

Application of microfluidics for the development of intensified aminotransferase (ATA) processes

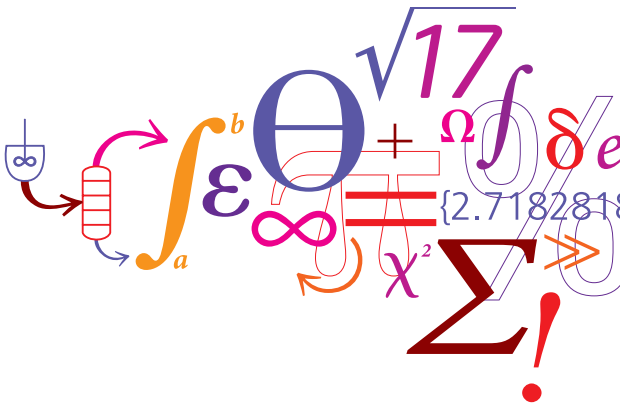

Søren Heintz

PhD Thesis

September 2015

DTU Chemical Engineering
Department of Chemical and Biochemical Engineering

Application of microfluidics for the development of intensified aminotransferase (ATA) processes

Technical university of Denmark
By:

Søren Heintz

PhD thesis

September 2015

DTU Chemical Engineering
Department of Chemical and Biochemical Engineering

Address: CAPEC-PROCESS Research Center

Department of Chemical and Biochemical Engineering

Technical University of Denmark

Building 229

Dk-2800 Kgs. Lyngby

Denmark

Phone: +45 4525 2800

Web: www.capec-process.kt.dtu.dk/

Print: GraphicCo.

DTU Chemical Engineering
Department of Chemical and Biochemical Engineering

Preface

This thesis was prepared at the Department of Chemical and Biochemical Engineering (DTU Chemical Engineering) at the Technical University of Denmark (DTU) in partial fulfilment of the requirements for acquiring the degree of Doctor of Philosophy (Ph.D.) in Chemical and Biochemical Engineering.

The work was performed at the joint CAPEC-PROCESS Research Center, Computer Aided Process Engineering Center/Process Engineering and Technology Center, in the period from September 2012 until September 2015. Professor Krist V. Gernaey (DTU Chemical Engineering, Head of CAPEC-PROCESS) was the principal supervisor of the project. Additionally, Professor John M. Woodley (DTU Chemical Engineering, CAPEC-PROCESS) and Associate Professor Ulrich Krühne (DTU Chemical Engineering, CAPEC-PROCESS) both functioned as co-supervisors of the project.

The project was partially funded by the BIOINTENSE project, financed by the European Union through the 7th Framework Programme (grant agreement n^o.: 312148). Hence, large parts of the presented work relate to specified goals within the BIOINTENSE project. Furthermore, the project received co-funding by the Technical University of Denmark (DTU).

Building 229, Søltofts plads, 2800 Kgs. Lyngby, September 2015

Søren Heintz

“Negative results are just what I want. They’re just as valuable to me as positive results. I can never find the thing that does the job best until I find the ones that don’t”

- *Thomas A. Edison, Inventor*

Acknowledgments

Before going into details with this Ph. D. thesis, I would like to acknowledge a great number of people for their valuable input, encouragement and support.

Firstly, I would like to thank my supervisors professor Krist V. Gernaey, professor John M. Woodley and associate professor Ulrich Krühne for their valuable input, for giving me the opportunity to work under their supervision and for letting me work on the BIOINTENSE project.

Secondly, I would like to thank all the BIOINTENSE partners for an excellent collaboration. It has been a great experience, with many fun times and interesting discussions. I have learned a lot through our collaboration. I would particularly like to thank my collaborators from Lund University (Tim Börner, Carl Grey and Patrick Adlercreutz), whom I worked and discussed intensively with while putting the two-step liquid-liquid extraction *in-situ* product removal system, presented in this thesis, in place.

Furthermore, I would like to thank all the people working in the CAPEC-PROCESS research group for an excellent work environment, with a fun and social work atmosphere. I would like to address a special thanks to Rolf H. Ringborg and Inês P. Rosinha for a fantastic collaboration on the BIOINTENSE project and many interesting and rewarding discussions. The project has been a lot of hard work, but I think the three of us made the best of it and have had a lot of fun at the same time. In addition, I would like to thank my office mates and training buddies (Aleksandar Mitic, Christian Bach and Asbjørn T. Pedersen) for keeping me in shape, good discussions and for many fun times.

Last, but not least, I would like to thank my mother, father, brother, other family and friends outside DTU (you know who you are) for your unlimited support and encouragement. It has been three tough years with many challenges in the project and privately, especially losing two close family members, and I would not have managed without your support. Especially I would like to thank my beloved girlfriend Carina L. Gargalo for her valuable input, discussions, encouragement and never ending support.

These three years have been an excellent learning experience, where I have truly developed my competences as a chemical engineer and as a person. Furthermore, it gave me the possibility of creating a great network across Europe through the BIOINTENSE project, courses and conferences.

Thanks to you all

Sincerely yours

Søren

Abstract

Development of biocatalytic processes is greatly dominated by well-established batch process based screening technologies, e.g. glass vials (mL) and microtiter plates (µL). However, there is still a need for improvement of currently available technologies and for new technologies enabling relatively easy screening and characterization of different process options. For example, small-scale microfluidic platforms enable testing of complex process options, by combining multiple process steps in a plug-and-play manner, that are difficult to assess with conventional methods. Early in the development of biocatalytic processes, most attention is given to developing and modifying the biocatalyst to reach required process targets. However, it is important to consider the downstream processing (DSP) early in the process development as well, i.e. the downstream costs and limitations to the separation steps will greatly influence the economic viability due to the constraints placed on the required process metrics. This thesis will therefore emphasize product recovery limitations and requirements in combination with the biocatalyst performance and limitations. Here the focus is mainly related to biocatalytic processes where it is found beneficial/necessary to implement *in-situ* co-product/product removal (IScPR/ISPR). For example, through combined operation of reactor and separation modules, as such applications require selective separation and sufficient driving force to influence the process significantly.

In recent years, many microfluidic applications have proven useful for process and synthesis development within the area of organic synthesis, i.e. flow chemistry. For example, the unique characteristics of the small scale enable safer and efficient handling and production of explosive and/or toxic compounds. Furthermore, development based on applying microfluidic platforms potentially enables easier introduction of continuous process aspects, when suitable. The motivation for this project is to investigate the potential of applying microfluidic technologies in the development and testing of biocatalytic processes. Within this thesis, microfluidic modules are applied as tools to screen, characterize, and test reactor and separation process options. Furthermore, multiple microfluidic modules are combined in order to test complex process configurations, i.e. reactor modules combined with separation modules, as a means of narrowing down and optimizing the most promising process options.

Throughout this thesis the applicability of microfluidics, as an integrated part of biocatalytic process development, is evaluated based on case studies focusing on the asymmetric synthesis of chiral amines using amine transaminases (ATAs). Chiral amines are valuable building blocks for many pharmaceuticals and precursors. The application of ATAs for asymmetric synthesis has many advantages, but it is also common that there are some challenges. In many cases, it is found beneficial/necessary to apply various process engineering strategies, e.g. IScPR and ISPR, to overcome these challenges and ensure the economic feasibility of such processes. With economic process feasibility in mind, it can be extremely useful to apply microfluidic platforms to enable fast screening and characterization of various process options in order to overcome the challenges. Due to the physicochemical properties of the compounds involved in the case studies in this thesis, the focus will be on the application/development of liquid-liquid extraction modules to operate in combination with reactor modules.

The main outcome of this PhD thesis is knowledge on the potential of applying microfluidics, in combination with conventional methods, for the development of biocatalytic processes. More specifically, microfluidics will enable testing of complex process options and strategies, which are very difficult to test with conventional methods. This is realized by combining microfluidic modules representing different process steps in a plug-and-play manner. The advantages and technology constraining disadvantages of microfluidics for biocatalytic process development are both identified in this thesis.

Novel applications of microfluidic development of ATA processes are investigated in detail, i.e. first by characterization of single microfluidic process steps (reactor and liquid-liquid extraction modules) and afterwards by testing of complex processes by combining multiple microfluidic process steps. This is realized by putting in place a microfluidic demonstration system, a plug-and-play combination of a reactor module with two liquid-liquid extraction modules and settlers. Another novelty of this thesis, is the application of the integrated liquid-liquid extraction steps to both recover the product, using *in-situ* product removal (ISPR), and at the same time feed the main substrate, i.e. *in-situ* substrate supply (ISSS). Furthermore, guidelines for identifying suitable ISPR/IScPR options – and, importantly, for eliminating unfeasible options – for ATA processes are proposed.

Resumé

Udvikling af biokatalytiske processer er stærkt domineret af veletablerede teknologier der er baserede på batchproceskoncepter, f.eks. mikrotiterplader (µL). Der er dog stadig behov for forbedringer af de konventionelle og tilgængelige teknologier, samt behov for nye teknologier, der gør det let at screene og karakterisere forskellige procesmuligheder. Et eksempel på en sådan ny teknologi er brugen af miniature-enhedsoperationer til at kontrollere fluider i små kanaler og derigennem teste komplekse procesmuligheder der ikke er mulige at teste med konventionelle teknologier. Dette kan opnås ved at kombinere flere miniature-enhedsoperationer, på samme måde som man leger med LEGO® (plug-and-play), og derved direkte teste kombinerede komplekse procesmuligheder.

Det er ydermere typisk for den indledende udvikling af biokatalytiske processer, at der bliver lagt vægt på at forbedre og modificere den benyttede biokatalysator for at leve op til de økonomiske krav der er for den givne proces. Det er dog lige så vigtig i den indledende procesudvikling at inkludere overvejelser om hvordan det syntetiserede produkt skal oprenses. Oprensningsomkostningerne og eventuelle begrænsninger vil i høj grad påvirke de økonomiske krav og begrænsninger for processer.

Formålet med denne afhandling er derfor at sætte fokus på vigtigheden af at overveje både ydeevnen og begrænsninger af biokatalysatorer og oprensningsprocesser i kombination, som et led i udviklingen af nye processer baseret på biokatalyse. I denne afhandling er det primære fokus på biokatalytiske processer hvor det er fordelagtigt/nødvendigt at implementere in situ produkt (ISPR) eller biprodukt fjernelse (IScPR). Det er specielt fordelagtigt for sådanne ISPR/IScPR applikationer at benytte miniature-enhedsoperationer til at teste reaktormoduler i kombination med separationsmoduler, som led i at undersøge effektive måder hvorpå inhiberende og ustabile produkter og biprodukter kan fjernes.

Et centralt element i denne afhandling er at evaluere brugen af miniature-enhedsoperationer, som en integreret del af biokatalytisk procesudvikling, baseret på et specifikt casestudie. Casestudiet omhandler brugen af amine transaminaser til asymmetrisksyntese af chirale aminer. Chirale aminer er vigtige og værdifulde komponenter i produktionen af mange lægemidler. Der er mange fordele ved amine transaminaser der gør denne gruppe af biokatalysatorer oplagte til at syntetisere chirale aminer. Der er dog samtidig nogle typiske udfordringer relateret til brugen af amine transaminaser, som for eksempel produkter der inhiberer og reaktionstermodynamik der ikke er favorable, der gør det udfordrende at bruge amine transaminaser i industrien. Disse mange udfordringer gør det i mange tilfælde nødvendigt at overveje alternative og komplekse processtrategier som ISPR/IScPR. Det er i den sammenhæng yderst relevant at bruge kombinerede miniature-enhedsoperationer til at teste sådanne processtrategier. Specifikt for casestudiet i denne afhandling er at de fysiske og kemiske egenskaber af de benyttede komponenter gør det oplagt at kigge på miniature væske-væske ekstraktionsmoduler i kombination med miniature-reaktormoduler. Denne kombination gjorde det muligt at teste et to-trins væske-væske ekstraherings ISPR koncept, hvor hydrofobiske og inhiberende aminprodukter effektivt blev ekstraheret og opkoncentreret. Ydermere, blev ekstraheringstrinnene brugt til samtidigt at tilføre substrat til reaktionsblandingen.

Et resultat af denne ph.d.-afhandling er omfattende viden om potentialet for brugen af miniature-enhedsoperationer, i kombination med konventionelle batchprocesmetoder, til udviklingen af nye alternative og komplekse biokatalytiske processer. Derudover, er en generel metode blevet foreslået til at identificere egnede ISPR/IScPR koncepter, når nødvendigt, til amine transaminase processer.

List of abbreviations

Abbreviation	Description
[AD]/[S]	Amine donor excess ratio
$[cP]_I$	Co-product inhibition
$[P]_I$	Product inhibition
Ace	Acetone
ACP	Acetophenone
AD	Amine donor
ADH	Alcohol dehydrogenase
Ala	Alanine
AlaDH	Alanine dehydrogenase
ALS	Acetolactate synthase
API	Active Pharmaceutical Ingredient
Aq.	Aqueous
ATA	Amine transaminase (EC.2.6.1.X) also known as Transaminase (TA)
BA	Benzylacetone
CAPEX	Capital expenses/Expenditure
CFD	Computational Fluid Dynamics
COP	Cyclic olefin polymers
cP	Co-Product
CST	Continuous stirred tank
CSTR	Continuous Stirred Tank Reactor
DKR	Dynamic Kinetic Resolution
DSP	Downstream processing
E	Evaporator
Enz.	Enzyme
Eq.	Reaction equilibrium
FDH	Formate dehydrogenase
FTIR	Fourier transform infrared spectroscopy
GC	Gas chromatography
GDH	Glucose dehydrogenase
GLE	Gas-Liquid extraction
GMP	Good manufacturing practice
HPLC	High Performance Liquid Chromatography
ID	Inner diameter
Imm.	Immobilized
IScPR	*In-Situ co*-Product Removal
ISPR	*In-Situ* Product Removal
ISSS	*In-situ* substrate supply
LDH	Lactate dehydrogenase

Abbreviation	Description
LFR	Laminar Flow Reactor
LLE	Liquid-Liquid Extraction
MIR	Mid-infrared spectroscopy
MPPA	1-Methyl-3-phenylpropylamine
MUO	Micro unit operation
MWD	Multiple wavelength detector
NIR	Near-infrared spectroscopy
OPEX	Operational expenses/expenditure
Org.	Organic
P	Product
P1-P4	Syringe pumps
PBR	Packed Bed Reactor
PDA detector	Photodiode array detector
PDC	Pyruvate decaroboxylase
PDMS	Polydimethylsiloxane
PEA	1-phenylethylamine also known as methylbenzylamine (MBA)
PEEK	Polyether ether ketone
PFR	Plug Flow Reactor
PI-diagram	Piping and Instrumentation diagram
PLP	Pyridoxal-5'-phosphate
PMMA	Poly methyl methacrylate
PMP	Pyridoxamine-5-'phosphate
PSE	Process systems engineering
PTFE	Polytetrafluoroethylene
PVA	Polyvinyl alcohol
Pyr	Pyruvate
R	Reactor
R1(a)	Reactor module
R1(b)	1st step LLE
R1(c)	2nd step LLE
Raman	Raman spectroscopy
RTD	Retention Time Distribution
S	Substrate
SLE	Solid-Liquid Extraction
SLM	Supported liquid membrane
ss	Steady state
UV	Ultraviolet spectroscopy
W1	Solvent waste
W2	Aqueous waste

Nomenclature

Nomenclature	Description	Unit
$\boldsymbol{a}$	Surface to volume ratio	$m^2 \cdot m^{-3}$
$\boldsymbol{A}$	Area	m^2
$[\boldsymbol{A^-}]$	Concentration of non-protonated amine donor	M
$[\boldsymbol{AD}]$	Amine donor concentration	M
$\boldsymbol{Bo}$	Bodenstein number	$-$
$\boldsymbol{C^*}$	Equilibrium concentration	M
$\boldsymbol{C_i}$	Concentration of component i	$M\ (mol \cdot L^{-1})$
$\boldsymbol{Ca}$	Capillary number	$-$
$[\boldsymbol{cP}]$	Co-product concentration	M
$\boldsymbol{d}$	Channel depth	m
$\boldsymbol{D}$	Taylor dispersion coefficient	$m^2 \cdot s^{-1}$
$\boldsymbol{D_{ab}}$	Diffusion coefficient of solute a in b	$m^2 \cdot s^{-1}$
$\boldsymbol{DF}$	Dilution factor	$-$
$\boldsymbol{d_H}$	Hydraulic diameter	m
$\boldsymbol{d_P}$	Spherical particle diameter	m
$\boldsymbol{d_t}$	Diffusion distance	m
$\boldsymbol{E_i}$	Uncertainty weight factor matrix	$-$
$[\boldsymbol{E}]$	Enzyme concentration	$g_{biocat} \cdot L^{-1}$
$\mathbf{E_{\theta,oo}}$	Exit age distribution	$-$
$\boldsymbol{e.e.}$	Enantiomeric excess	$-$
$\boldsymbol{Eo}$	Eötvös number	$-$
$\boldsymbol{F_1, F_2}$	Aqueous flow rates	$mL \cdot min^{-1}$
$\mathbf{F_{oo}}$	F curve	$-$
$\boldsymbol{Fo}$	Fourier number	$-$
$[\boldsymbol{HA}]$	Concentration of protonated amine donor	M
$\boldsymbol{i}$	Component nominator	$-$
$\boldsymbol{ID}$	Inner diameter	m
$\boldsymbol{k}$	Reaction rate constant	s^{-1}
$\boldsymbol{K_{eq}}$	Reaction equilibrium constant	$-$
$\boldsymbol{k_H}$	Henry's law constant	$L \cdot atm \cdot mol^{-1}$
$\boldsymbol{K_L}$	Mass transfer coefficient	s^{-1}
$\boldsymbol{K_La}$	Overall mass transfer coefficient	$s^{-1} \cdot m^2 \cdot m^{-3}$
$\boldsymbol{K_M^S, K_M^{AD}}$	Michaelis parameters	M
$\boldsymbol{L}$	Length	m
$\boldsymbol{L_{aq}}$	Length of aqueous slugs	m
$\boldsymbol{L_{org}}$	Length of organic slugs	m
$\mathbf{log}\,\boldsymbol{P}$	Octanol-water partition coefficient	$-$
$\boldsymbol{m}$	Mass	g
$\boldsymbol{M}\ (\boldsymbol{M_w})$	Molecular weight	$g \cdot mol^{-1}\ or\ kDa$
$\boldsymbol{n}$	Number of components	$-$
$\boldsymbol{N_{i,x}}$	Flux of component i in the x direction	$mol \cdot m^{-2} \cdot s^{-1}$
$\boldsymbol{P}$	Pressure	Pa
$[\boldsymbol{P}]$	Product concentration	M
$\boldsymbol{P^*}$	Purity	%
$\boldsymbol{PC_i}$	Partitioning coefficient of component i	$-$
$\boldsymbol{pK_a}$	Acid dissociation constant	$-$
$\boldsymbol{P_{vap}}$	Vapor pressure	$mmHg$

Nomenclature	Description	Unit
$\boldsymbol{q}$	Volumetric flow rate	$m^3 \cdot s^{-1}$
$\boldsymbol{r}$	Reaction rate	$mol \cdot min^{-1} \cdot g_{enz}$
$\boldsymbol{R}$	Ideal gas constant	$8.31\, J \cdot K^{-1} \cdot mol^{-1}$
$\boldsymbol{R^*}$	Recovery efficiency	%
$\boldsymbol{R_G}$	Radius of gyration	Å
$\boldsymbol{Re}$	Reynolds number	–
$[\boldsymbol{S}]$	Substrate concentration	M
$\boldsymbol{S_1}$	Solvent flow rate	$mL \cdot min^{-1}$
$\boldsymbol{s_i}$	Selectivity for component i	–
$\boldsymbol{STY}$	Space-Time-Yield	$g_P \cdot L^{-1} \cdot s^{-1}$
$\boldsymbol{t}$	Time	s
$\boldsymbol{T}$	Temperature	K *or* ℃
$\boldsymbol{T_b}$	Boiling point	℃
$\boldsymbol{T_F}$	Flash point	℃
$\boldsymbol{v}$	Linear flow rate	$m \cdot s^{-1}$
$\boldsymbol{V}$	Volume	m^3
$\boldsymbol{v_0}$	Fluid velocity based on an empty channel	$m \cdot s^{-1}$
$\boldsymbol{v_{avg}}$	Average linear flow rate	$m \cdot s^{-1}$
$\boldsymbol{v_{\max}}$	Maximum linear flow rate	$m \cdot s^{-1}$
$\boldsymbol{V_{max}}$	Maximum reaction rate	$mol \cdot min^{-1} \cdot g_{enz}$
$\boldsymbol{V_x}$	Discretized reactor volume	m^3
$\boldsymbol{We}$	Weber number	–
$\boldsymbol{W_x}$	Discretized biocatalyst loading in reactor	g
$\boldsymbol{x}$	Length direction and fragment length	m
$\boldsymbol{x}$	Number of elements in discretization	–
$\boldsymbol{X_{inh}}$	Parameter applied to determine the loss in initial enzyme activity	$\%_{loss} \cdot g_P^{-1} \cdot L$
$\boldsymbol{\beta}$	Channel specific parameter for estimation of the Taylor dispersion coefficient (48 for a tube)	–
$\boldsymbol{\varepsilon}$	Particle porosity	–
$\boldsymbol{\eta}$	Viscosity	$Pa \cdot s$
$\boldsymbol{\mu}$	Dynamic viscosity	$kg \cdot m^{-1} \cdot s^{-1}$
$\boldsymbol{\rho}$	Density	$kg \cdot m^{-3}$
$\boldsymbol{\sigma}$	Surface tension	$N \cdot m^{-1}$
$\boldsymbol{\tau}$	Dimensionless residence time	–
$\boldsymbol{\tau_{mix}}$	Characteristic diffusion controlled mixing time	s
$\boldsymbol{\theta}$	Mean residence time	–
$\boldsymbol{\theta_{n,i}}$	Measurement uncertainty	M
$\boldsymbol{\theta_{re}, \theta_{ad}}$	Receding and advancing contact angle, respectively	°
$\boldsymbol{\phi}$	Thiele modulus	-
$\boldsymbol{\Delta G}$	Gibbs free energy of formation	kJ/mol
$\boldsymbol{\Delta P}$	Pressure drop	Pa
$\boldsymbol{\Delta P_L}$	LaPlace pressure	Pa

Contents

Chapter 1

Introduction

1.1 Background and motivation

The increasing academic and industrial interest in biocatalytic processes (chemical reactions catalyzed by an isolated enzyme, immobilized enzyme, or whole cells containing one or more enzymes) is to a large extent driven by the need for selective chemistry [1]. Even more noteworthy is that such selectivity is achieved with enzymes under mild reaction conditions. While high selectivity may be easily achievable using biocatalysis, for implementation in industry, it is also necessary to develop processes that are sufficiently efficient, which sometimes is a challenge, in order to be economically feasible. For example, in the scientific literature it has been proposed that for a pharmaceutical intermediate, a product concentration of 50 g/L as a minimum must be achieved and a high yield of product on biocatalyst (termed biocatalyst yield) must be achieved as well [2,3]. The exact threshold values depend on the type of biocatalyst, the ease of separation and the industry sector (or more accurately the value of the product relative to the cost of the substrate). However, almost without exception, a new biocatalytic process studied in the laboratory will not fulfill these requirements, since enzymes are usually evolved to convert natural substrates at low concentrations.

This presents an interesting challenge for process chemists and engineers, since the wish to implement processes with new (non-natural) substrates at high concentrations can only be addressed by a concerted development effort with a combination of biocatalyst modification and process modification [4]. To date there are many examples where modification of the biocatalyst and the process has led to successful industrial implementation [1,3,5,6]. This is a strong indicator and motivator that it is indeed possible to either modify poorly performing biocatalysts, or to optimize the process, or to combine biocatalyst modification and process optimization, to reach economically viable process targets.

This work is solely focusing on the process aspects of the biocatalytic process development, e.g. application of advanced strategies combining reactor modules with separation modules to overcome severe inhibition and low solubility of reaction species. During the process development there are many options, e.g. reactors and recovery methods, to choose from and different routes to solve a given problem [7]. It is many times the case that processes are focused on the performance of the biocatalyst, which ultimately can come as a compromise of the efficiency of the following DSP [8]. While some process solutions are more effective than others, and some are easier to implement than others, there remain many choices to be made. Furthermore, in many cases, at an early development stage it is not clear where to put the research effort and which direction to focus the process.

It is therefore highly desirable to specify generic methods and develop/apply new technologies for high throughput screening and testing of complex process options, e.g. reactors combined with separation methods, to facilitate this decision process. The ultimate goal is to find optimal process solutions and to reach fast exclusion of infeasible options.

To address this problem, one potential vision for the future could be a systematic procedure for automated data collection, followed by testing of a more limited number of alternatives at a miniature scale, such that

operations can be carried out with a reduced reagent inventory and potentially even in parallel. Indeed, such schemes already exist for chemical synthetic systems [9], and while the level of complexity involved with a biocatalytic process is frequently greater, it is also frequently the case that biocatalytic processes give economic benefits. At the very least, testing at miniature scale would enable more process options, both complex and simple, to be evaluated in a shorter time, due to the automated control and the easy plug-and-play combination of microfluidic modules. Combined with process modeling techniques [10], microfluidics could provide a way to map the solution space for a given biocatalyst and enable design decisions to be made more rapidly and with greater confidence.

1.2 Scope, aim and specific thesis goals

The scope of this thesis is the application of microfluidic technologies and methods as novel tools to aid in accelerating the development of biocatalytic processes. The main aim and novelty of this work is the application of microfluidic technologies and methods for characterization of biocatalytic processes and testing of complex process options, when needed, that are difficult to test with conventional batch based methods. This will enable the characterization of single process steps and also multiple process steps in combination, e.g. reactors combined with separation operations. The rationale for selecting the miniaturized technology is to reduce the quantity of expensive and/or scarce resources needed for evaluation of potential process options, and to have experiments performed in an automated manner. Furthermore, this type of technology should make it easier to consider more complex process options, i.e. processes with *in-situ* product removal (ISPR), and should potentially yield easier development of continuous biocatalytic processes as well.

Specifically in this thesis, there is focus on the application of microfluidics for development of amine transaminase (ATA) processes for the asymmetric synthesis of chiral amines. Unfavorable thermodynamics and severe inhibitory effects from both substrates and products typically challenge ATA processes. Therefore, such biocatalytic processes often benefit from the implementation of ISPR and/or IScPR strategies. This makes it an ideal case study for applying microfluidics to test complex process options, i.e. ISPR by liquid-liquid extraction (LLE). Therefore, the goal of this thesis is to apply combined microfluidic modules to intensify ATA processes by putting in place a two-step LLE ISPR strategy that selectively removes the amine product during the reaction course.

The following objectives are addressed in this thesis:

- Demonstration of the application of microfluidic modules to characterize and evaluate individual process steps for ATA processes, i.e. reactor modules and liquid-liquid extraction modules.
- Combination of microfluidic modules, in a plug-and-play manner, to test complex process options and process steps, i.e. intensification of ATA processes by putting in place ISPR based on a two-step LLE strategy.
- Application of the LLE modules as a substrate supply strategy in combination with the product removal, to address the issue of low aqueous substrate solubility, rather than applying complex reaction media to increase the solubility.
- Investigation of the possibility of putting in place on-line and in-line analytical methods to avoid manual sample handling and increase the data throughput from the microfluidic systems.
- Reflection on how the knowledge obtained in the microfluidic systems can be applied for scale-up when suitable, and highlighting specific conditions when scale-out (numbering-up) is more suitable.

Though the focus of this project is on the development and application of miniaturized platforms and toolboxes for development of ATA processes, it is believed that microfluidic technologies and methods are easily applicable to other biocatalytic processes as well.

1.3 Thesis structure

This PhD thesis includes 9 chapters, covering theoretical and practical aspects of the application of microfluidic platforms for development of biocatalytic processes. The main content of the different chapters is as follows:

Chapter 1 provides an overview of the content, motivation and goals of this thesis.

Chapter 2 gives a general introduction to biocatalysis in the chemical industry, with focus on application of amine transaminases (ATAs). Special emphasis is given to the advantages and motivation for applying ATAs for synthesis of chiral amines and an overview of general limitations and the reaction mechanism is provided. Furthermore, the motivation for considering microfluidics in development of such processes is identified.

Chapter 3 gives an introduction and a general overview on microfluidics, where basic microfluidic mixing theory is presented and discussed. In addition, this chapter aims at identifying the potential of applying microfluidic modules for development of complex biocatalytic processes with ISPR.

Chapter 4 presents and discusses development considerations for ATA processes assisted by implementation of ISPR/IScPR strategies. Emphasis is put on the use of common separation metrics that are suitable to determine when putting in place ISPR/IScPR is appropriate. In relation to this, a review was performed on commonly applied ISPR/IScPR strategies and implementation strategies.

Chapter 5 describes experimental work focused on characterizing microfluidic packed bed reactors (PBRs), containing two ATA mutants, i.e. ATA-50 and ATA-82, entrapped in a polyvinyl alcohol (PVA) matrix. For the characterizations, a HPLC system was modified to operate as an on-line HPLC to completely avoid manual handling of small sample volumes.

Chapter 6 describes experimental work focused on selecting a suitable solvent for extracting a chiral amine product from a reaction mixture and characterization of two microfluidic extraction steps. The characterization was performed to get an idea about the partitioning and to ensure that equilibrium was achieved in each of the two LLE steps.

Chapter 7 demonstrates the ability to put a microfluidic system together in a plug-and-play manner to test an ISPR system. The system combines the micro PBR module with two-step micro LLE modules that were characterized in chapter 5 and chapter 6, respectively. The combined system truly highlights how easily relatively complex process options can be tested by applying automated microsystems.

Chapter 8 contains a discussion mainly on how the knowledge obtained in microsystems can be applied across scales to fulfill industrial production requirements in terms of throughput. The discussion will focus on when to perform conventional scale-up, i.e. from µL to m^3, and when to perform scale-out (numbering-up), i.e. moving from one module to a large number of identical modules in parallel in order to ensure sufficient product throughput.

Chapter 9 highlights the main findings and concludes the thesis. Furthermore, some open challenges are identified and future perspectives are briefly discussed.

1.4 Contributions

Throughout this project, a lot of feedback was given at various conferences, seminars, project meetings and through collaborations established in the course of the project. These actions gave important input and provided inspiration to the conclusions of this PhD thesis. The following subsections lists the events that contributed to this work.

1.4.1 Publications

Below a list of journal publications, either completely or partially resulting from the work described in this thesis, is provided. In addition, the publications are attached in appendix A.

- Krühne U., Heintz S., Ringborg R. H., Rosinha I. P., Tufvesson P., Gernaey K. V. & Woodley J. M., 2014, Biocatalytic process development using microfluidic miniaturized systems, Green Processing and Synthesis, 3(1), 23-31.

- Krühne U., Larsson H., Heintz S., Ringborg R. H., Rosinha I. P., Bodla V. K., Santacoloma P. D. G. A., Tufvesson P., Woodley J. M. & Gernaey K. V., 2014, Systematic development of miniaturized (bio)processes using Process Systems Engineering (PSE) methods and tools, Chemical and Biochemical Engineering Quarterly, 28(2), 203-214.

- Mitic A., Heintz S., Ringborg R. H., Bodla V. K., Woodley J. M. & Gernaey K. V., 2013, Applications, benefits and challenges of flow chemistry, Chimica Oggi, 31(4), 4-8.

1.4.2 Oral presentations

Provided here is a list of oral presentations given at conferences during this PhD project. The presentations focused on presenting the findings of this PhD project.

- Heintz S., Ringborg R. H., Rehn G., Börner T., Grey C., Adlercreutz P., Krühne U., Gernaey K. V. & Woodley J. M., 2015, Microfluidics for development and testing of ISPR options for the synthesis of chiral amines using ω-transaminases, Transam 2.0: Chiral amines through (bio)catalysis, 4-6 of March, Greifswald, Germany.

- Heintz S., Krühne U., Woodley J. M. & Gernaey K. V., 2015, Process intensification of ω-transaminase processes applying microfluidics, 3rd International Conference on Implementation of Microreactor Technology in Biotechnology (IMTB2015), 10-13 May, Opatija, Croatia.

1.4.3 Poster presentations

Provided here is a list of poster presentations given at conferences during this PhD study. The presentations focused on highlighting the findings in this PhD project.

- Heintz S., 2014, Challenges and opportunities of product recovery technologies for ω-transaminase processes, Bioprocess Engineering Course, 21-27 September, Supetar Island Brac, Croatia.

- Heintz S., Ringborg R. H., Rosinha I. P., Tufvesson P., Krühne U., Woodley J. M. & Gernaey K. V., 2014, Challenges and opportunities of product recovery technologies for ω-transaminase processes, CHISA/PRES 2014, 23-27 August, Prague, Czech Republic.

- Heintz S., Krühne U., Woodley J. M. & Gernaey K. V., 2014, Microfluidics for the development of biocatalytic processes with *in-situ*(co-) product removal, 13th International conference on microreaction technology (IMRET(, 23-25 June, Budapest, Hungary.

- Heintz S., Woodley J. M., Krühne U. & Gernaey K. V., 2013, Enzymatic process intensification across scales, 2nd International Conference on Implementation of Microreactor Technology in Biotechnology (IMTB2013), 5-8 May, Cavtat, Croatia.

- Rosinha I. P., Ringborg R. H., Heintz S., Tufvesson P., Schürmann M., Lavinia P., Wohlgemuth R., Krühne U., Gernaey K. V. & Woodley J. M., 2013, Miniaturized experimental toolbox for ω-transaminase technology (BIOINTENSE), 1st International Symposium on Transaminase Biocatalysis, 28 February- 1 March, Stockholm, Sweden.

Chapter 2

Biocatalysis overview

In this chapter, a general introduction is given on the topic of biocatalysis in the chemical industry, where the general benefits and challenges are highlighted. The chapter serves as an introductory chapter to the topic of applying microfluidics for development of advanced and complex biocatalytic processes. Furthermore, this chapter gives a general overview of the application of amine transaminases (ATAs) for the synthesis of high value optically active chiral amines, with emphasis on advantages and challenges. The challenges, e.g. inhibition and unfavorable thermodynamics, are highlighted to identify where microfluidics can aid in the development of such processes.

2.1 Introduction

In recent years, the number of applications of biocatalysis in the production of fine chemicals and pharmaceuticals has increased tremendously [3,5–7,11,12]. The term biocatalysis refers to the application of isolated enzymes, immobilized enzymes or whole cells containing one or more enzymes as catalysts for chemical reactions [1]. Many times biocatalysis is integrated as an intermediate step in the overall synthesis route, where the majority of the steps are chemical [13]. The majority of industrial applications of biocatalysis is somewhat related to the synthesis of pharmaceuticals and fine chemicals, with a trend towards applications for production of bulk chemicals [1,14–16]. Furthermore, as biocatalysis has matured tremendously in recent years it has broadened the potential application scope of biocatalysis [7].

The increased interest for industrial biocatalysis is motivated by the many advantageous features that biocatalysts are generally known for, e.g. exquisite selectivity, mild operating conditions, less process steps, high atom efficiency and safety [5,15,17–20]. Additionally, depletion of non-renewable resources and increasing political pressure on the chemical industry to promote sustainability also motivates increased focus on alternatives, like biocatalysis, in the chemical industry [18,19,21,22]. Furthermore, the continuous discovery and isolation of a variety of enzymes from biological sources and the development of enzyme libraries (toolboxes) has enabled a broad application range of biocatalysts compatible with a multitude of operational conditions.

Despite the many advantages and tremendous progress in the development of biocatalysts and biocatalytic processes, there are still common challenges that need to be resolved. The most common challenge is the ability, in due time, to tune the chosen biocatalyst to perform sufficiently efficient at the required process conditions [20,23] and/or the ability to modify the process to be compatible with the available biocatalyst [8]. For example, in the pharmaceutical industry the time to market has to be as short as possible [1], which will cause compromises to be made in terms of achievable biocatalyst and process performance. Table 2.1, gives an overview of common advantages and challenges associated with biocatalysis for organic synthesis.

Therefore, there is a need to explore new technologies and methods that can aid in accelerating the development of biocatalysts and biocatalytic processes. The application of microfluidic technologies in the development has the potential to aid in both accelerated and systematic high throughput characterization and testing of promising biocatalysts and process options (automation, parallelization and small consumptions of available resources) [4]. Hence, the aim in this chapter is to give a general introduction to different elements that play an important role in the development of biocatalysts and biocatalytic processes, and to identify the potential role of microfluidics in that development process. Special emphasis is put on the production of chiral amines through biocatalysis based on amine transaminases (ATAs), which is chosen as the case study in this thesis.

Table 2.1: Overview of common advantages and challenges associated with biocatalysis for organic synthesis.

Advantages:

- Stereo- & regio-selectivity
- Mild operating conditions (T, P, pH)
- Reduced process steps
  (e.g. avoid (de-)protection steps)
- Versatile in operating media
  (e.g. Aqueous and/or solvents)
- Few by-products
- Biodegradable
- Reusable
- Safe operation

Challenges:

- Compatibility with required conditions:
  (Low activity and stability under non-natural conditions)
  1) High/low pH
  2) High/low temperatures
  3) Solvents
  4) High substrate concentrations (Inhibition/toxicity)
  5) High product titers (Inhibition/toxicity)
- Unfavorable thermodynamics
- Solubility of substrates (Aqueous)
- Biocatalyst development time
- Selectivity not guaranteed
- Interfacing process steps
  1) Chemical and biocatalytic process step compatibility
  2) Biocatalytic process step and separation method compatibility

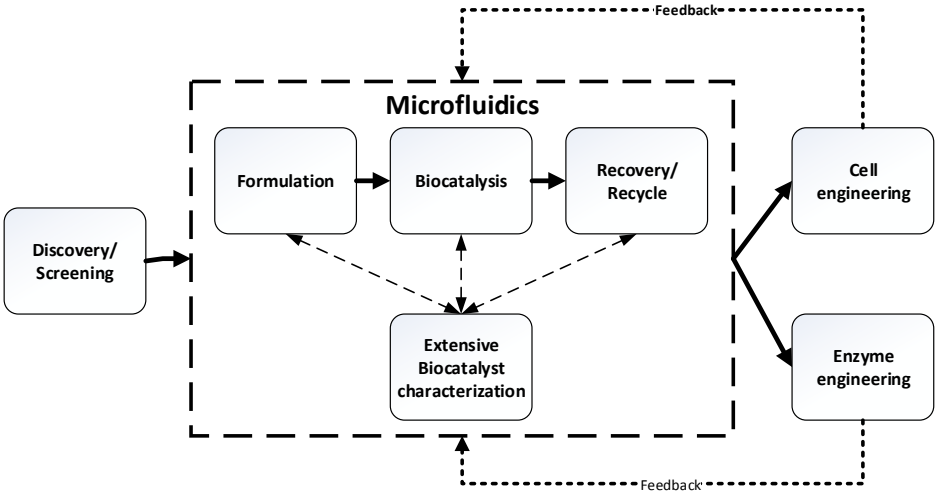

Figure 2.1: Overview of the application area of microfluidics focused on in this work, i.e. as a technology coupling the biocatalyst characterization and application that ultimately will aid in guiding further development of the biocatalyst and the process.

2.2 Microfluidics in biocatalytic process development

In the development and application of biocatalysis for chemical synthesis, there is a multitude of aspects that needs to be considered, which in a simplified manner can be divided into three categories: 1) Biocatalyst application; 2) Biocatalyst production; and 3) Biocatalyst development. This multitude of different aspects makes it highly relevant to consider new methods and technologies for robust development of biocatalytic processes. One such technology can at least in part be microfluidics, where – at least in this PhD thesis – the focus of microfluidics is directed to the characterization of biocatalysts and process scenarios (illustrated in Figure 2.1).

Biocatalyst application:

Implementation of biocatalytic based process steps in chemical synthesis is motivated by the ability of the biocatalyst to perform a complex synthesis in a simple manner and with high selectivity, which fulfills economic requirements [5]. The value of the final product of the biocatalytic process steps relative to the operational costs (OPEX: substrates, media, biocatalyst, labor and energy) partly determines the economic constraints of the process. The economic constraints are also influenced by the capital cost of equipment, e.g. reactors and separation units, needed to perform the specific synthesis step and ensure final product quality.

Specifying the economic targets is a rather complex task, and it is highly dependent on how the biocatalytic process step is implemented. For example, if the biocatalyst is performing poorly, resulting in low space-time yields (g/L/h), low product titer (g/L) and low biocatalyst productivity (g_P/g_{biocat}), then it is necessary to consider how to improve the biocatalyst (biocatalyst development) and/or the process (depends on process flexibility) to reach the required economic feasibility targets [2,7,8,15]. It is outside the scope of this work to go into detail with specifying economic requirements for biocatalytic process steps in chemical synthesis.

Biocatalyst production:

Another aspect is the cost impact of the applied biocatalyst. The cost impact of the biocatalyst is determined by the cost to produce, recover and formulate a biocatalyst with a specific performance [2,24]. In contrast to the biocatalyst application, the biocatalytic production method is rather fixed, i.e. fermentation with a suitable production host (microorganism).

The following recovery and final formulation of the biocatalyst is highly dependent on how the biocatalyst will be applied and how the production host expresses the biocatalyst, i.e. intracellularly or extracellularly. For extracellularly expressed biocatalysts, a crude biocatalyst liquid extract can be achieved by removing the cells from the culture broth, e.g. filtration or centrifugation. The biocatalyst can then be further purified and/or immobilized dependent on the process needs. For intracellularly expressed biocatalysts, the biocatalyst can be applied as whole cells (whole cells, lyophilized whole cells, immobilized whole cells), which can be recovered by filtering the culture broth. Alternatively, it might be required to disrupt the cells and either apply the crude cell lysate or further purify the biocatalyst before direct application or immobilization.

Immobilization of the biocatalyst, when considered beneficial and necessary, can be done by a multitude of different methods [25,26]. The method of choice for a specific application depends both on the form of the recovered biocatalyst and the nature of the immobilization technique relative to the application. For example, whole cells can be immobilized by flocculation [27] or different forms of the biocatalyst can be entrapped in or onto a porous solid support [25].

Biocatalyst development:

Before producing and applying the biocatalyst, in a feasible manner, extensive efforts are needed to develop and characterize the biocatalyst, the production host and the process [8,15]. As highlighted in the two previous sections there are many choices to be made, which has to be based on the process and knowledge obtained from identifying the performance of available and modified biocatalysts (e.g. through protein engineering or directed evolution [7]). The development is a labor-intensive and iterative cycle that can benefit from high-throughput technologies such as microfluidics. The exact role of microfluidics in this context is for extensive characterization of developed biocatalysts, formulations and process options to serve as an input for further development of the biocatalyst and identify economic feasibility. This aspect of microfluidics in the development of biocatalytic processes is illustrated in Figure 2.1.

In general, the aim of the iterative biocatalyst and process characterization is to map the optimal operational window and requirements. Additionally, the extensive characterization enables the possibility of identifying dominating limitations to both the process and the biocatalyst. It is important to be thorough and focus the characterization relative to what is required to investigate (you get what you screen for) [28,29]. Listed below are some general aspects and parameters that in many cases need to be considered in the characterization of novel biocatalysts and biocatalytic processes [5,14].

Biocatalyst characterization:

- Kinetics
- Inhibition
- Stability
- Reaction conditions: T, P, pH
- Co-factor recycle/regeneration
- Solvent compatibility: 1- /2-phase
- (substrate scope)

Process characterization:

- Reactor
  Thermodynamics
  Flow dynamics
  Operational requirements relative to biocatalyst: titer (g_P/L), STY (g_P/L/h), Yield (%), biocatalyst productivity ($g_P/g_{biocat.}$).
- Product recovery
  Driving force ([C])
  Selectivity
  Capacity
  Rate kinetics
  Recovery

In some cases, one may fail to modify the biocatalyst sufficiently and thereby severe process limiting challenges need to be overcome in alternative ways. For example, in cases of severe inhibitory effects from the products it can be beneficial to consider the implementation of process strategies to continuously remove inhibitory products during operation, i.e. *in-situ* product removal (ISPR). Such alternative process strategies can also be useful to investigate in cases, where groups of products with similar physicochemical properties need to be synthesized and the biocatalyst is inhibited. Development and testing of such alternative

processes can be difficult with conventional batch process based technologies. It is believed that microfluidics can enable easy testing of such untraditional and potential complex ISPR process options, and thereby contribute greatly to the development of novel and efficient biocatalytic processes.

2.3 Chiral amines

A promising application of biocatalysis is for the synthesis of chiral compounds, e.g. chiral amines. Chiral compounds are present in a vast number of, presently available and applied, active pharmaceutical ingredients (APIs) making such compounds highly demanded and valuable [30,31]. Listed in Table 2.2 are examples of such chiral amine compounds. Emphasized in the table is chiral amines that can be achieved through amine transaminase (ATA) synthesis routes, which is the focus of this work.

A still remaining challenge in the synthesis of such chiral compounds is the number of process steps required and the selectivity of the applied chemistry [30]. This drives the motivation for simpler synthesis routes with exquisite selectivity, which indeed can be achieved through biocatalysis.

Table 2.2: APIs containing chiral amines, which can be achieved using amine transaminase synthesis steps.

APIs	Structure	Comments	Refs.
Labetalol	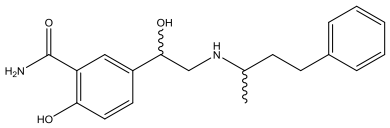	Application: α- and β-adrenoceptor blocking activities (antihypersensitives) Four possible stereoisomers, where the (R,R) form has the highest API potency (also called dilevalol)	[32]*
Sitagliptin (Januvia®)	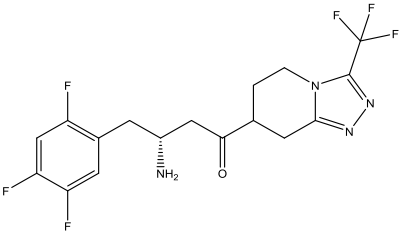	Application: Antidiabetic The (R) stereo isomer is required, which can be synthesized directly from prositagliptin ketone in >99.95% e.e.	[33]
(S)-(+) amphetamine (dextroamphetamine)	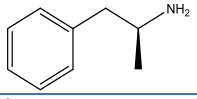	Application: ADHD and narcolephsy	[34]
(R)-3,4-dimethoxy-amphetamine (3,4-DMA)	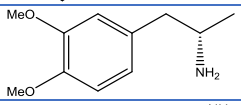	Application: Psychedelic drug	[34]
(S)-aminotetralin	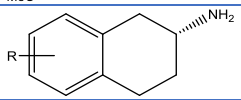	Applications: Parkinson's disease, depressions, cardiovascular problems	[35]

* In this work the main focus is related to synthesizing 1-methyl-3-phenylpropylamine (MPPA) from benzylacetone catalyzed by amine transaminases (ATAs). MPPA is a key building block in the synthesis of Labetalol.

2.3.1 Routes to chiral amines

There are numerous routes to chiral amines, both chemical and biocatalytic. The choice of synthesis route is greatly dominated by the availability and cost of the starting material and the complexity of the synthesis route. In the scientific literature, common chemical and biocatalytic routes are highlighted for the synthesis of primary chiral amines. These routes are:

Chemical routes to chiral amines are [36–38]:

- Reductive amination (single step) from enantio pure imines
- Reductive amination (multistep) from ketones incorporating chiral alcohol formation
- Crystallization of diastereomeric salts of chiral carboxylic acids

Biocatalytic routes to chiral amines are [34,36,39,40]:

- Amine transaminases for asymmetric synthesis
- Amine transaminases for dynamic kinetic resolution (DKR) and deracemization
- Oxidases for DKR and deracemization
- Hydrolases for DKR and deracemization
- Hydrolases for kinetic resolution
- Imine reductases for asymmetric synthesis

In Figure 2.2, an overview is given of the commonly identified biocatalytic routes to primary chiral amines and their corresponding substrates.

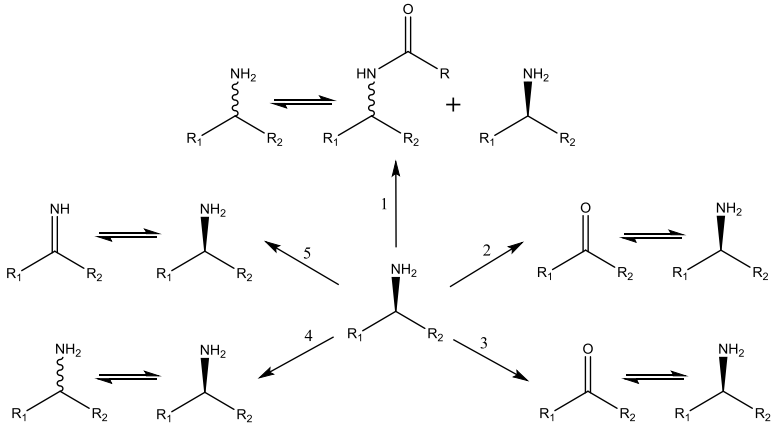

Figure 2.2: Commonly identified biocatalytic routes to chiral amines. 1) Resolution by lipases. 2) Asymmetric synthesis by amine transaminases (ATAs), these biocatalysts can also be applied for resolution and deracemzation. 3) Asymmetric synthesis by amine dehydrogenases, which conceptually can also be applied for resolution and deracemization. 4) Resolution by amine oxidases. 5) Asymmetric synthesis by imine reductases. R_1 and R_2 can be a variety of side groups, e.g. alkyl or aryl groups, which is dependent on the substrate scope of the given biocatalyst [41,42].

2.3.2 Amine transaminases (ATAs)

In this work, it was decided to focus on the synthesis of primary chiral amines by applying amine transaminases (ATAs, EC. 2.6.1.X). ATAs are highly versatile biocatalysts that can both be applied for DKR,

deracemization and asymmetric synthesis of a variety of chiral amines [41,43–45]. The motivation for focusing on ATAs is related to this versatility in combination with ATAs ability to synthesize enantiomerically pure amines directly from prostereogenic ketones [46]. Furthermore, compared to chemical routes, ATAs are not dependent on potentially toxic and scarcely available metal catalysts and the chiral amine is synthesized in one step.

In the scientific literature, there is some confusion on the name of these enzymes, and especially on the use of the name in a consistent manner. For example, some people call them transaminases (TAs) and others call them the aminotransferases (ATAs), which for historical reasons can be explained by IUPAC changing their recommendation from aminotransferases to transaminases in 1992 [47]. However, recently it has been argued that amine transaminases (ATAs) is a more correct name [45]. Here it is decided to apply the name amine transaminase (ATA).

ATAs belong to the enzyme class of transferases and have catalytic activity for the transfer of an amine group from an amine donor to an acceptor ketone [44]. The transfer is facilitated by the co-factor pyridoxal 5'-phosphate (PLP), which is converted to pyridoxamine-5'-phosphate (PMP) and back to PLP during the catalytic cycle [44]. The automatic recycle of the co-factor is of great importance as co-factor recycle strategies do not need to be considered.

Commonly, ATAs are further divided into two subcategories that are α-amino acid amine transaminases (α-ATAs) and ω-transaminases (ω-ATAs). The general reaction scheme of the two subcategories are shown in Scheme 2.1. The subcategory α-ATAs is named according to the ability to catalyze the transfer of an amine group between α-amino acids and corresponding keto-acids. The subcategory ω-ATAs is named according to the ability to transfer an amine group from an amine donor onto a carbonyl moiety of an amine acceptor, whereby at least one of the two substances is not an α-amino acid or an α-keto acid [44]. This definition will be applied throughout this work. In the scientific literature, it is also argued that ω-TAs transfer amine groups from ω-amino acids that are more distant from the carboxylic group [45]. Recently, it has been proposed that amine transaminases is the correct naming of the group of ATAs that are independent of the presence of carboxylic groups [31,39,43,45,46,48,49]. The reaction scheme of amine transaminases is the same as the one for ω-transaminases, just with different side groups.

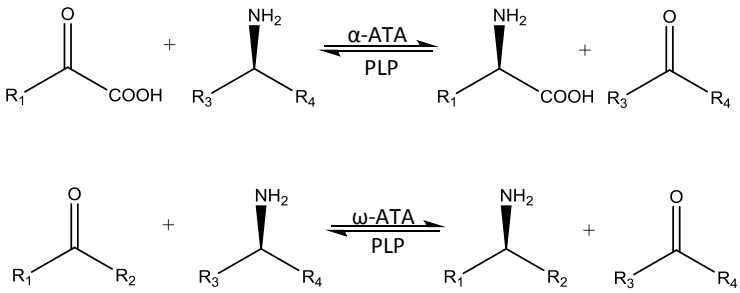

Scheme 2.1: Generalized reaction schemes of α-amino acid amine transaminases (Top, α-ATAs) and ω-amine transaminases (Bottom, ω-ATAs) for asymmetric synthesis of chiral amines. R_1 and R_3 are H, alkyl, aryl or alkene groups. R_2 and R_4 are H, alkyl, aryl, arylalkyl, alkene or carboxyl groups. Specifically for ω-ATAs, if R4 is a carboxyl group then R_2 should not be a carboxyl group and vice versa.

2.3.3 Amine transaminase mechanism

ATAs are known to follow a ping pong bi bi reaction mechanism [50,51], which consists of two half reactions. Generally for ATAs, PLP is believed to be bound in the active site as a Schiff base to lysine (internal aldimine: E-PLP) [51]. During the ATA reaction, the amine group from the amine donor binds to PLP and result in the formation of PMP (E-PMP) and the corresponding ketone product (cP) from the amine donor (first half reaction) [52]. Thereafter, the ketone substrate binds to the formed PMP and the ketone group is replaced with the amine group of PMP, resulting in the regeneration of PLP (E-PLP) (second half reaction). In Figure 2.3, the general reaction mechanism of ATAs is shown. Included in the figure are four complexes that indicate inhibitory effects from substrates and products of the reaction, i.e. E-PLP-S, E-PLP-cP, E-PMP-AD and E-PMP-P. Application of ω-ATAs for asymmetric synthesis of chiral amines is known to be heavily influenced by (competitive) inhibition of the keto substrate and corresponding amine product [50].

The small and large pockets in the active site dictate the variety of amine donors and ketone substrates that can bind in the active site of ATAs (substrate scope). At the same time these pockets are also directly responsible for the regio- and stereo selectivity of ATAs [53,54].

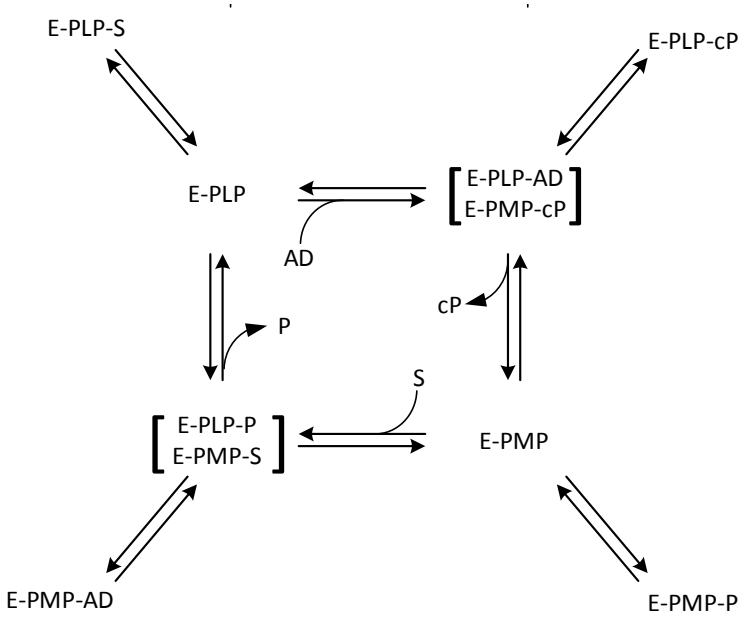

Figure 2.3: King-Altman representation of the amine transaminase reaction mechanism. Adapted and modified from Al-Haque et al. [50].

2.3.4 Challenges

Despite the many valuable features of ATAs, making it an interesting choice as an industrial synthesis route to optically active chiral amines, and despite the tremendous progress with these enzymes, there are still some common challenges that need to be overcome. The most common of these challenges are the

inhibitory effects from the products and substrates, sometimes toxic effects on the enzyme (denaturation), and low aqueous solubility of the ketone substrates. Furthermore, many times for the asymmetric synthesis of chiral amines, the thermodynamics are unfavorable in the desired direction [24].

The tremendous developments in protein engineering tools and methods, e.g. directed evolution, have indeed made it possible to overcome the majority of such challenges and to a great extent fit novel biocatalysts to the desired application and process [7]. However, protein engineering is still considered a time- and labor-intensive task that cannot solve all the challenges, e.g. unfavorable thermodynamics.

Therefore, in some cases it may be beneficial and faster to consider implementation of process engineering strategies, such as *in-situ* product removal (ISPR) to overcome severe product inhibitory effects and shift unfavorable thermodynamics. ISPR refers to the continuous selective removal of products during the reaction course. ISPR strategies are fast to implement, compared to protein engineering, as they commonly are based on conventional separation methods. The latter methods are well known and well-established, and are driven by differences in physicochemical properties and concentration gradients (ISPR and IScPR strategies will be discussed in detail in chapter 4).

The challenge of implementing ISPR/IScPR strategies is the ability to test and evaluate the practical feasibility of such a strategy, which is difficult to do with conventional methods and equipment. This challenge is addressed in this work by considering the application of microfluidics, in a plug-and-play manner, for performing such advanced and complex testing of novel and alternative process concepts. Microfluidics is introduced in chapter 3. A supplement to the microfluidic experimental platform is the development and application of robust kinetic models of the ATA reaction mechanism. Such kinetic models can be applied to set targets and requirements for considered ISPR concepts based on scenario analysis, i.e. the impact of the product removal efficiency on the biocatalyst performance. It was outside the scope of this work to apply available kinetic models from the literature [50] or to develop new general kinetic models for ATA reactions.

Chapter 3

Microfluidics for biocatalytic process development

The following chapter has been written as a joint chapter with Rolf H. Ringborg. This was done, as microfluidic mixing effects are a core element in both our theses and by combining efforts a more comprehensive understanding was achieved.

Application of microfluidics in the development of biocatalytic processes, where the main advantage is the low consumption of scarce and valuable resources has great potential. However, exploiting this potential fully requires a fundamental understanding of the dominating phenomena and effects at the microfluidic scale.

It is therefore the aim here to give an overview of these dominating phenomena and effects in order to highlight how to exploit them in the development of biocatalytic processes. Special emphasis is given to microfluidic mixing/mass transfer effects, which is considered the most important feature for successful application of microfluidics for development of biocatalytic processes. Furthermore, the concept of combining microfluidic modules in a plug-and-play manner is described and introduced as a novel option for testing complex biocatalytic process strategies that otherwise are very difficult to test with conventional methods. Biocatalytic process concepts that are complex are of interest as potential solutions for biocatalytic processes that are particularly challenging to operate as conventional batch processes.

3.1 Introduction

Microfluidics is in this context referred to as the analysis, control and manipulation of fluids in geometrically constrained channels, having characteristic dimensions in the micrometer range [55,56]. Microfluidics can be classified as a sub-category of flow chemistry, which covers continuous reactions conducted in microreactors, and is currently being considered an improvement and greener alternative compared to conventional batch processing in organic synthesis [57,58]. Furthermore, it has several times been pointed out that the use of microfluidics is in accordance with the 12 principles of green chemistry [59,60], in terms of improved safety [55,61], reduced waste generation [62] and energy efficiency to name a few metrics [63]. All these features are also considered requirements of efficient processes [58].

In 2007, a roundtable with the pharmaceutical industry ranked the most important research topics as being continuous processing, bioprocesses and separation and reaction technologies [64]. Hence, it is the focus of this work to address these topics and apply microfluidics as a tool in doing so.

Jensen et al. [62] presented the most recent developments in the microfluidic toolbox and further addresses major challenges for the technology. The Jensen group has published many papers regarding the field of microscale technology, and most relevant here are the creation of plug flow conditions at microscale [65], batch-like reaction time courses [66], automatic reaction optimization [67], and automatic kinetic model validation [68]. Furthermore, there is increased focus on the application of microfluidics for multistep synthesis systems [69,70] and continuous-flow chemical [71] and biochemical [72] processing, which is considered highly relevant as well.

The application of microfluidics for development of biocatalytic processes has a great potential. In fact, the main product resulting from the application of microfluidic process technology is information and fundamental knowledge that can be channeled towards accelerated process development. The exception to this is when reactions are difficult to control in conventional batch systems, causing microfluidics to be a suitable production method [73,74], which is in fact rarely the case for biocatalytic processes. For biocatalytic processes, one clear benefit of applying microfluidics is the low consumption of scarce and valuable resources, especially in the early development phase where for example only a few milligrams to a few grams of the catalyst is available [4]. More importantly, the information gathered per mass of biocatalyst spent is much higher in micro-scale reactors. Consequently, investigations that are more detailed can be carried out in comparison to conventional lab-scale studies. Furthermore, the small characteristic length scale and the large surface-to-volume ratio in microsystems enable faster heat and mass transfer. Compared to larger scale equipment this enables better control of concentration and temperature gradients in the microfluidic systems [55,63].

To fully exploit microfluidics for biocatalytic process development it is essential to have a fundamental understanding of the physical effects at the scale of interest. The dimensional effects are the majority of what is changing by using microscale technology as opposed to conventional lab scale and large scale equipment. In particular the smaller intrinsic volume, large surface to volume ratio and small hydraulic diameter are worth mentioning [75]. Microsystems commonly operate in well-defined laminar flow conditions, where heat and mass transfer will mainly be governed by diffusion and convection. Especially the mass diffusion time in microfluidic modules has a significant impact on the development of biocatalytic processes as it dictates the ideality of the mixing in the system. The diffusion time can be calculated by:

$$\tau_{mix} = \frac{d_t^2}{4D_{ab}} \qquad \text{(Eq. 3.1)}$$

, where $d_t[m]$ is the diffusion distance, τ_{mix} [s] is the characteristic mixing time and D_{ab} [m^2s^{-1}] is the diffusion coefficient of solute a in b.

Therefore, an important tool for understanding the phenomenal behavior at microscale, is to perform dimensional analysis which gives insights into opportunities that can emerge from miniaturization. Examples of different effects of miniaturization are highlighted in Table 3.1. For example, the short distances in microsystems cause the transport times of mass and heat to be shortened, where especially short mixing times are important when testing biocatalytic processes. The highly increased surface to volume area gives fast energy control and important operation parameters can be regulated precisely. The assumptions of ideal (constant) conditions are therefore approached, and modeling of the system will be more accurate. Microfluidic systems are expected to form the practical tool that will make us realize high-speed, functional, and compact instrumentation [76]. This will aid in improving and accelerating the characterization and development of biocatalytic processes. After investigating the effect of miniaturization, different dimensionless numbers will be introduced in this chapter, in order to better understand the fluid dynamic behavior occurring at this scale. These numbers can also be used to define regions of operation where desired behavior can be exploited.

Table 3.1: Highlights of the benefits of miniaturization.

Parameter	Factor change	Macroscale	Mesoscale	Microscale
Hydraulic diameter	d_H	1 m	1 cm	100 µm
Surface	d^2	1 m^2	1 cm^2	10^4 μm^2
Volume	d^3	1000 L	1 mL	1 nL
Surface / Volume (m^2/m^3)	$d^2/ d^3 = 1/d$	1	10^2	10^4
Diffusion time over d ($D_{ab} = 10^{-5}$ cm^2s^{-1})	d^2	8 y	7 h	2.5 s
Diffusion time over d ($D_{ab} = 10^{-6}$ cm^2s^{-1})		80 y	70 h	25 s
Example: in flowing systems				
Linear flow rate	d	1 m/s	1 cm/s	1 mm/s
Re (µ = 0.001 kg m^{-1} s^{-1}, ρ = 1000 kg m^{-3})		10^6	10^3	0.1
Volume / Experiment		>1 m^3	]1000: 1[mL	<<1 mL

In order to get a better feeling for the ranges one applies in the different overall flow regimes, common values are given in Table 3.2 and illustrated in Figure 3.1.

Table 3.2: common values for the hydraulic diameter (d_H) and the flow rate (q)

	d_H [mm]	q [L/min]
Plug flow	6.4	>100
Laminar flow	1-3	1-500
Low-dispersed flow	0.1-0.5	50-400

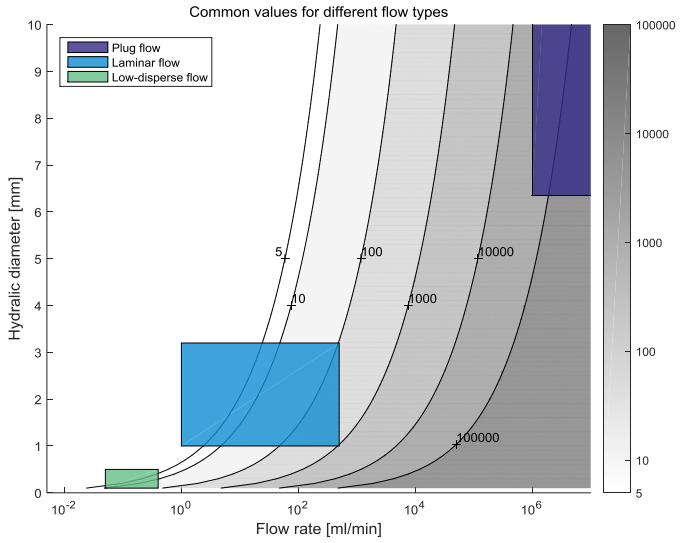

Figure 3.1: Illustration of common values for different types of flow, Re numbers are indicated by the grey contour.

3.2 Phenomena at the microfluidic level

A core element in the development of processes is to develop a proper understanding of the transport phenomena across scales, i.e. small scale in the development phase and large scale for industrial implementation. In order to efficiently use the information collected at the different scales such differences must be accounted for. It is therefore essential to understand the dominating transport phenomena in the microfluidic regime, relative to large-scale applications, when applying microfluidics for process development.

The topic of transport phenomena is a well-developed branch of physics with many standardized methods to calculate the dominating physical phenomena at the given scale and operational conditions, i.e. through dimensionless numbers [77,78]. Here a brief overview is given of common dimensionless numbers that are applied to understand the transport phenomena in microfluidics. The dimensionless numbers are crucial when dimensioning microfluidic modules for specific applications.

3.2.1 Reynolds number

The Reynolds number is applied to describe the ratio of momentum forces relative to viscous forces. The Reynolds number is calculated by:

$$Re = \frac{momentum\ force}{viscous\ force} = \frac{\rho v d_h}{\mu} = \frac{\rho\left(\frac{q}{A}\right)d_H}{\mu} \qquad \text{(Eq. 3.2)}$$

, where $\rho\ [kg/m^3]$ is the fluid density, $d_h[m]$is the hydraulic diameter, $\mu\ [kg/(m \cdot s)]$ is the dynamic viscosity, $v\ [m/s]$ is the average linear flow velocity in the channel, $A\ [m^2]$ is the cross-sectional area and $q\ [m^3/s]$ is the volumetric flow rate in the channel.

At low Reynolds numbers, viscous forces become dominant, which causes the fluid to move with a laminar flow profile, i.e. a parabolic velocity profile. At high Reynolds numbers, the momentum forces become dominant causing chaotic mixing effects, i.e. turbulent flow. The two types of flow regime are illustrated in Figure 3.2. In the scientific literature different regions of Reynolds numbers are applied to identify where the two types of flow regimes are dominant. It is stated in the literature that the different flow regime regions are in the ranges of [63,77]:

Turbulent flow regime: $Re > 3000$

Transition from turbulent flow to laminar flow: $1500 < Re < 3000$

Laminar flow regime: $Re < 1500$

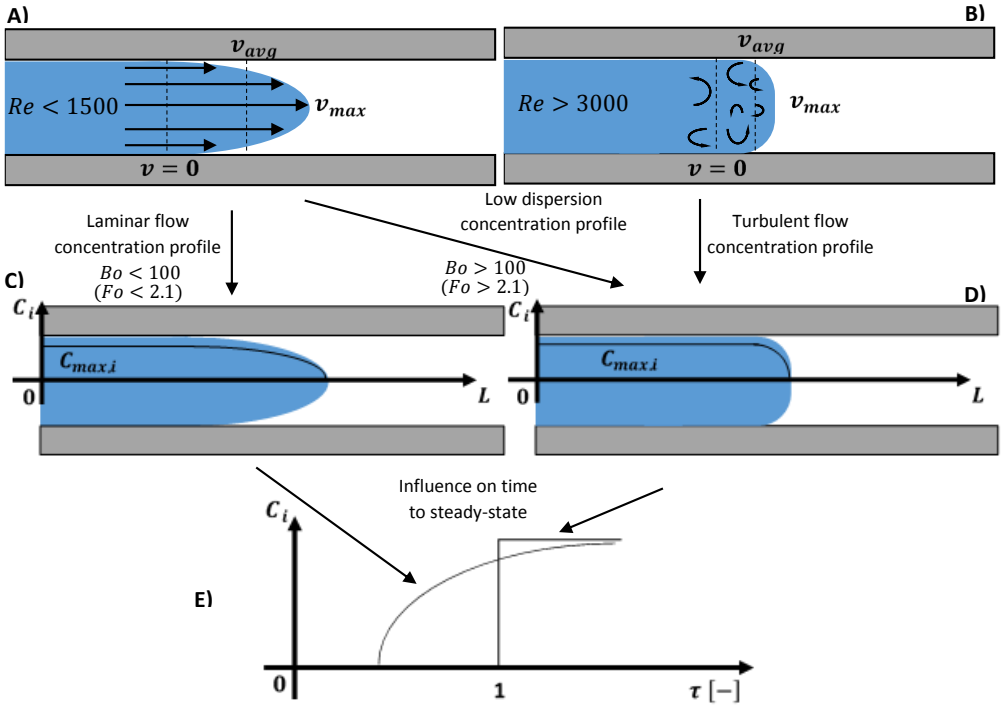

Figure 3.2: Overview of flow characteristics and concentration distribution profile scenarios. A) Laminar flow velocity profile. B) Turbulent flow velocity profile. C) Laminar flow concentration profile, where convection is dominating over radial dispersion. D) Turbulent flow concentration profile, which will appear similar to laminar flow when radial dispersion is dominating. E) Residence time concentration profiles of laminar flow and plug-flow dominated systems.

In Figure 3.3, the Reynolds number is calculated for a range of tube diameters and flow rates that are commonly applied for microsystems. Also highlighted in the figure are the Reynolds numbers, at various flow rates, for standard PTFE tubes, which are easily applicable in microsystems. The calculated Reynolds numbers clearly indicate that microsystems operate in the laminar flow regime, i.e. $Re \ll 1500$. In comparison, it is common that large-scale systems operate in the turbulent flow regime, which causes some fundamental differences in the mixing behavior across scales. This also makes it challenging to scale up processes based on knowledge obtained in microfluidic systems, which will be discussed in more detail in chapter 8.

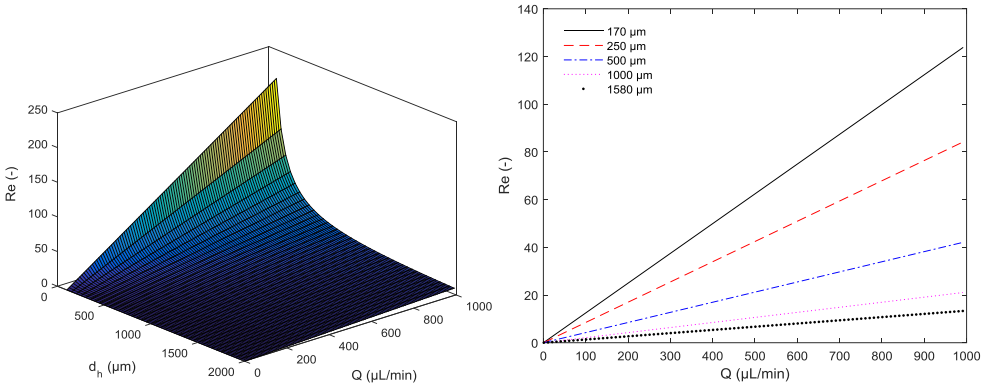

Figure 3.3: Left) Reynolds numbers for various inner tube diameters at various flow rates. Right) Reynolds numbers at various flow rates for standard PTFE tube dimensions.

3.2.2 Bodenstein & Fourier numbers

The Reynolds number only indicates the flow regime at the specified dimensions and flow conditions. Therefore, in order to get an idea about the mixing effects and concentration profiles in the microsystem of interest at various process conditions, it is essential to consider the Bodenstein, Fourier and/or Péclet numbers. The Bodenstein number is applied to describe the ratio of convection relative to that of dispersion. The Bodenstein and Péclet numbers both describe momentum transfer relative to molecular mass transfer. Consequently, the focus here is solely on the Bodenstein number. The Bodenstein number is described as:

$$Bo = \frac{total\ momentum\ transfer}{molecular\ mass\ transfer} = \frac{vL}{\mathbf{D}} \qquad \text{(Eq. 3.3)}$$

, where $\mathbf{D}$ is the Taylor dispersion coefficient [65,78]. Convection dominates most small scale flow systems and as a result the diffusive portion of the expression can be neglected:

$$\mathbf{D} = D_{AB} + \frac{v^2 d_H^2}{4\beta D_{AB}} \cong \frac{v^2 d_H^2}{4\beta D_{AB}} \qquad \text{(Eq. 3.4)}$$

, where $\beta[-]$ is a channel specific parameter, i.e. 48 for cylindrical channels [65].

Large Bodenstein numbers indicate low dispersion and operation will resemble that of a plug-flow reactor. At low Bodenstein numbers, dispersion will be dominant and the flow profile will be that of a laminar flow reactor. This is illustrated in Figure 3.4, where the flow profile will develop towards parabolic flow if convection is dominant (small Bo numbers), whereas radial dispersion will move the behavior towards plug flow when diffusion becomes significant.

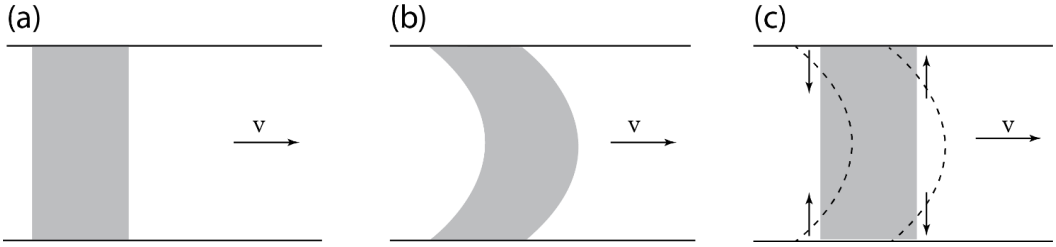

Figure 3.4: Explaining convection with and without diffusion, (a) impulse injected, (b) convection of impulse without diffusion and (c) convection of impulse with diffusion

Both concentration profile scenarios and their relative system response times (retention time distributions, RTD) are schematically presented in Figure 3.2. The inverse of the Bodenstein number can be said to describe the intensity of dispersion, and follows the inverse explanation of the Bodenstein numbers. Nagy et al. [65], coupled the Bodenstein number with the Fourier number, the ratio of residence time relative to the time to diffuse halfway across the channel, described by:

$$Fo = \frac{residence\ time}{transverse\ diffusion\ time} = \frac{4D_{AB}\tau}{d_t^2} \qquad \text{(Eq. 3.5)}$$

This coupling made it possible to specify ranges of the Bodenstein number, which resembles plug-flow dynamics and the transition to Taylor dispersion/convective flow dynamics. The specified ranges are as follows for step changes in the flow rate and/or concentration composition [65]:

Convective profile:	$Bo < 10$	($Fo < 0.16$)
Large deviations from plug-flow profile:	$10 < Bo < 100$	($0.16 < Fo < 2.1$)
Small deviations from plug-flow profile:	$100 < Bo < 1000$	($2.1 < Fo < 21$)
Plug-flow profile:	$1000 < Bo$	($21 < Fo$)

Based on the specified regions it was possible to make predictions about the magnitude of dispersion effects and the corresponding flow characteristics for different diffusion coefficients. These predictions are presented in Figure 3.5, inspired by Nagy et al. [65]. The location of the different regions, relative to residence time and tube diameter, is greatly dependent on the diffusion coefficient of the solute. Practically, this means that slowly diffusing compounds are prone to having flow dynamics, which are dominated by axial dispersion. The main problem of having such flow dynamics is the time it takes to reach steady state, which is greatly increased compared to plug-flow dynamics. This can be observed in Figure 3.6.

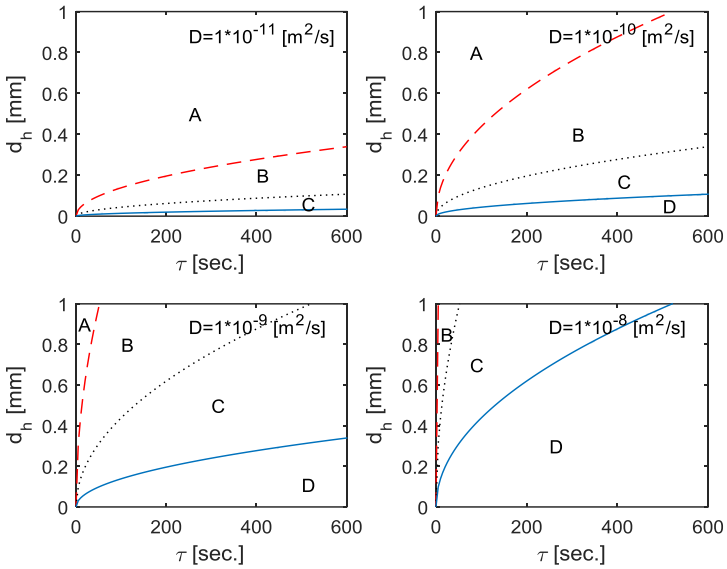

Figure 3.5: Influence of the diffusion coefficient on the flow dynamics/mixing dynamics of the system. A) fully developed laminar flow dynamics, B) large deviations from plug-flow dynamics, C) small deviations from plug-flow dynamics, and D) plug-flow dynamics

Enzymes and other proteins are known for having low diffusivities, which as earlier stated makes it time consuming to achieve steady state. This problem is repeated for each step change with regard to the enzyme concentration. However, it is possible to circumvent this by acquiring a steady state condition profile for the enzyme in the system and hereafter only introduce step changes to the substrate composition. In other words, the mass balance over the reactor for the enzyme is kept constant. Hereby, it can be assumed that the system operation will depend on the substrates diffusion coefficient, as shown in Figure 3.5. The substrates applied for enzymatic reactions are commonly very small molecules, and consequently fast diffusing molecules.

Estimation of the time required to reach the initial steady state shows that this time is still highly dependent on the specific diffusion coefficient of the investigated enzyme. Significant research efforts have been invested into development of quick and robust methods and models for predicting protein diffusion coefficients. He et al. [79], for example, included the radius of gyration [80] to the molecular weight correlation [81] to get within 15% deviation of most experimentally determined values. The addition of gyration radius gives a correction for non-globular shaped proteins, which is for example important in the case of rod shaped proteins. The radius of gyration needs to be calculated and should not be looked up as a general value. It can be calculated directly from protein database files by applying the HYDROPRO software [82]. It is suitable to apply the HYDROPRO software when the protein crystal structure is available, as the software not only calculates the radius of gyration, but also directly calculates the diffusion coefficient. For globular proteins, it is possible to correlate the diffusion coefficient directly to the molecular weight of the protein. The molecular weight correlation [81] and the model including the radius of gyration [79] are defined as follows:

$$D_{AB} = 8.34 \cdot 10^{-11} \left(\frac{T}{\mu \cdot M^{1/3}}\right) \quad \text{(Eq. 3.6)}$$

$$D_{AB} = \frac{6.85 \cdot 10^{-15} T}{\mu \cdot \sqrt{M^{1/3} \cdot R_G}} \quad \text{(Eq. 3.7)}$$

, where $T\ [K]$ is the absolute temperature, $\mu\ [PA \cdot s]$ is the dynamic viscosity, $M\ \left[\frac{g}{mol}\right]$ is the molecular weight and $R_G [\text{Å}]$ is the radius of gyration.

HYDROPRO requires knowledge of the specific volume, $\nu\ \left[\frac{cm^3}{g}\right]$, which is the inverse density, ρ^{-1}. The protein density can be estimated by the following correlation [83]:

$$\rho(M) = \left[1.410 + 0.145 \exp\left(-\frac{M}{13}\right)\right] \quad \text{(Eq. 3.8)}$$

, where the molecular weight M is expressed in kDa units. If the molecular weight exceeds 20 kDa the model has been identified to slightly over predict the molecular density.

Predicted diffusion coefficients from the above-mentioned models and correlations for two transaminases are presented in Table 3.3. The two transaminases 3A8U and 4A72 originates from *Pseudomonas putida* and *Chromobacterium violaceum*, respectively. It was assumed for the calculations that $T = 303.15\ K$ (30℃) and $\eta = 0.001\ Pa \cdot s$.

Table 3.3: Predicted diffusion coefficients of two transaminases obtained from various models and correlations.

PDB ID.	Enzyme	M	R_G (from hydropro)	ρ	Young et al. [81]	He et al. [79]	HYDROPRO
-	-	g/mol	Å	g/cm^3		$10^{-11} m^2/s$	
3A8U	ω-ATA-monomer	48916	23.1	1.41	6.91	7.14	7.23
4A72	ω-ATA-tetramer	205613	40.7	1.41	4.28	4.23	4.49

The Taylor dispersion coefficient described earlier (equation 3.4) can be combined with dispersion models to predict the exit age distribution. For open-open systems, where the system boundaries represent similar flow dynamics as that of the control volume, the exit age distribution can be described by [84]:

$$\mathbf{E}_{\theta,\mathrm{oo}} = \frac{1}{\sqrt{4\pi \mathbf{D}/vL}} \exp\left[-\frac{(1-\theta)^2}{4\theta \mathbf{D}/vL}\right] \quad \text{(Eq. 3.9)}$$

, where $\theta\ [-]$ is the mean residence time.

The F curve can then be calculated by:

$$\mathbf{F}_{\mathrm{oo}} = \int_0^{\theta} \mathbf{E}_{\theta,\mathrm{oo}}\, dt \quad \text{(Eq. 3.10)}$$

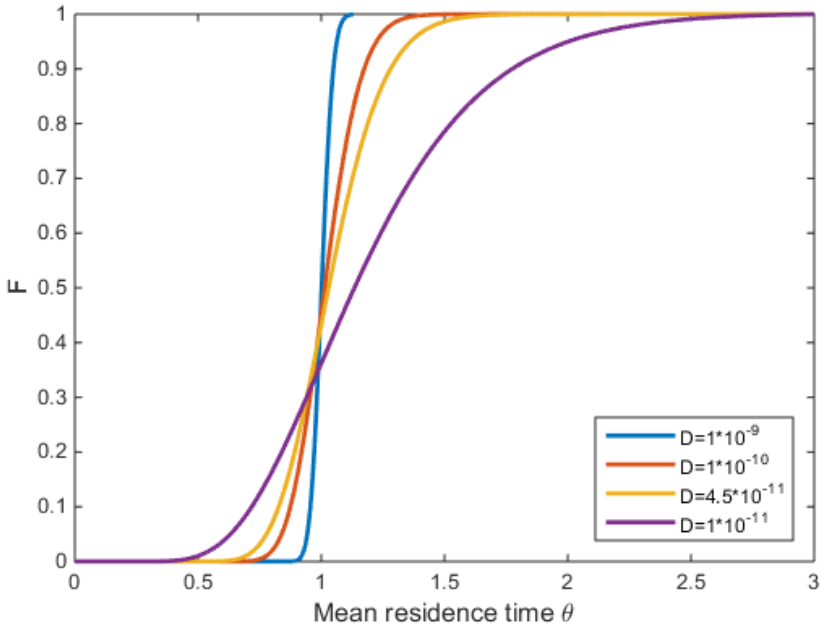

Figure 3.6: F curve as a function of mean residence time accounting for different diffusion coefficients. The curves were calculated with v=0.023 m/s, L= 7 m, beta = 48 and ID=200 µM

From Figure 3.6, it is clear that the substrates (D = 10^{-9} m^2/s) and enzymes (D = 10^{-11} m^2/s) move very different through the reactor, as expected. The required times to reach steady state have been estimated and can be observed in Table 3.4. Levenspiel [84] states that for dispersion numbers above $\mathbf{D}/\bar{v}L = 0.01$ other models should be applied to calculate the exit age distribution. For the diffusion coefficient $D_{ab} = 1 \cdot 10^{-11}\ m^2/s$, the steady state calculation can therefore only be used as a guidance.

Table 3.4: Required time to reach steady state (ss) dependent on diffusion coefficient. Calculations were done with v=0.023 m/s, L= 7 m, beta = 48 and ID=200 µM

Diffusion coefficient $D_{ab}\ [m^2/s]$	Dispersion number $\mathbf{D}/\bar{v}L$	95% ss	99% ss	Region defined from above
$\mathbf{1 \cdot 10^{-9}}$	0.0006	1.06θ	1.09θ	"plug-flow"
$\mathbf{1 \cdot 10^{-10}}$	0.0066	1.22θ	1.32θ	Small deviations from plug flow
$\mathbf{4.5 \cdot 10^{-11}}$	0.015	1.36θ	1.52θ	Large deviations – mixed flow
$\mathbf{1 \cdot 10^{-11}}$	0.066	2.00θ	2.47θ	Dispersed flow.

In cases where the dispersion number is high more complex numerical models, i.e. computational fluid dynamics (CFD) solving the Navier-Stokes equations, are required to describe the dispersion in the system. As an example, such CFD calculations were done for a specific cylindrical tube with the characteristic

dimensions of 1 mm inner diameter and a length of 10 cm. Various diffusion coefficients were applied and the flow rate was fixed to 21 µL/min. The given flow rate was specified as that flow rate was applied for some experimental investigations, which are not included in this thesis. The commercial software ANSYS CFX 14.0 was applied to solve this problem, and the results are shown in Figure 3.7. Additionally, the analytical solutions are compared with the step responses of an ideal continuous stirred tank reactor (CSTR) and a plug-flow reactor (PFR).

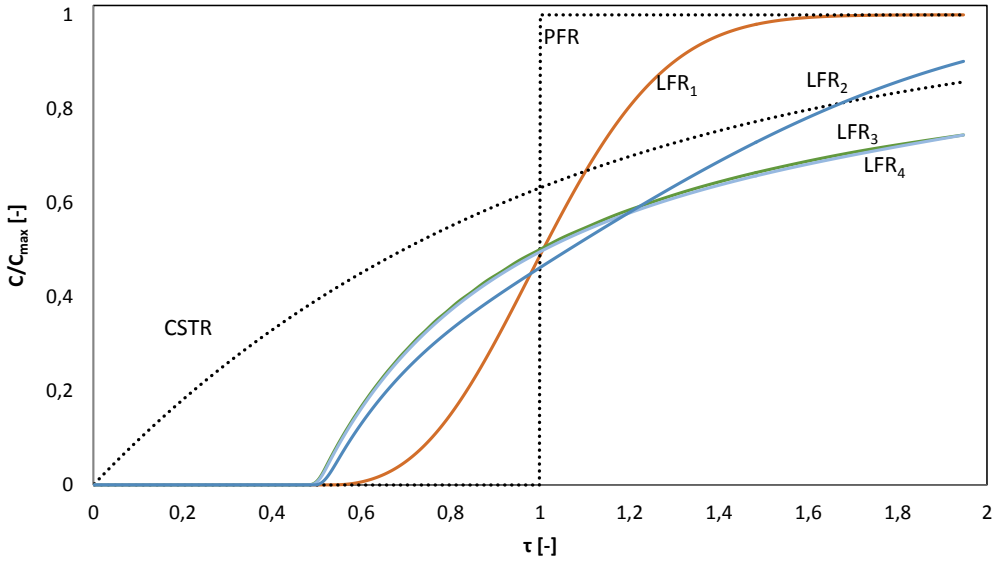

Figure 3.7: Mapping of compounds with different diffusion velocities, *i.e.* $D_{ab} = 1 \cdot 10^{-9} \frac{m^2}{s}$ *(orange),* $D_{ab} = 1 \cdot 10^{-10} \frac{m^2}{s}$ *(blue),* $D_{ab} = 1 \cdot 10^{-11} \frac{m^2}{s}$ *(light blue) and* $D_{ab} = 1 \cdot 10^{-12} \frac{m^2}{s}$ *(green),* based on CFD simulations. The curves for the two latter diffusion coefficients are very similar to one another in the simulated time interval. The length of the simulated tube is in this case 10 cm, and the tube has a diameter of 1 mm. The initial concentration was set to $1\ kg/m^3$ and the mass flow rate was specified to be $3.5 \cdot 10^{-7}\ kg/s$. Nomenclature: PFR - *plug flow reactor,* CSTR - *continuous stirred tank reactor,* LFR - *laminar flow reactor*

Regarding the similarities of the dispersion profiles for slowly diffusing solutes presented in the figure, $D_{ab} \geq 1 \cdot 10^{-11} \frac{\mathrm{m}^2}{\mathrm{s}}$, it is obviously difficult to distinguish between them in the given modelling framework. However, it should be possible to distinguish between them. This can be done by extending the RTD experimental time which will cause the difference in the profiles to become more prominent as $time \rightarrow \infty$. Based on the performed experiments the dispersion numbers were also calculated, and the values are presented in Table 3.5. It can be seen that the numbers are all significantly higher than the boundary specified by Levenspiel [84].

Table 3.5: Diffusion coefficients, dispersion coefficients and dispersion intensity of the simulation examples in Figure 3.7.

D_{ab}	D	$\frac{D}{vL}$
10^{-9}	$1.04 \cdot 10^{-6}$	0.023
10^{-10}	$1.03 \cdot 10^{-5}$	0.232
10^{-11}	$1.03 \cdot 10^{-4}$	2.323
10^{-12}	$1.03 \cdot 10^{-3}$	23.210

3.2.3 Capillary, Eötvös (Bond) and Weber numbers (for two-phase flow)

Another application in microfluidics is to operate with immiscible fluids, e.g. gas-liquid or liquid-liquid. This type of application is beneficial for the development of separation processes and/or biocatalytic processes where it is required to feed and/or remove various compounds during the reaction course. The interfacial behavior in this type of application can be described through a different set of dimensionless numbers [85,86]. Two of the numbers are the Eötvös number (also known as the Bond number) and the Weber number.

The Eötvös number represents the ratio of gravitational forces relative to surface tension forces. It is described by:

$$Eo = \frac{\Delta\rho g d_h^2}{\sigma} \quad \text{(Eq. 3.11)}$$

, where $\Delta\rho\ [kg/m^3]$ is the density difference between two immiscible fluids and $\sigma\ [N/m]$ is the surface tension.

The Weber number represents the ratio of the fluids inertia relative to its surface tension. It is described by:

$$We = \frac{\rho\mu^2 d_h}{\sigma} \quad \text{(Eq. 3.12)}$$

However, the Weber number is usually not the most important dimensionless number for microfluidic applications, i.e. the Reynolds number is small for such applications meaning that inertial effects can be neglected. Furthermore, the Eötvös number is only essential when operating with two immiscible fluids with significant density differences, like gas-liquid systems [87,88]. Besides these two numbers, which are not used for microfluidic liquid-liquid applications, there is a third dimensionless number that is commonly applied. This is the Capillary number which describes the ratio of viscous forces, shear stresses, relative to surface tension forces [88]. The Capillary number is defined by:

$$Ca = \frac{viscous\ force}{surface\ tension\ force} = \frac{\mu v}{\sigma} \quad \text{(Eq. 3.13)}$$

The Capillary number is an important parameter for understanding the droplet formation, size and shape in microsystems [89]. Dependent on the magnitude of the Capillary number it is possible to predict different droplet formation regimes, i.e. squeezing, dripping and jetting [90,91]. The different droplet formation regimes are illustrated in Figure 3.8. At low Capillary numbers, e.g. $Ca \leq 0.01$, the system operates in the squeezing regime, which causes the formation of slug-like droplets [87,88,90], as shown on top of Figure 3.8. Larger Capillary numbers, e.g. $Ca \geq 0.02$, cause formation of dripping droplets, which have a significantly lower droplet volume than the slugs [87,88,90], as shown in the center part of Figure 3.8. As the Capillary number increases in the dripping regime, the behavior of the system moves towards the jet regime. Here the detachment in the dripping regime gradually moves further down the channel. This trend is then further

amplified with increasing Capillary number and increasing ratio of the continuous flow phase relative to the droplet phase ratio, as shown at the bottom of Figure 3.8.

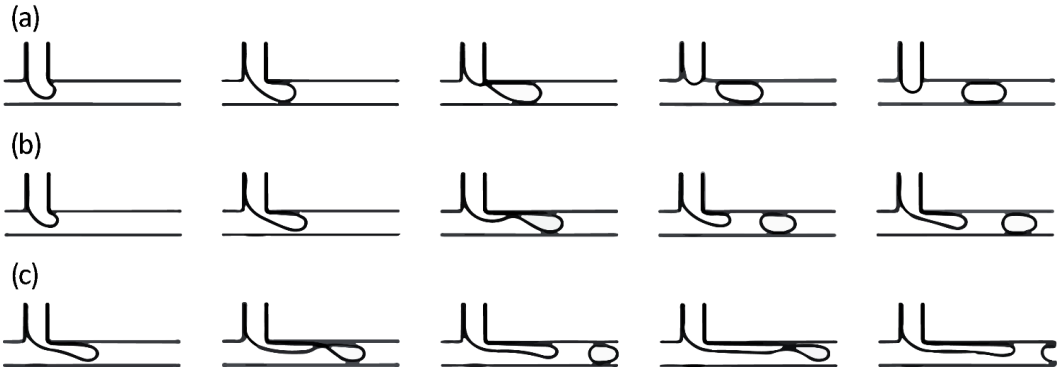

Figure 3.8: Squeezing (a), dripping (b) and jetting (c) based droplet formation mechanisms.

Dependent on the channel dimensions, flow rates, surface tensions etc. it is possible to achieve different types of multi-phase flow patterns in the channels [92]. In addition, modifying the wetting properties of the wall surfaces will enable to operate with fluid streams in co- or counter side-by-side flow [93]. Maintaining this type of flow is dependent on stabilizing the pressure gradient between the two phases by the Laplace pressure at the interface [71]. These different types of flow are sketched in Figure 3.9 [92,94]. The shape of the liquid-liquid interphase is dependent on the interfacial tension between the two phases.

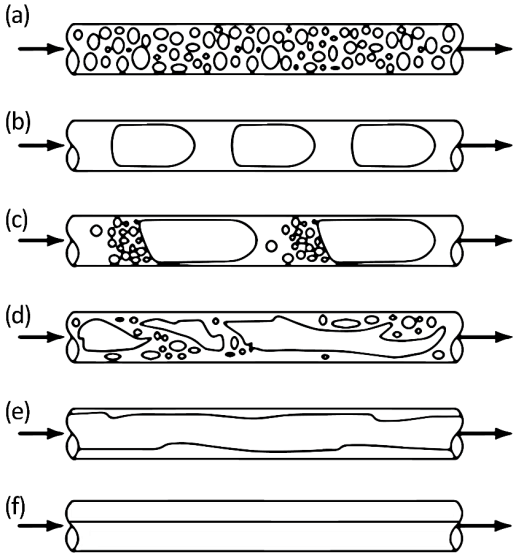

Figure 3.9: Overview of different multi-phase flow scenarios: (a) bubble flow, (b) slug flow, (c) transitional slug/churn flow, (d) churn flow, (e) annular flow, (f) side-by-side flow.

Table 3.6: Overview of important dimensionless numbers and their ranges for various applications.

	Re	Bo	Ca	Application	Comments
Plug flow	>3000	N/A	N/A	Production	
Laminar flow	<1500	<10	N/A	Transport of homogenous solution	Well-defined flow regime and easy to simulate through CFD.
Low dispersed flow	<10	>100	N/A	Determine kinetics	Laminar flow regime where concentration profiles appear similar to plug flow profiles.
Slug flow (sweeping)	N/A	N/A	≤ 0.01	Study of LLE, GLE, ISSS, ISPR, individual batch reactors	Formation of slugs is greatly dominated by the inlet diameter and the diameter of the operating channel – for microfluidic channels it is common to talk about slugs/droplets for this range of capillaries
Side-by-side flow	N/A	N/A	N/A	Study of LLE, ISSS, ISPR	Note: Requires that the pressure gradient is stabilized between the two phases by the Laplace pressure and/or by modifying the channel hydrophobicity.
Droplet flow (dripping)	N/A	N/A	≥ 0.02	Study of LLE, GLE, ISSS, ISPR	Similar to slug flow.

In Table 3.6, an overview is given of the different dimensionless numbers, along with ranges that are of interest for different applications. The different highlighted applications of interest in relation to the development and application of biocatalytic processes are:

- **Plug-flow:** Plug-flow mixing characteristics are commonly experienced at large scale (larger hydraulic diameters and flow rates) and thereby such flow dynamics are relevant for production purposes. The required dimensions and flow rates to achieve plug flow dynamics make this flow regime unsuited for development purposes, as it would be too costly.
- **Laminar flow:** For development purposes, it is common to operate with laminar flow dynamics, due to the small scale and flow rates. This however gives some challenges for scale-up, as the flow dynamics change with increasing scale. Transport of homogenous solutions and steady state measurements are here the direct application. However, the study of dynamic responses with such a flow profile is either relative to the system, or should be corrected by residence time distributions. Nonetheless, it is here possible to quickly assess the dynamics of various flows and operating conditions on the biocatalyst performance and/or separation. The comparison of similar systems with different units can thereby still be quite useful for process optimization.
- **Low dispersed flow:** The application of this regime is for simulating plug-flow dynamics of a system. As plug-flow reactors has identical behavior as batch reactors, it is here possible to determine kinetics in flow.
- **Slug, side-by-side and droplet flow:** These microfluidic flow applications are useful for testing and optimizing separation based processes, such as liquid-liquid extraction, gas-liquid extraction, ISSS and ISPR. Furthermore, droplet and slug flow can also be operated as single reactors making it possible to perform high-throughput reaction screening and characterization. A limitation to side-by-side flow is that its application is restricted to small scale applications and that its main purpose is to gain knowledge about mass transfer between phases. It is also dependent on phase separation at

the end of the module. The advantage of slug flow over droplet flow is the possibility to apply optical analytical methods to follow the progress in the slugs, which is significantly more difficult with freely flowing droplets. For development of extraction methods, droplet and/or slug flow applications are more appropriate than side-by-side flow. This is because the high throughput characterization of such applications is easily adaptable to a broad range of different operating conditions.

3.3 Pressure drop

When designing a specific microfluidic module it is important to consider the limitations of the pumps available to operate the specific system, i.e. not all pumps can operate at high pressure. It is therefore important to evaluate the pressure drop in each module and in combined modules. The Hagen-Poiseulle equation describes pressure drop in laminar flow with incompressible and Newtonian fluids, where the length of the channel is much greater than the diameter [63].

$$\Delta P = \frac{128 \eta L q}{\pi d_H^4} \qquad \text{(Eq. 3.14)}$$

, where $\Delta P\ [Pa]$ is the pressure drop across length L $[m]$ of the channel diameter, for a flow $q\ [m^3/s]$ of a fluid with viscosity $\eta\ [Pa \cdot s]$. As the channel diameter ($d_H\ [m]$) decreases, the pressure needed to achieve the same flow increases dramatically. In Figure 3.10, the influence of flow rates and channel diameters on the pressure drop can be seen for various tube lengths, assuming a maximum allowable pressure drop of 3 bar, which was indeed the pressure limit of the pumps utilized in this project.

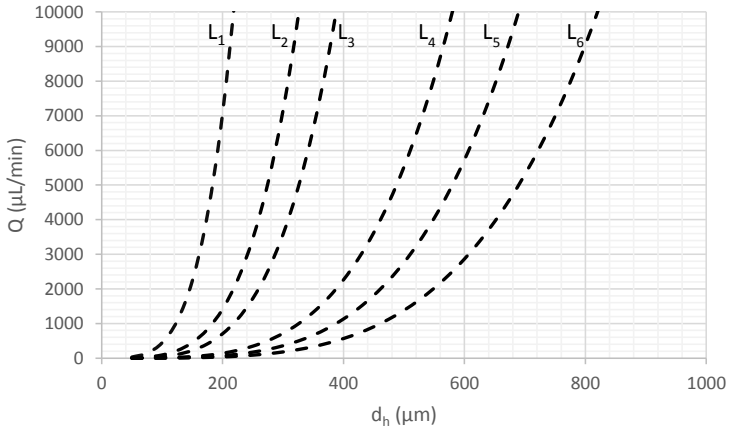

Figure 3.10: Representation of a 3 bar pressure drop in microfluidic modules with changing flow rates and diameter at various tube lengths, i.e. L_1=0.1 m, L_2=0.5 m, L_3=1 m, L_4=5 m, L_5=10 m and L_6=20 m. Everything to the left of the curves corresponds to regions where the pressure drop is higher than 3 bar.

For modules with porous domains, e.g. packed bed reactors, one can apply Erguns equation to describe the pressure drop [95]. Erguns equation is defined as:

$$\Delta P = 1.75 \frac{v_0^2 \rho L(1-\varepsilon)}{\varepsilon^3 d_p} + 150 \frac{v_0 \eta L(1-\varepsilon)^2}{\varepsilon^3 d_p^2} \quad \text{(Eq. 3.15)}$$

, where $\varepsilon\ [-]$ is the particle porosity, $v_0\ [m/s]$ is the fluid velocity based on an empty channel, and $d_P\ [m]$ is the diameter of the spherical particles. However, in many cases it might be difficult to get an exact prediction of the pressure drop in porous domains. For example, there can be many variations in packing densities, whereas particles come in a range of sizes and shapes, and are rarely completely spherical [96].

3.4 Microfluidic reactor and separation modules

The development of biocatalytic processes is greatly dominated by lab scale batch process based technologies. Liquid handling at lab scale for batch type experiments requires manual handling. This type of liquid handling is directly related to the amount of labor required to run an experiment. Furthermore, conducting reaction and separation sequentially in different containers requires that people are available to conduct the transfer of liquid. It is clear that this form of experimentation is laborious and requires relatively large volumes for every cycle. The alternative is to conduct microfluidic experiments in a continuous fashion by connecting reactors with separation directly and by handling the liquids by pumps. The labor requirement for constructing such a setup is of course much larger compared to the sequential "batch" lab scale. Therefore, such an effort should only be done when more than a couple of experiments are required. Flow chemistry has evolved a lot in the recent years, and has moved into microscale and microfluidics, where many unit operations have been translated to this scale. It is possible to mix [97], introduce an extraction phase, phase separate [98], distil [99], adsorb/absorb [85] and implement optical analytical methods. The available microfluidic modules enable the testing of various unit operations in combination (plug-and-play combination of the microfluidic modules). An advantage of this type of testing is that it will be possible to test complex biocatalytic process options, where reactor modules and separation modules are integrated to some extent. In order to understand the simplicity of combining units at this scale, different unit operations relevant for biocatalytic processes have been sketched and can be seen in Table 3.7.

Table 3.7: Different unit operations at µ-scale.

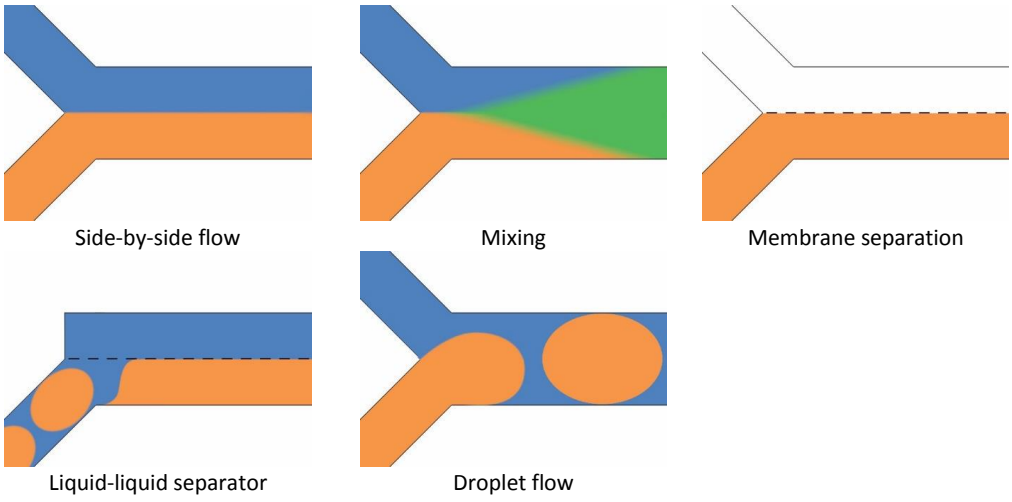

The sketched unit operations can be combined rather easily with a simple interface consisting of tubing and fittings. The realization that this is possible makes the hurdle of continuous setup construction less time consuming. To illustrate this, a PI diagram (Figure 3.11) describing a generalized process flow for synthesis of chiral amines catalyzed by amine transaminases (ATAs) [100] has been translated to microscale unit operations (MUO's), as shown in Figure 3.12.

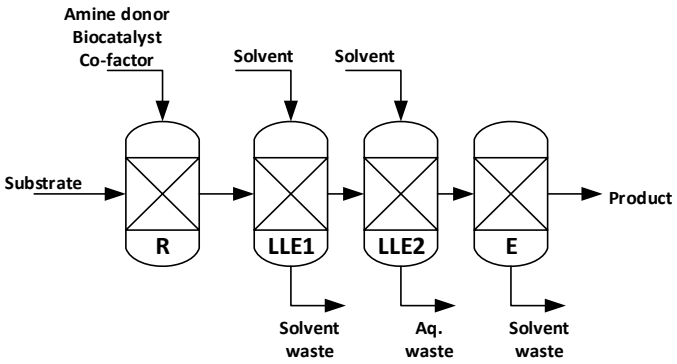

Figure 3.11: Generalized amine transaminase (ATA) process flow chart for synthesis and recovery of chiral amines. The generalized scheme consists of a reactor (R), two liquid-liquid extraction steps (LLE1 and LLE2) and an evaporation step (E).

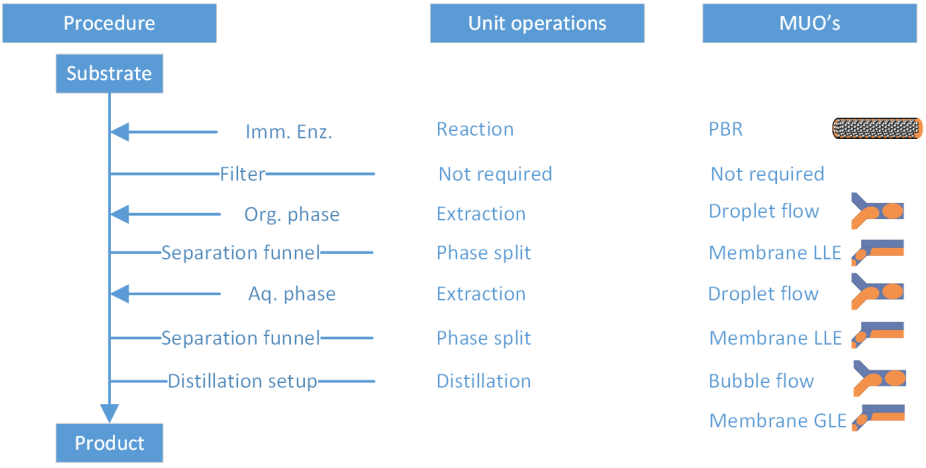

Figure 3.12: Translation from standard sequential batch processing to microscale unit operations.

The concept of modularity is not new, and creating a framework for such modularization has been attempted a number of time [101–103]. Projects defined with the specific objective of developing generic approaches to somewhat different operating regimes compared to the one investigated in this thesis are summarized in the list below. However, applications of such modules in a plug-and-play manner for biocatalytic applications has to date only been attempted a few times [70].

The European project BIOINTENSE intended to design units with fixed dimensions to fit all purposes for biocatalytic applications, and an obviously clear result is that this is impossible. In order to navigate the space of microfluidics, as outlined in this chapter, one should be able to manipulate the characteristic dimension, length and flow rate of the modules. Commercialization of the technology for flow chemistry, which can be adopted to biocatalytic applications, is becoming more widespread and platforms are available such as the Lonza flow plate [104], the Syrris system [105], Fluidgent [106] or Chemtrix [107]. The increasing number of industrial producers of such systems can be considered as a direct proof of the commercial importance of this research, and can be extended to how relevant this work is to the wider world. Along with the history of other international projects, this indicates that this type of work is a relatively high priority in industry.

3.5 Materials and fabrication

It is from a qualitative point of view nice to work with systems that are easy to manufacture, and from a quantitative point of view, systems characterized by complete inertness are important. Polymers are relatively easy to manipulate, and 3D printing lightens the burden of constructing a microscale reactor even further [108]. It is within such a flexible design space that rapid investigations of geometry can take place. Several trade-offs can be observed in Table 3.8. Glass is the preferred material for inert reactor construction, and can be made at microscale to have a high pressure rating and fair heat transfer capacity as well. Unfortunately, glass has a rather rough surface and adsorption is therefore unavoidable when working with proteins. It is possible to work around this by using polyethylene glycol, or by working with an enzyme concentration that is high enough to make monolayer surface coverage insignificant. A semi-quantitative comparison of different materials is given in Table 3.8.

Table 3.8: Comparison of materials for construction of microreactors

	Chemical Resistance	Transparency for optical measurements	Heat transfer	Prototype cost	Mass produced device cost
Polymers (PDMA, PMMA)	Very Low	Good	Poor	Low	High
Hard Polymers (COP, COPF)	Low	Good	Medium	Medium	Low
Glass (SiO_2)	High	Very good	Good	High	Medium
Quartz (SiO_4)	High	Excellent	Good	Very high	Medium - High
Metal (steel)	High	N/A	Very good	Medium	Medium
Silicon	High	N/A	Good	Very high	Medium
Tubing (PTFE, Glass capillary)	High	PTFE is IR transparent, but pathlength is small	Good	Low-medium	Low

Based on the experience gained from working with microfluidics it has become clear that when experimental methods are established and experiments are to be reproduced hundreds of times it is suggested to apply microfluidic chip designs. This is exactly what Lab-on-a-chip has been about, i.e. scaling down analysis with a fixed method. When the method is being developed and while working with complex fluid dynamics (precise droplet flow, side by side flow) or extremely small volumes it is suggested to use 'standard' options from chip manufacturers. In general, for research purposes, it is desired to be as flexible as possible and unless it is required to have optical readout it is suggested to do experiments in tubing. In the latter approach, changing the length of the reactor is as simple as cutting a new piece of tubing.

A decision roadmap for when to use which technique or tool has previously been described, but this was in relation to organic chemistry where fast reactions and high temperatures and pressures are present [109,110]. The following paragraph will focus on describing where experiments should be conducted in relation to the specific goals of a project. Three different goals can be distinguished to categorize the different efforts, which are carried out in the course of biocatalytic process development, namely discovery, development/optimization and production. For biocatalyst discovery, testing is usually conducted in a binary form and for that reason the use of containers in parallel provides an easy accessible platform. In the biocatalyst development and optimization phase, it is very important to have proper control of the experimental conditions. Microfluidics as described in this chapter, displays these qualities along with small resource consumption. Well plates also have small resource consumption, but will to a lesser extent allow control over the reaction conditions. These methods require automation for efficient and precise handling of the small volumes. In such an automated set-up, samples are directly drawn from the reactors, be it wells or channels, and injected into the analysis system. Without this automated handling and analysis ability one should probably stick to working on a slightly larger scale, such as small vials (4 mL) in thermoshakers. For production is it obvious that the smaller type equipment will have problems handling very large scale throughputs. However, with microfluidics one of the major advantages is that one can set up systems in parallel, and numbering up can in this way generate a considerable throughput. The main elements of the discussion in this last paragraph have been summarized in Table 3.9.

Table 3.9: Considerations on when to use microfluidic technology

Goals	Labscale batch	Well plates	Labscale continous	microfluidic
Volume	>1 mL	<400 µL	>1mL	<1 mL
Discovery	Good	Good	Bad	Bad
Development and optimization	Fair	Good	Bad - Fair	Good +
Production	Fair	Bad	Good	Bad-fair

Chapter 4

Considerations for amine transaminase processes assisted by ISPR strategies

The following chapter has been written in the style of an article manuscript. The manuscript is to be submitted to the peer-reviewed scientific journal Biotechnology Advances.

Asymmetric synthesis of optically pure chiral amines using amine transaminases (ATAs) is a promising process pathway, starting from ketone substrates, towards valuable building blocks for many active pharmaceutical ingredients and their precursors. However, in many cases, it is necessary to overcome unfavorable thermodynamics and inhibitory effects, for example by implementing in-situ product (ISPR) and/or co-product (IScPR) removal strategies. Implementation of ISPR and IScPR strategies adds significant complexity to the process, which gives some challenges in evaluating the feasibility and potential gain related to applying such strategies. Therefore, this chapter reviews important considerations and requirements for the development of ATA processes with ISPR and IScPR strategies. A simple methodology is proposed to guide the selection and/or exclusion of ISPR/IScPR strategies, when required, during the development of ATA synthesis routes and processes. Furthermore, an overview is given of the most commonly applied ISPR and IScPR strategies for ATA processes and some of the associated challenges. Additionally, evaluation of the requirements of various, commonly applied, ISPR and IScPR strategies is provided based upon three case studies. The chosen ATA based case studies focus on the asymmetric synthesis of 1-methyl-3-phenylpropylamine (MPPA) from benzylacetone (BA) using three alternative amine donors, i.e. 1-phenylethylamine (PEA), isopropylamine (IPA) and alanine (Ala). The case studies represent various thermodynamic, inhibitory, and separation related challenges. Hence, they form a good basis for broad coverage of the requirements and feasibility of ISPR and IScPR strategies for amine transaminase processes. The case studies indicated that the choice of amine donor might improve the thermodynamics of the synthesis route and/or reduce inhibitory effects, but there can be tradeoffs in terms of the separation efficiency. For example, for the case study with PEA as the amine donor, implementation of ISPR was found unsuited because the separation was assessed as being difficult and non-selective. However, for the two other case studies, with IPA and Ala as amine donors, it was found feasible to implement an ISPR strategy based upon liquid-liquid extraction.

4.1 Introduction

One specific application of biocatalysis, which has received particular attention in recent years, is the production of optically pure chiral amines applying amine transaminases (ATAs) [111]. ATAs facilitate the transfer of an amine group from a primary amine to a carbonyl compound mediated by pyridoxal-5'-phosphate (PLP) [39,112]. Chiral amines are valuable building blocks for a vast number of pharmaceuticals and precursors [20,113,114]. The advantage of ATAs, is the potential of performing asymmetric synthesis of pure chiral amines with enantiomeric excess (e.e.) >99%, under mild reaction conditions [24,115]. Furthermore, ATA processes potentially use simplified process pathways, compared to conventional chemical synthesis [7,20,116]. Additionally, ATAs are not dependent on the use of scarce, valuable and potentially toxic metal catalysts [33], which are many times applied in chemical synthesis routes, and can only be accepted in very low concentrations in the final product [117].

Despite the advantageous features of ATAs for the synthesis of chiral amines, the number of industrial applications is still somewhat limited. The limited number of applications is the consequence of the fact that ATAs commonly experience toxic and/or inhibitory effects from substrates and/or products, especially at high concentrations. For some compounds, e.g. pharmaceuticals, there can also be problems with product degradation and/or stability issues [111,118,119]. Furthermore, for the synthesis of non-natural products from non-natural substrates it is often experienced that the reaction can be severely challenged thermodynamically [1,7,119].

All these factors make it difficult and time consuming to develop such biocatalytic processes and ensure economic feasibility. Hence, it is therefore necessary to invest significant effort in modifying the biocatalysts, e.g. by means of protein engineering. The tremendous developments and achievements in protein engineering strategies and techniques have indeed made it possible to develop biocatalysts for specific applications and requirements [7,120]. Improving the biocatalyst performance will always be done by modifying the biocatalyst and when considered necessary and beneficial, process engineering strategies are applied supplementary. Protein engineering is a powerful technology, which can greatly improve the biocatalyst performance, e.g. aiming at decreased inhibitory effects from reaction species, broadening the substrate scope and/or improving activity and stability [5,7,116].

Despite the great benefits of protein engineering, it is for example not always easy and fast to overcome severe inhibitory effects with that strategy. Moreover, protein engineering will only influence the performance of the biocatalyst and not directly influence reaction related issues, e.g. it will not have an influence on thermodynamics and/or product degradation. Particularly for such issues, it is required to consider various process engineering strategies, such as *in-situ* product (ISPR) or co-product removal (IScPR), which aim to reduce the influence of such limitations and optimize the productivity of the biocatalyst, ideally yielding intensified and economically viable processes [118,121,122]. ISPR/IScPR refers to removal of a product/co-product from the reaction mixture during the reaction course [5,121].

What is specifically investigated in this thesis, is the aspect of applying process engineering strategies, such as ISPR and IScPR, as complementary strategies to the modification of the biocatalyst. For ATA process applications, ISPR and IScPR are applied to overcome severe (co-)product inhibition and, to some extent, unfavorable thermodynamics. Highlighted here are important considerations for the planning and implementation of process engineering strategies, and technologies for biocatalytic process intensification. Therefore, a focused review of the currently applied ISPR and IScPR strategies for ATA processes is presented

here. Furthermore, general requirements for the ISPR and IScPR are highlighted and discussed. Moreover, three case studies will be discussed regarding the selection of ISPR/IScPR strategies and their respective case-specific limitations.

4.2 ISPR/IScPR requirements

The choice of ISPR and/or IScPR method(s), to overcome inhibitory and toxic effects, is based on removing the compound(s) of interest either through additional reaction steps or selectively by conventional separation methods during the course of reaction.

Additional reaction steps, e.g. multi-enzyme cascades (commonly applied as IScPR strategies), are challenging to implement and add significant complexity to the following product recovery steps. Conventional separation methods are driven by differences in pure component properties, such as solubility or volatility. Despite the increased process complexity, it is still considered beneficial to consider the possibility of implementing ISPR/IScPR strategies during the process development. For example, considering product recovery options and identifying separation limitations can be useful for setting development targets for the biocatalyst.

An overview of important separation metrics, useful for identifying the efficiency and the feasibility of ISPR/IScPR strategies, is reported. Moreover, an overview of commonly applied ISPR/IScPR strategies specifically for ATA applications is provided.

4.2.1 ISPR and IScPR separation metrics

The performance of ISPR and IScPR strategies can be reflected in how efficiently the chosen method/strategy removes the desired compound, product and/or co-product, from a given reaction mixture. Hence, it is necessary to characterize the performance firstly and then to evaluate the economic viability of a proposed process (before considering implementation). The chosen method/strategy can be characterized using some general separation metrics, i.e. selectivity, capacity, rate kinetics and stability.

Selectivity: This separation metric indicates how efficiently specific components are separated relative to all other components present in the reaction mixture. The selectivity, of any given ISPR and/or IScPR method, or for any given separation based downstream processing (DSP) method, is highly dependent on the physicochemical properties of the components in the reaction mixture. The selectivity of different separation methods can generally be estimated as the relative partitioning of each component between the original reaction mixture phase, e.g. aqueous, and the separating phase, e.g. organic solvent, resin or gas. This can mathematically be expressed by:

$$s_i = \frac{PC_i}{\sum_{i=1}^{n} PC_i} \quad \text{(Eq. 4.1)}$$

$$PC_i = \frac{[C_i]_{removed}}{[C_i]_{aq}} \quad \text{(Eq. 4.2)}$$

, where s_i[-] is the selectivity fraction, PC_i[-] is a unique partitioning coefficient for the ISPR method, both for component i, and n is the number of involved components in the mixture.

It is important to calculate the partitioning coefficients in a standardized way, in order to ensure objective comparison of various configurations and methods. Good separation, of the single components, is achieved with large partitioning coefficients, i.e. $PC_i \gg 1$. The selectivity metric can be useful to determine achievable product purity. At the same time, the selectivity can be used to identify the fraction of product which can be recovered and thereby give an indication about the permissible costs of the required product purification steps [123]. It is desired to achieve selectivity as close to unity as possible, i.e. $s_i \rightarrow 1$, and with good partitioning in order to achieve good product recovery.

Additionally, the selectivity can be applied to evaluate the potential impact of the given separation method on the reaction thermodynamics. For example, highly selective separation (close to unity) of the main product and/or co-product is a necessity to overcome unfavorable thermodynamics.

Removal rate kinetics: The removal rate kinetics is used to describe how fast it is possible to remove the desired reaction species. It is important to note that the separation method needs to be as fast as the reaction rate, or faster, so optimal process intensification is achieved with the chosen ISPR/IScPR method. Hence, it is ideal if the rate of reaction is the rate limiting step. If the rate of separation is the rate limiting step it will cause a build-up of inhibitory and/or unstable compounds and thereby the system will not operate optimally. Furthermore, when the rate of separation is the rate limiting step it will prolong the time it takes to shift unfavorable equilibria, and will thereby delay the time it takes to achieve sufficiently high yields. These effects are highlighted in Figure 4.1.

The rate of removal is related to the flux from the reaction phase into the separation phase, i.e. the rate of mass transfer. In addition to the capacity metric, the flux is dependent on the area of separation and thereby dictates the required size of the separation unit and thereby the related separation costs [123].

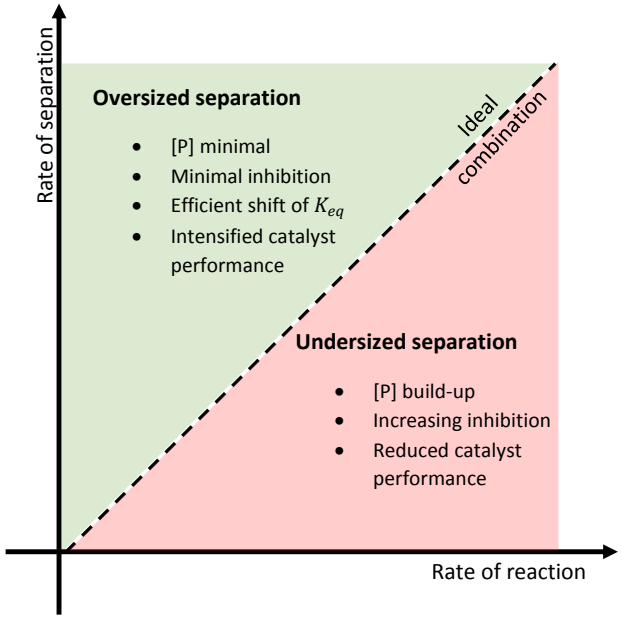

Figure 4.1: Process effects expressed in terms of rate limitations for the rate of separation relative to the rate of reaction.

Biocatalyst stability: Here, the biocatalyst stability is concerning the direct impact of the ISPR/IScPR method on the biocatalyst. For example, will the presence and/or interface to the ISPR/IScPR cause increased denaturation of the biocatalyst. The stability of the biocatalyst can be tested by comparing the initial activity of the biocatalyst to the remaining activity after timely exposure to the separation method at its process conditions. For example, biocatalysts are not always compatible with auxiliary phases such as gas and/or organic solvents, causing the biocatalyst activity to drastically decrease over a short period of time [7,116]. Therefore, testing how the ISPR/IScPR method influences the biocatalyst activity is important to know how to operate the process satisfactorily. Such knowledge will be useful for determining the implementation strategy (internal/external and direct/indirect), a topic which is discussed in detail in section 4.2.3.

Stability of separation: The stability of the actual ISPR/IScPR method is related to the performance consistency of the separation method over time, with a certain set of operating conditions, e.g. concentrations, fouling, temperature and pH. It is desired to have separation methods that are as stable, and consistent, as possible to reduce the costs related to maintaining a sufficient separation performance. The performance consistency can be determined as a measure of how easily the chosen separation method can be regenerated, i.e. loss of relative performance after regeneration.

Capacity: The capacity metric gives an indication of the required size of the separation method, in order to ensure sufficient component removal during operation. Hence, the capacity metric dictates how often it is required to regenerate and/or replace the media/material facilitating the separation. Thereby, it has a direct impact on the ISPR/IScPR implementation and reaction times. The capacity metric depends on the chosen separation methods. For example, the separation capacity of resins, i.e. solid-liquid extraction (SLE), can be measured as the total amount of product, which can be retained by a certain amount of resins.

The application of the proposed separation metrics in combination with thermodynamic and kinetic data on the biocatalyst performance, serves as the foundation for the evaluation of the economic feasibility of processes. Additionally, the metrics compose a powerful tool for identifying process bottlenecks, which hinder the economic feasibility for different process configurations. The specified metrics can be determined by characterizing the desired separation method. However, the characterization is highly dependent on the separation method, due to operating differences.

4.2.2 Identification of suitable ISPR/IScPR strategy

A considerable challenge for the implementation of ISPR/IScPR strategies is to identify and evaluate the most feasible process options. Firstly, it is necessary to identify the process limitations that need to be overcome, such as unfavorable thermodynamics, inhibition and/or product stability. Thereafter it is important to review the significant differences in pure component properties, in order to ensure selective separation, or the applicability of cascade reaction systems, which can be beneficial. In Figure 4.2, a methodology is proposed for the identification of suitable ISPR/IScPR strategies for ATA applications based on the experienced process limitations and differences in pure component properties, which is the driving force for the separation. This methodology is inspired by previously published work by De Wever et al. [124].

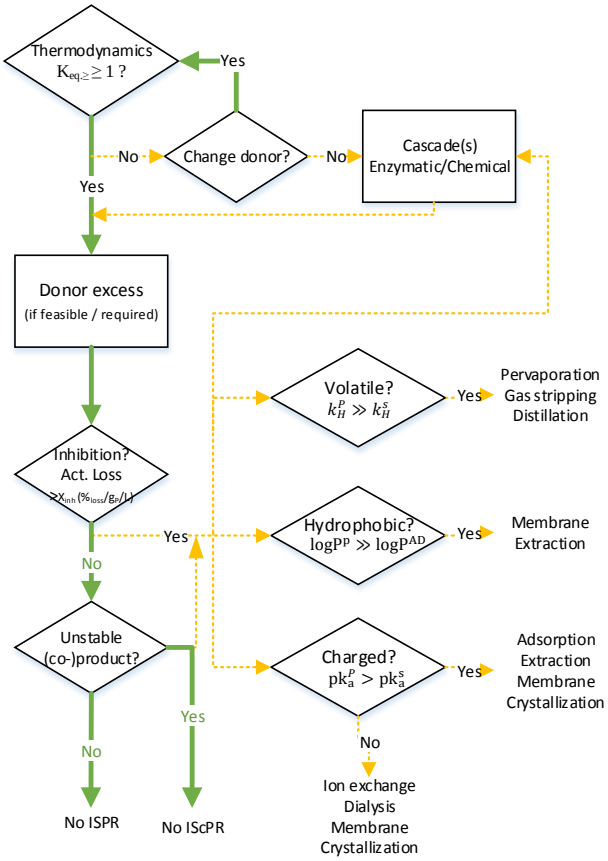

Figure 4.2: Methodology for identification of suitable ISPR/IScPR strategies for ATA based processes. The full lines indicate preferred process solutions. The dotted lines represent possible solutions when experiencing process limitations [124].

The main motivation for the implementation of ISPR and/or IScPR strategies, based on conventional separation methods, is to overcome inhibition from the product, co-product, and/or intermediates from cascade reaction systems.

In case of severe inhibition, it is useful to consider implementation of cascade reactions, but in many cases, it can be sufficient to implement strategies that are based upon conventional separation principles. Cascade reaction systems can only be used as ISPR when the product in the given reaction is an intermediate of the final product. If inhibition of the product and/or co-product composes a severe problem, and the thermodynamics is unfavorable, it could be very beneficial to operate with a low conversion in the reactor, if the separation step is implemented externally. Through this strategy, the inhibitory effects will be reduced. However, it requires efficient substrate and amine donor recycling, along with product separation and purification. Ultimately, it could be possible to operate the reaction under highly unfavorable thermodynamic conditions and hence avoid implementation of cascade reaction systems. A limitation to this recycle concept

is that it might not be possible and/or allowed by regulatory authorities for production of APIs, e.g. there can be risks of cross-contamination. Severe inhibition can be characterized as the loss in relative activity with increasing (co-)product titer. It is difficult to quantify the degree of inhibition a given process needs to experience, before ISPR/IScPR strategies need to be considered, as this decision is influenced by multiple correlated factors. Examples of such factors are: 1) The required remaining activity at the needed product titer (g_P/L) to ensure the space time yield (STY: g_P/L/h) of the reactor. 2) Dependent on the cost of the biocatalyst and the remaining activity at the desired product titer, it is the easiest solution to add additional biocatalyst if economically feasible. However, it is important to note that the required additional biocatalyst will increase exponentially with increasing inhibition.

For example, for pharmaceuticals it is advised to reach product titers in the range of 50 g_P/L [125] without compromising the required STY of the reactor. In such case, a theoretical inhibition scenario could be a requirement to maintain minimum 25% of the initial biocatalyst activity at 50 g_P/L to ensure the STY. It is assumed in this example that the cost associated with adding additional biocatalyst cannot be economically justified. For this specific scenario, it could be justified to implement ISPR/IScPR options if the loss of initial activity of the given biocatalyst is greater than X_{inh} = 1.5 $\%_{loss}/g_P$/L. For fine chemicals and bulk chemicals it is commonly advised to operate with even higher product titers than 100 g_P/L and 200 g_P/L, respectively, which would make this constraint even tougher [125]. In Figure 4.3, an overview is given on how the loss of relative initial activity, due to inhibition, will influence the constraint X_{inh} ($\%_{loss}/g_P$/L) for when to consider implementation of ISPR/IScPR strategies. This form of calculation is useful early in the process development to identify if the experienced inhibition makes it suitable to consider ISPR/IScPR options. As more knowledge is acquired, it is possible to develop and apply more sophisticated and reliable models and economic evaluations to specify the thresholds.

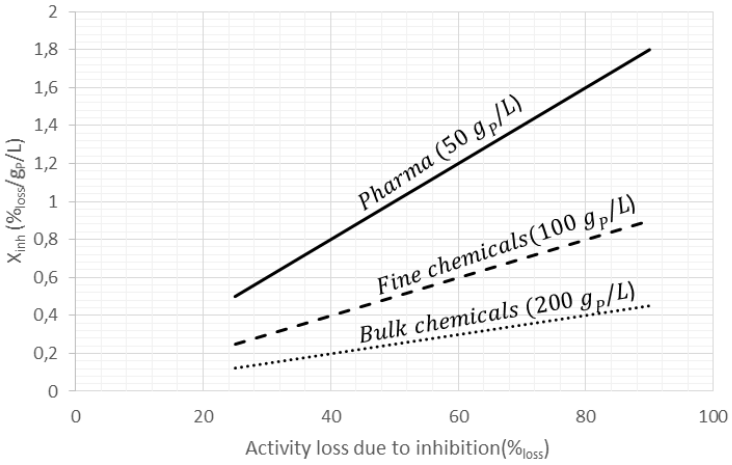

Figure 4.3: Overview on how the loss of relative initial activity, due to inhibition, will influence the constraint for when ISPR/IScPR methods should be considered ($\%_{loss}/g_P$/L). It is assumed that the cost associated with adding additional biocatalyst cannot be economically justified.

In cases where stability of the product is a reason of concern, ISPR strategies can be advantageous in order to stabilize the product and thereby ensure improved recovery yields. If the co-product is unstable, and the formed compound(s) does not intervene in any way with the main reaction, there is no rationale to implement IScPR options.

In cases where it is found suitable and beneficial to implement an ISPR/IScPR strategy it is common to exploit differences in physicochemical properties, i.e. volatility, hydrophobicity and charge or a combination of the three. Alternatively, implementation of cascade reaction systems is considered. Volatility differences are only applicable when the (co-)product is significantly more volatile than the substrate and amine donor, i.e. $k_H^P \gg k_H^S$, $T_b^P \ll T_b^S$ and $P_{vap}^P \gg P_{vap}^S$, and when no azeotropes are formed. Hydrophobic differences are exploitable either when the substrate and amine donor are hydrophilic or have small partition coefficients ($logP$) relative to the hydrophobic (co-)product, i.e. $logP^{AD} < 1$ and $logP^P > 1$ and/or $logP^{AD} \ll logP^P$. However, it is common that the main substrate for ATA reactions is hydrophobic and has low aqueous solubility, which makes it difficult to achieve selective product removal unless the separation is combined with charge differences simultaneously (the ketones are not charged, while the amines can be charged at various pH values). Differences in the charge can be exploited when there is a significant difference in the acid dissociation constant (pK_a) of the pure components, e.g. $\Delta pK_a > 1$. And dependent on whether the pK_a of the (co-)product is larger or lower than that of the amine donor then separation processes based on either hydrophobicity or charge, respectively, will be applied.

As highlighted, unfavorable thermodynamics ($K_{eq} < 1$) can mostly be overcome by implementation of a cascade reaction system, which is highly selective and operates efficiently at low concentrations. If the cascade reaction system is not sufficient to shift the equilibrium, or if it is too costly, then the investigated reaction route may potentially only be useful for dynamic kinetic resolution and not asymmetric synthesis. However, when having semi-unfavorable to semi-favorable thermodynamics ($K_{eq} \geq 1$), implementing cascade systems adds significant complexity to the process and greatly increases the complexity of DSP. Therefore, in such cases, if economically feasible, it may be easier to either apply an excess of the amine donor, implement a conventional separation process or a combination of the two. Implementation of a conventional separation method will also add complexity to the process, but not to the same extent as with cascade reaction systems that will make the DSP more complex. However, conventional separation methods are not as selective as cascade reaction systems and for that reason not suited to shift highly unfavorable thermodynamics (this is explained based on basic calculations in the supplementary material). Currently, having an excess of the amine donor is considered the easiest strategy to shift the equilibrium and overcome thermodynamic limitations [24]. However, limitations to this approach are potential inhibitory effects and the cost contribution from the amine donor.

Conceptually, conventional separation methods can also be used to shift highly unfavorable thermodynamics. However, conventional separation methods are in general not as selective, and therefore not as efficient, as enzymatic cascade systems. Therefore, in cases where it is required to shift unfavorable thermodynamics the choice of ISPR/IScPR will in most cases be based on implementation of a cascade reaction, which is further underlined in section 4.4. In appendix B, results are shown indicating the maximum allowable (co-)product concentrations in the reaction mixture if the equilibrium is to be shifted sufficiently. In the methodology, shown in Figure 4.2, it is specified that for $K_{eq} < 1$ it is required to either consider replacing the amine donor or implement a cascade reaction to shift the equilibrium efficiently. This is defined

based on the required amine donor excess to achieve high conversion (>90%), without implementation of ISPR/IScPR options, at various reaction equilibrium constants. It is assumed that a donor excess of 10 is the maximum feasible for any given donor [126] (there might be rare cases where it is suitable to apply a larger excess). The reaction equilibrium constant, K_{eq}, represents the change in Gibbs free energy of formation, ΔG. The equilibrium concentrations can be calculated as shown in equation 4.4 following the general transaminase reaction scheme presented in equation 4.3 [24].

$$S + AD \rightleftarrows P + cP \qquad \text{(Eq. 4.3)}$$

$$K_{eq} = e^{-\Delta G^{\circ}/RT} = \frac{[P][cP]}{[S][AD]} \qquad \text{(Eq. 4.4)}$$

, where R (8.31 $J \cdot K^{-1} \cdot mol^{-1}$) is the ideal gas constant, T (K) the absolute temperature, [S] (M) the substrate concentration, [AD] (M) the amine donor concentration, [cP] (M) the co-product concentration and [P] (M) the product concentration.

Based on the presented definitions, it is possible to calculate the required excess of the amine donor to achieve a certain degree of conversion at various reaction equilibria scenarios, which is shown in Figure 4.4

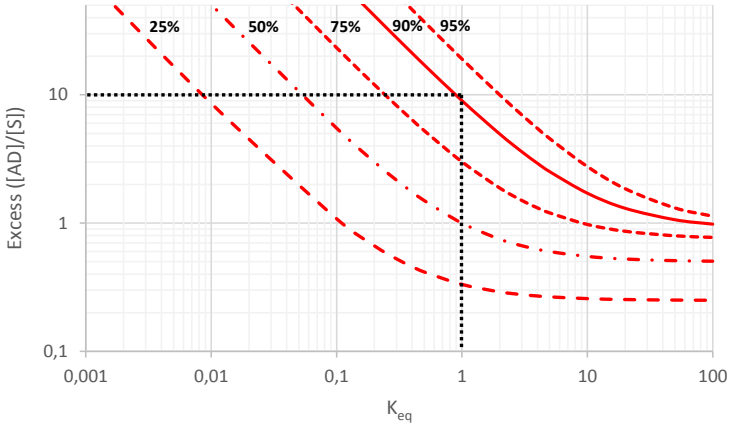

Figure 4.4: Required donor excess to reach various degrees of conversion for a range of equilibrium constants for ATA processes. The vertical dashed line represents the region of different reaction equilibria, from where it is considered suitable to apply an amine donor excess [24].

Alternatively, if the separation and recycling of the main substrate ([S]) (and/or amine donor ([AD])) is possible, a feasible process could consist of recycling the substrate rather than trying to achieve high conversion in one step. If it is possible to efficiently recycle the amine donor, it will be possible to use a larger excess and still have an efficient and economically feasible process. For pharma applications, it might not be possible to apply such recycle strategies as there is increased risk of cross-contamination and build-up of impurities. Alternatively, the replacement of the amine donor with a stronger donor will potentially make it

possible to achieve more favorable reaction thermodynamics and overcome some challenges in this way [127,128].

4.2.3 Implementation strategies

The implementation of IPSR/IScPR methods is not straightforward and several implementation strategies need to be considered. Two main points should be considered: (i) whether the separation should occur internally or externally of the reactor; and, (ii) whether the separation should be directly or indirectly in contact with the biocatalyst [119,122,129,130]. It is a complex decision procedure and as an example there can be cases, where one is confronted with compatibility concerns between the separation method and the biocatalyst. Furthermore, the separation/implementation strategy may be limited to equipment availability and flexibility. Identifying a suitable implementation strategy will potentially make it possible to significantly reduce harmful effects from the separation method on the biocatalyst. When compatibility issues between the biocatalyst and the separation method are of concern, having the biocatalyst indirectly in contact with the separation is potentially less harmful than having direct contact. Table 4.1 presents an overview of the potential advantages and disadvantages of the mentioned implementation strategies [119,121,122,129,131,132].

Table 4.1: Overview of the prospects of considering implementation of ISPR/IScPR strategies into biocatalytic processes.

Implementation strategies		Advantages	Disadvantages
Internal – direct	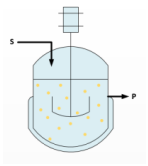	• Simple construction • Good operational control • Multi-phase operation	• Complex system modelling • Difficult recycling • Difficult separation control • Biocatalyst compatibility
Internal – indirect	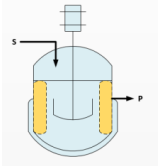	• Biocatalyst compatibility • Improved separation control • Possibility of recycling	• Dedicated construction • Complex reactor module • Complex system modelling • Difficult operational control
External – direct	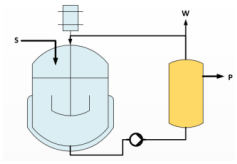	• Simple construction • Good separation control • Good operational control • Possibility of recycling	• Additional equipment (CAPEX increase) • Biocatalyst compatibility • Complex system modeling
External - indirect	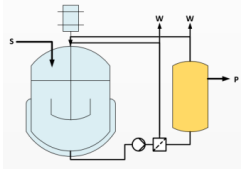	• Simple construction • Simple system modelling • Biocatalyst compatibility • Good separation control • Good operational control • Possibility of recycling	• Additional equipment (CAPEX increase)

Factors such as biocompatibility and reactor configuration limitations significantly influence the selection of the implementation strategy. In addition, the implementation of process engineering strategies will cause significant additional costs, operational expenses (OPEX) and in some cases capital expenses (CAPEX). For example, retrofitting conventional flexible equipment might be a relatively cheap solution, but it comes as a tradeoff to the flexibility. It might therefore be a better option not to consider dedicated equipment. Instead, it might be better to have flexible modular equipment where it is possible to operate various ISPR/IScPR methods directly connected with the reactor, without significant additional modifications, and/or by combining the reactor with modular separation units.

4.2.3 Commonly applied ISPR/IScPR strategies for amine transaminases

There are numerous examples of different applications where ISPR and/or IScPR strategies have been applied [129,130]. However, for ATA processes the investigated types of ISPR/IScPR strategies are rather limited. The applied ISPR/IScPR strategies for ATA processes are generally based upon a few conventional separation methods and cascade reactions. Table 4.2 provides an overview of ISPR/IScPR strategies based on conventional separation methods, whereas Table 4.3 provides a summary of ISPR/IScPR strategies based on the implementation of cascade reactions. Using ISPR/IScPR strategies for transaminases has as main goal to overcome unfavorable thermodynamics and to reduce inhibitory effects from either the co-product or product. Commonly, the investigated options focus on the internal configuration of the reactor in direct contact with the biocatalyst, with few exceptions. Furthermore, most scientific literature applies one of three very specific amine donors, i.e. alanine (Ala), isopropylamine (IPA) and 1-phenylethylamine (PEA). ISPR/IScPR strategies based on conventional separation methods are mostly based on hydrophobicity, volatility, and charge differences.

Table 4.2: Examples of conventional separation methods applied for ISPR and IScPR in amine transaminase (ATA) processes.

Tech.	Driving force	Specification	Rationale	Amine donor	Removed compound	Comments	Ref.
SLE	Charge	Ion exchange resins	$[P]_I$	Ala	MBA	Issue with amine selectivity	[133]
		Hydrophobic polymeric resins	$[cP]_I$	MBA	ACP	Issues with selectivity and loading capacity	[134]
Evaporation	Volatility	N_2 carrier (H_2O sat.)	Eq.	IPA	Ace	Issues of foaming and selectivity	[135]
		Vacuum	$[cP]_I$	MBA	ACP	Issue of water removal	[134]
		Vacuum	$[cP]_I$	Pyr[1)]	2-butanone	Issue of water removal	[136]
LLE	Hydrophobicity	Multiple solvents	$[cP]_I$	MBA	ACP	Issue of catalyst and solvent compatibility.	[137]
		Toluene	$[cP]_I$	MBA	ACP	-	[31]
		Isooctane	$[cP]_I$	MBA	ACP	Issue of interfacial inactivation	[138]
		Cyclohexanone	$[P]_I$	Pyr[1)]	ACP	Issue of catalyst and solvent compatibility	[139,140]
		Isooctane	$[P]_I$	Ala	MBA	Issue of selectivity	[141]
Membrane	Hydrophobicity	Membrane contactors[2)]	$[P]_I$	Pyr[1)]	ACP	Membrane to avoid emulsions with isooctane	[142]
		Hollow fiber membrane contactor[2)]	Eq.	IPA	MBA + Ace	Undecane as solvent support, issue of selectivity	[143]
		Hollow fiber membrane contactor[2)]	Eq. +$[P]_I$	Ala	Pyr + MPPA	Issue of pH stability and substrate extraction	[144]

Ala: alanine, MBA: 1-phenylethylamine (PEA) also known as methylbenzylamine, IPA: isopropylamine, ACP: Acetophenone, MPPA: 1-methyl-3-phenylpropylamine, Eq.: shift equilibrium, $[cP]_I$: overcome inhibitory effects from co-product, $[P]_I$: overcome inhibitory effects from product, SLE: Solid-Liquid extraction, LLE: Liquid-Liquid extraction. 1) Based on dynamic kinetic resolution using pyruvate as the substrate for deracemization. 2) Implemented externally of the reactor and in indirect contact with the catalyst

Table 4.3: Examples of cascade reactions applied for ISPR and IScPR in amine transaminase (ATA) processes.

Technology		Driving force	Specification	Rationale	Amine donor	Removed compound	Comments	Ref.
Cascade:	**Chemical**	Reaction selectivity	Spontaneous cyclisation	$[P]_I$ + Eq.	IPA	6-methyl-2-piperidone	-	[133]
			Spontaneous cyclisation	Eq.	Ala	2,6-disubstituted piperidines	-	[145,146]
			Spontaneous tautomerization	Eq.	*	3-hydroxybenzoic acid	Expensive amine donor	[147,148]
	Biocatalytic	Reaction selectivity	ADH/GDH	$[cP]_I$	MBA	Acetophenone	A), B), C)	[134]
			ADH/GDH	Eq.	IPA	Acetone	A), B)	[148]
			LDH/GDH	Eq.	Ala	Pyruvate	A), B), C)	[46,133,148–150]
			AlaDH/FDH or GDH	Eq.	Ala	Pyruvate	A), B), E)	[145,146,148,150,151]
			PDC	Eq.	Ala	Pyruvate	C), D), E)	[148]
			ALS	$[cP]_I$	Ala	Pyruvate	E)	[141]

LDH: Lactate dehydrogenase. GDH: Glucose dehydrogenase. ADH: Alcohol dehydrogenase. FDH: Formate dehydrogenase. AlaDH: Alanine dehydrogenase. PDC: Pyruvate decarboxylase. ALS: Acetolactate synthase. Ala: alanine, MBA: 1-phenylethylamine (PEA) also known as methylbenzylamine, IPA: isopropylamine, ACP: Acetophenone, Eq.: shift equilibrium, $[cP]_I$: overcome inhibitory effects from co-product, $[P]_I$: overcome inhibitory effects from product. *: 3-aminocyclohexa-1,5-dienecarboxylic acid. A) Gluconic acid formation might require pH control, B) Co-factor recycle required, C) Inhibition of new intermediates might be a problem, however inhibitory pyruvate removed simultaneously, D) Side reactions might occur, i.e. reaction selectivity is a problem, E) CO_2 formation may require pH control

4.3 Case studies

In this work, some remarks for the implementation of ISPR and IScPR strategies will be highlighted through three case studies. The case studies investigate how the choice of amine donor influences the rationale for implementation of ISPR or IScPR strategies for a specific reaction using transaminases. The investigated reaction is the asymmetric synthesis of the chiral amine 1-methyl-3-phenylpropylamine (MPPA) from benzylacetone (BA), using three commonly applied amine donors, i.e. 1-phenylethylamine (PEA), isopropylamine (IPA) and alanine (Ala). The general reaction schemes of the case studies are illustrated in Scheme 4.1.

CS	Substrate	Amine donor	Product	Co-product	K_{eq}
1	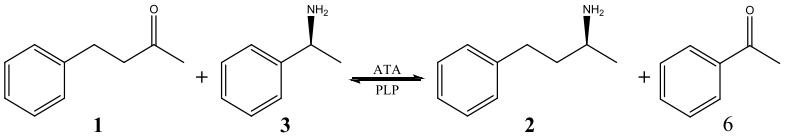				$\approx 15.1 - 22.2$
2	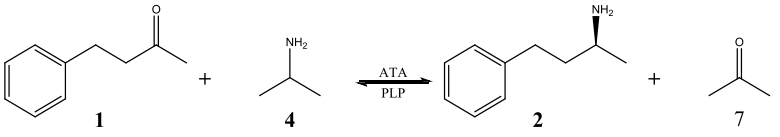				≈ 0.74
3	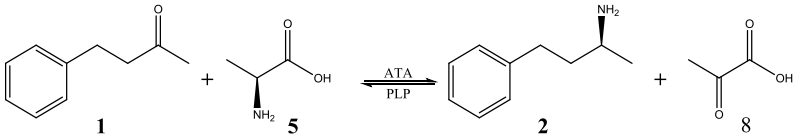				$\approx 6.1 \cdot 10^{-4}$

Scheme 4.1: The general reaction schemes for the three case studies (CS) and the apparent equilibrium constants reported by Tufvesson and co-workers [152]*. The case studies evolve around the transamination of benzylacetone (BA)(**1**) to 1-methyl-3-phenylpropylamine (MPPA)(**2**) using three different amine donors. The chosen amine donors are 1-phenylethylamine (PEA)(**3**), isopropylamine (IPA)(**4**), and alanine (Ala)(**5**). These amine donors give cause to the formation of the co-products acetophenone (ACP)(**6**), acetone (Ace)(**7**), and pyruvate (pyr)(**8**), respectively.*

Each of the case studies imposes various process challenges, e.g. solubility issues, thermodynamic issues, inhibition and separation difficulties, which motivates to investigate the possibility of implementing ISPR/IScPR options. Conventional separation methods are relatively fast and easy to put in place, which makes them a good choice for overcoming inhibitory effects. Application of conventional separation methods is also very useful because the final product has to be recovered at some point.

Presently, no scientific literature indicating these compounds to be unstable has been discovered, and therefore the discussion of the three case studies will purely be based on the parts of the methodology (Figure 4.2) concerning thermodynamics and inhibition. Tufvesson et al. [152] have experimentally identified equilibrium constants for two of the cases studies, i.e. for the IPA based case study ($K_{eq} = 0.74$) and for the Ala based case study ($K_{eq} = 6.1 \cdot 10^{-4}$). Tufvesson et al. did not experimentally investigate the case study with PEA as the amine donor. However, PEA is a strong amine donor, and it should be reasonable to assume that the reaction equilibrium is somewhat favorable [126]. Also, based on the determined equilibrium

constants by Tufvesson et al. it is possible to calculate the apparent equilibrium constant, i.e. $K_{eq} = [15.1: 22.2]$ [152]. The pure component properties of the involved reaction species are highlighted in Table 4.4. This data, found in the Chemspider database, will be referred to throughout the case studies when referring to the driving force of potentially feasible ISPR/IScPR strategies [153].

Table 4.4: Pure component properties of the reaction species involved in the case studies [153].

COMPOUNDS	BA (1)	MPPA (2)	PEA (3)	ACP (6)	IPA (4)	ACE (7)	ALA (5)	PYR (8)
-	Substrate	Product	Case study 1		Case study 2		Case study 3	
CAS. NO.	2550-26-7	22374-89-6	618-36-0	98-86-2	75-31-0	67-64-1	302-72-7	127-17-3
$M_w\left(\frac{g}{mol}\right)$	148.2	149.2	121.2	120.2	59.1	58.08	89.09	88.06
T_b (℃)	235-237	220-222	183.0	202	33-34	56	-	165
$log\ P\ (-)$	1.671	2.18±0.20	1.3	1.58	0.21±0.19	-0.16±0.19	-0.679	-1.24±0.39
$Solubility\ (aq.)\left(\frac{g}{L}\right)$	1.625	12.05	54.38	4.484	Miscible	Miscible	164	High
$pKa*$	-	10.63	9.83	-	10.6		2.35/9.69	2.5
$P_{vap}(mmHg\ 25℃)$	0.1±0.4	0.1±0.4	0.8±0.3	0.3±0.4	460	180	0.1±0.9	1.0±0.6
$k_H\left(\frac{atm \cdot m^3}{mol}\right)$	1.2-7.8· 10^{-6}	0.1-1.4· 10^{-6}	0.8-1.6· 10^{-6}	1.0· 10^{-5}	4.5· 10^{-5}	4.0· 10^{-5}	1.5· 10^{-9}	3.2· 10^{-9}

A common challenge for the chosen case studies is the low aqueous solubility of the main substrate BA, which gives some challenges to achieve high space time yields ($g_P/L/hrs$). This can be overcome by improving the solubility by using an alternative reaction medium than water, which will also influence the biocatalyst performance and stability. Alternatively, an efficient substrate feeding strategy can be put in place. Furthermore, the low solubility of BA in aqueous media gives some restriction with respect to how low concentrations the desired ISPR/IScPR method should be able to achieve if the equilibrium is to be shifted. Using equation 4.4, it is possible to calculate how low product or co-product concentrations are required to achieve sufficient conversion. The results from these calculations can be found in the supporting material. Based on these calculations, it is clear that cascade reactions, which are commonly highly selective and capable of operating at very low concentrations, form a better choice for shifting unfavorable thermodynamics, especially when operating with compounds of low solubility. Increasing the solubility or applying an excess of the amine donor will make it possible to apply conventional separation methods, but it requires extensive modification of the biocatalyst.

4.3.1 Case study 1: 1-Phenylethylamine

This case study involves the formation of MPPA from BA using PEA as the amine donor. Applying a racemic mixture of PEA will enable simultaneous asymmetric synthesis of MPPA and dynamic kinetic resolution of PEA. This will potentially yield two valuable pure chiral products, which theoretically is very appealing. Furthermore, it is desirable to apply a racemic mixture of PEA as it is significantly cheaper than applying the pure chiral compound as amine donor [126]. However, it requires the correct enantiomer of the amine donor to be completely converted by the biocatalyst, i.e. >99% conversion, and no amine donor excess can be applied. Therefore, ISPR or IScPR are not suitable for this reaction route, as it needs to go to completion for the separation to be feasible.

The favorable thermodynamics of the reaction, i.e. $K_{eq} = 15.1 - 22.2$ [152], will enable relatively good yields without using excess of the amine donor. This will potentially enable to operate the process with

ISPR/IScPR. However, based on the pure component properties it appears that the separation of these amines and ketones is somewhat challenging making this process challenging and even more so to operate with ISPR/IScPR. The pure component properties listed in Table 4.4 for the components involved appear very similar, which makes the selective separation of the amine and ketone products very difficult and costly. The separation of the amines from the ketones will be relatively easy, as the amines become charged at a pH below the pK_a values, while the ketones remain unchanged. This result in the possibility of applying separation methods based on either charge or hydrophobic differences, such as ion exchange or hydrophobic resins.

Nevertheless, the separation of the two ketones in order to, simultaneously, recycle the main substrate BA, does not seem feasible. Regarding the separation of the two amines, there is a small difference between the pK_a values, which can be useful for separation purposes. Using the Henderson-Hasselbalch equation (equation 4.5), it is possible to predict the distribution of charged and uncharged amine, for each one of the amine compounds, at various pH set points.

$$pH = pK_a + log\frac{[A^-]}{[HA]} \qquad \text{(Eq. 4.5)}$$

The fraction of uncharged molecules of the two amines (PEA and MPPA) is presented in Figure 4.5 at several pH set points.

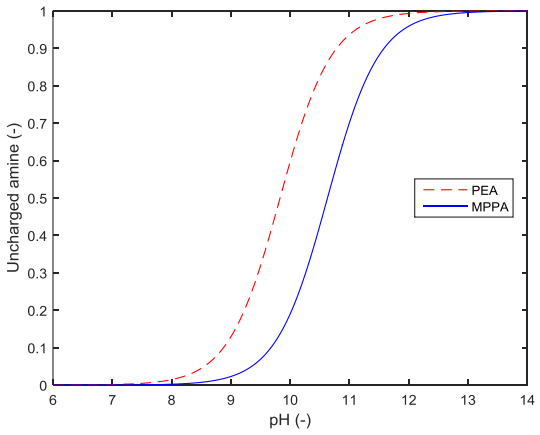

Figure 4.5: Fractions of charged and uncharged molecules at various pH values for the two amine products, i.e. MPPA and PEA.

Figure 4.5 indicates that operating at a pH in the range of 8.5-10, will give a significant difference between charged and uncharged amine fractions for the two compounds. This will potentially make it possible to separate the compounds by extracting the uncharged compound, e.g. using liquid-liquid extraction. However, MPPA is more hydrophobic than PEA which will have significant influence on the selectivity of the separation. Ion exchange might be useful at pH set points above 11, where PEA will mainly be uncharged and a small fraction of MPPA will remain charged. Another possibility for separation of the two amines would be

distillation, which is energy intensive, as there is a significant difference in the boiling points ($\Delta T_b \approx 40$°C). Alternatively, chromatography could be applied to efficiently separate the two compounds, but this is also costly and will only be a possibility if justified by the value of the two pure chiral products. Moreover, the involved reaction species are known to be inhibitory, which means that the reaction will have to operate at relatively diluted conditions to avoid severe inhibition, unless a suitable catalyst is developed. Hence, achieving sufficient space-time-yields and product titers for this system would be severely challenging to the economic viability of the process.

Application of a racemic mixture of an amine donor to perform asymmetric synthesis in combination with dynamic kinetic resolution has great potential theoretically. However, the feasibility is highly dependent on how easy it is to separate the two amine products, and on the extent of product and co-product inhibition. In this case, there were no significant differences between the amine products, making it difficult to achieve good separation selectivity. Nonethless, the application of racemic PEA does not appear feasible for the production of MPPA with or without ISPR/IScPR strategies. Potentially it may be suitable for the sytnthesis and purification of valuable amino acids and/or other amines.

4.3.2 Case study 2: Isopropylamine (IPA)

This case study involves the formation of MPPA from BA using IPA as the amine donor. IPA is an achiral amine donor and hence not dependent on whether the used biocatalyst is R- or S- selective. This case study involves slightly unfavorable thermodynamics, i.e. $K_{eq} = 0.74$ [152], which will require either implementation of an ISPR/IScPR strategy, application of an excess of IPA or a combination of the two to achieve a sufficient degree of conversion. Furthermore, in the case that the produced MPPA and/or acetone give cause to significant inhibition and/or toxic effects it will be beneficial to implement an ISPR/IScPR strategy. IPA is considered an inexpensive amine donor making it possible to apply a relatively large excess [126]. This will at the same time ease the separation requirements of the ISPR/IScPR method(s) in order to achieve sufficient conversion. In Figure 4.6, it is shown how the application of an excess of the amine donor will influence the requirements for minimum allowable product or co-product concentration as a complement to the amine donor excess to shift the reaction equilibrium. The calculations are based upon equation 4.4, assuming $K_{eq} = 0.74$ and an initial BA (**1**) concentration of 10 mM (close to the solubility limit).

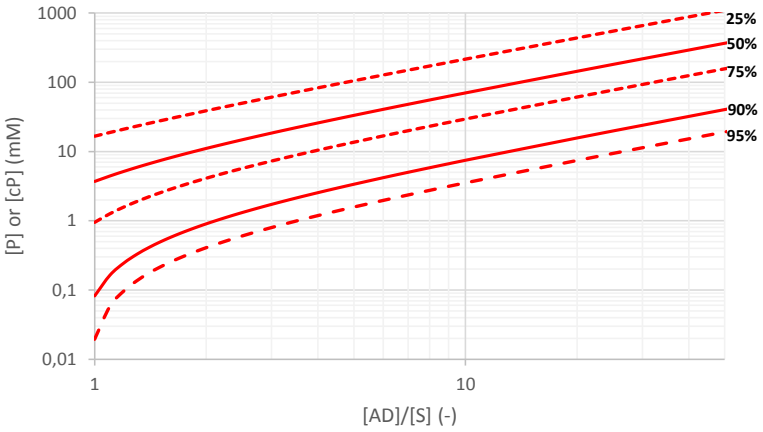

Figure 4.6: Degrees of conversion expressed by the relation between minimum allowable product ([P]) and/or co-product ([cP]) concentrations and various amine donor to substrate excess ratios ([AD]/[S]), for an initial substrate concentation of 10 mM BA.

An alternative or supplement to applying an amine donor excess, in order to loosen the requirements for product and co-product separation to achieve high conversion, is to increase the solubility of the main substrate by modifying the reaction medium. However, using an alternative reaction medium, to increase the substrate solubility, will influence the catalyst performance as well. Overall, using an excess of the amine donor, within a feasible ratio, and increasing the substrate solubility is very useful for achieving relatively high yields, i.e. shift the equilibrium, and product titers. However, potential issues of inhibition and/or toxic effects from the substrate and the amine donor will limit the impact of these strategies. In addition, none of these strategies will aid in overcoming inhibitory effects from the products. In case of severe inhibitory effects from the product(s) implementation of an IPSR or IScPR strategy needs to be considered, supplementary to modifying the biocatalyst. Tremendous progress in protein engineering strategies has indeed made it possible to significantly improve the biocatalyst performance and ultimately overcome product inhibition and toxic effects [7]. However, protein engineering is not a guarantee that product inhibition and toxcicity will be overcome and the time it takes to overcome these factors is unknown. Therfore, in case of severe inhibition and/or toxic effects it may be less of a risk and faster to consider implementation of ISPR/IScPR strategies based on well-known and developed conventional separation methods.

For this specific reaction system it is adding considerable complexity and cost to the process by implementing cascade reaction based IScPR strategies to overcome inhibition. Moreover, the pure component physicochemical properties highlighted in table 4 indicate that it might be suitable, less complex and faster to put in place an ISPR/IScPR strategy based on conventional separation methods. The main differences in the pure component properties relates to the volatility, where IPA and acetone are quite volatile compared to BA and MPPA. Implementation of IScPR based on removing acetone during the reaction course via stripping is an easy way to overcome significant inhibitory effects. Also, this strategy of continuously removing acetone has been attempted quite extensively to shift the equilibrium [135]. However, this separation method is not particularly selective and significant amounts of the other reaction species, especially IPA which is also volatile, are lost simultaneously causing this method to be very challenged

economically [135]. An alternative could be to apply membranes to perform pervaporation, which would be more selective to some extent.

Another useful feature of this reaction system is the hydrophobic nature of MPPA compared to IPA, making it possible to implement a somewhat selective ISPR strategy based on extraction, e.g. hydrophobic resins or liquid-liquid extraction. However, BA is also hydrophobic and will be removed simultaneously [144], and therefore will require the introduction of a recycling strategy of BA for this ISPR strategy to be feasible.

In Figure 4.7 an ISPR strategy, two-step liquid-liquid extraction (LLE), is proposed for this case study which enables simultaneous feeding of the substrate whilst allowing for product separation through the LLE steps. The suggested ISPR configuration should be generally applicable for ATA processes as long as the amine product is hydrophobic and the amine donor is hydrophilic. The ISPR strategy can either be operated based on the supported liquid-membrane concept [143,144] and/or in more flexible equipment in the form of a system with two coupled hydrophobic membranes or as two mixers and settlers. The main benefit of the supported liquid-membrane is the response time of the extraction due to the low overall volume of the solvent in the system. However, there might be some operational challenges of maintaining the solvent in the membrane and limitations to the quantity of BA, which can be loaded into the membrane modules during operation and/or the need to feed BA in another way. The main drawback of operating the system with mixers and settlers or the hydrophobic membranes is the required solvent volume, which will cause long system response times and increased losses of the main substrate and product in the solvent. Independent on how the proposed configuration is operated, it is conceptually possible to achieve significant upconcentration of the product leaving the reactor module [154–156], with a good recovery [157], high product titers and high product purity in the outgoing stream [143,144,158].

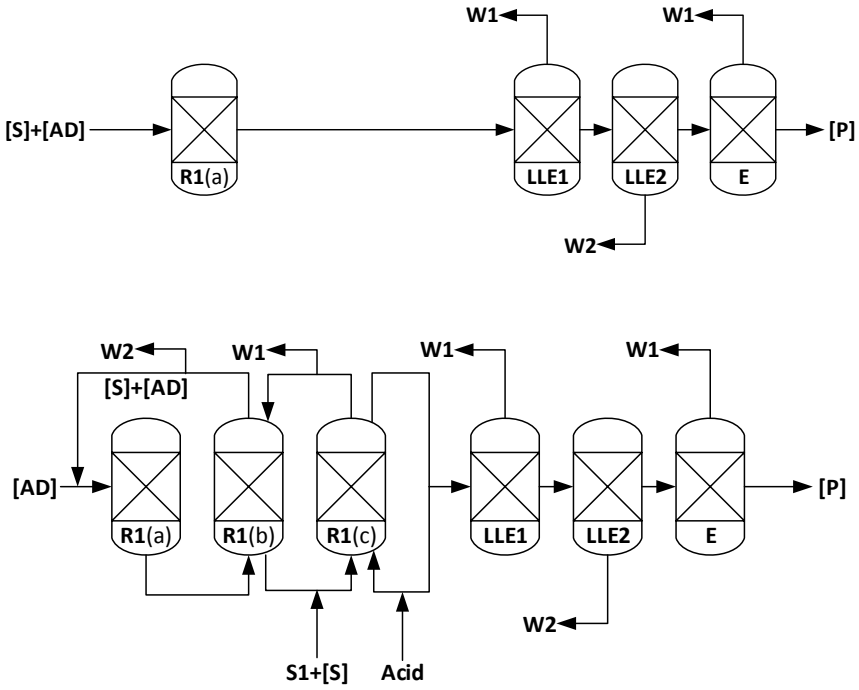

Figure 4.7: The top figure indicates the general flow chart for the synthesis and recovery of chiral amines proposed by Tufvesson et al. [126]*. The bottom figure indicates the suggested ISPR configuration with a two-step liquid-liquid extraction (LLE), which can be operated as a supported liquid membrane, either by using two hydrophobic membrane contactors in combination or as two coupled mixers and settlers. R1(a): Reactor module with catalyst (Immobilized or free – if free it may be required to isolate the catalyst before the 1st extraction step), R1(b): 1st Extraction step at pH close to amine pK_a, R1(c): 2nd extraction step at low pH, solvent with main substrate is recycled, LLE1: ketone substrate in the product stream is extracted at low pH, LLE2: amine is extracted at $pH > pK_a$, E: Solvent is evaporated to achieve high purity amine product (alternatively precipitation might be applicable), W1: solvent waste for incineration and W2: aqueous waste*

4.3.3 Case study 3: Alanine

This case study involves the formation of MPPA from BA using alanine as the amine donor (case study 3 shown in Scheme 4.1). A challenge for this case study is the highly unfavorable thermodynamics, i.e. $K_{eq} = 6.1 \cdot 10^{-4}$ [152], which will require ISPR/IScPR strategies with a very strong driving force, i.e. cascade reaction systems, to shift the reaction equilibrium sufficiently and ensure good conversion. For example, calculating the conversion using equivalent amounts of the amine donor and BA initially (10 mM) it would require the product/co-product concentration to be in the range of about 0.01 mM to achieve 25% conversion and 0.01 µM to achieve 95% conversion for batch operation (based on equation 4.4 and the highlighted K_{eq}). Achieving sufficient selectivity and operating at very low concentrations, to achieve good conversion, will be extremely challenging and maybe even impossible with conventional separation methods. Hence implementation of a highly selective cascade reaction system that is efficient at low concentrations is currently the most feasible solution. This is also strongly indicated in Table 4.2 and Table 4.3 where most

applications involving alanine consider the implementation of a cascade reaction system. If it is not feasible to implement a cascade reaction system, this reaction route with alanine might only be feasible for performing dynamic kinetic resolution instead of asymmetric synthesis. Using an excess of the amine donor is not realistic for this case study due to the highly unfavorable reaction equilibrium.

In case of strong inhibitory effects of MPPA it will potentially be required to implement a supplementary ISPR strategy. For this case study there is a significant difference in the hydrophobicity of the amines, i.e. MPPA is hydrophobic and alanine is hydrophilic making it possible to ensure selective separation of the two amines, e.g by means of hydrophobic resins or liquid-liquid extraction. However, similar to case study 2, this case study also faces the issue of having simultaneous removal of the hydrophobic substrate BA, which will also require introduction of a recycling strategy of BA for this ISPR method to be feasible. It is therefore considered equally suitable to apply the same ISPR concept as suggested for case study 2 in Figure 4.7 in combination with a cascade reaction in the reactor to shift the equilibrium. This has been demonstrated succesfully, achieving high product purity and titers, by Börner and co-workers [144].

An alternative to this could be to exploit the zwitter ionic behavior of alanine to selectively remove MPPA. For example, operating the biocatalytic process close to the isoelectric point of alanine (pH 6) would potentially allow to selectively separate MPPA by applying electrophoresis as ISPR strategy. However, it would require the biocatalyst to be compatible with these operating conditions.

Another alternative is the application of ion exchange resins and operating at a pH above the isoelectric point of alanine, which would potentially allow to separate the positively charged MPPA from the negatively charged alanine. However, the pH should be kept lower than the pK_a value of MPPA. The fraction of uncharged molecules of the two amines at changing pH can be exploited for optimizing the ISPR method. The distribution of the charge of the two amines is presented in Figure 4.8, where the calculated curves are based upon using the Henderson-Hasselbalch equation (equation 4.5). It should be noted that extensive work would have to be put into screening selectivity and capacity of different ion exchange resins. Furthermore, it should be considered how the choice of operational conditions impacts the biocatalyst performance and stability.

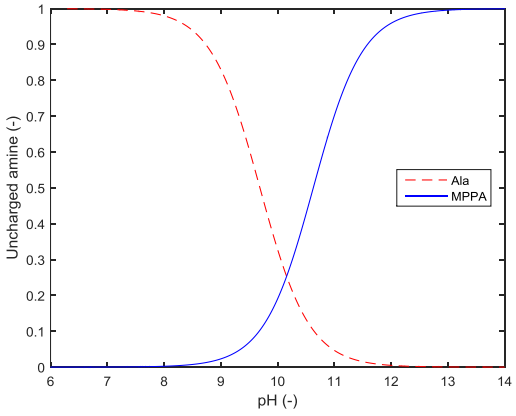

Figure 4.8: Distribution of charged and uncharged molecules at various pH values for the two amine products, i.e. Ala and MPPA.

4.4 Conclusions

This chapter focused on the applicability, feasibility and limitations of *in-situ* product (ISPR) and co-product (IScPR) removal strategies for amine transaminase (ATA) processes. Fundamental requirements, as well as important development and implementation considerations of ISPR/IScPR strategies were highlighted and discussed. In addition, state of the art ISPR and IScPR application for ATA processes were reviewed. Introducing ISPR/IScPR strategies adds significant complexity to processes and it is essential to consider the impact and feasibility of such an implementation, during the process development. Based on this a generic methodology for rational selection of proper ISPR/IScPR strategies, when found necessary and beneficial to implement, was proposed. Commonly applied ISPR and IScPR strategies were evaluated with the methodology based upon three case studies.

The case studies represented various thermodynamic, inhibitory, and separation related challenges. Hence, the case studies formed a good basis for broad coverage of the requirements and feasibility of ISPR and IScPR strategies for ATA processes. In conclusion, in the case studies it was found that the choice of amine donor might improve the thermodynamics of the synthesis route, but it comes with a trade-off in terms of the separation efficiency. It is therefore convenient to base ATA processes on amine donors, which can be considered easy to separate, i.e. donors with significant physicochemical differences from the main product and the substrate. In cases with unfavorable thermodynamics where the amine donor cannot be changed, it was found necessary to implement IScPR strategies based on cascade reaction systems. In cases with severe inhibitory and/or toxic effects from the (co-) product it is convenient to apply ISPR/IScPR strategies based on conventional separation methods. Furthermore, in cases where the product is hydrophobic and the amine donor is relatively hydrophilic it was found suitable to implement ISPR strategies based upon liquid-liquid extraction, which will enable good recovery, high purity and high concentrations of the amine product. In some cases, it might be necessary to apply a combination of both ISPR and IScPR if the inhibitory nature of both products from the ATA synthesis route is inhibitory and/or if the thermodynamics are highly unfavorable. It is problematic to identify unique and generic ISPR/IScPR solutions for the majority of potential ATA synthesis routes as each ISPR/IScPR solution is very case dependent. For example, the economic gain, in terms of improved process intensity, needs to justify the added costs by the implementation. In addition, there are many tradeoffs associated with the implementation of ISPR/IScPR strategies, which needs consideration as well. Some of the most prominent tradeoffs relate to altered biocatalyst performance in terms of activity and stability, along with the selectivity and efficiency of the applied separation method.

Overall, it is concluded that it is a suitable approach to implement ISPR/IScPR strategies for ATA synthesis routes and processes suffering from severe inhibitory effects and unfavorable thermodynamics. Processes suffering from unfavorable thermodynamics benefit the most from IScPR strategies based upon cascade reaction systems. However, processes experiencing severe inhibitory issues from the products might benefit more from easy and fast implementation of ISPR/IScPR strategies based upon conventional separation processes and principles, such as LLE.

Chapter 5

Characterization of microfluidic packed bed reactor (PBR) modules

In the development of biocatalytic processes, it is important to investigate, modify and develop robust technologies and methods to accelerate the development of the process using the available resources optimally. This chapter aims at highlighting the potential of microfluidic platforms, as such a novel technology. A major advantage of microfluidic platforms and technologies in this context is the possibility to perform extensive experimental investigations using a minimum of the available and valuable resources, e.g. expensive enzyme. In addition, the control interface of microfluidics is somewhat automated, enabling systematic testing with a minimum of manual labor. Here these advantages are demonstrated through characterization of immobilized biocatalysts, i.e. two ATA mutants (ATA-50 and ATA-82) entrapped in a lentil shaped polyvinyl alcohol (PVA) matrix, in specific microfluidic packed bed reactor (PBR) modules. Furthermore, the investigated microfluidic reactor modules were coupled to an on-line HPLC system to minimize manual labor, avoid handling of small volumes, and ensure fast and reliable characterization of the biocatalysts in the reactor modules. Despite the efficiency and reliability of this microfluidic platform there are also some limitations that are identified and discussed as well. The performed characterizations are based on the two mutants performing asymmetric synthesis of 1-methyl-2-phenylpropylamine (MPPA(2)) from benzylacetone (BA(1)), using isopropylamine (IPA(4)) as the amine donor, which was introduced as case study 2 in chapter 4. The general reaction scheme is illustrated in Scheme 5.1.

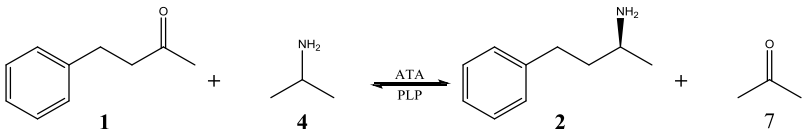

Scheme 5.1: General ATA reaction scheme for the synthesis of 1-methyl-3-phenylpropylamine (MPPA(2)) from benzylacetone (BA(1)) using isopropylamine (IPA(4)) as the amine donor. The co-product of this synthesis route is acetone (Ace(7)).

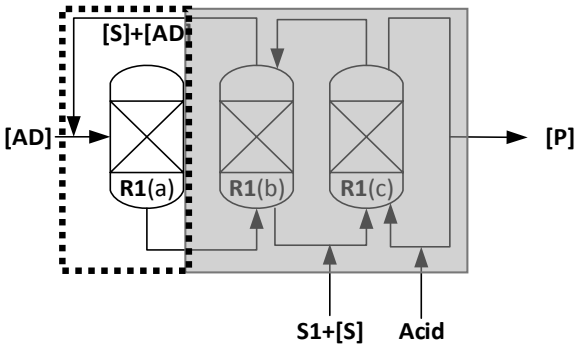

Figure 5.1: Flowsheet of the two-step liquid-liquid extraction ISPR concept for selective removal of hydrophobic amines from ATA processes, which was introduced in chapter 4. This chapter will solely focus on the reactor module as indicated with the dashed box in the figure. [AD]: Amine donor, [S]: substrate, S1: solvent, [P]: product, R1(a): reactor module, R1(b): 1st LLE module (High pH ~9.5) and R1(c) 2nd LLE module (Low pH ~3).

5.1 Introduction

In the development of biocatalytic processes, extensive efforts go into discovery and development of new biocatalysts, with activity for the reaction of interest. Once activity for the desired reaction has been discovered, the performance of the biocatalyst can indeed be enhanced by protein engineering, to improve the desired properties, such as substrate repertoire and selectivity as well as activity and stability [120]. Today, there are many examples where new biocatalytic routes are established through significant improvement of an existing biocatalyst, via iterative rounds of mutagenesis and screening [7,116,159,160]. When such a biocatalyst, with the desired properties, is discovered/developed, it is essential to characterize it and evaluate its performance and limitations. Biocatalyst characterization refers to the study on how various process parameters influence the performance of the biocatalyst in terms of activity and stability. Commonly, a large number of process parameters will significantly influence the biocatalyst performance. For many biocatalysts, e.g. ATAs, it is quite common that the performance is influenced by process parameters such as:

- Temperature
- pH
- Salt concentration
- Solvent compatibility
- Concentrations of reactants, co-factors and products: [S], [AD], [P], [cP], [PLP]

Performing extensive catalyst characterization and identifying how all these parameters influence the biocatalyst performance, either separately and/or in combination, is extremely labor intensive, costly and requires significant resources in terms of raw materials as well. Hence, application of automated microfluidic platforms for the characterization will make it possible to perform extensive characterization with the available resources in an easy and cost efficient manner.

The obtained knowledge from the characterization is extremely useful for directing modification and optimization of the catalyst. Furthermore, the knowledge gives an idea about current process limitations, such as inhibition from products, which potentially motivate the implementation of an ISPR and/or IScPR strategy. Furthermore, at this point in the process development, resources are commonly scarce, e.g. only small-scale production of the biocatalyst has been established. It is therefore highly relevant to consider the application of microfluidic platforms in this part of the process development. Microfluidics operate with small volumes of material, in the µL range, which makes it possible to perform extensive testing with the available resources compared to conventional mL scale batch testing [4]. Additionally, the possibility of performing extensive testing will ultimately make it possible to develop and apply advanced models for evaluating the process performance, e.g. ease the application of process systems engineering (PSE) tools and methods in the process development. The analytical limitations form a limitation to the scale-down of experiments and the application of microfluidics, which will dictate the minimum required sample volume. The concept behind this philosophy is sketched in Figure 5.2 [73]. Furthermore, the small scale gives challenges in terms of performing manual sampling, which motivates the development and implementation of on-line and in-line analytical methods.

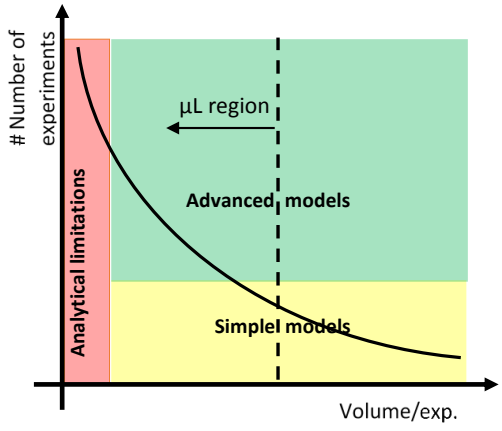

Figure 5.2: Sketch of the philosophy underlying miniaturization in the context of process development for biocatalytic processes [73].

5.2 On-line HPLC

In this work, an on-line HPLC system was put in place to overcome and minimize experimental bottlenecks, e.g. minimize manual labor and resource consumption, in the characterization of novel biocatalysts. Furthermore, it is believed that the implementation of on-line analytical methods in microfluidic platforms will facilitate and ensure high throughput of the systems. This feature in combination with the exquisite flow control, mass and heat transfer in closed microfluidic systems will ultimately ensure a competitive advantage compared to conventional methods. The on-line HPLC system was implemented by discarding the auto-sampler from a standard Dionex Ultimate 3000 HPLC system, and by implementing a dual loop injection port valve instead. The flowsheet of the setup and a picture of the actual setup are both shown in Figure 5.3. Please note that the magnetically stirred heater, used to control the reactor temperature, is not included in the flowsheet and the picture.

In general, HPLC systems can be categorized as advanced microfluidic platforms, and for that exact reason this analytical method and flow system are easily compatible with microfluidic modules. Furthermore, only small and simple changes in the application of the Chromeleon control software (Chromeleon® 6.8) was required in order to operate the modified system, i.e. it was required to exclude the auto-sampler operation in the program sequences by choosing the blank sample option. The setup was inspired by conceptual similar setups found in the scientific literature and commercialized products [161–166].

The basic concept of the implemented system is that a low-pressure microfluidic system operates in parallel with the high-pressure HPLC system. The injection port valve enables continuous introduction of samples from the low-pressure side into the high-pressure side, by sequentially switching the valve position. The two valve positions are shown in Figure 5.4. A requirement for this operation is that the valve only switches when each of the sample loops is completely filled with new sample, and the previous sample has had sufficient time in the HPLC system ensuring that peaks do not overlap. Another constraint might be the injected volumes of the samples, i.e. oversaturation of the detector and/or overlapping peaks due to tailing might occur. For the specific system used here, it was found feasible to apply two 2 µL sample loops. In addition,

the interfacing of the loops to the valve can cause small differences in internal dead volumes and thereby different sample injection volumes. The applied dual loop injection port valve was manually operated. Hence, the valve was required to be operated manually for each sample injection. However, there are automatic valves available, so it would conceptually be possible to make this setup fully automatic and/or invest in a costly commercial solution. In cases where it is not possible to inject the undiluted sample from the reactor, it is possible to dilute and/or quench the outgoing reactor mixture before entering the sample loop, e.g. by acid or base, and thereby achieve diluted samples.

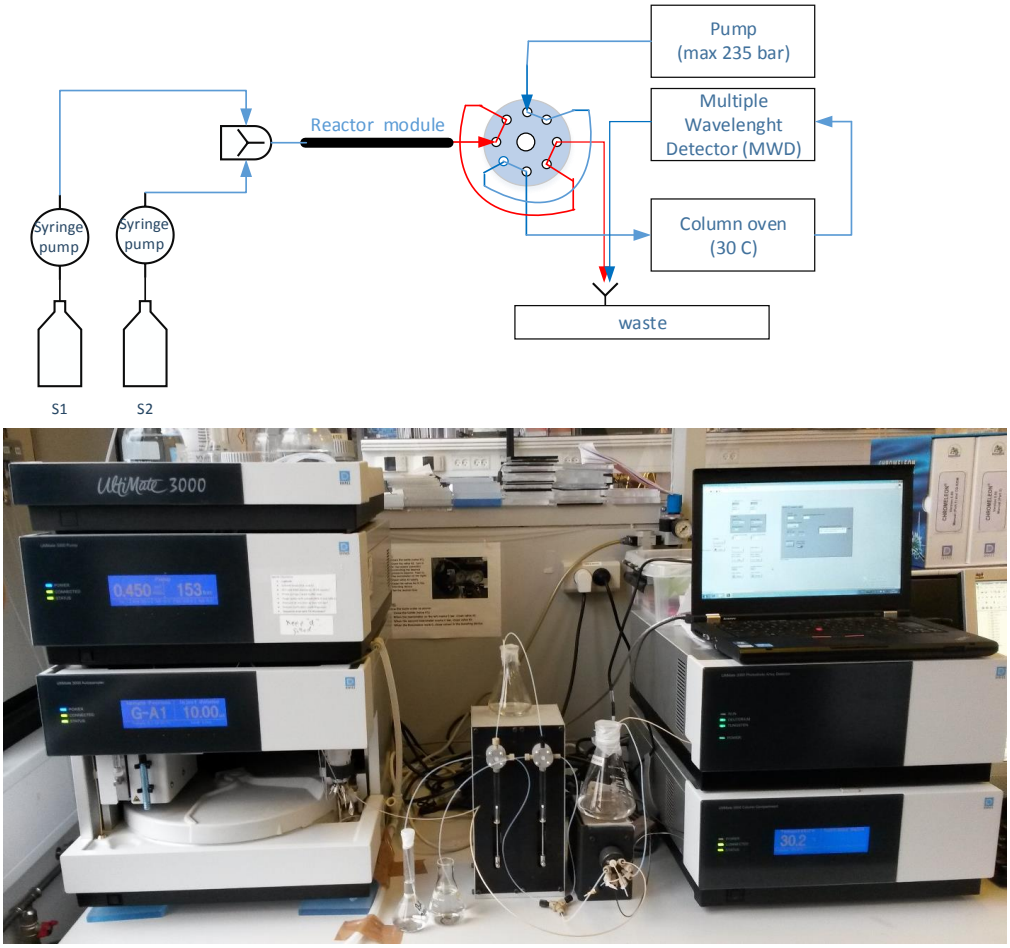

Figure 5.3: Top: Flowsheet of the applied on-line HPLC setup. Bottom: Figure of the actual set-up as it looks in the lab.

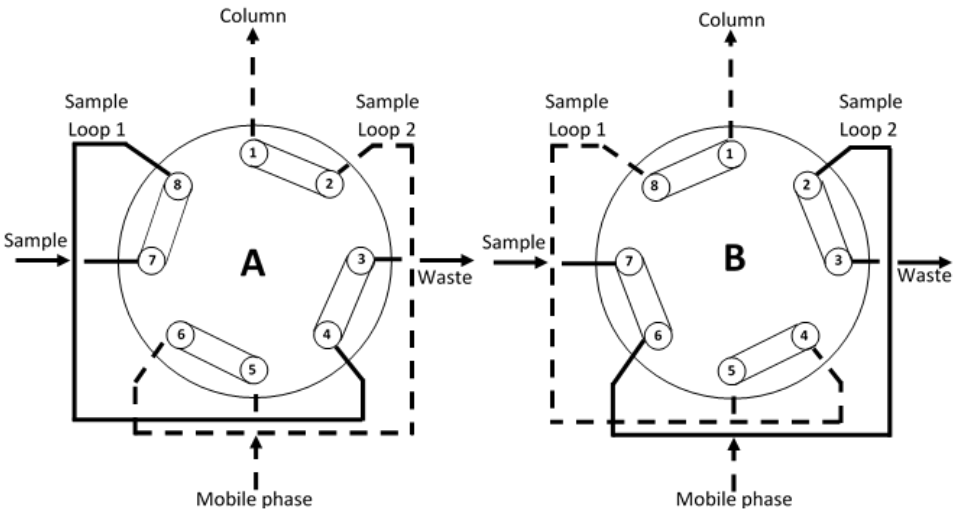

Figure 5.4: Different operating positions of the dual loop injection port valve applied in the on-line HPLC system, i.e. position A for injection of sample loop 2 and position B for injection of sample loop 1.

Despite the fact that such advanced and robust on-line HPLC systems are commercially available the application of on-line HPLC systems is still rather limited in terms of development and characterization of biocatalysts and biocatalytic processes. A reason for this can be that biocatalytic processes are commonly operated in batch. Hence, people test the process in the same manner as the application is operated in practice, and characterizing the biocatalyst in flow gives fundamentally some major differences.

The main motivation for implementing the specific on-line HPLC system was to operate the biocatalyst in a closed well-controlled system and to avoid costly and intensive manual sampling while performing extensive biocatalyst characterization. In addition, accurate manual handling of samples in the µL range can be difficult, which motivates the use of an automated sample handling procedure. Furthermore, it was a logical choice to focus on the on-line analysis by HPLC, rather than other analytical methods, as HPLC is a frequently applied analytical method for analysis of amines and monitoring ATA reactions [46,143,144,154,156,167,168]. The advantages of the HPLC include specificity, sensitivity, and fast chromatographic procedures.

5.3 Biocatalyst formulation

In this work, it was decided to focus on characterization of immobilized ATAs, i.e. wild type ATA-50 and ATA-82 immobilized by entrapment in lentil shaped polyvinyl alcohol (PVA) particles, in microfluidic packed bed reactor modules. The main reasons for focusing on immobilized ATAs in this work are listed below:

- Easy separation, retaining and recycling of the biocatalysts
- Suitable biocatalyst formulation for continuous applications
- Possible to follow biocatalyst stability at process relevant conditions
- No need to quench the product stream after the reactor
- Enables easy implementation of ISPR applications without direct contact with the biocatalyst

Despite the many benefits of applying immobilized biocatalysts in microfluidic packed bed reactors (PBR) for characterization of novel biocatalysts there are also multiple drawbacks. Some of the main drawbacks are the additional added costs of the biocatalyst, additional mass transfer limitations, potentially reduced volumetric activity, large particles, stability and packing of the bed. For example, non-uniform packing will cause altered fluid dynamic behavior in the packed bed, channeling, which makes it difficult to reproduce experimental results. Channeling comes as a cause of changed flow dynamics in the packed bed, i.e. regions with low and high flow resistance, and thereby not all the loaded catalyst will operate equally efficiently. The concept of channeling together with potential dead zones (no flow zones) is illustrated in Figure 5.5 [169]. All these effects will influence the reliability of the measured data. It is therefore crucial to put extensive efforts into proper packing of the particles and into removing air bubbles in microfluidic packed bed reactors prior to use, to ensure reproducibility. However, as long as there is good reproducibility of experimental results, then the microfluidic PBR experiments give a good indication of the relative performance of the biocatalyst at various tested process conditions.

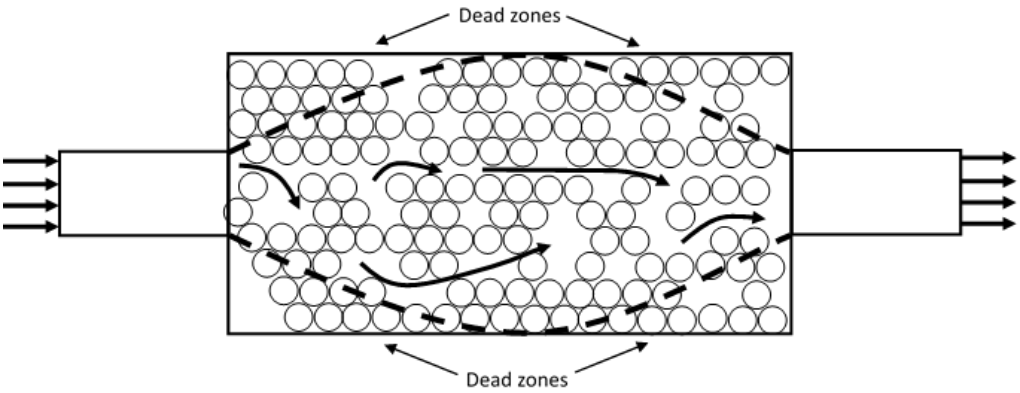

Figure 5.5: Illustration of the concept of channelling and occurrence of dead zones in packed bed reactors [169].

In this work, it was decided to mainly focus on a specific immobilization form, i.e. immobilization by entrapment in porous lentil shaped PVA particles. The main benefits of this particular immobilization form is related to the physical and mechanical properties of the PVA hydrogel, i.e. cheap, biologically inert, long-term mechanical stability, chemical inertness and non-toxic [170]. Furthermore, the porous lentil shape of the formed particles gives a number of advantages such as short diffusion distances across the particles, i.e. good mass transport properties [171–174]. The general concept and functionality of the porous LentiKats PVA lentil particles and the mass transfer in the particles is illustrated in Figure 5.6, whereas pictures of the actual lentils are shown in Figure 5.7.

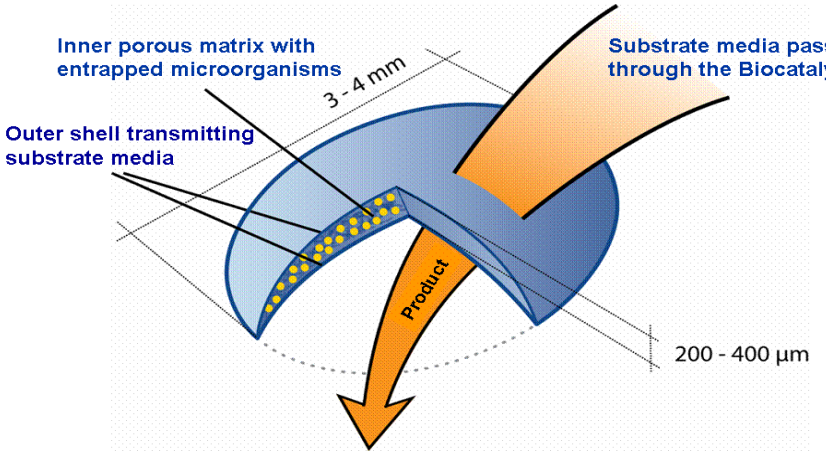

Figure 5.6: General concept and functionality of the porous LentiKats PVA lentils (Adopted with permission from LentiKat's® [175]).

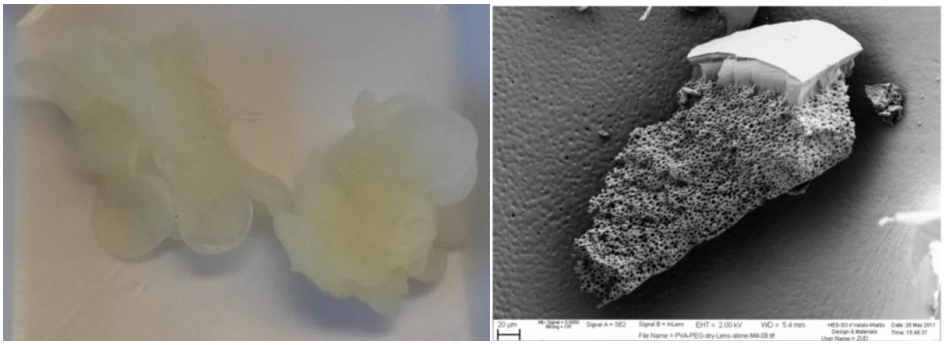

Figure 5.7: Left: Picture of lumps of the LentiKat's porous lentil shaped PVA particles. Right: microscopic picture of the matrix structure of the PVA particles (Adopted with permission from LentiKat's® [175]).

Conveniently, LentiKats® is an industrial partner in the BIOINTENSE project, and performed immobilization of ATA-52 and ATA-82, in the PVA particles [175]. The immobilization procedure is simple and based upon mixing the biocatalyst formulation with a PVA polymer solution. After the mixing, the lentil shaped particles are generated by dripping the solution onto a plate where gelatination occurs. The size of the particles can be altered by changing the size of the applied syringe for the dripping. The general concept of the immobilization strategy is illustrated in Figure 5.8 [176]. The manufacturing procedure causes the formation of a surface membrane layer on the PVA particles, with permeability in the range of 7-14 kDa, which enables entrapment of the biocatalyst and passage of the reaction species. The PVA matrix has an inner porous structure, with pore sizes in the range from 1-10 µm. A specific value of the overall porosity of the particles is not provided by the supplier and has not been experimentally determined.

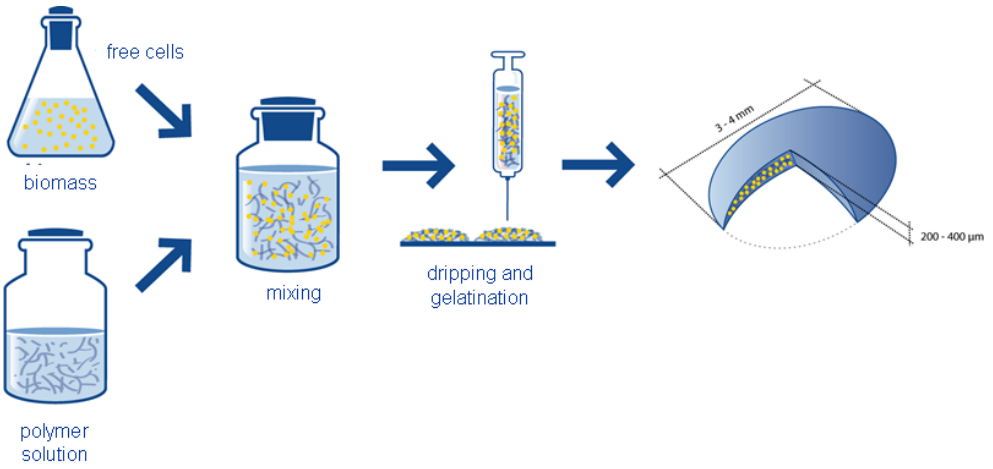

Figure 5.8: Lentikat's manufacturing scheme(Adopted with permission from LentiKat's® [175]).

5.4 Experimental method

5.4.1 Chemicals

Recombinant amine transaminase ATA-82 produced in an *Escherichia coli* production host, was provided by c-LEcta GmbH (Leipzig, Germany). Formulation of the polyvinyl alcohol matrix (PVA) for immobilization of purified ATA-82 was performed and provided by LentiKat's a.s. (Czech Republic, www.lentikats.eu); the formulation contained $50\ mg_{ATA-82}/g_{PVA}$. Benzylacetone (BA; synthesis grade; Cas no. 2550-26-7) was purchased from Merck KGaA. Potassium carbonate (99+%; Cas no. 584-08-7) was purchased from Acros Organics. All other chemicals were purchased from Sigma-Aldrich, i.e. 1-methyl-3-phenylpropylamine (MPPA; 98%; Cas no. 22374-89-6), pyridoxal 5'-phosphate monohydrate (PLP; ≥97.0%; Cas no. 41468-25-1), acetone (Ace; ≥99.5%; Cas no. 67-64-1), isopropylamine (IPA; ≥99.5%; Cas no.75-31-0), sodium bicarbonate (99.5-100.5%; Cas no. 144-55-8).

5.4.2 Analytical method

The concentration of the substrates and products in aqueous solutions was determined by HPLC (Dionex Ultimate 3000) with UV detection (Dionex Ultimate 3000 PDA detector). The applied method for the on-line measurements only allowed analysis of benzylacetone (BA) and 1-methyl-3-phenylpropylamine (MPPA). The method is operated isocratic (0.450 mL/min mobile phase) at 30°C with a Gemini-NX C18 column (100mmx2mm, 3µm, 110Å, Phenomenex, Torrance, CA, USA). The mobile phase consists of 35% acetonitrile and 65% Milli-Q water adjusted to pH 11 by addition of NaOH. The retention times for MPPA and BA were 2.9 min and 3.6 min, respectively, and the detection was performed at 265 nm. Isopropylamine (IPA) and acetone (Ace) were not detected during the characterization. (See appendix C for detailed information on the applied standard, validation, etc.)

5.4.3 Method

A set of standard conditions (fixed temperature at 30℃, pH 9.5 and a PLP concentration of 0.1 mM) were applied for characterization of the microfluidic PBR modules with the immobilized biocatalysts. The pH of the reaction mixtures was ensured by applying a 100 mM carbonate buffer solution, where the pH was adjusted with HCl after addition of the amine compound. Due to the nature of the performed characterization experiments the concentrations of all other reaction species were varied sequentially, by changing the flow to the reactor from different substrate reservoirs. In order to compare different prepared reactor modules a standard experiment was performed at the start and end of the testing of each reactor module. The standard experiment was carried out using 10 mM BA and 500 mM IPA. This type of testing also gives an indication on the loss of activity throughout the performed experiments. Furthermore, the standard test was performed at various flow rates, while the characterization tests were performed at fixed flow rates, 25 µL/min for ATA-50 and 100 µL/min for ATA-82. For each experimental set point, a minimum of 5 reactor volumes was flushed through before commencing the sampling. All samples were repeated 4-6 times. For these experiments, an on-line HPLC setup, with 2 µL sample loops, was put in place in order to automate and accelerate the characterization, and thus minimize manual handling. The flow diagram of the applied setup is shown in Figure 5.3.

The applied reactor modules for the characterization of the performance of ATA-82 and ATA-50 entrapped in PVA particles consisted of PTFE tubes (Length 5 cm, OD 1/8”, and ID 1/16”, giving a working volume of ~100 µL). The used PVA particles for the characterization were lentil shaped and had diameters in the range of 1-1.5 mm, i.e. smaller than normal size (3-4 mm) produced in the large scale manufacturing at LentiKat’s [175]. The thickness of the 1-1.5 mm particles is in the range of 0.1-0.2 mm, while the thickness of the 3-4 mm particles is in the range of 0.2-0.4 mm.

The quantity of biocatalyst loaded into the reactor modules was determined by weight. The loading was performed by sucking up the PVA particles from an aqueous suspension and retaining them in the reactor by dead end filtration. The water from the suspension was thereafter removed, before weighing, by blowing air through the filled reactor module (PVA matrix maintained wet).

5.5 Characterization of ATA-50 and ATA-82 entrapped in PVA

In this study, the aim is to characterize the performance of ATA-50 and ATA-82 to perform asymmetric synthesis of MPPA from BA using IPA as the amine donor (case study 2 introduced in chapter 4). The characterization is performed by testing how various concentrations of the reaction species influence the initial rate of the biocatalyst. The motivation for choosing this particular case study is related to the physicochemical properties, which in this case enable somewhat selective separation based on LLE as proposed and discussed in chapter 4. Furthermore, this case study has semi-favorable thermodynamics, which makes it possible to get somewhat reasonable conversions using an excess of the amine donor.

A potential problem with this simple characterization relates to the first law of directed evolution: “You get what you screen for” [28]. For example, with this type of testing we only get an indication of the impact of the reaction species on the biocatalyst performance and neglect the potential influence of pH, temperature, buffer, solvent compatibility and PLP. These parameters are of high importance for the biocatalyst

performance and their impact needs to be classified simultaneously in the characterization, unless they do not influence the initial rate of the biocatalyst significantly. However, it was outside the scope of this thesis to fully characterize the applied biocatalysts, i.e. the focus here is to determine if the applied ATAs can benefit from implementation of ISPR process options. Furthermore, various BIOINTENSE project partners, i.e. Lund University and c-LEcta GmbH, have tested the dependence of the biocatalyst on [PLP], temperature, solvent compatibility and pH.

In addition, LentiKats® has addressed the aspect of mass transfer limitations in the PVA particles. It was determined that the remaining activity after the immobilization of ATA-50 and ATA-82 to be 94% and 98%, respectively. These numbers are relative to the activity of non-immobilized ATA-50 and ATA-82 for the conversion of BA into MPPA using IPA as the amine donor. This is a good indication that the reaction rate, for the given reaction, is the rate limiting step and not the mass transport into the particles.

LentiKats® performed a similar study with a faster reaction, i.e. the asymmetric synthesis of PEA from ACP, where it was shown that mass transport limitations are more dominating. For the faster reaction, the remaining activity after immobilization was in the range of 50% for both ATA-50 and ATA-82. The loss in activity is not considered a consequence of loss in biocatalyst during immobilization, i.e. the loss in activity for the slower reaction was very low indicating that potential loss of biocatalyst must be fairly low.

However, when packing the particles in a PBR some of the loaded particles will face the wall. For particles facing the wall, diffusion will only occur from one side and thereby increase the diffusion distance and time significantly. For example, for PVA particles where diffusion can occur from both sides, the diffusion distance in the particles will be in the range of 0.05-0.1 mm (half the thickness), giving diffusion times of 1.25-5 seconds. Assuming the diffusion velocity of the molecules of interest is approximately $\mathrm{D_{AB}} = 10^{-9}\frac{\mathrm{m^2}}{\mathrm{s}}$. However if the particles are facing the wall the diffusion distances will conceptually be doubled causing the diffusion time to be in the range of 5-20 seconds. Consequently, this will increase diffusion limiting effects and thereby cause somewhat slower reactions as a consequence of increased mass transfer limitations. Calculating the Thiele modulus ($\phi = \mathrm{L}\sqrt{\frac{\mathrm{k}}{\mathrm{D_{AB}C_{BA}}}}$ for a zero order reaction) and internal effectiveness factor of the particles ($\eta = \frac{3}{\phi^2}(\phi \cdot \coth\phi - 1)$), makes it possible to quantify if mass transfer limitations will be a concern. Based on the identified maximum rate determined in section 5.5.2, table 5.1 ($\frac{\mathrm{k}}{[\mathrm{E}]} = \sim 156.9\ \frac{\mu\mathrm{mol}}{\mathrm{min}\cdot \mathrm{g_{enz}}}$), worst case estimates are made of ϕ and η (Assuming: $\mathrm{D_{AB}} = 10^{-9}\frac{\mathrm{m^2}}{\mathrm{s}}$, $\mathrm{L} = 0.2\ \mathrm{mm}$, $\mathrm{C_{BA}} = 10\ \mathrm{mM}$, $[\mathrm{E}] = 100\frac{\mathrm{g_{enz}}}{\mathrm{L_{PVA}}}$). These estimates resulted in $\phi \approx 1.0$ and $\eta \approx 0.93$. Consequently, this confirms mass transfer is not expected to be the rate limiting mechanism even when the large particles stick to the surface. It is off course a necessity that channeling does not occur in the packed bed reactors as this would significantly increase the diffusion distance to some of the particles. The applied enzyme concentration in the particles in the calculation, $[\mathrm{E}] = 100\frac{\mathrm{g_{enz}}}{\mathrm{L_{PVA}}}$, was chosen higher than what can be expected in the provided PVA particles, 50 $\mathrm{mg_{enz}/g_{PVA}}$, as a means to illustrate worst case scenario.

5.5.1 Residence time

Before starting the actual characterization, the impact of the substrate feed flow rate to the microfluidic PBR was investigated. The aim of this investigation was to identify suitable residence times in the PBR to achieve sufficient conversion to monitor the impact of changing feed concentrations. For example, if the

characterization is performed with low conversion in the PBR, the sensitivity of the HPLC method will have a significant impact on the results. On the other hand, if the characterization is performed with high conversion in the PBR the influence of inhibitory effects from products, experimental time and throughput will increase significantly. Furthermore, at high conversion, the measured differences may be a direct effect of altered equilibrium concentrations and/or the lack of differences can be a result of achieving full conversion. It is therefore important to operate with a reasonable residence time to ensure that the experimental data is not compromised. Here, it was decided to aim at an approximate conversion of 20%, which corresponds to formation of ~2 mM MPPA. The results from these investigations are summarized in Figure 5.9.

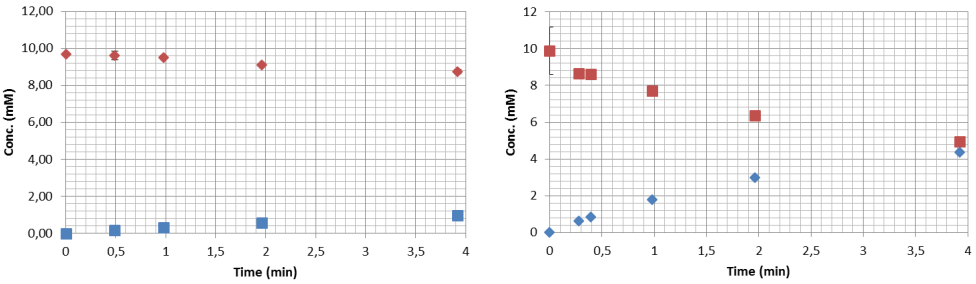

Figure 5.9: Investigation of the influence of increasing residence time in packed bed reactors, with ATA-50 (left – ~311 g_{PVA}/L ≈16 g_{ATA50}/L) and ATA-82 (right – 594 g_{PVA}/L ≈ 30 g_{ATA82}/L), using a standard reaction mixture of 9.53 mM BA, 482.23 mM IPA and 0.1 mM PLP in 100 mM carbonate buffer (pH 9.5). The data points in the upper part of the plot correspond to the measured BA concentrations, while the lower points correspond to MPPA.

These investigations indicate that it is suitable to operate with residence times of approximately 4 min (25 µl/min) and 1 min (100 µL/min) for ATA-50 and ATA-82, respectively. The need for different residence times in the PBR modules will cause different laminar flow behavior for each of the characterized biocatalysts. However, the relative influence of the different reaction species at steady state should still be comparable.

The significant difference in the required residence time, for the two biocatalysts, to achieve various degrees of conversion can be related to significant improvements and differences in active enzyme content in the ATA-82 formulation compared to the wild-type ATA-50 formulation. Note that it can be erroneous with such conclusion if the purity and active enzyme content is not known precisely before such comparison is made.

The estimated residence times correspond to the residence time if the reactor was empty. Filling the reactor with porous particles will take up some of the void space end thereby influence the flow dynamics and residence time in the reactor. The routes resulting in lowest fluid resistance dictate the flow in the packed reactors. Hence, filling the 1.59 diameter tube with 1-1.5 mm wide and 0.1-0.2 mm thick particles will cause the actual residence time in the PBR to be lower as the flow is likely to go around the particles rather than through them. Performing standard experiments is therefore essential to identify if the prepared PBR behaves similarly to other experiments. Furthermore, performing sets of experiments, e.g. characterization of the impact of the different components individually in each prepared PBR, makes it possible to identify trends in those experiments, as the fluid dynamics in those experiments will be the same.

5.5.2 Characterization

Applying the proposed residence times from section 5.5.1, the influence of the various reaction species on the reaction rate of the two biocatalysts was tested. The results from these tests are summarized in Figure 5.10 and Figure 5.11 for ATA-50 and ATA-82, respectively. It was attempted to fit the expression for the forward reaction rate in the absence of products for reactions following ping-pong bi-bi kinetics, in the same manner as described by Al-Haque et al. [50], to the data describing the influence of BA and IPA on the reaction rates. The kinetic expression is shown in equation 5.1. The estimated parameters from this data fitting are presented in Table 5.1. The model predictions for each of the biocatalysts are included in the figures.

$$r = \frac{V_{max} \cdot [S][AD]}{K_M^S[AD] + K_M^{AD}[S] + [AD][S]} \quad \text{(Eq. 5.1)}$$

, where $K_M^S\ [M]$ and $K_M^{AD}\ [M]$ are the Michaelis parameters and $V_{max}\ [mol \cdot min^{-1} \cdot g_{enz}]$ is the maximum rate [50].

Table 5.1: Estimated parameters for the initial forward reaction velocity in the absence of products for biocatalysts following ping-pong bi-bi kinetics.

	V_{max}	K_{BA}	K_{IPA}	r_{BA}^2	r_{IPA}^2
	$\frac{\mu mol}{min \cdot g_{enz}}$	mM	mM	$-$	$-$
ATA-50	9.56	3.1	329.7	0.77	-1.3
ATA-82	156.9	13.2	160.9	0.99	0.96

Overall, these results indicate that the formulation of ATA-82 has significant higher activity than the ATA-50 formulation. Furthermore, the low activity of ATA-50 causes large deviations in the performed measurements as well as inaccurate model fitting, relative to ATA-82 where the influence of both BA and Ace is predicted well by the model.

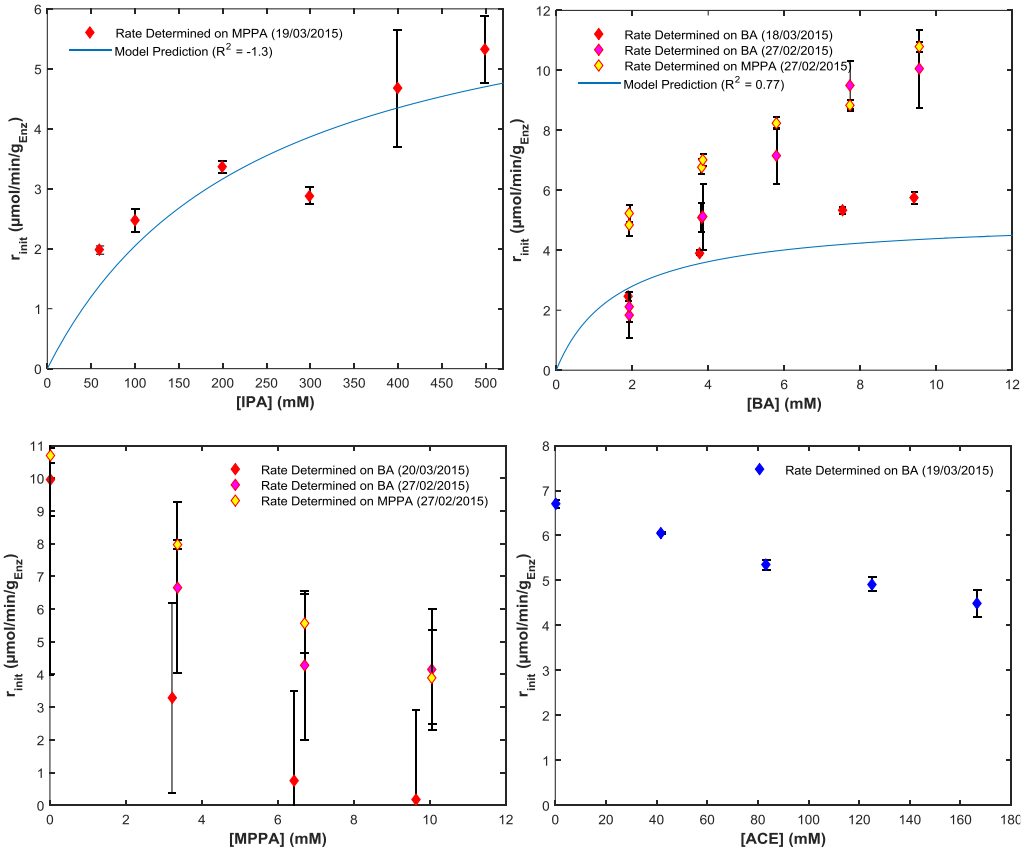

Figure 5.10: Characterization profiles of a µ-PBR containing PVA particles with entrapped ATA-50. A: fixed [IPA] (500 mM) and varying [BA] (2-10 mM). B: fixed [BA] (10 mM) and varying [IPA] (50-500 mM). C: fixed [BA] (10 mM) and [IPA] (500 mM) with varying [MPPA] (0-10 mM). D: fixed [BA] (10 mM) and [IPA] (500 mM) with varying [Ace] (0-170 mM). All experiments were performed at 30 °C, in the presence of 0.1 mM PLP and applying a feed of 25 µL/min (4 min residence time).

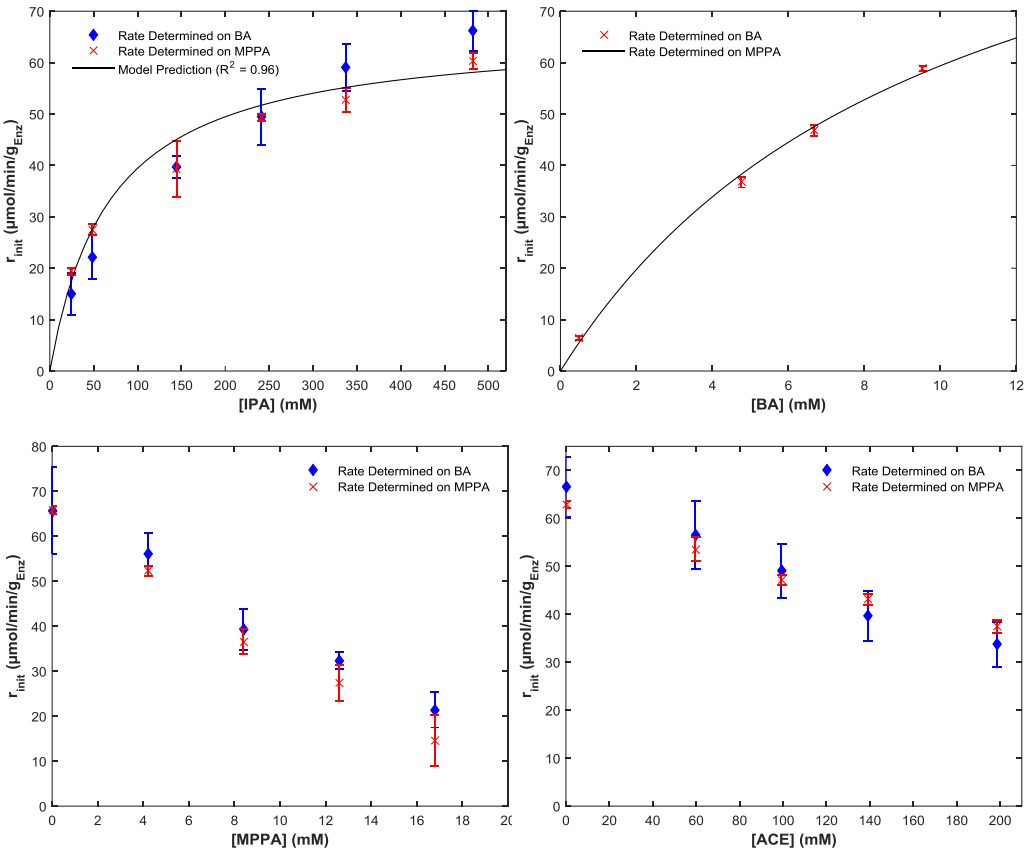

Figure 5.11: Characterization profiles of µ-PBR containing PVA particles with entrapped ATA-82. A: fixed [IPA] (500 mM) and varying [BA] (2-10 mM). B: fixed [BA] (10 mM) and varying [IPA] (50-500 mM). C: fixed [BA] (10 mM) and [IPA] (500 mM) with varying [MPPA] (0-10 mM). D: fixed [BA] (10 mM) and [IPA] (500 mM) with varying [Ace] (0-170 mM). All experiments were performed at 30 °C, in the presence of 0.1 mM PLP and applying a feed of 100 µL/min (1 min residence time).

Looking into the influence of varying the initial MPPA content in the feed, the results indicate that MPPA gives cause to a significant decrease in the reaction rate for both biocatalysts. Hence, it is a strong indication of severe product inhibition, ~4% loss in initial rate per mM MPPA for ATA-82, which motivates to investigate the possibility of implementing an ISPR strategy. Similarly, acetone also appears inhibitory, ~0.2% loss in initial rate per mM Ace for ATA-82, for both biocatalysts. However, the inhibitory nature of MPPA is greater, ~20 times higher, than that of acetone making it the first priority to focus on MPPA removal by ISPR. Therefore, it is found reasonable to proceed with the development and implementation of the highlighted two-step liquid-liquid extraction ISPR strategy that was described in chapter 4.

In parallel to this work, Börner et al. [144] did some similar characterization investigations on ATA-50 in batch, which also gave an indication of strong inhibitory effects from MPPA (with alanine as the amine donor). In

their work, they also measured rates of ATA-50, either as crude enzyme or cells, for the reaction of BA with IPA to MPPA and found values that were an order of magnitude greater than what was measured here. There can be multiple reasons for the difference in observed behavior, where the main reason is believed to be caused by the altered reaction conditions. Here the reaction operated with 100 mM carbonate buffer at pH 9.5 and Börner et al. [144] applied 20 mM sodium phosphate buffer at pH 8. Hence, a direct comparison of these experimental results is not possible. However, it is still interesting to consider potential features in conventional batch systems and in microfluidic reactor modules that potentially give cause to altered reaction behavior, which will be further discussed in section 5.7.

For the characterization of ATA-50 there was almost 3 weeks between the first and the last characterization experiments, which had a significant impact on the remaining activity, i.e. on 27/02/2015 the maximum measured activity was around 10 mmol/min/mg and on 17/03/2015 the remaining activity was slightly lower than half the initial value. This gives some challenges for collection of reproducible data if the enzyme is not characterized relatively fast after it is immobilized. Considering the potential for industrial application, it causes some challenges as well because it is not possible to have the biocatalyst in storage for long periods before one should apply the biocatalyst. Hence, a more stable biocatalyst is required, which is also the case for ATA-82.

5.5.3 Stability

In connection to the performed characterizations, standard experiments (10 mM BA and 500 mM IPA) were performed to get an indication of the relative stability of the tested biocatalysts, i.e. remaining activity after each characterization. The results from these stability tests are summarized in Figure 5.12.

The results indicate minor differences in the reduction of relative activity during the performed characterizations between the two biocatalysts, i.e. the relative activity of ATA-50 decreases slightly more than for ATA-82 in the tested periods. For both biocatalysts, the remaining relative activity is above 90% after a few hours, which is an important feature when intending to operate the system for a longer time as is intended with the combined ISPR system, because the microfluidic PBR modules can operate for longer periods before replacement is required.

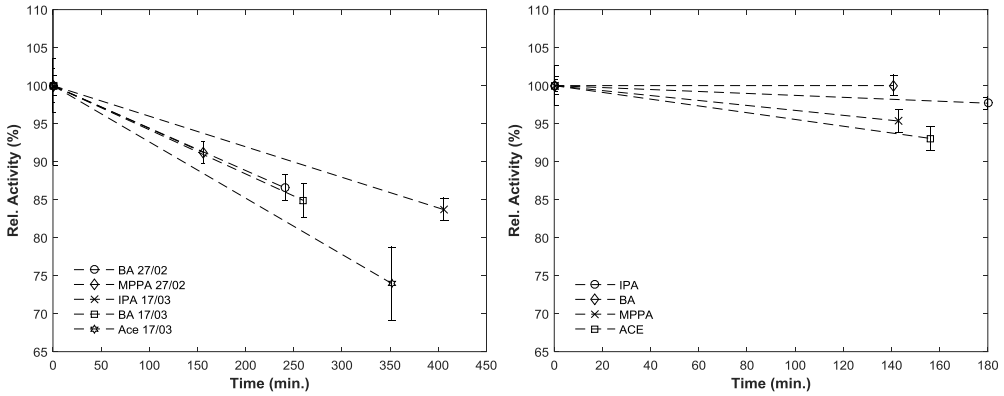

Figure 5.12: Measured remaining activity for the various performed experiments for characterization of ATA-50 (left) and ATA-82 (right) entrapped in PVA particles presented as the remaining activity after exposure to various concentrations of the various reaction species.

5.6 On-line HPLC sensitivity

An important aspect of the application of the on-line HPLC system is to reflect on the sensitivity of this analytical method. The relatively large quantity of data points generated during the characterizations, around 300, makes it possible to reflect on the sensitivity and some general limitations with this setup and current application.

In general, the quality of the collected data, with this on-line HPLC setup, is as good as the applied method and it really pays off to put some effort into developing a sensitive and robust analysis method. Some of the general limitations for this on-line HPLC setup, which influences the data quality and throughput, are:

- **Analysis time:** The sample analysis time dictates the throughput of an on-line HPLC system. Hence, fast methods are required to ensure high throughput. Furthermore, biocatalysts with low stability will require frequent replacement of the biocatalyst in the reactor module, so a fast method will make better use of the applied biocatalyst. However, a catalyst with low activity will require a certain residence time in order to monitor sufficient conversion and in this case, nothing is gained by having a fast HPLC method.
- **Absorbance:** Compounds with strong UV absorbance require small sample loops and/or dilution before going to the sample loops in order not to exceed the detection limit of the UV detector. However, this is also a positive effect as it potentially gives highly sensitive measurements.
- **Dead volumes:** It was difficult to achieve two identical sample loops, i.e. small deviations in the dead volumes between sample-loops occurred, which requires a standard for each loop. Having a standard for each loop makes it vital to keep track of the valve position, to ensure correct analysis of the samples.
- **Column contamination:** If the injected samples are dirty and/or contain small particles, compounds and/or traces of protein might damage the column after relatively few samples. Hence, it is required to either implement a way to clean the samples before injection and/or to evaluate if the costs saving achieved by avoiding manual sampling can counterbalance the reduced lifetime of the columns.

- **Column stability:** Increased peak tailing and loss of column separation performance over time make it crucial to validate the standards relatively frequently, which increases manual labor and analytical downtime. It is the same problem when reaction species cause irreversible inhibition and/or increased enzyme denaturation over time. Alternatively, performing a standard experiment relatively frequently to determine the relative remaining activity would to some extent make it possible to consider such effects.
- **Overlapping peaks:** If the sampling is not timed correctly, overlapping peaks can be experienced and hence erroneous measurements, i.e. it is desired to have perfect timing of the sample injections to ensure the throughput. For example, for the applied method here, some of the compounds (IPA, Ace and PLP) lump together, appearing approximately 1 minute after the sample injection, and thereby cannot be quantified. Those compounds are the sole reason why the method took 4 minutes per sample and analysis time could not be decreased to 2 minutes, i.e. MPPA and BA both appear from 2 to 4 minutes after injection.

Figure 5.13, provides two examples of how the spectra can appear when applying the on-line HPLC, i.e. an example of a long sample sequence and a short sample sequence is provided. In case of a long sample sequence, it can be difficult to distinguish between different peaks. Hence, shorter sample sequences are easier to handle, unless a systematic method is implemented for peak recognition. Interfacing the microsystem control with the Chromeleon software is probably the most suitable solution to this problem.

External standards are applied for the quantitative analysis of the spectra. The generated standards for each sample loop can be seen in Figure 5.14. It was required to generate a standard for each of the sample-loops, as there was a small difference in their dead volumes. The difference was in the range of 1 µL based on the differences in measured areas from the external standards. Also included in the figure is the validation of the generated standards by independent external standards. The validation is performed to ensure that the generated standards remain reliable throughout the characterization studies. In the presented validation, it can be seen that the MPPA standards start to under-predict the MPPA concentration with about 5% when time goes by, in the period from 16/02/2015 to 17/03/2015. This will have some impact on the experimental uncertainty, and since ATA-50 was characterized last, in the period from 26/02/2015 to 17/03/2015, it may explain some of the larger uncertainties in those experimental results. However, since ATA-82 was characterized first and within a few days, those data should not be compromised. The standard curves and the following characterization of ATA-50 were not repeated, due to ATA-82 was chosen as the candidate for further experimental work.

The estimated standard deviation in each experimental point is presented in Figure 5.15, i.e. based on 4 to 6 sample repetitions, for both BA and MPPA. From the presented data, large deviations can be found in some of the experimental points. Some of these deviations can be explained as sample points, where the peaks have minor overlaps, due to poorly timed sampling. Overall, the relative error in the single point measurements is below 5% for both MPPA and BA, meaning that the data is somewhat trustworthy. However, the sensitivity in the MPPA measurements is 5-6 times better than for BA. Therefore, it is concluded that it is better to perform model fitting based on the MPPA experimental data. The sensitivity can also be improved by choosing a different wavelength with stronger MPPA and BA absorbance, i.e. 210-220 nm rather than 265 nm. This would however require sample dilution before injection in order to ensure that the saturation limit of the detector is not reached.

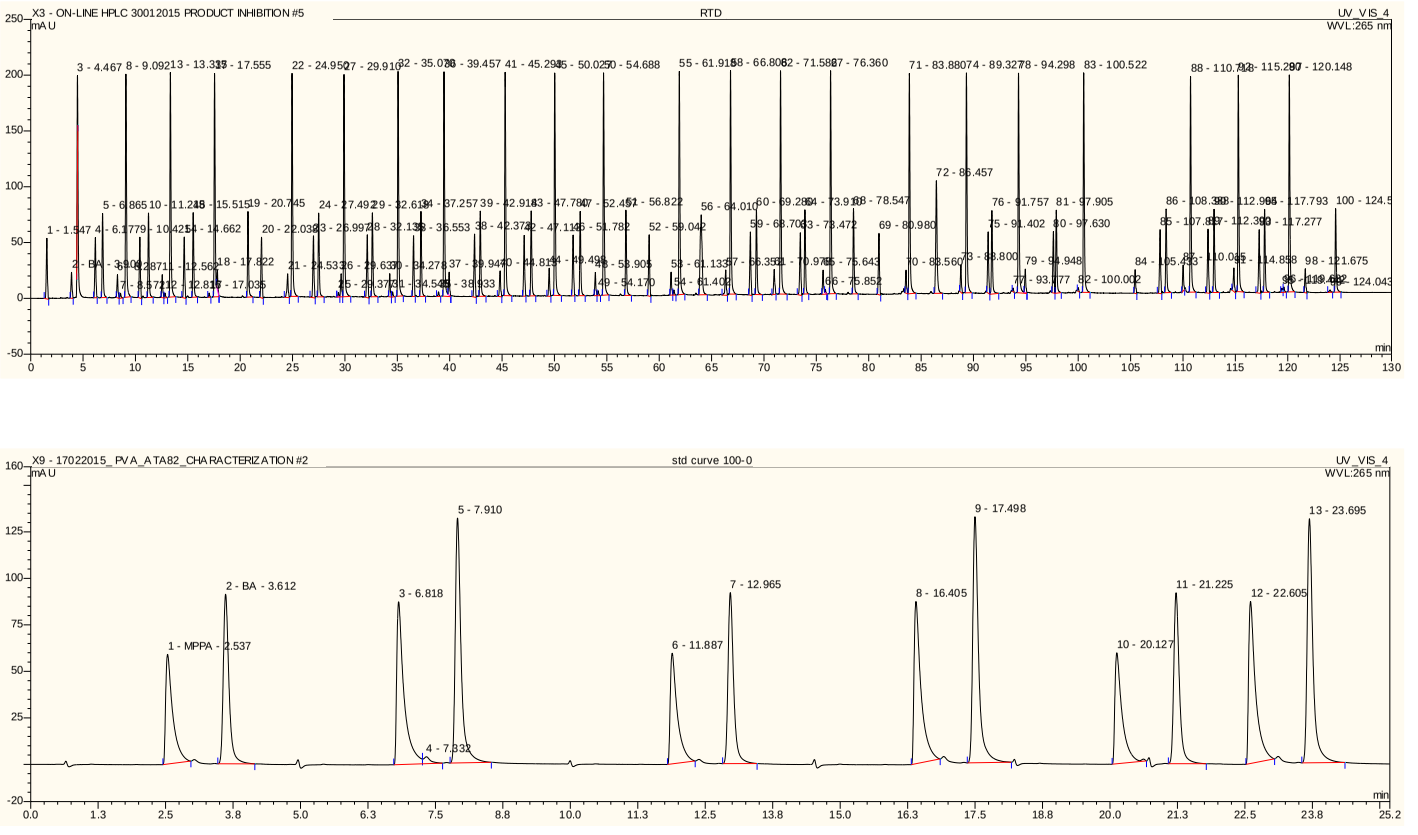

Figure 5.13: Examples of spectra from the on-line HPLC set-up. The upper figure forms an illustration of many sample injections in a row, and the lower figure is an example of a limited set of sample points in a spectrum simulating a single experimental set point.

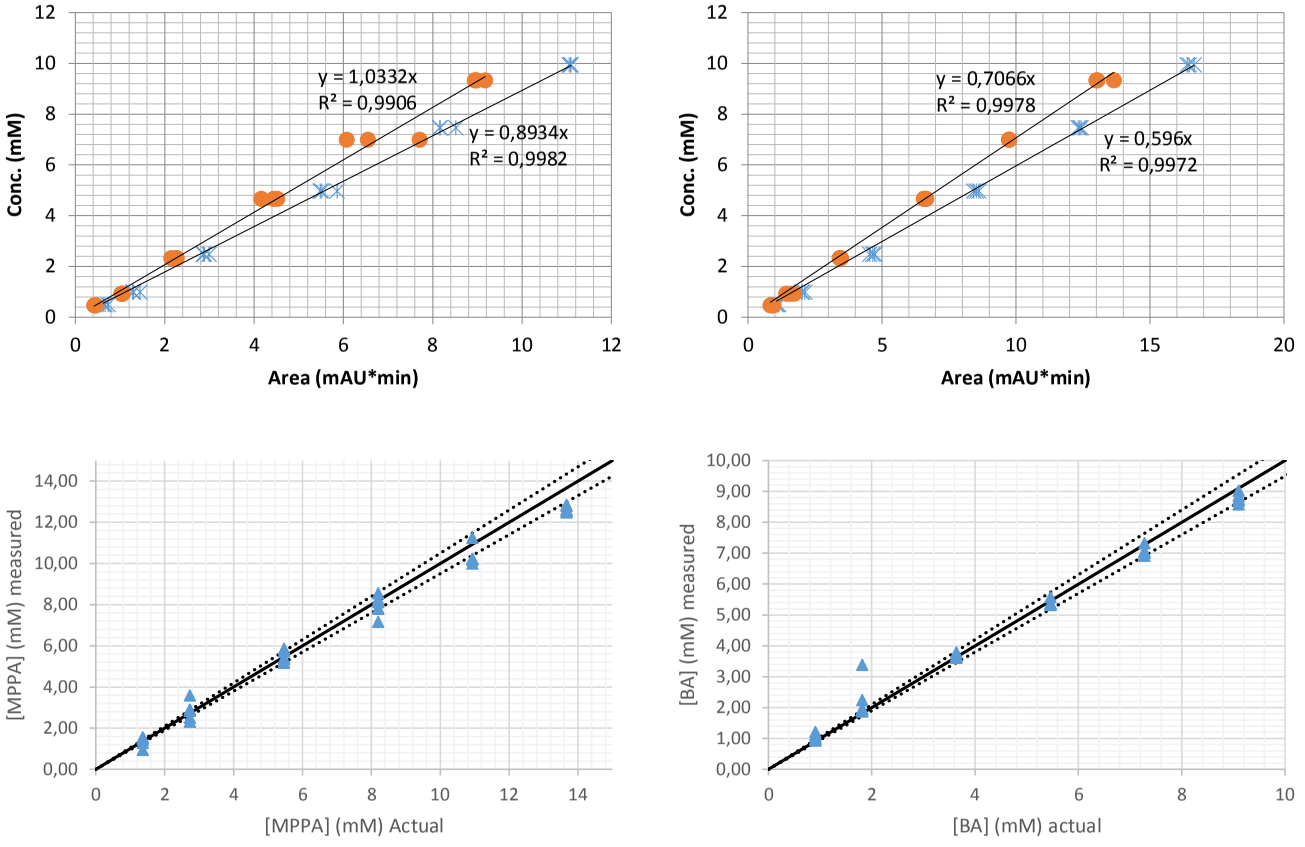

Figure 5.14: Standard curves for the two sample loops and the experimental validation of the standards over time (the solid line corresponds to 100 % prediction and the dashed lines correspond to ±5% error in the predictions). The circles correspond to the standard curves for MPPA and the crosses correspond to the standard curves for BA.

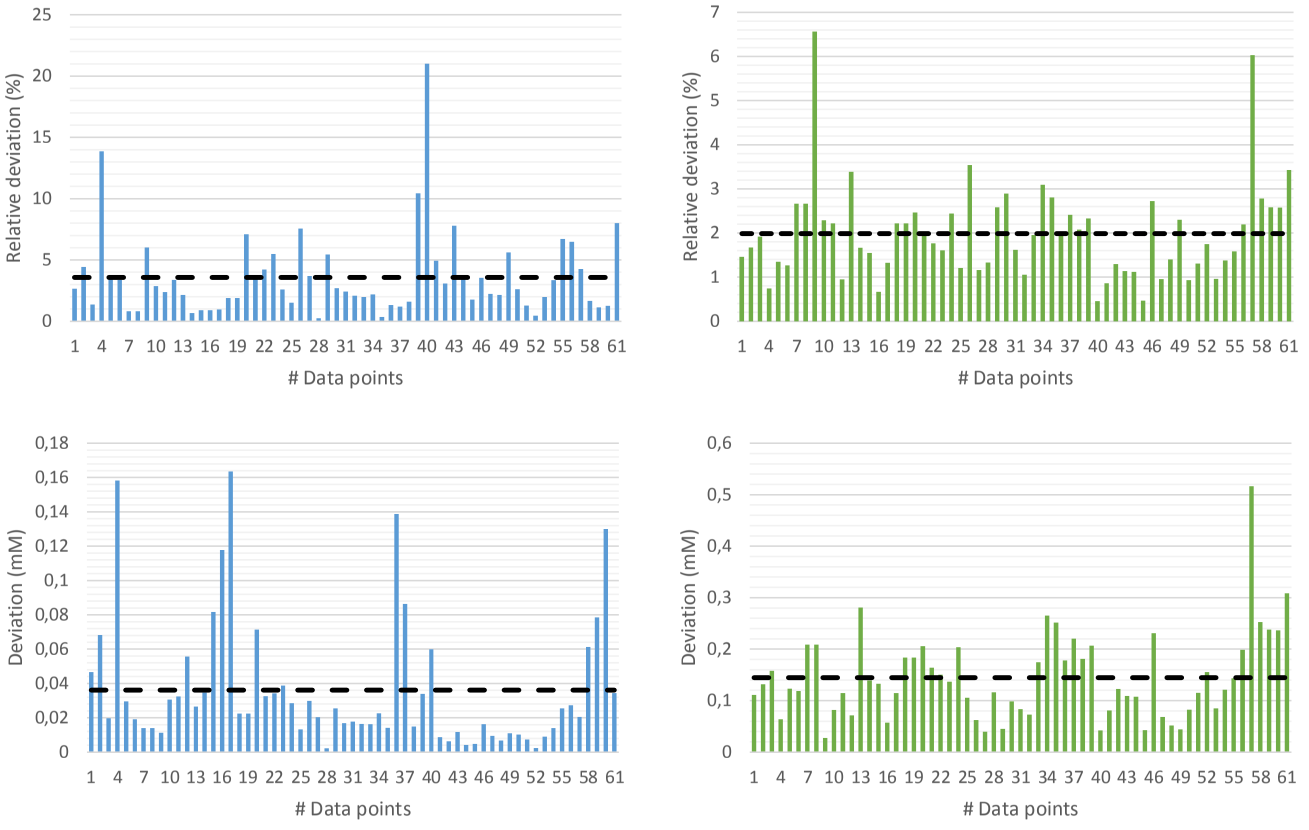

Figure 5.15: Examples of relative deviation from the measured values and the actual measured standard deviations in mM for MPPA (left) and BA (right) for each experimental point, consisting of 4 to 6 data repetitions.

5.7 Discussion

The benefits, the advantages and the potential of applying microfluidics for characterization of biocatalysts is emphasized throughout this chapter. However, there are different aspects of the general applicability of microfluidics for the characterization that need to be considered in the further application of microfluidics and of the acquired data in such systems.

Firstly, an important aspect in any biocatalytic process is the formulation of the applied biocatalyst, which is case specific. For example, characterizing purified free enzymes is relevant when improvements of specific characteristics of various mutants are to be identified, or when the purified form of the enzyme is required for actual production. However, for industrial applications, the pure enzyme is often not suitable for direct application in a process and/or it is not economically feasible to apply free purified enzymes in the process. In such cases, other formulations and immobilization techniques need to be exploited and characterized. Therefore, an essential aspect is the general applicability of microfluidics, i.e. a requirement is that it is easy and fast to characterize different biocatalyst formulations, which in most cases is easily performed in conventional batch experiments. Conceptually, microfluidics can be applied to test various immobilization forms, but different formulations will give altered fluid dynamics behavior that has to be taken into account and considered carefully. For example, formulations with the biocatalyst freely in suspension will cause the flow dynamics in microfluidics to be dominated by diffusion, and dispersive effects will become prominent which will make it time consuming to reach steady state when introducing step changes (explained in detail in chapter 2). On the other hand, this is also a strong motivation for characterizing immobilized biocatalysts in a microfluidic PBR as this application is solely dependent on the fluid dynamic behavior of the relatively fast diffusing reaction species compared to the slowly diffusing proteins. However, for immobilized forms other effects may cause altered and unpredictable fluid dynamic behavior, e.g. packing density and channeling effects. A result of this will be erroneous information about the catalyst performance and activity. However, despite these effects it may still be feasible and fast to apply microfluidics to determine the relative biocatalyst performance under various process conditions, e.g. test the relative influence of temperature, pH, and component concentrations, in a similar way as a HPLC operates, and determine relative concentrations based on external standards.

That being said, it is important to emphasize that despite the benefits associated with application of microfluidics for characterization of biocatalysts demonstrated in this chapter, this technology is not always the ideal choice. In many cases, it may be easier, faster and more reliable to characterize the biocatalyst in conventional batch experiment based methods. The latter is especially the case when it is required to determine accurate kinetics of the biocatalyst, which in microfluidic systems would be greatly influenced by the fluid dynamics while small scale batch systems many times are operated such that they form close to homogeneous mixtures.

In addition, when operating with biocatalyst formulations that are free in the reaction media it is required to quench the reaction at the outlet of the reactor. As such, it is easy to quench the reaction in microfluidics, e.g. by implementation of heated spots/segments and/or to quench it by acid or base through feeding such solutions immediately after the reactor modules.

Applying biocatalysts in suspension in the on-line HPLC system gives problems related to the fact that dirty samples are injected to the column, and hence reduced column lifetime is the result. Applying immobilized biocatalysts in PBR modules will overcome this issue, but it requires that the biocatalyst is stable for longer

periods so the module can be operated for a longer time before replacement is required. A significant problem of applying PBR modules is the issue of flushing out gas bubbles. The latter can be difficult, and for non-transparent systems, it might be an issue to verify whether bubbles appear. An alternative to the HPLC system would be to implement spectroscopic methods (UV, NIR, MIR, FTIR, Raman etc.) combined with chemometrics instead of having a column to do the separation of the amines and ketones. Such implementation would increase the throughput of the microfluidic systems. However, with implementation of such analytical methods it might be easier, more flexible, faster and more reliable to consider operating with microtiter plates. The exception to this would be when continuous flow applications, e.g. PBR and PFR, are considered.

5.8 Conclusion

In this chapter, the applicability of microfluidic reactor modules for characterization of novel biocatalysts was investigated in detail. It was found in this work that the main advantage of applying microfluidics for such characterization is the possibility of performing extensive testing of various process conditions, i.e. one can find optimal operating conditions in an easy manner using relatively small quantities of available resources. Limitations to the application of microfluidics for characterization were also identified and discussed, e.g. the fluid dynamics in microfluidics make it challenging to develop generally applicable kinetic models.

The advantages were demonstrated through characterization of immobilized biocatalysts, i.e. two ATA mutants (ATA-50 and ATA-82) entrapped in lentil shaped polyvinyl alcohol (PVA) particles, in specific microfluidic packed bed reactor modules. The reaction of interest was the asymmetric synthesis of the chiral amine 1-methyl-3-phenylpropylamine (MPPA) from benzylacetone (BA) using isopropylamine (IPA) as the amine donor. For both biocatalysts, the inhibitory nature of the products was identified and it was found reasonable to consider development and implementation of ISPR strategies as a means to overcome these effects. Furthermore, the performed characterization gave indications of optimal operating conditions in terms of concentrations of substrates for the biocatalysts.

In relation to these characterizations, an on-line HPLC system was installed to perform the characterization of two amine transaminases (ATAs), i.e. ATA-50 and ATA-82, in an automated manner. Furthermore, this experimental setup is recognized to significantly reduce manual activities related to characterization of the biocatalysts. For example, no sample handling, preparation and/or transportation were required during the characterizations, i.e. only stock solutions and reactor modules needed to be prepared.

Chapter 6

Characterization of microfluidic liquid-liquid extraction modules

In the development of biocatalytic processes, considerable emphasis is put into development of the biocatalyst and well performing reactors. However, it is equally important to consider in the development how to recover the product efficiently at reasonable costs. This is especially the case, where it is required to implement *in-situ* product removal (ISPR) strategies (the selective removal of product during the reaction course) to overcome some process challenges, such as severe inhibitory effects caused by the product(s). This issue was discussed in detail in chapter 4.

In this chapter, the potential of applying microfluidics in the development of product recovery strategies for amine transaminase (ATA) based processes based on liquid-liquid extraction (LLE) is illustrated. LLE is commonly applied for recovery of chiral amines, and ATAs are known to experience severe inhibition by the product, which was also underlined in chapter 5. More precisely the focus in this chapter is on the characterization of single step microfluidic LLE modular units for putting in place a two-step LLE ISPR concept for extraction of hydrophobic chiral amine products from ATA processes, which is described in detail in chapter 4 and highlighted here in Figure 6.1. Chosen as case study is the ATA facilitated asymmetric synthesis of MPPA from BA, using IPA as the amine donor. The latter was also introduced in chapter 4, as case study 2, which is again shown here as Scheme 6.1.

The performed characterization of the LLE modules is based on both conventional batch and microfluidic methods. It was found that multiple solvents give selective separation of MPPA relative to the other investigated reaction species. From these solvents, undecane was found to be the best choice for this application. Issues of simultaneous removal of BA in the extraction steps were overcome by dissolving 1 M BA in undecane, which enabled applying the extraction steps for feeding the main substrate (BA) as well.

Furthermore, it was found that applying microfluidics in the development of extraction steps gives some significant advantages in terms of ease of use, high throughput and fast optimization of extraction steps. In addition, it was established that implementation of spectroscopic based analytical methods will enable easy and somewhat reliable determination of the overall mass transfer coefficients in the microfluidic extraction modules.

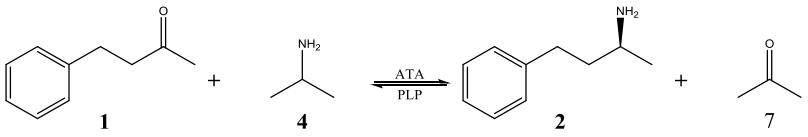

Scheme 6.1: General ATA reaction scheme for the synthesis of 1-methyl-3phenylpropylamine (MPPA(2)) from benzylacetone (BA(1)) using isopropylamine (IPA(4)) as the amine donor. The co-product of this synthesis route is acetone (Ace(7)).

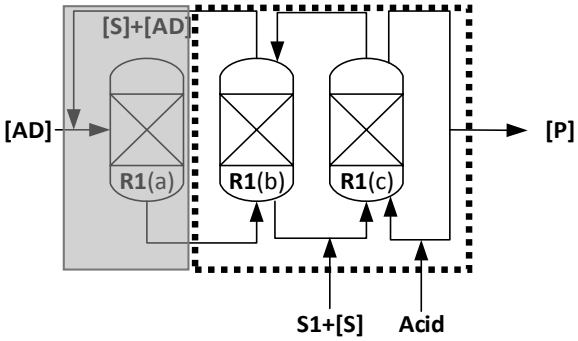

Figure 6.1: Flowsheet of the two-step liquid-liquid extraction ISPR concept for selective removal of hydrophobic amines from ATA processes, which was introduced in chapter 4. This chapter will solely focus on the liquid-liquid extraction modules as indicated with the dashed box in the figure. [AD]: Amine donor, [S]: substrate, S1: solvent, [P]: product, R1(a): reactor module, R1(b): 1st LLE module (High pH ~9.5) and R1(c) 2nd LLE module (Low pH ~3).

6.1 Introduction

As proposed in chapter 4, for case study 2 with IPA as the amine donor to form MPPA, the focus here is to apply a solvent bridge concept in a two-step LLE operational mode as an ISPR concept to remove the inhibitory product MPPA. LLE is applied as MPPA is hydrophobic relative to the hydrophilic IPA. In addition, LLE is commonly applied for extraction of amine compounds from aqueous solutions [126,154,155,157,158,177,178]. Furthermore, it is possible to protonate both amines, thereby opening up for selective separation of the amines from the ketone compounds involved in the reaction. However, before testing the combined system it is required to characterize the two LLE steps and specify the required capacity of the individual LLE modules, which is the aim of this chapter.

LLE is a well-developed separation method in the chemical industry that is based upon exploiting the relative solubility of compounds in two immiscible liquids [179]. The performance of the LLE modules can be evaluated by identifying the selectivity, partitioning and mass transfer of all the reaction species between the two immiscible liquids in each extraction step at the desired operational conditions. The general metrics applied to describe the selectivity and partitioning of each component in the system are described in chapter 4, while the mass transfer theory is described here (section 6.1.1). Knowledge of the mass transfer between the phases is important, as it will dictate the design and sizing of the extraction units, e.g. size of the extraction modules required to achieve equilibrium in each extraction step. In this chapter, these parameters are determined based upon a combination of microfluidic and conventional lab scale batch experiments. The motivation for this combination is that in conventional batch experiments, it is easy to get an idea about the equilibrium concentrations (identifying partitioning and selectivity), while microsystems are highly applicable to determine mass transfer rates and test various operating conditions in an easy manner.

6.1.1 Mass transfer theory

The driving force in LLE is the concentration difference of a specific compound between two liquids, e.g. a liquid containing the compound of interest and an extracting liquid with larger affinity for that specific compound. The velocity of the mass transfer between the liquids is dependent on the diffusion of the extracted compound. This transfer can be generally described by Fick's law of molecular diffusion [77]:

$$N_{i_x} = -D_{ab,i}\frac{dc_i}{dx} \qquad \text{(Eq. 6.1)}$$

, where $N_{i_x}\left[\frac{mol}{m^2 s}\right]$ is the flux of component i, in the x [m] length direction. $D_{ab,i}\left[\frac{m^2}{s}\right]$ is the diffusion coefficient of solute a (i) in b and $c_i\left[\frac{mol}{m^3}\right]$ is the molar concentration, both of component i.

There are several theories describing the mechanism of mass transfer between the two liquid phases, taking into account the mass transfer resistance effects at the liquid-liquid interface, i.e. the film, penetration, surface-renewal and film-penetration theories [179]. All these theories have in common that they assume well-mixed bulk phases and address the aspect of the gradient appearing close to the interface. In each theory, a mechanism representing resistance to mass transfer at the phase interface is described. However, since it is difficult to measure on the actual phase interface mechanistic behavior, it is convenient to determine the mass transfer in terms of overall mass transfer coefficients, which can be described by [179–181]:

$$\frac{dC_{i,L_1}(t)}{dt} = K_{L,i}a\left(C^*_{i,L_1} - C_{i,L_1}(t)\right) \quad \text{(Eq. 6.2)}$$

, where $K_{L,i}a$ $[s^{-1}]$ is the overall mass transfer coefficient of a component i, from phase L_1 [-] to the extracting phase. C^*_{i,L_1} $[mol/m^3]$ and $C_{i,L_1}(t)$ $[mol/m^3]$ represent the equilibrium concentration at the phase interface and the time dependent concentrations of component i in phase L_1, respectively.

From the above expression for the mass transfer, it is clear that the extraction is limited by the phase equilibrium, which is a direct function of the partition coefficient. Hence, for $t \gg 0$ s the system goes towards equilibrium and the partition coefficient (PC) can be described as:

$$PC_i = \frac{C^*_{i,L_2}}{C^*_{i,L_1}} \Leftrightarrow \quad \text{(Eq. 6.3)}$$

$$PC_i = \frac{\left(C_{i,L_1}(t=0) - C^*_{i,L_1}\right)}{C^*_{i,L_1}} \quad \text{(Eq. 6.4)}$$

, where C^*_{i,L_2} $[mol/m^3]$ is the equilibrium concentration of component i in the extracting phase L_2. Equation 6.4 assumes that the change in concentration over time is solely caused by the extraction from L_1 into L_2, which is assumed because only the aqueous phases are analyzed in this work. The expression is applied in combination with the experimental data to evaluate the extraction performance of the screened solvents.

6.1.2 Microfluidic extraction phenomena

In chapter 2, a general introduction to different multi-phase flow phenomena that occur in microfluidics was given. Two of the presented phenomena are of special interest for the characterization of LLE modules, i.e. slug and side-by-side flow scenarios, because it is possible to predict the phase interfacial area to volume ratio rather accurately based on the slug size and system dimensions. In Figure 6.2, the general concept of the two types of flow and the associated mass transfer effects are illustrated.

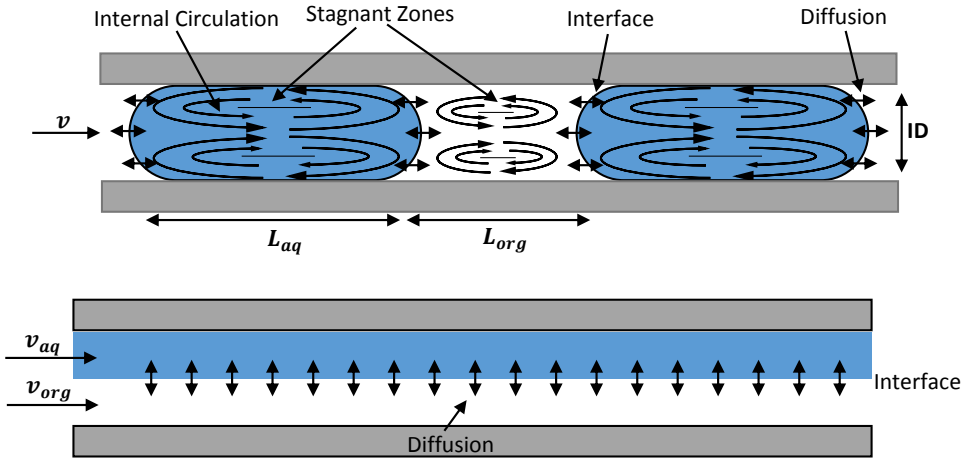

Figure 6.2: Droplet/slug (top) and side-by-side (bottom) flow extraction concepts in microfluidics.

In the case of side-by-side laminar flow applications, the mass transfer is solely based on diffusion through and in between the two fluids. The interface area and curvature between the two phases is determined based on the pressure difference (ΔP_F) and the Laplace pressure (ΔP_L) caused by the interfacial tension between the two phases that stabilizes the phase interface, respectively. ΔP_F can be determined by applying the Hagen-Poiseulle equation, introduced in chapter 2, for each phase. The Laplace pressure is restricted as follows, for parallel multi-phase flows [71]:

$$\frac{2\sigma\sin(\theta_{re}-90°)}{d} < \Delta P_L < \frac{2\sigma\sin(\theta_{ad}-90°)}{d} \quad \text{(Eq. 6.5)}$$

, where d $[m]$ is the depth of the microchannel, and θ_{re} and θ_{ad} are the receding and advancing contact angles of the organic phase.

As long as ΔP_F is between the higher and lower limits of ΔP_L it should be possible to maintain the parallel multi-phase microflows. The side-by-side flow can also be stabilized by having a combination of hydrophobic and hydrophilic channels [182] and/or structural support in parts of the channel [183].

In the case of slug flow applications, the mass transfer will be dominated by the diffusion at the phase interfaces at the ends of the slugs and by internal mixing in the droplets. The internal mixing effects in the droplets are also known as Hadamard-Ryczniski circulation, which is illustrated in Figure 6.2 [77]. Another effect that might occur in microscale slugs are Marangoni effects, which are caused by surface tension gradients in the slugs, that potentially influence the mass transfer rate of the slugs significantly [77,88,92,179]. It is therefore important to keep in mind that measured mass transfer coefficients in micro slugs, influenced by Marangoni effects, will make the values unreliable across scales.

In this work, it was chosen to apply standard hydrophilic polytetrafluoroethylene (PTFE) tubing. This choice was based on the good chemical resistance, the low cost, the compatibility with the applied pumps and the easy handling of PTFE tubing relative to fabrication of specific microfluidic chips and/or glass capillaries. The hydrophilic behavior and pressure drop in the channels gave cause to the formation of aqueous slugs in the applied standard tubes. This is illustrated in Figure 6.3. Furthermore, side-by-side flow scenarios can result in inaccurate prediction of the mass transfer because of different flow velocity profiles in the two liquid phases caused by viscosity differences [184]. Unless the flow velocity profiles are known this is difficult to take into account.

Based on the measured droplet dimensions presented in Figure 6.3, it was possible to determine some characteristic dimensional features of the droplets in the tubes at various flow rates. These features are important for identifying and characterizing different dimensional characteristics of the formed slugs, which will have an impact on the mass transfer in the microfluidic LLE modules. The measured and calculated dimensional features are presented in Table 6.1. The low capillary numbers form a strong indication that these tubes are operated in the squeezing flow regime, hence the formation of slugs (theory described in chapter 2). Furthermore, it is noteworthy that the slug length to diameter ratio increases as the inner diameter (ID) of the tubes decreases, which causes the surface area (where mass transfer occurs) to volume ratio to decrease alongside the ID. This effect is represented in Figure 6.4. This effect needs to be taken into account when comparing measured mass transfer coefficients, as it might have a severe impact on the mass transfer occurring in extraction experiments with small ID tubing. For the rest of this work these

characteristics will be applied, bearing in mind that there might be small deviations in the slug size and slug length distribution at various flow rates. The slug lengths can be influenced by varying the flow rates, relative to one another, but further investigation of such effects was considered to be outside the scope of this work.

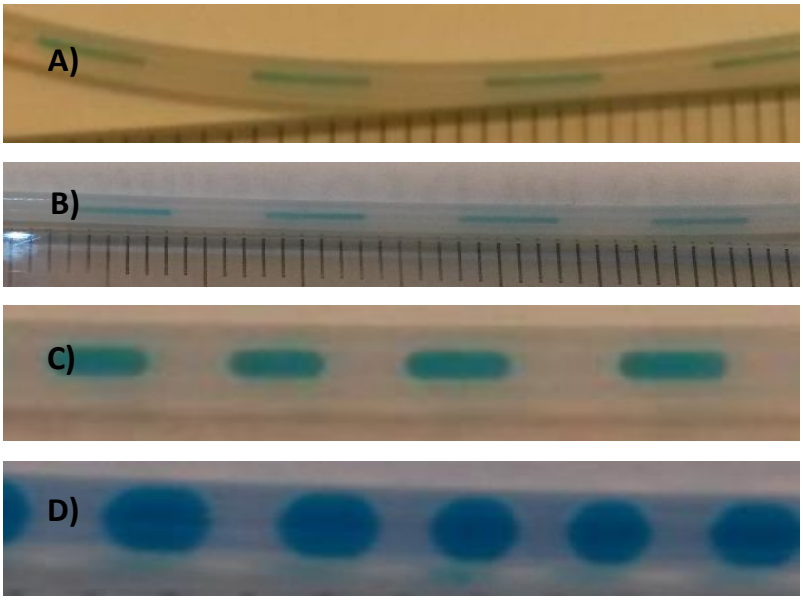

Figure 6.3: Influence of tube inner diameter (ID) on the slug length, aqueous blue slugs and transparent undecane fluid segments, for 4 different tube diameters: A) 170 µm ID gave ~4 mm slugs, B) 250 µm ID gave ~5 mm slugs, C) 500 µm gave ~1.5 mm slugs and D) 1000 µm gave ~1mm droplets/slugs.

Table 6.1: Measured and calculated features of slugs formed in PTFE tubing of various inner diameter (ID) when mixing water and undecane at various flow rates (25-1000 µL/min). The Capillary number was introduced in chapter 2 ($\mu = 0.001\ Pa \cdot s$ [185] and $\sigma = 0.025\ N/m$ [153]).

ID	L_{slug}	L/ID	A_{sphere}	V_{slug}	a	v	Ca
µm	mm	-	mm^2	µL	m^2/m^3	µL/min	$\cdot 10^{-7}$
170	4.5	26.5	0.09	0.10	889	25-400	$1.8 - 29.0$
250	5	20	0.20	0.25	800	25-400	$0.8 - 14$
500	1.5	3	0.79	0.29	2667	25-500	$0.2 - 4.2$
1000	1	1	3.14	0.79	4000	25-500	$0.1 - 1.1$

Note: The phase interface where mass transfer occurs is assumed only to be located in both ends of the slugs. The ends are furthermore assumed spherical for each droplet and the volume of the slugs is then estimated by assuming cylindrical slugs.

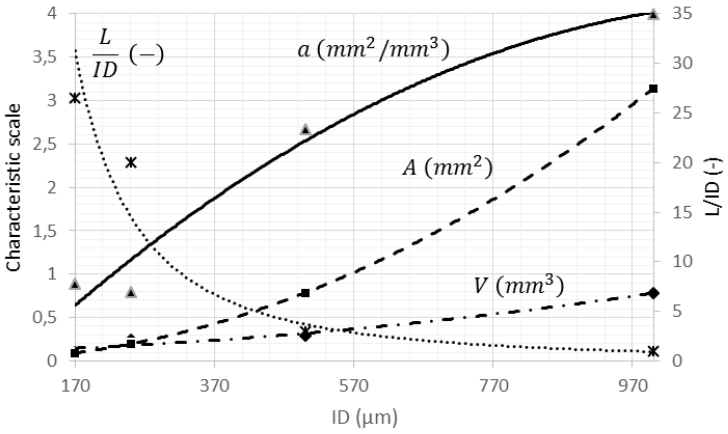

Figure 6.4: Representation of the increasing slug lengths with decreasing inner diameter (ID) (L/ID, which follows the right hand side y-axis) and the impact it has on the area to volume ratio of the slugs in the tubes.

6.2 Solvent selection

For LLE applications, it is important to select a solvent that performs the desired separation satisfactorily, e.g. sufficient selectivity and partitioning. However, also other aspects in the choice of solvent need to be addressed. For example, aspects such as safety, environmental impact, separation efficiency, recyclability, enzyme compatibility and costs need to be considered as well. In the scientific literature there are multiple methods and guides for selecting appropriate solvents [186–188]. Highlighted below are a few important considerations related to the choice of a solvent for a particular application:

Safety, health & Environment: A point of concern when deciding to apply a specific solvent in a given process and/or during development are the safety, health and environmental risks associated with handling and operating the process with the given solvent [186,189]. For example, carcinogenic solvents potentially impose unnecessary health risks, explosive/highly flammable solvents may impose unnecessary safety risks, and some solvents have severe toxic effects on the environment. It should therefore always be the aim, when applying solvents, to apply solvents where these issues do not cause any concerns. However, for some applications, it may not be possible to avoid solvents that cause such concerns and appropriate precautions need to be made.

Solvent separation: From an operational point of view, it is important to select a solvent that is easy to handle, allowing easy product recovery, and in some cases, the solvent should be easy to recycle as well. For example, if the solvent of choice causes formation of emulsions the phase separation can be difficult. Furthermore, if the solvent is not selective and difficult to separate from the product(s), e.g. by distillation, it may not be suitable. In addition, if the chosen solvent is costly it may be a requirement to have efficient solvent separation and recovery to ensure that it can be recycled multiple times. For pharmaceutical applications, it may not always be possible to recycle the solvent,

e.g. potential cross-contamination is to be avoided, and it might be difficult to get approval from regulatory authorities.

Biocatalyst Compatibility: Solvents can have toxic effects on the applied biocatalysts, which can significantly reduce the stability and thereby greatly inactivate/denature the catalyst over short time periods. In general, such toxic effects can be divided into two categories:

1. Inactivation/denaturation caused by the phase interface between two immiscible fluids, which also motivates separation of the biocatalyst before the LLE. This form of inactivation/denaturation only occurs when operating with immiscible fluids.
2. Inactivation/denaturation caused by dissolved solvent in the aqueous reaction media, where the effect will depend on the hydrophobicity ($logP$). This form of inactivation/denaturation can be experienced with both water miscible and immiscible solvents. In the scientific literature, it is argued that high relative water-octanol partition coefficients, $logP > \sim 4$, are prone to have minor toxic effects on biocatalysts relative to solvents with lower partition coefficients [190,191].

Inertness: Another compatibility aspect is the inertness of the chosen solvent. It is important that the chosen solvent does not intervene with the desired reaction, i.e. the biocatalyst should not have affinity for the solvent and thereby cause the solvent and substrate(s) to compete. Furthermore, it is important that the chosen solvent does not react in an uncontrolled manner with the substrates and/or products resulting in the formation of unwanted side-products.

Considering these aspects in addition to the methods, guidelines and reported solvents in the scientific literature [143,186–188] a list of 5 solvents was chosen for further testing. The list is shown in Table 6.2. Solvents with a range of different $logP$ values were chosen to identify how the polarity of the solvents influences the separation performance. Furthermore, one of the chosen solvents is the main substrate (BA) applied in the investigated case study (case study 2), which ideally will decrease the complexity of the process if suitable for the extraction.

Table 6.2: List of selected solvents focused on in this work [153].

Solvents	$logP$	ρ	$Aq.Sol.$	P_{vap}	T_b	T_F	σ
-	$[-]$	$\left[\frac{g}{cm^3}\right]$	$\left[\frac{mg}{L}\right]$	$[mmHg]$	[°C]	[°C]	$[mN/m]$
BA	1.671	1	1625	0.1	235-237	105	34.2
Undecane	6.60	0.7	0.2571	0.6	196	60	25
Heptane	4.47	0.7	3.554	45.2	97-99	-4	21.6
Xylene	3.12	0.9	242.4	7	143-145	32	28.8
Toluene	2.73	0.9	573.1	21	111	4	28.8

6.3 Experimental methods

A combination of conventional batch and microfluidic experiments was performed to characterize the extraction performance of the chosen solvents.

6.3.1 Chemicals

Benzylacetone (BA; synthesis grade; Cas no. 2550-26-7) was purchased from Merck KGaA. Potassium carbonate (99+%; Cas no. 584-08-7) was purchased from Acros Organics. All other chemicals were purchased from Sigma-Aldrich: 1-Methyl-3-phenylpropylamine (MPPA; 98%; Cas no. 22374-89-6). Pyridoxal 5'-phosphate monohydrate (PLP; ≥97.0%; Cas no. 41468-25-1). Acetone (Ace; ≥99.5%; Cas no. 67-64-1). Isopropylamine (IPA; ≥99.5%; Cas no.75-31-0). Citric acid monohydrate (99.5-102%, Cas no. 5949-29-1). Sodium citrate dehydrate (≥99%; Cas no. 6132-04-3). Sodium bicarbonate (99.5-100.5%; Cas no. 144-55-8). Undecane (≥ 99%; Cas no. 1120-21-4). Xylenes (Cas no. 1330-20-7). Toluene (≥99.5%; Cas no. 108-88-3). Heptane (HPLC grade; ≥99%; Cas no. 142-82-5).

6.3.2 Equipment

The pumps used in the experimental set-ups were TECAN cavro® XLP6000 pumps (Tecan Systems Inc., San Jose, CA, USA) equipped with TECAN cavro® XLP 250 µL syringes (Tecan Systems Inc., San Jose, CA, USA). The applied tubing for the systems was PTFE based. Standard HPLC PEEK fittings and connectors were used to connect pumps, tubing and micro-scale modules. These items were purchased from Mikrolab Aarhus A/S (Højbjerg, Denmark). Sampling was performed with a 10 µL 10F syringe (SGE Analytical Science, Trajan Scientific Australia Pty Ltd).

6.3.3 Analytical methods

The concentration of the substrates and products in aqueous solutions was determined by HPLC (Dionex Ultimate 3000) with UV detection (Dionex Ultimate 3000 PDA detector). One method was applied for the separation of benzylacetone (BA) and 1-methyl-3-phenylpropylamine (MPPA) and another method was applied to separate isopropylamine (IPA) and acetone (Ace). Both methods are isocratic and operate at 30°C with the same column, i.e. a Gemini-NX C18 column (100mmx2mm, 3µm, 110Å, Phenomenex, Torrance, CA, USA). The first method is operated with a flow rate of 0.450 mL/min with a mobile phase consisting of 35% acetonitrile and 65% Milli-Q water adjusted to pH 11 with NaOH. The retention times for MPPA and BA were 2.9 min and 3.6 min, respectively. Both BA and MPPA are detected at 215 nm. The second method is operated with a flow rate of 0.300 mL/min with a mobile phase consisting of 5% acetonitrile and 95% Milli-Q water adjusted to pH 11 with NaOH. The retention times for Ace and IPA were 1.6 min and 2.7 min, respectively. Acetone is detected at 265 nm, while IPA is detected at 200 nm.

6.3.4 Batch experiments

The performed batch experiments were based on the methodology published by Grey et al. [143]. Mixtures of the different reaction species, from case study 2 (IPA, Ace, BA, MPPA), were fully dissolved in aqueous solutions containing either 100 mM citrate based buffer (pH 3) or 100 mM carbonate based buffer (pH 9.5).

The pH of the mixtures were adjusted with HCl after the addition of the reaction species. Each of the two buffer solutions represents the aqueous mixture in one of the LLE modules. The aqueous solutions are mixed with the organic solvents (volume ratio 1:1, total volume 2 mL) and shaken (900 rpm) for 24 hours at $30℃$ using a thermomixer (HLC BioTech Model MHR 11, Germany). After 24 hours of mixing, the samples are left to phase separate (o rpm) for an additional 24 hours at $30℃$ on the thermomixer. 100 µL samples are then extracted from the aqueous phases and analyzed by HPLC-UV. The organic phases are not analyzed. Hence, the mass balances are closed by assuming that the extracted compounds are located in the solvents, i.e. assuming insignificant quantities of the reaction species in the headspace of the vials. Experiments are performed in triplicate.

6.3.5 Microfluidic experiments

The characterization of the microfluidic LLE modules is based on forming slugs by combining streams of aqueous mixtures with streams of the different solvents in a standard PEEK Y-connector at the entrance to the PTFE LLE modules (the volume ratio remained 1:1). The same types of aqueous mixtures as for the batch experiments are applied. The characterization of the modules is performed by varying the flow rates of the applied syringe pumps (TECAN Cavro® XLP6000 pumps, 250 µL syringes, Tecan Systems Inc., USA) and varying the dimensions of the LLE modules (varying length and varying inner diameters), giving a range of mixing times and behavior. The different inner diameters of the applied PTFE tubes are highlighted in Table 6.1. The slugs in the microfluidic LLE modules are separated in a mini settler at the outlet of the modules (borosilicate HPLC glass vials with micro inserts, 200µL), similar to how Zhao et al. [192] separated the phases. The settlers are long and thin to minimize additional extraction of the reaction species while filling the settler (small surface to volume ratio). 10 µL samples are extracted from the aqueous phases and analyzed by HPLC-UV. The organic phases are not analyzed. Hence, it is necessary to close the mass balances by assuming that the extracted compounds are located in the solvents. The experiments are performed in triplicate at ambient temperatures. i.e. $22 \pm 1℃$. The experimental setup is sketched in Figure 6.5. For experiments, where the amine(s) is initially added to the solvent, the pH cannot be adjusted during the extraction of the amine, and hence the successful execution of these experiments is dependent on the fact that the applied amine concentrations do not exceed the buffer strength.

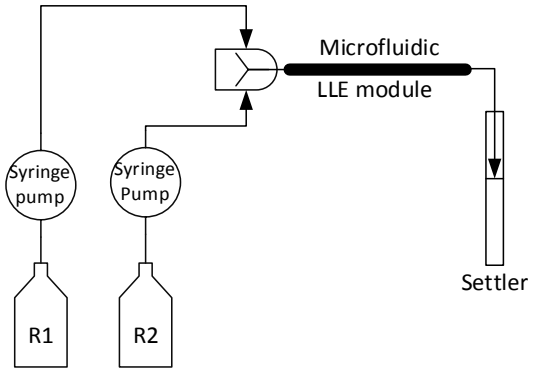

Figure 6.5: Microfluidic LLE characterization experimental setup, where R1 and R2 corresponds to the reservoirs containing the aqueous and solvent solutions, respectively.

6.4 Results: Preliminary solvent screening

The first step in the implementation of the proposed LLE based ISPR option is to identify the most suitable solvent from the list of selected solvents from section 6.2. It is therefore required to do some basic characterization experiments identifying the partitioning and selectivity of the various solvents. Furthermore, these basic characterization experiments give a good indication of potential operational problems with the applied solvents.

6.4.1 Influence of pH

An important aspect in the driving force of the two-step LLE ISPR configuration is the pH in the two aqueous reservoirs. In the first extraction step, it is required to operate the aqueous phase at a pH close to or above the pK_a value of the amine of interest. This will ensure that a sufficient fraction of the amine is uncharged and will thereby drive the extraction into the chosen solvent [193]. In Figure 6.6, it is shown how the pH influences the fraction of uncharged amines at various pH values for IPA and MPPA. There is no significant difference in the pK_avalues of IPA and MPPA and thereby the selectivity of the extraction of MPPA is solely dependent on the differences in the hydrophobicity. Hence, the optimal pH for extraction for this reaction system is dependent on the optimal pH for the biocatalyst. However, since the characterization of ATA-82, in chapter 5, was performed at pH 9.5 and was found to be active and somewhat stable at this pH, this pH value is also chosen for further testing. It should be noted that BIOINTENSE partner ULUND investigated the performance of the wild type ATA-50 at various pH values and found this catalyst to have optimal performance at pH ~8. However, at pH 8 almost all the present MPPA will be in the charged form and the driving force for the extraction will be reduced, which is another reason why pH 9.5 is chosen here. Future work should focus on coupling the extraction and biocatalyst pH dependence to identify optimal pH operational conditions.

In the second extraction step, it is important that the pH is kept well below the pK_a value of the amine of interest. This will ensure that the amine is charged and thereby drive the extraction into the aqueous phase, which is why it is chosen to operate with pH 3 ($pH\ 3\ << pK_a\ 10.63$ for MPPA).

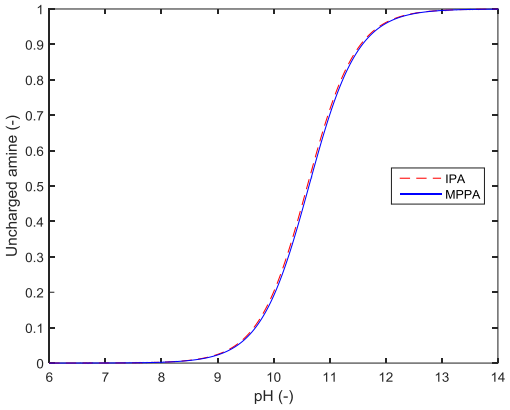

Figure 6.6: Influence of pH on the distribution of uncharged amines in solution.

6.4.2 Solvent screening

For the selected solvents, an initial screening was performed to identify the partition coefficients and selectivity of the various reaction species in the given solvents. The screening was performed with aqueous mixtures with pH ~3 and pH ~9.5 using 100 mM citrate and 100 mM carbonate based buffers, respectively. The screening was performed in batch experiments following the procedure described in section 6.3.4 and in triplicate.

6.4.2.1 BA extraction

Firstly, the partitioning of BA was investigated to identify the impact of the extraction steps on unreacted BA from the reactor module. The results are listed in Table 6.3.

The results show that the aromatic solvents that have similar structure to BA (xylene and toluene) have a high affinity for BA and will thereby extract the remaining BA. On the other hand, applying solvents like undecane and heptane will minimize the BA loss during operation relative to xylene and toluene due to the lower affinity. Another aspect is to apply BA as the solvent that, as long as it is possible to recycle BA extensively, will make it possible to minimize overall BA losses.

Table 6.3: BA partitioning coefficients (PC) in various solvents, ~10 mM BA dissolved in aqueous buffer solutions at 30 °C.

Solvent	pH 3.13	pH 9.45
BA	-	-
Undecane	30.6 ± 0.7	26.3 ± 0.3
Xylene	147 ± 27	137 ± 35
Toluene	230 ± 94	146 ± 32
Heptane	33.4 ± 2.5	29.1 ± 1.0

6.4.2.2 Amine extraction

In addition, a screening of the partitioning of the other reaction species in the various solvents was performed. Extraction of BA was not considered in the calculation of the selectivity of the solvent. The reason for not including BA in the estimation of the selectivity was because it was desirable to obtain a relative measure of the selectivity for the other reaction species. Furthermore, it was the intention to feed BA to the aqueous solutions through the solvent. The results for the first extraction step (pH 9.5) are shown in Table 6.4.

These results also indicate that the aromatic solvents (BA, xylene and heptane) have a high affinity for extracting MPPA. Furthermore, BA was found to have the highest affinity for MPPA making it ideally suited for applying the main substrate BA as the extracting solvent in terms of good separation of the main product. However, there are operational aspects that make it challenging to apply BA, which is discussed further in section 6.4.4. An important feature of all the solvents is their relatively low affinity for IPA, ensuring high extraction selectivity for MPPA at pH 9.5, i.e. $s_{MPPA} \geq 87.0\%$. High affinity for IPA would cause severe losses of IPA during the extraction. This feature will enable the possibility to apply a large excess of IPA on the reaction side of the ISPR setup and recycle IPA to improve the atom efficiency. The affinity for acetone is also low. However, acetone build-up is not considered a severe issue in the specific case study, as ATA-82 seemed to be able to handle relatively large quantities before a significant loss in activity was experienced, see also chapter 5. Furthermore, at higher acetone concentrations it becomes relatively easy to selectively strip off the majority of the formed acetone, e.g. Tufvesson et al. [135] easily stripped off all acetone higher than 20 to 30 mM.

Experimental results for the second extraction step (pH 3) indicated the partition coefficients to approach 0 for MPPA. Values of the partition coefficients were found in the range of [0.006:0.02] for all solvents. This means that the majority of the extracted MPPA from the first extraction step will be extracted into the low pH reservoir. This is also as expected, and it is common that the amines have a high affinity for acidic aqueous phases [143,157,158]. It is expected that IPA will behave similarly as MPPA, i.e. IPA extracted in the first extraction step will extract into the acidic aqueous phase in the second extraction step [143]. The acetone partitioning is not expected to be influenced by changing pH.

Table 6.4: Measured partition coefficients and selectivity, in various solvents, of 441 ± 9 *mM IPA,* 34.2 ± 0.4 *mM Ace and* 8.95 ± 0.02 *mM MPPA at 30 ℃ and pH 9.53.*

Solvent		PC_i [-]	s_i [%]
BA	IPA	0.10 ± 0.04	0.2
	Ace	1.24 ± 0.05	2.2
	MPPA	55.82 ± 9.74	97.7
Undecane	IPA	0.03 ± 0.02	1.6
	Ace	0.17 ± 0.00	8.4
	MPPA	1.83 ± 0.01	90.0
Xylene	IPA	0.11 ± 0.02	1.0
	Ace	0.73 ± 0.01	7.0
	MPPA	9.56 ± 0.65	92.0
Toluene	IPA	0.09 ± 0.03	0.7
	Ace	0.86 ± 0.08	6.5
	MPPA	12.21 ± 0.70	92.8
Heptane	IPA	0.07 ± 0.02	2.6
	Ace	0.26 ± 0.04	10.4
	MPPA	2.20 ± 0.05	87.0

An issue with this characterization procedure is that the performed experiments are based on having the components dissolved in the acidic aqueous solutions at the start of the experiment. Therefore, a similar test was performed with the components initially present in undecane, with 1 M BA, which is similar to the way Peng et al. [158] did their investigations. The thermodynamics are not dependent on the initial location of the reaction species, which the results from Peng et al. also indicated, but the water solubility in the solvent is suspected to influence the degree of protonation and thereby the extraction. In this work it was found that performing the extraction experiments in the reverse direction caused the partition coefficients to differ from the initially found values, i.e. $PC_{MPPA} = 0.7 \pm 0.1$ and $PC_{Ace} = 0.7 \pm 0.2$. The analytical method did not enable reliable detection of IPA in the aqueous phase.

The cause of this deviation is suspected to be linked with the highly hydrophobic behavior of undecane ($log\ P\ =\ 6.6$), which is causing limited quantities of acid to dissolve in the solvent in order to protonate and extract the amines. In comparison, Peng et al. applied solvents with more hydrophilic nature (log P < 2). Rehn et al. [143] tested undecane, but only reported the partitioning of the extraction from the acidic aqueous solution to the solvent. For future work, it could be interesting to test the influence of ionic strength of the acid solution on the partitioning and investigate how it will affect the partitioning.

6.4.3 Influence of buffer

In the scientific literature, it has previously been pointed out that the applied buffer and/or acid concentration can significantly influence the partitioning between the phases [154]. Therefore, a simple set of tests was performed to investigate the influence of the applied buffers and the initial concentration of the reaction species on the extraction performance. For example, will high buffer concentrations cause

significant effects on the partitioning or vice versa? The reason for applying buffers for these extraction experiments in the first place, is due to the basic nature of the amines that will influence the pH and the extraction, where the result of the latter operation is pH dependent. The experiments are based on testing how different buffer concentrations in mixtures containing MPPA (~40 mM) influence the extraction. The standard mixtures are prepared with and without buffer to identify the influence of the buffer. The solutions containing buffer were prepared at pH 3 (100 mM citrate buffer) and pH 9.5 (100 mM carbonate buffer), while for the solutions without buffer the pH was adjusted to pH 3 and pH 9.5 by addition of HCl and NaOH respectively. BA was applied as solvent for these extraction experiments. The prepared solutions containing MPPA with and without buffer were diluted with a solution not containing MPPA and buffers, to see how it influenced the extraction. The dilution factor (DF [-]) is determined by:

$$DF = \frac{V_{total}}{V_{mix}} = \frac{V_{aq}+V_{mix}}{V_{mix}} \quad \text{(Eq. 6.6)}$$

The results from these experiments are shown in Figure 6.7. Noteworthy, these results indicate that the buffer does not have a significant impact on the extraction of MPPA. Additionally, these results once again underline that the amines tend to remain in the acidic aqueous solution. However, these experiments were also based on extraction from the aqueous solutions into BA and not the other way around. In contrast to undecane, then BA is not as hydrophobic and thereby the water content in BA might be higher and have less influence on the partitioning, as the protonation of the amines might be higher.

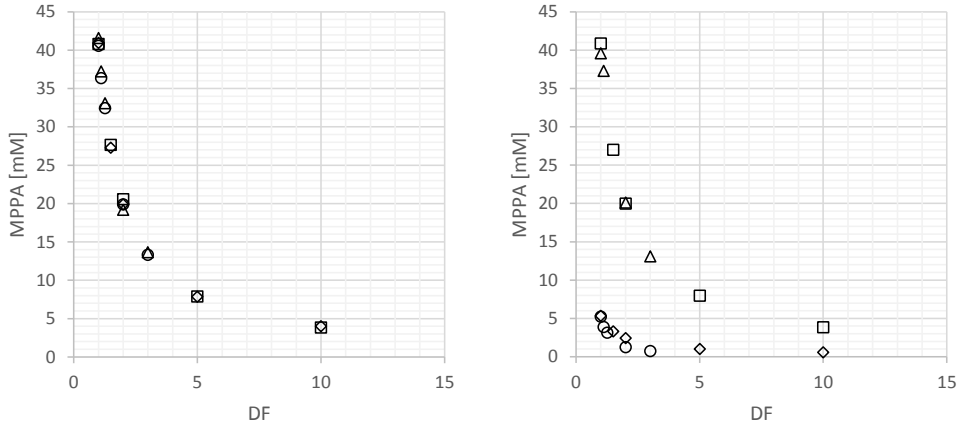

Figure 6.7: Experimental results indicating the influence of the buffer, relative to no buffer, on the MPPA extraction by BA at various initial MPPA concentrations. Left) Experimental results at pH 3.0. Right) Experimental results at pH 9.6. (Δ) and (□) initial MPPA concentrations for various dilution factors with and without buffer, respectively. (○) and (◊) MPPA concentrations for various dilution factors with and without buffer after extraction, respectively.

6.4.4 Water solubility in solvent

Based on the preliminary screening it was found ideal to apply the main substrate as the extracting solvent. However, amines are prone to react with acids and form salts [194], which may give some restrictions to the application of solvents where significant quantities of water can be dissolved, i.e. solvents with high uptake of water should be avoided. It was in this relation experienced that applying BA as extracting solvent caused the solvent to become milky white, which is suspected to be caused by salt formation in BA. In Figure 6.8 it is shown how the BA phase, with dissolved MPPA and IPA, appears after mixing with water (pH ~6-7), 100 mM citric acid buffer (pH 3) and HCl (pH ~1). It can be seen that the milky appearance of the solvent is only visible with the two acid solutions. The samples were centrifuged to investigate the possibility of splitting the salt from the solvent, but the solvent phase maintained turbid after intense centrifugation. Furthermore, centrifugation was not suited for the proposed microfluidic two-step LLE ISPR concept.

In order to avoid this effect it was decided to mainly focus on undecane, which is a highly hydrophobic solvent. In relation to this it was tested which quantities of BA that could be dissolved in undecane before the milky appearance became dominant. The results from these tests, with various loadings of BA in undecane, are shown in Figure 6.9. It is desirable to add BA to undecane in order to apply the first extraction step as a BA saturation step as well, i.e. continuously supply BA during the reaction course. It was found that BA concentrations below 1.25 M were less prone to causing the milky effect, and therefore it was decided to apply 1 M BA concentrations for testing the combined system, which is done in chapter 7.

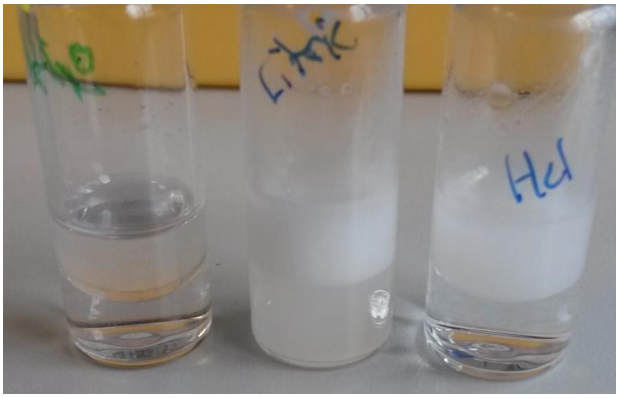

Figure 6.8: Visual test of how the presence of acids and amines in BA causes a milky appearance, i.e. suspected insoluble salt formation causes increased turbidity. From left to right: Water (pH ~6-7), 100 mM citrate buffer (pH ~3) and HCl (pH ~1), respectively.

Figure 6.9: Visual turbidity investigations of various BA loadings in undecane, to identify optimal BA loading. The BA concentration increases from left to right, both top and bottom ([0.5; 0.75; 1.0; 1.25; 1.5; 2.0; 3.0] M BA in undecane, respectively). The top picture also indicates that a lower BA concentration reduces the time needed for achieving phase splitting.

6.4.5 BA supply

As it is desirable to feed the BA from the applied solvent, which avoids implementation of a feeding strategy after the extraction and before the reactor, it is required to identify how the BA will distribute between the solvent and the aqueous phase. The partition coefficients determined for BA between the various solvents in Table 6.3, can be applied to calculate the minimum required BA loading in the solvents to ensure full BA saturation of the aqueous phase. Hence, due to the low partition coefficients for undecane and heptane, relatively to xylene and toluene, these solvents are better suited for supplying BA (less BA will be lost in the solvent) of the screened solvents. The minimum required BA concentrations in the solvents calculated from the measured partition coefficients are presented in Table 6.5.

Table 6.5: Minimum required BA concentrations in the tested solvents for ensuring saturation of the aqueous phase. The applied partition coefficients are based on the extraction results presented in table 6.3, which are based on LLE experiments with ~10 mM BA dissolved in aqueous buffer solutions at 30 °C.

	PC	$[BA]_{min}$
BA	-	(mM)
Undecane	26.3±0.3	288
Xylene	137±35	1502
Toluene	146±32	1601
Heptane	29.1±1.0	319

In addition to the calculated values, this was experimentally verified by testing the partitioning at various initial BA concentrations. These results are highlighted in Figure 6.10, where the same trends are observed, which is a good indication that the measured partition coefficients are somewhat reliable. However, some of the measured concentrations in the aqueous phase exceed the solubility limit of BA in water, which is suspected to be a cause of small solvent droplets compromise the sampling.

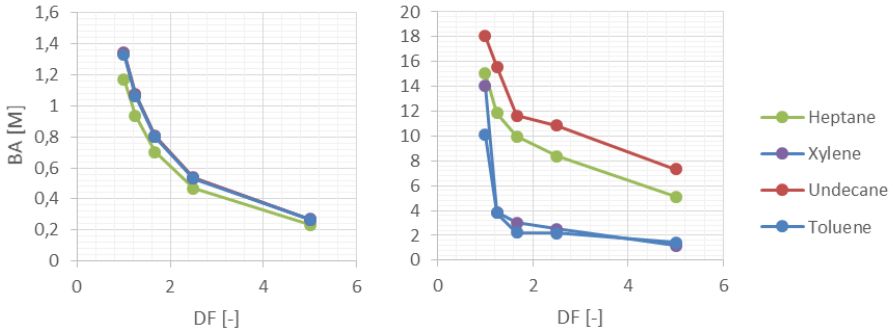

Figure 6.10: Left) Initial BA concentrations, at various dilution factors, in four solvents. Right) The monitored aqueous concentration at equilibrium at 30 °C. DF = 1 corresponds to the initial concentration of BA in the solvents before dilution.

6.5 Results: Micro LLE characterization

Here it is intended to apply microfluidics as a means to obtain an idea about the mass transfer, which is important for specifying the required dimensions of the extraction modules. Nevertheless, as mentioned in the introduction to this chapter, section 6.1.2, there might be different aspects that make it difficult to perform actual scale-up of the measured mass transfer values, i.e. different dominating mixing phenomena across scales. However, the measured partition coefficients are not scale dependent making them suitable to focus on achieving equilibrium in the extraction steps across scales.

6.5.1 Module dimensions

Different microfluidic LLE modules consisting of PTFE tubing with various inner diameters (ID) were characterized. The different modules were tested with various flow rates (50-500 µL/min) and tube lengths (10-75 cm) to change the residence times in the modules. The characterization of the modules was carried out with various solvent mixtures and initial concentrations of the reaction species present in the IPA case study presented in chapter 4. The acquired experimental data is fitted with the model defined in eq. 6.2 to determine the overall mass transfer coefficient and based on the estimated equilibrium concentrations the partition coefficients are determined based on eq. 6.4. The estimation was performed in MATLAB® using the fminsearch function, where the difference between the experimental data and the model predictions is minimized by changing the input parameters, i.e. $K_L a$ and C^*_{i,L_1}.

The estimated parameters and the experimental conditions are presented in Table 6.6. Examples of the model predictions relative to experimental data are shown in Figure 6.11 and Figure 6.12 for pH 9.51 and pH 3.03, respectively. The uncertainty of the single point measurements, determined by the experiments performed in triplicate, is implemented in the parameter estimation as a weight factor (E).

$$E_i = \begin{pmatrix} \frac{1}{\theta_{1,i}^2} & \cdots & 0 \\ \vdots & \ddots & \vdots \\ 0 & \cdots & \frac{1}{\theta_{n,i}{}^2} \end{pmatrix}$$

, where $\theta_{n,i}$ [mM] is the uncertainty in the n^{th} measurement for component i.

This weight factor is multiplied with the matrix of residuals of the experimental results relative to the model predictions in the fminsearch function. The uncertainty of the estimated parameters is evaluated based on the bootstrap method [195], which is applying random sampling with replacement from the residuals of the experimental data relative to the model predictions.

The microfluidic characterization experiments were not applied for characterizing the extraction of IPA and Ace. The relatively small partition coefficients determined in the batch experiments will only cause small quantities of the added IPA and Ace to be extracted. This in combination with the poor sensitivity of the HPLC method to detect these compounds makes it unreliable and difficult to determine the extraction of these compounds accurately, i.e. it is difficult to distinguish small changes over time considering the uncertainty of the analytical method. It would require an improved and sensitive analytical method to get reliable predictions of the extraction performance of these compounds. It was however not the focus of this thesis to go further in the direction of developing such an improved HPLC method.

Table 6.6: Microfluidic LLE extraction results and estimated parameters in various LLE modules and under varying conditions.

ID	pH	Solv.	$[BA]_{in}$	$[C_i]^*_{init}$	BA				MPPA				
-	-	-	-	-	k_La	k_L	C^*	r^2	k_La	k_L	C^*	PC	r^2
µm	-	-	mM	mM	s^{-1}	$\frac{m^2}{s \cdot m^3}$	mM	-	s^{-1}	$\frac{m^2}{s \cdot m^3}$	mM	-	-
170	9.51	BA	-	6/516/7/5	7.47±3.96	0.008	15.33±0.18	0.987	2.91±2.42	0.003	0.59	11.02±0.09	0.997
250					3.17±2.24	0.004	14.66±0.27	0.943	6.08±0.69	0.008	0.62	10.52±0.36	0.999
500					5.61±0.25	0.002	15.01±0.33	0.811	6.04±0.33	0.002	0.62	10.45±0.11	0.994
1000					2.41±0.10	0.001	14.69±0.08	0.997	5.42±0.43	0.001	0.53	12.44±0.21	0.988
170	9.51	Und	319	5/500/5/5	3.52±0.42	0.004	9.14±0.04	0.998	25.99±1.16	0.029	1.98	1.41±0.01	1.000
250					7.14±2.62	0.009	8.97±0.12	0.992	2.01±1.02	0.003	1.98	1.41±0.01	0.998
500					5.45±0.21	0.002	8.93±0.01	1.000	0.44±0.02	$1.7 \cdot 10^{-4}$	1.92	1.48±0.01	1.000
1000					5.19±0.36	0.001	9.06±0.04	0.999	3.61±0.19	0.001	1.84	1.59±0.03	0.988
250	9.43	Und	1049	5/328/5/6	15.41±11.93	0.019	12.35±0.12	0.992	31.95±11.11	0.040	1.77	1.56±0.05	0.970
170	9.52	BA	-	-/-/42/-	-	-	-	-	4.59±0.24	0.005	10.44	3.03±0.02	0.999
250					-	-	-	-	1.88±0.12	0.002	10.29	3.09±0.03	0.998
500					-	-	-	-	9.44±0.50	0.004	11.20	2.76±0.06	0.988
1000					-	-	-	-	10.58±0.63	0.003	10.37	3.06±0.04	0.997
170	3.03	Und	507	507/104/8/7	3.80	0.004	20.23	0.998	5.04	0.006	5.58	0.43	0.999
250					1.57	0.002	18.67	0.997	2.34	0.003	5.49	0.46	1.000
500					0.57	$2.1 \cdot 10^{-4}$	17.89	0.993	0.43	$1.6 \cdot 10^{-4}$	5.48	0.46	1.000
1000					1.19	$3.0 \cdot 10^{-4}$	17.17	0.999	1.19	$3.0 \cdot 10^{-4}$	4.99	0.60	0.995

Und: undecane, BA: benzylacetone, ID: inner diameter, $[BA]_{init}$: Initial BA concentration in solvent, $[C_i]^*_{init}$: initial BA/IPA/MPPA/Ace concentrations, C^*: equilibrium concentration [mM]. The experiments was performed at ambient temperature, i.e. 22 ± 1°C. The uncertainties of the estimated parameters are calculated using the bootstrap method and sample sizes of 500.

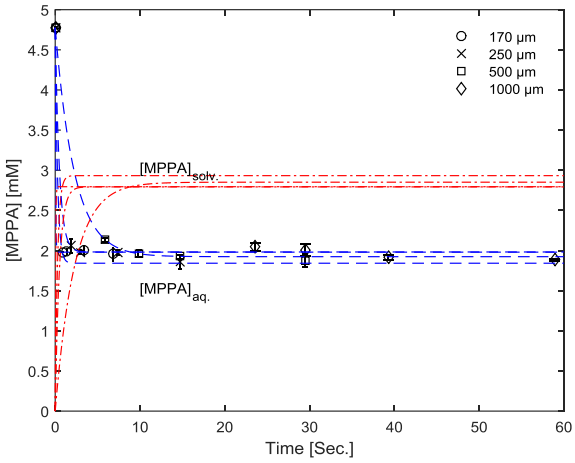

Figure 6.11: Model predictions relative to experimental data for the first extraction from a pH 9.51 aqueous mixture of the reaction species into undecane, with 309 mM BA.

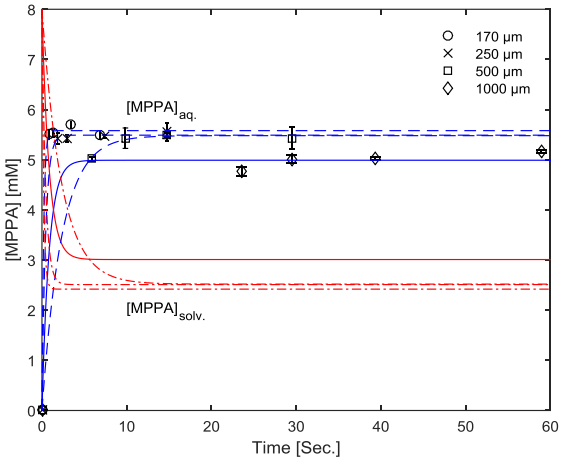

Figure 6.12: Model predictions relative to experimental data for the second extraction from undecane, with 507 mM BA, into a pH 3.03 aqueous solution.

From the results, it is not possible to identify unique trends in the estimated overall mass transfer coefficients relative to the ID of the applied PTFE tubes. If accounting for the surface area to volume ratio, one can argue that there are some trends of improved mass transfer with decreasing ID, but there are many exceptions and/or outliers in the results making it unreliable to make definitive conclusions from these data. The reasons for these deviations are most likely associated with errors caused by the manual experimental approach and

in a lesser degree with altered mixing effects in the various LLE modules. A problem in the estimation of the mass transfer coefficients is the lack of data in the region where mass transfer is dominating, i.e. most of the acquired data appears close to the equilibrium concentration and thereby the mass transfer effects are not caught by the experimental method. Furthermore, there can easily be measurement time errors in the range of ± 1 seconds in the given experimental setup caused by delays in the system that increase the effective extraction time. For example, the need for a settler will cause additional mass transfer while the phases split, and this will influence the results. The additional mass transfer before phase separation in the settler and mass transfer at the interface make it difficult to assess data in the mass transfer region. The interfacial area of the micro inserts is ~9.6 mm^2 while the surface area in the various tubes and the tube lengths are in the range of 7.5-1177.5 mm^2. However, the mass transfer at the interface is slow relative to the mass transfer distances in the settler and will have a minor effect. Therefore, the residence time of the two phases in the settler before splitting will cause overestimation of the mass transfer coefficients, i.e. it introduces longer residence times. Because of the surface area to volume ratio of the droplets in the different tubes and thereafter in the settler, this effect will be more prominent for smaller bubbles relative to larger bubbles. Assessing data in the mass transfer dominated region, with improved accuracy, for this type of experiments can be achieved by implementing in-line analytics. Alternatively or in combination, it is possible to implement a settler module where the residence time and interfacial area are known precisely. Therefore, in conclusion the applied manual experimental setup is not suited for determination of mass transfer coefficients, but merely useful for determination of equilibrium concentrations and thereby partition coefficients.

The measured saturation concentration, C^*, of BA in the experiments is in many cases higher than the maximum aqueous solubility (see Table 4.4 in chapter 4). Droplets of solvent being transferred during the sampling, which gives erroneous measurements, will potentially cause this result, and due to the high concentration of BA in undecane, it has a significant impact. This can be overcome with in-line monitoring of BA, which also avoids manual sample handling.

The determined partition coefficients for MPPA with undecane as the solvent are in good correlation with the values determined via batch experiments. It is however noteworthy that the second extraction step also shows that the extraction of MPPA from undecane into the aqueous solution with pH 3 is not complete. Once again, this confirms that the direction of the performed extraction makes a difference when applying highly hydrophobic solvents.

The determined partition coefficients for MPPA, with BA as the solvent, deviate significantly from the values obtained with the batch experiments. The cause of this was not investigated in detail as it was decided to apply undecane as the solvent at this point of time. A potential cause may be the differences in temperature between the batch and microfluidic experiments. The temperature difference between batch and microfluidic experiments was approximately $\Delta T \approx 8°C$. Furthermore, a cause may be erroneously determined pH value that will give cause to altered partitioning. At pH 9.5 small deviations of the pH will have a large influence on the fraction of uncharged MPPA and thereby the extraction.

The applied pumps for the micro LLE characterization experiments are highly accurate and thereby the flow rates and ratios between the solvent and the aqueous streams are considered highly accurate. The only cause of deviations is in these cases where air bubbles occur in the experimental setup. However, extensive efforts were made before each experiment to avoid the presence of any air bubbles, e.g. by flushing through the system and the syringes extensively.

From these investigations, it was found that most of the tested LLE modules and residence times resulted in extractions that were close to the equilibrium concentrations. Hence, the given modules will enable the combined two-step LLE system to be operated as equilibrium steps. Therefore, it was decided to apply oversized LLE modules (250 µm ID and lengths of 30 cm that result in ~15 µL dead volumes) for the combined system, enabling some flexibility to alter flows in the system without compromising the extraction performance.

6.5.2 Extraction optimization

Despite the challenges of applying the current microfluidic experimental setup to determine mass transfer coefficients accurately, it has a lot of potential for extraction optimization. Small modifications to the setup will enable fast testing of various extraction conditions, e.g. pH and temperature. For example, implementation of a pH sensor in the aqueous stream, before the inlet to the LLE modules, will make it possible to test the influence of changing pH on the extraction and equilibrium in a fast and easy manner (buffers are prepared and mixed upstream of the sensor). Another modification is to implement temperature control of the LLE modules, which will enable the possibility to test the influence of temperature on the extraction performance.

These modifications in combination with a battery of aqueous buffer solutions and solvent mixtures connected to multiple pumps before the LLE module will facilitate the possibility of operating this setup as a microfluidic high throughput, extraction characterization platform in the future.

However, in order to ensure the high throughput, improve data accuracy and avoid extensive manual sampling it is required to consider the implementation of on-line or in-line analytics as well. If a continuous settler had been put in place, it would have been possible to apply the on-line HPLC system from chapter 5 for characterization of ATA-50 and ATA-82. However, implementation of NIR spectroscopy was attempted here as such an in-line analysis method. The choice for NIR was made partly because a continuous settler was not readily available and because in-line spectroscopy was thought to simultaneously provide information about slug size distributions at various conditions and dimensions. NIR relative to other spectroscopic methods was chosen due to the availability of the equipment.

In order to determine the slug size distribution it is required that the data acquisition rate of the NIR equipment (Networkir, Q-interline/ABB Inc.) is fast relative to the linear velocity in the LLE modules. The available equipment and software (Grams/AI, Thermo Galactic) have a maximum acquisition rate of 1 spectrum per second, which makes it difficult to test droplet size distributions at a variety of different flow rates. In Figure 6.13 two examples are shown of such droplet size distribution data at various flow rates. A challenge for the data collection is when the linear velocity of the slugs exceeds the data acquisition rate, making it difficult to determine the start and end of each droplet, and thus making it difficult to distinguish between the different slugs.

From the presented data, it can be seen that each time an aqueous slug passes by the optical fiber the absorbance detection is saturated, i.e. water absorbs strongly in the NIR wavelength range. This feature enables the possibility to determine droplet size distributions if the data acquisition is accelerated, e.g. by means of updated software and/or equipment.

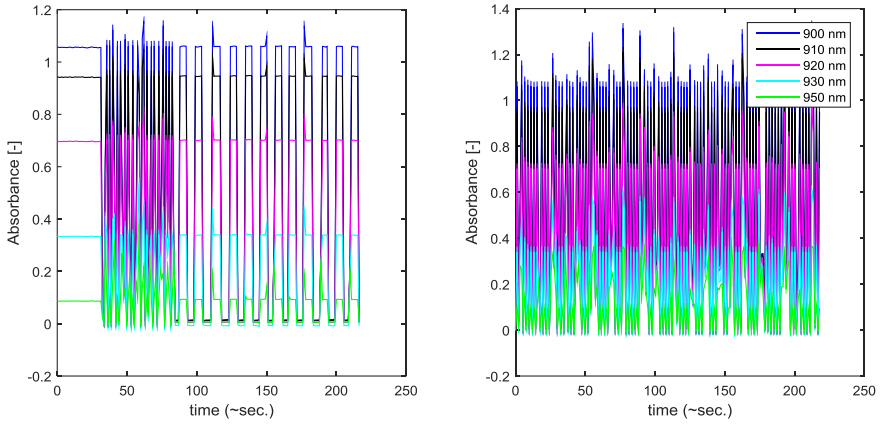

Figure 6.13: Examples of NIR spectra at various wavelengths of water slugs in BA and PTFE tubing for two different flow rates, i.e. at a low (left) and a high (right) flow rate.

Despite the fact that the available equipment was not ideally suited to determine droplet size distributions accurately, it was still tested if the equipment could be applied to measure different amines and ketones in solvents. In this relation, mixtures were prepared and tested (1 cm path length). The composition of the tested mixtures in BA as solvent are presented in Table 6.7, and the measured spectra, with various backgrounds, are shown in Figure 6.14.

The results indicate that the different compounds in the mixtures have significant absorbance in the wavelength range from 7500-4500 cm^{-1}. In order to distinguish between the compounds it is necessary to apply chemometrics. However, in this specific region water is also absorbing strongly making it difficult to develop an accurate PLS model in the presence of small quantities of water in the solvent. Alternatively, the water content in the solvent can be determined by the PLS model, if the content does not cause the NIR spectra to be saturated. In Figure 6.15, the absorbance of water in the NIR region is shown relative to the absorbance of the amines and ketones. In case water is saturating the spectra it is possible to minimize the path length of the sensors, but this will at the same time compromise the absorbance intensity of the amines and ketones. Applying highly hydrophobic solvents, e.g. undecane, may reduce the impact of water absorbance due to the low water solubility and make NIR applicable in such cases. However, because of the impact of water absorbance in most solvents it was assessed that NIR is not generally applicable and thereby not pursued further in this project.

Table 6.7: Dilution sequences of a standard reference sample in BA.

	ACP	MPPA	(S)-PEA
Ref. 1	0.35 M	0.33 M	0.35 M
Dil. 1	0.18 M	0.17 M	0.17 M
Dil. 2	0.058 M	0.055 M	0.058 M
Dil. 3	0.0083 M	0.0079 M	0.0083 M

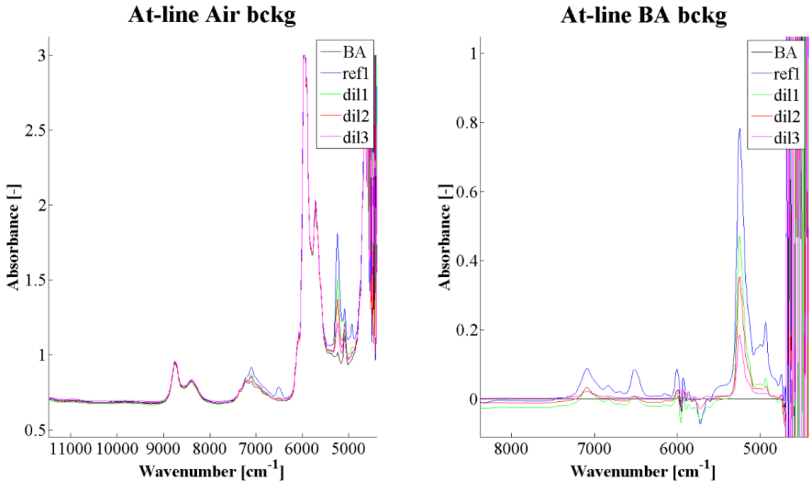

Figure 6.14: At-line spectral data based on the dilution sequence from table 1, with air and BA as the background (the solvent is BA), the path length is ~5 mm and the material used is a glass vial.

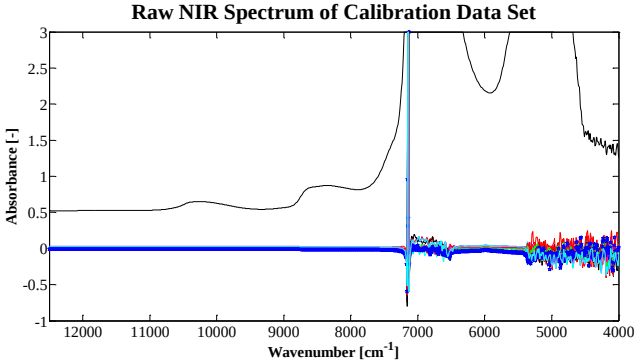

Figure 6.15: Example of spectra of aqueous mixtures with 10 mM BA, MPPA, MBA and ACP with water as the background. The spectrum of water with air as the background (black line) is also shown for comparison. The noise in the spectra occurs in the regions where water saturates the absorbance, which is in the same regions where the tested components are detectable making it challenging to apply NIR for analysis.

6.6 Conclusion

In this chapter the potential of applying microfluidics, combined with conventional batch methods, was assessed for the development of product recovery strategies for ATA processes based on LLE. This was done by characterizing single step microfluidic LLE modules for putting in place a two-step LLE concept, which is described in chapter 4, for the selective extraction of MPPA from mixtures also containing BA, IPA and Ace.

In this relation, multiple solvents were screened for their capacity to selectively separate MPPA from the mixtures. The screening results indicated that applying the main substrate BA as the solvent gave the best selectivity and capacity for extracting MPPA. However, the aqueous solubility of this solvent gave an issue with what is believed to be salt formation in the solvent. Therefore, it was found more suitable to apply a highly hydrophobic solvent, undecane, with 1 M of BA dissolved. BA was added to the solvent to enable simultaneous extraction of MPPA and feeding of BA in the extraction steps.

In the process of characterizing the two extraction steps, it was found that the applied microfluidic experimental platform gives some advantages in comparison to conventional batch experiments. The advantages include the potential for high-throughput extraction characterization and optimization. In addition, it was identified that the implementation of on-line and/or in-line analytical methods, when possible, will greatly increase the throughput and the quality of acquired data.

In conclusion, it is decided to apply oversized LLE modules (250 µm ID and lengths of 30 cm that result in ~15 µL dead volumes) for performing tests with the combined system proposed in chapter 4. This will give sufficient flexibility to alter flow rates in the combined system without compromising the extraction performance in the two modules.

Chapter 7

ISPR testing by combined microfluidic modules

The development of biocatalytic processes is greatly dominated by the application of batch-based technologies, e.g. well plates and glass vials. A limitation to the batch based approaches is that it is not possible to test and validate complex process options and scenarios. For example, in conventional batch based technologies it is very difficult to test and validate complex ISPR and IScPR concepts that are not implemented internally and directly in contact with the applied biocatalyst. It is always desirable to keep the process as simple as possible, but in some cases it can be beneficial to consider more complex alternatives, such as when severe inhibitory effects from products are of concern.

Therefore, the purpose of this chapter is to emphasize the potential of applying combined microfluidic modules (plug-and-play) in order to test complex biocatalytic process concepts. More precisely this is done by combining microfluidic modules to experimentally test the two-step LLE ISPR concept proposed in chapter 4 (also shown in Figure 7.1). Additionally, in order to get a better understanding of the dynamic behavior of the evaluated ISPR concept, a simple mathematical model describing the system is developed.

Similarly, to the previous chapters, the ATA facilitated asymmetric synthesis of MPPA from BA using IPA as the amine donor forms the basis for the case study in this chapter. Furthermore, as shown in chapter 5 increasing MPPA concentrations caused a significant reduction in the rate of the tested ATAs, which motivates the implementation of and efficient ISPR strategy.

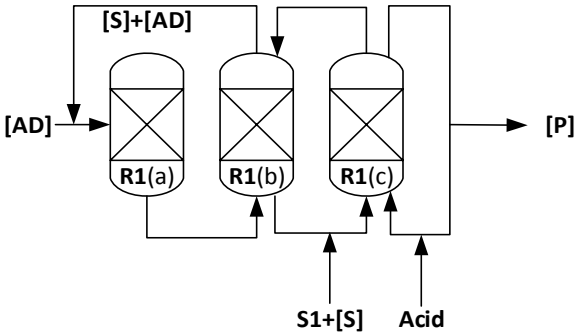

Figure 7.1: Flowsheet of the two-step liquid-liquid extraction ISPR concept for selective removal of hydrophobic amines from ATA processes, which was introduced in chapter 4. This chapter will focus on the entire setup. [AD]: Amine donor, [S]: substrate, S1: solvent, [P]: product, R1(a): reactor module, R1(b): 1st LLE module and R1(c) 2nd LLE module.

7.1 Introduction

A generic methodology was presented earlier in chapter 4 to select appropriate ISPR/IScPR options according to specific ATA process limitations and pure component properties. Moreover, chapter 4 highlights general ISPR/IScPR implementation strategies and requirements. However, when suitable ISPR/IScPR options and implementation strategies are identified, further identification of their performance is required. A way to approach this objective is through extensive experimental characterization and modelling of the isolated single process steps of the identified strategy. However, testing single process steps will only provide an indication of the performance under artificial conditions and, possibly, fail to catch the dynamics of the combined process. Microfluidics, when compared to conventional batch methods, gives a distinct advantage by providing an easier way of testing combined complex biocatalytic processes, in a plug-and-play manner [196]. Furthermore, it is useful to identify the influence of different process steps on each other and, hence, aid in understanding the actual dynamic behavior of the system, contributing to the development of more reliable descriptive system models. Therefore, the main goal of this chapter is to underline the advantages of applying microfluidics for testing complex ISPR concepts, which are difficult to perform by means of conventional batch process based methods.

The focus of the present chapter is to apply microfluidics to test the performance of the two-step LLE ISPR concept (firstly presented in chapter 4, shown in Figure 7.1), where hydrophobic amines are selectively separated from hydrophilic amines.

The ISPR concept is inspired by the solvent bridge concept published by Yun and Kim [141], which has later been modified, to a supported liquid membrane (SLM) concept, and has been explored for chiral amine production applications by Rehn et al. [143] and Börner et al. [144]. Up to now, very limited work has been presented on the application of different combinations of microfluidic modules for ISPR testing of biocatalytic processes [70]. Therefore, this is also one of the most significant contributions of this work. The microfluidic setup ($\leq \sim 5\ mL$), in comparison with the already tested SLM concept ($\geq \sim$60 mL [143,144]), enables experimental testing with at least a factor 12 lower volumes. In addition, simultaneous substrate supply and product extraction are performed in the two-step LLE modules. Furthermore, a mathematical model has been developed to describe the dynamic behavior of the system as well.

In line with the previous sections, the case study of interest for testing the ISPR concept is the formation of MPPA from BA using IPA as the amine donor (case study 2) and applying undecane with dissolved BA as the solvent. The motivation for testing this ISPR concept, for this specific reaction, is related to the outcome of the ATA-50 and ATA-82 characterizations in chapter 5. There it was identified that increasing MPPA concentrations cause a drastic reduction of the reaction rates for both of the tested biocatalysts. Furthermore, in chapter 6 it was found that undecane is a suitable solvent for performing actual tests with the proposed ISPR system.

7.1.1 Two-step Extraction dynamics

In the proposed two-step LLE ISPR concept, the partitioning between the different phases and the degree of conversion achieved in the microfluidic packed bed reactor, controls the dynamics of the system. Because the two LLE steps operate as equilibrium steps, these parts of the system are not rate dependent. The ISPR

concept can be divided into three elements: 1) the reactor module, R1(a), 2) the 1st LLE module, R1(b), and 3) the 2nd LLE module, R1(c), where the functionality of each module is illustrated in Figure 7.2.

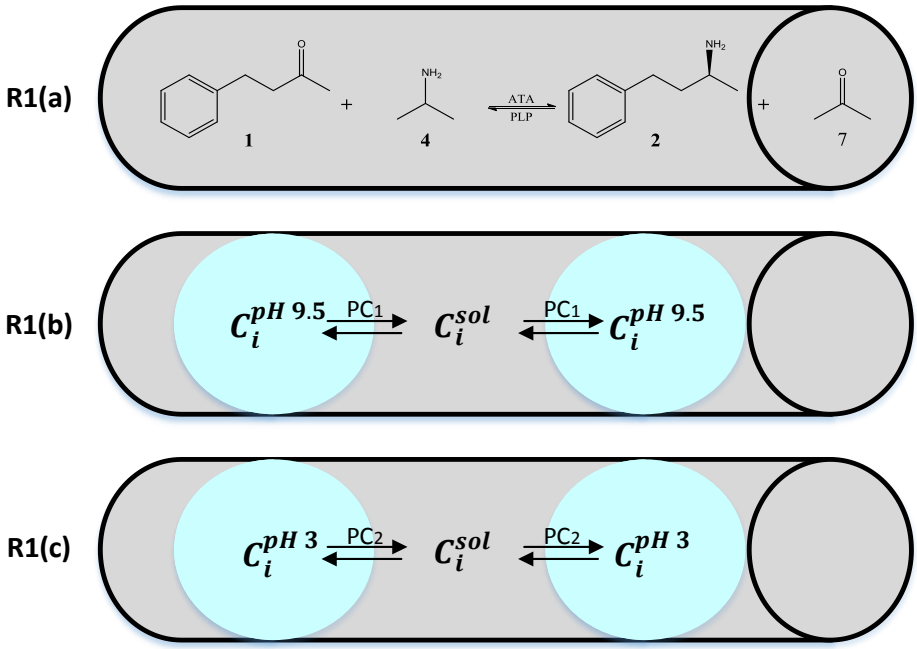

Figure 7.2: Schematic illustration of the functionality of each element in the proposed ISPR concept, where pH 9.5 and pH 3 are chosen as operating conditions in the two LLE modules.

In the reactor module, R1(a), the Immobilized ATA-82 will convert BA and IPA into MPPA and Ace. In the 1st LLE module, R1(b), the formed MPPA, along with small quantities of the other reaction species, will be extracted by the applied solvent. The high pH will cause only a fraction of the amine compounds to be uncharged and thereby they can be extracted. In the 2nd LLE module, R1(c), the extracted components from R1(b) will be extracted into the low pH aqueous phase, i.e. by protonation of the amine compounds in the solvent. The relative quantities depend on the partitioning of the reaction species. The combination of these dynamic effects is shown in Scheme 1.

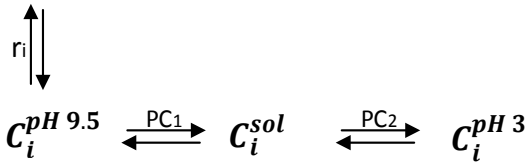

Scheme 7.1: Simplified scheme of the dynamic behavior of the component i between the different phases in the two-step LLE ISPR system, and the effect of the biocatalyst causing a change in the quantities of the reaction species in the system.

An important aspect of this ISPR concept, is the ability of the LLE modules to ensure low MPPA concentrations in the reactor, i.e. shown by R1(a) and R1(b). This is directly influenced by the residence time and loading in the reactor module, in combination with the solvent to aqueous phase ratio in the extraction modules and the partitioning. For example, in the 1st LLE module it might be beneficial to have an excess of the solvent relative to the aqueous solution to reach minimal product concentrations in the aqueous phase. Excess in the LLE modules refers to the volumetric flow rate and not the overall volume ratio, as it would compromise the final product titer. The reservoirs form a limitation of the system, which causes prolonged response times and thereby influences the time it takes to reach equilibrium between the phases.

The efficiency of the ISPR concept can be defined as the ability to recover the desired product relative to the recovery of the other compounds. A way of evaluating this is by identifying the degree of recovery and purity of the amine product in the low pH reservoir throughout the course of reaction. The product recovery and purity are defined as shown in equations 7.1 and 7.2, respectively.

$$R^* = \frac{m_i^{pH\ 3}(t)}{m_i^{tot}(t)} \cdot 100\% \qquad \text{(Eq. 7.1)}$$

, where $m_i^{pH\ 3}(t)$ [g] and $m_i^{tot}(t)$ [g] represent the recovered quantity, of component i, in the pH 3 reservoir and the total quantity in the system, respectively.

$$P^* = \frac{M_i \cdot C_i^{pH\ 3}(t)}{\sum_n^{i=1} M_i \cdot C_i^{pH\ 3}(t)} \cdot 100\% \qquad \text{(Eq. 7.2)}$$

, where M_i [g/mol] is the molar mass of component i and $C_i^{pH\ 3}(t)$ [mol/L] is the molar concentration of component i in the product reservoir.

7.2 Materials and Methods

The chemicals, equipment and off-line analytical methods described in the materials and methods sections in chapter 5 and 6 are also applied here. Only the experimental method differs.

7.2.1 Experimental method

The combined system consists of a packed bed reactor module and two LLE modules. The applied PBR reactor consists of a glass cylinder with PEEK connectors in the top and bottom (ID = 10mm, L = 11mm, V ≈ 864 µL). The two LLE modules consist of PTFE tubing (ID = 0.25mm, L = 300mm, V ≈ 15 µL).

The flows in the system are obtained by operating 4 TECAN cavro® XLP6000 pumps (Tecan Systems Inc., San Jose, CA, USA) equipped with TECAN cavro® XLP 250 µL syringes (Tecan Systems Inc., San Jose, CA, USA). The pumps are equipped with an inlet tube (ID = 1 mm, L = 300mm, V ≈ 236 µL) and an outlet tube (ID = 0.25 mm, L = 200mm, V ≈ 10 µL), all composed of PTFE. The tubes, pumps and the microfluidic modules are connected by standard PEEK flangeless fittings. The solvent and aqueous streams are combined before the LLE units in standard PEEK Y-connectors. Two glass vials (2 mL borosilicate glass, 8x70mm) are applied in the combined system as both settlers and reservoirs. The reservoirs are sealed with caps with PTFE septum. The various tubing entering into the reservoirs only come in through the septum. The flow scheme of the setup with the relative locations of tubing, modules and reservoirs/settlers is presented in Figure 7.3.

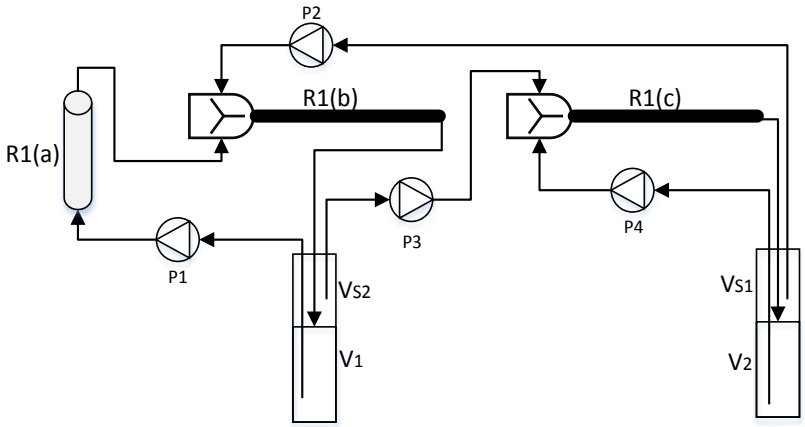

Figure 7.3: Microfluidic experimental setup. P1-P4 syringe pumps with 250 µL syringes, V1 and V2 aqueous reservoirs 1 mL of pH 9.5 and pH 3, respectively, Vs1 and Vs2 solvent reservoirs 750 µL. R1(a) PBR, R1(b) 1st LLE module, R1(c) 2nd LLE module

One reservoir is initially filled with 1000 µL (V_1) of a pH 9.5 mixture (100 mM carbonate buffer solution with 10 mM BA, 500 mM IPA and 0.1 mM PLP) and 750 µL (V_{S2}) undecane with 1 M BA dissolved. The second reservoir is initially filled with 1000 µL (V_2) of a pH 3 mixture (100 mM citrate buffer) and 750 µL (V_{S1}) undecane with 1 M BA dissolved. The buffer concentrations will be the limiting factor for the quantities of amines that can be removed and added to the two aqueous reservoirs before the pH changes significantly. Magnets are placed in the bottom of each reservoir providing mixing of the aqueous phases. Before initializing the experiments, the respective solutions are flushed through the system and disposed of. This serves the purpose of priming the system, by removing air bubbles and filling dead volumes with the respective solutions.

The loading of the PBR module is determined by weight and the pH 9.5 mixture is applied to dispense the particles before sealing the packed bed, hence, enabling easy removal of air bubbles that can potentially be stuck in the PBR. Before testing the combined system, the performance of the PBR module is evaluated by flushing the standard pH 9.5 mixture through, at various flow rates, followed by measuring the achieved conversion.

The tests are performed with the reactor module submerged into a water bath (30℃) on a magnetic stirrer (IKA® C-MAG HS7 - Werke GmbH & Co. KG, Staufen, Germany). The two reservoirs and LLE modules are operated at ambient conditions (22±1℃) and the pumps are set to operate with a flow rate of 250 µL/min. Sampling is performed by introducing a 10 µL syringe (10F syringe SGE Analytical Science, Trajan Scientific Australia Pty Ltd) through the PTFE septum into the lower aqueous reservoir.

In cases where the system is tested without a reactor module, the sizes of the reservoirs are altered to: V_1 = 10 mL, V_2 = 2 mL, V_{S1} = 1 mL and V_{S2} =2 mL. In those experiments, the applied solvent(s) are used without added BA, and the pH 9.5 mixture contains: ~8.5 mM MPPA, ~6.5 mM BA, ~50 mM Ace and ~250 mM IPA.

7.3 System model

A model of the system (Figure 7.3) is developed to get in depth understanding of the dynamic behavior of the ISPR concept. The developed model divides the proposed two-step LLE ISPR strategy into different modules and equilibrium steps describing the different functionalities. The model is composed of four reservoir modules, two liquid-liquid extractor modules and a reactor module, all connected by streams S1-S9. Figure 7.4 shows the different modules and respective streams as they interact in the model.

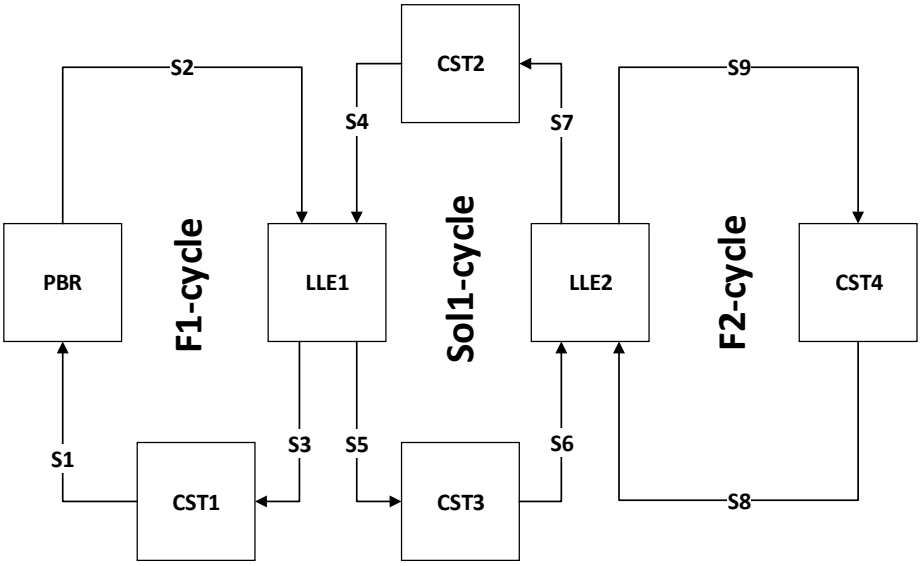

Figure 7.4: Visualization of the different modules and streams included in the developed model. F1-cycle is the high pH and reactor side of the system. Sol1-cycle is the solvent cycle in the system and F2-cycle is the low pH extracting side of the system. PBR: Packed Bed Reactor. CST1: High pH aqueous reservoir. CST2: Solvent reservoir on top of the low pH reservoir. CST3: Solvent reservoir on top of the high pH reservoir. CST4: Low pH aqueous reservoir. LLE1: 1st LLE module. LLE2: 2nd LLE module. S1-S9: The different streams in the system.

Noteworthy is that the concept of the model should be applicable to predict the dynamic behavior of the SLM concept exploited by Rehn et al. [143] and Börner et al. [144]. It would require small modifications of

the dynamic behavior of the solvent cycle, which is stagnant in the SLM. Verifying the general applicability of the developed model for two-step LLE based ISPR options was outside the scope of this work.

In the model, the reservoirs are defined as well mixed continuous stirred tanks (CST). However, this is a rough approximation as the experiments are performed with low intensity mixing in CST1 and CST4 solely. No active mixing was applied in CST2 and CST3. The change in the outlet concentration of component i (BA, IPA, MPPA and Ace) from these reservoirs can then be described by the following equations:

CST1: $$\frac{dC_{i,1}}{dt} = \frac{F_1}{V_1} \cdot \left(C_{i,3} - C_{i,1}\right) \quad \text{(Eq. 7.3)}$$

CST2: $$\frac{dC_{i,4}}{dt} = \frac{S_1}{V_{s1}} \cdot \left(C_{i,7} - C_{i,4}\right) \quad \text{(Eq. 7.4)}$$

CST3: $$\frac{dC_{i,6}}{dt} = \frac{S_1}{V_{s2}} \cdot \left(C_{i,5} - C_{i,6}\right) \quad \text{(Eq. 7.5)}$$

CST4: $$\frac{dC_{i,8}}{dt} = \frac{F_2}{V_2} \cdot \left(C_{i,9} - C_{i,8}\right) \quad \text{(Eq. 7.6)}$$

, where $F_1\ [mL/min]$, $F_2[mL/min]$ and $S_1[mL/min]$ correspond to the flow rates in the two aqueous cycles and the solvent cycle, respectively. $V_1[mL]$ and $V_2[mL]$ are the volumes of the high and low pH reservoirs, respectively. $V_{S1}[mL]$ and $V_{S2}[mL]$ are the volumes of the two solvent reservoirs located on top of the low and high pH aqueous reservoirs, respectively. $C_{i,1-9}$ corresponds to the concentrations of component i in the different streams S1-S9.

The two LLE modules are modelled by assuming that in each pass the solvent and aqueous streams reach equilibrium, which should be a good approximation based on the chosen LLE module designs (described in chapter 6). The partition coefficient relationship of each component is applied to describe the partitioning relative to the flow rates of the two fluids. Based on the mass balance over the LLE modules, it is possible to derive the following expressions to determine the outlet concentrations, assuming $F_1 = S_1 = F_2$ (similar to how the experiments are operated):

LLE1 (Aq.): $$C_{i,3} = \frac{1}{1+PC_{i,1}} \cdot \left(C_{i,2} + C_{i,4}\right) \quad \text{(Eq. 7.7)}$$

LLE1 (Sol.): $$C_{i,5} = C_{i,4} + \left(C_{i,2} - C_{i,3}\right) \quad \text{(Eq. 7.8)}$$

LLE2 (Aq.): $$C_{i,9} = \frac{1}{1+PC_{i,2}} \cdot \left(C_{i,8} + C_{i,6}\right) \quad \text{(Eq. 7.9)}$$

LLE2 (Sol.): $$C_{i,7} = C_{i,6} + \left(C_{i,8} - C_{i,9}\right) \quad \text{(Eq. 7.10)}$$

, where $PC_{i,1}$ [-] and $PC_{i,2}$ [-] are the partition coefficients of component i in the 1st and 2nd LLE module, respectively. For BA there is a limitation to the application of the partition coefficients as the concentration in the aqueous mixtures cannot exceed the solubility limit of BA in water, i.e. in cases with high BA concentration in the solvent then $C_{BA,3} = C^*_{BA}$ and $C_{BA,9} = C^*_{BA}$. For this particular case study, the other components in the system are not operated close to their respectively solubility limits.

It is possible to implement the applied PBR modules as large series of continuous stirred tank reactors (CSTRs), which are easier to describe and implement in MATLAB® than as a PBR. A large number of CSTRs in

series will approximate the behavior a PBR. The behavior of the PBR modules with reaction can be described by:

$$\frac{dC_{i,x}}{dt} = \frac{F_1}{V_x}\left(C_{i,x-1} - C_{i,x}\right) \pm r_{i,x-1} \cdot \frac{W_x}{V_x \cdot 10^{-3}} \quad \text{(Eq. 7.11)}$$

, where X [-] corresponds to the number of CSTRs in series, i.e. discretization of the PBR. V_x $[mL]$ and W_x $[mg_{enz}]$ are the volume and biocatalyst loading in each of the CSTRs, respectively. The term $\pm r_i$ $[mmol/min./mg_{enz}]$ corresponds to the rate of formation, which is positive for the products of the asymmetric synthesis (formation) and negative for the substrates (consumption).

A rate expression for the forward reaction of the given case study was previously determined and presented in chapter 5. However, due to the specific laminar flow profile for that reactor module at the given operational conditions, the derived rate expression is unique for the tested reactor modules and not feasible in other modules. A larger reactor module was applied for testing of the combined system, due to the presence of larger quantities of PVA particles with a larger average diameter of 3-4 mm relative to the smaller particles applied for the characterization performed in chapter 5. Consequently, this change in reactor module did not enable the possibility of implementing the reactor performance into the proposed model framework.

In the tested cases without a reactor module, the PBR functionality can be excluded from the model by implementing equation 7.13 that represents the PBR when no reaction is occurring.

$$\frac{dC_{i,2}}{dt} = \frac{dC_{i,1}}{dt} \quad \text{(Eq. 7.12)}$$

7.4 Results

Here the proposed two-step LLE ISPR concept is tested using a combination of microfluidic. The experimental results consist of three parts: 1) identifying extraction performance without PBR modules, 2) identifying system performance with PBR modules with ATA-82 immobilized in PVA, and 3) Identifying the system flexibility, by testing ATA-50 immobilized by chitosan. The developed model is applied in parallel with the experiments without PBR modules.

7.4.1 Preliminary testing

A set of preliminary experiments, without reactor modules, were performed to verify that the microfluidic system, with the proposed ISPR setup, works as intended. This form of testing will aid in identifying operating difficulties and the overall extraction performance. Furthermore, excluding the reactor module makes it accessible to evaluate the performance of the model to understand the dynamic behavior of the two-step LLE and, potentially, identify losses in the solvent phase.

The set of preliminary experiments were performed in triplicate with undecane, xylene and toluene as solvents. The achieved results for each of the applied reaction species (BA, IPA, MPPA and Ace) are highlighted in the following sections.

7.4.1.1: Benzylacetone (BA)

The measured concentrations of BA over time, in the high and low pH reservoirs, are highlighted and shown for the three tested solvents in Figure 7.5. Additionally, the BA concentration predicted by the model in the two reservoirs is presented. For the model, it is assumed that BA in the aqueous streams entering the LLE modules will fully extract into the solvent (no initial BA in the solvent), which is a good approximation relative to the measured partitioning coefficients (values presented in Table 6.3 in chapter 6).

The experimental results and the model predictions are shown to be consistent (Figure 7.5), which forms a strong indication that the model represents the dynamics of the system properly (behavior of the main substrate in the two reservoirs for all three solvents being tested). There is a small increase in the BA concentration in the pH 3 reservoir for the undecane experiments. This is believed to be a result of the lower partition coefficient of BA in undecane relative to the other solvents, which will cause a higher quantity of BA to appear in the aqueous reservoirs (results presented in Table 6.3 in chapter 6). This can be accounted for by directly implementing the measured partition coefficients of BA in the model. However, for experiments including PBRs and dissolved BA in the solvent, the aqueous phases will appear completely saturated with BA and, therefore, no additional efforts were made to include this in the model.

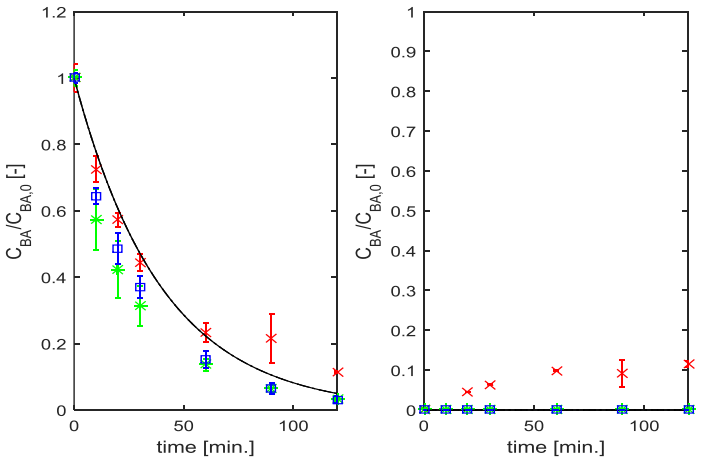

Figure 7.5: Comparison of model predictions relative to experimental results of BA in the pH 9.5 (Left) and pH 3 (Right) reservoirs, with undecane (x), Xylene (×), and Toluene (□) as solvents. The dotted, full and dash-dotted lines indicate the model predictions of BA in undecane, xylene and toluene, respectively. The model assumed full partitioning of BA into the solvents.

7.4.1.2: Isopropylamine (IPA)

Similarly, the measured time dependent IPA concentrations in the two reservoirs were compared to the model predictions. These results are shown in Figure 7.6. Interestingly, here the model fails to predict the behavior of IPA in the two reservoirs. It is believed that this is due to the uncertainty of the measured parameters, i.e. partition coefficients of IPA (Table 6.4 in chapter 6). Furthermore, the applied analytical method for identifying the IPA content is highly inaccurate, which is also, reflected in the large deviations in the measured IPA concentrations in the reservoirs.

Consequently, the extraction of IPA in the system is excluded from the model by fixing the partition coefficients of IPA in both reservoirs to 0, i.e. $PC_{IPA,1} = PC_{IPA,2} = 0$. This avoids the erroneous prediction of the IPA extraction for experiments where reactor modules are implemented. This assumption will also maintain the IPA concentration in the pH 9.5 reservoir artificially high, which will influence the rate of reaction. However, this assumption will be applicable when operating with an initial IPA concentration of 500 mM or higher, 3 times higher than the determined K_{IPA} in chapter 5, and for experiments with a short time horizon, e.g. 2 hours operation. Rehn et al. [143] showed that, for long-term experiments, the removal of IPA is significant. In such cases, the assumption fails and the model cannot be applied. The model results, with the altered partition coefficients, relative to the IPA measurements are represented in Figure 7.7.

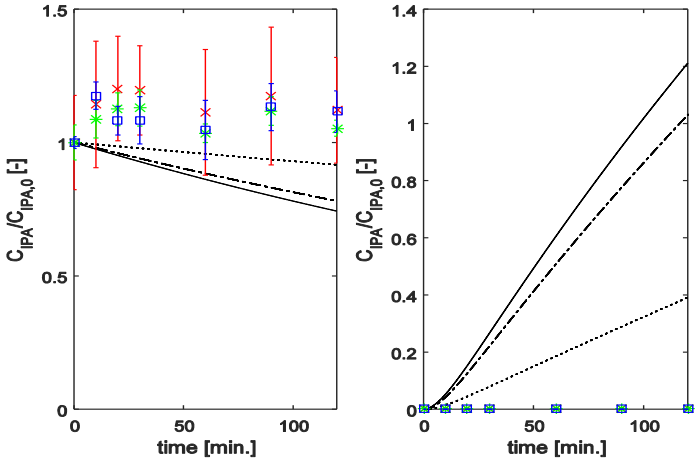

Figure 7.6: Comparison of model predictions relative to experimental results of IPA in the pH 9.5 (Left) and pH 3 (Right) reservoirs, with undecane (x), Xylene (×), and Toluene (□) as solvents. The dotted, full and dash dotted lines indicate the model predictions of IPA in undecane, xylene and toluene, respectively. The model applies $PC_{IPA,1} = [0.03; 0.11; 0.09]$ *and* $PC_{IPA,2} = [0; 0; 0]$ *for undecane, xylene and toluene, respectively.*

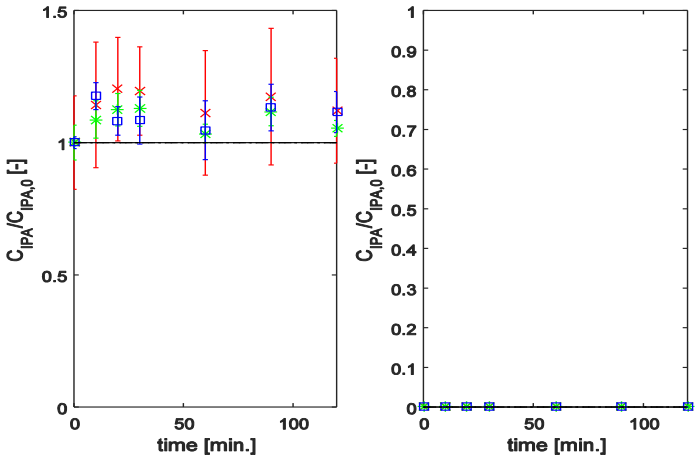

Figure 7.7: Comparison of model predictions relative to experimental results of IPA in the pH 9.5 (Left) and pH 3 (Right) reservoirs, with undecane (x), xylene (x), and toluene (□) as solvents. The dotted, full and dash-dotted lines indicate the model predictions of IPA in undecane, xylene and toluene, respectively. The model applies $PC_{IPA,1} = [0; 0; 0]$ and $PC_{IPA,2} = [0; 0; 0]$ for undecane, xylene and toluene, respectively.

7.4.1.3: 1-Methyl-3-phenylpropylamien (MPPA)

Likewise, the measured time dependent MPPA concentrations in the two reservoirs were also compared with the model predictions; the results are presented in Figure 7.8. Noteworthy is the fact that the model somewhat accurately predicts the dynamic behavior of MPPA in both reservoirs for the different solvents. The exception to this is the prediction for undecane in the pH 3 reservoir, where the model fails to predict the MPPA concentration profile. However, this is believed to be closely related to the difficulty of identifying a unique partitioning coefficient for MPPA in the 2nd LLE module with undecane (see chapter 6). Hence, this is also the reason why multiple partition coefficients are highlighted in the figure, in order to identify, which of the measured values represents best the experimental data. Figure 7.8 shows that, in the case of $PC_{MPPA,2} = 0$, the data is better represented and therefore, it is more suitable to apply this coefficient when modelling the extraction in the 2nd LLE module.

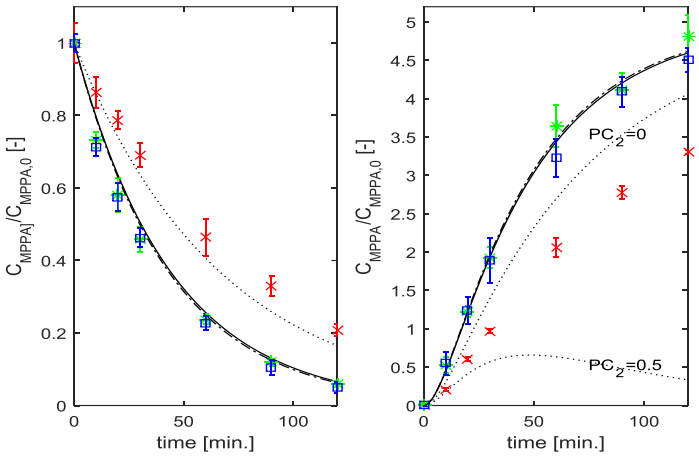

Figure 7.8: Comparison of model predictions relative to experimental results of MPPA in the pH 9.5 (Left) and pH 3 (Right) reservoirs, with undecane (x), Xylene (×), and Toluene (□) as solvents. The dotted, full and dash-dotted lines indicate the model predictions of IPA in undecane, xylene and toluene, respectively. The model applies $PC_{MPPA,1} = [1.5; 9.6; 12.21]$ and $PC_{MPPA,2} = [\#; 0; 0]$ for undecane, xylene and toluene, respectively. The value of # is indicated on the figures.

Moreover, for MPPA it is also interesting to evaluate the degree of recovery by using the various solvents. In Figure 7.9, the estimated degrees of recovery determined by the model (based on equation 7.1) are presented together with the experimental results. From these estimations, it can be found that applying xylene or toluene enables recoveries in the range of 90% of the initial MPPA. For undecane, the relative recovery of MPPA, in the same scale, is approximately in the range of 65%, which poses a significant decrease. This can to some extent be explained by the lower partition coefficient determined for MPPA with undecane.

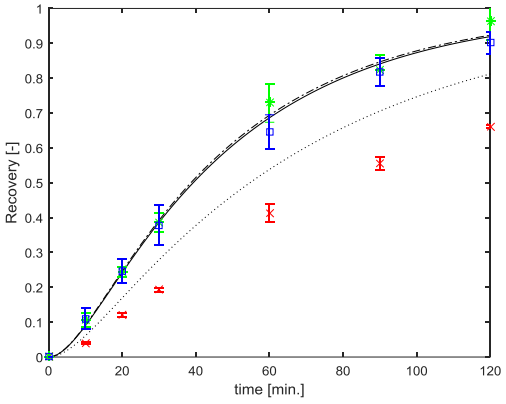

Figure 7.9: Representation of the experimentally achieved degrees of MPPA recovery in undecane (x), xylene (×), and toluene (□) as solvents The dotted, full and dash-dotted lines indicate the model predictions of IPA in undecane ($PC_{MPPA,2} = 0$), xylene and toluene, respectively.

7.4.1.4: Acetone (Ace)

Lastly, the measured time dependent Ace concentrations in the two reservoirs were compared to the model predictions and are presented in Figure 7.10. Similarly, to the results achieved for IPA, the model fails to predict the dynamic extraction behavior of Ace accurately. The poor model performance in predicting the dynamic behavior can be due to the relative uncertainty of the analytical method. However, it is also believed to be caused – at least partly – by over-predicted partition coefficients, i.e. acetone is rather volatile and significant quantities may appear in the headspace of the vials. Hence, the predicted partition coefficients appear to be larger than they actually are.

Better predictions for the extracting behavior of acetone were achieved by manually reducing the measured partition coefficients. Figure 7.11 shows the results with the modified partition coefficients ($PC_{Ace,1} = PC_{Ace,2} = [0.1; 0.3; 0.25]$) relative to the experimental results.

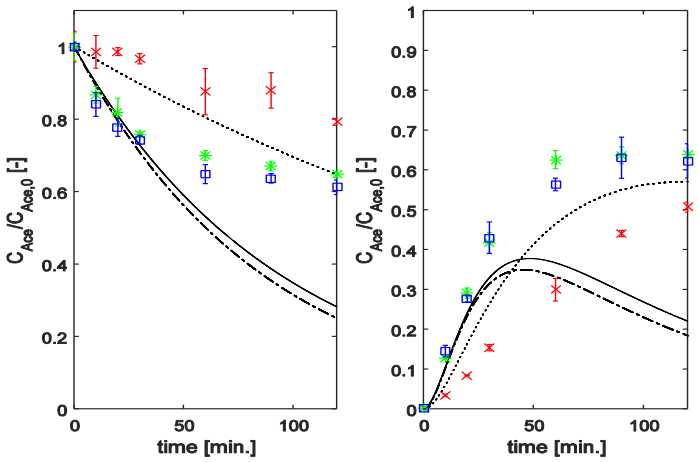

Figure 7.10: Comparison of model predictions relative to experimental results of Ace in the pH 9.5 (Left) and pH 3 (Right) reservoirs, with undecane (x), Xylene (x), and Toluene (□) as solvents. The dotted, full and dash-dotted lines indicate the model predictions of IPA in undecane, xylene and toluene, respectively. The model applies $PC_{Ace,1} = [0.17; 0.73; 0.86]$ and $PC_{Ace,2} = [0.17; 0.73; 0.86]$ for undecane, xylene and toluene, respectively.

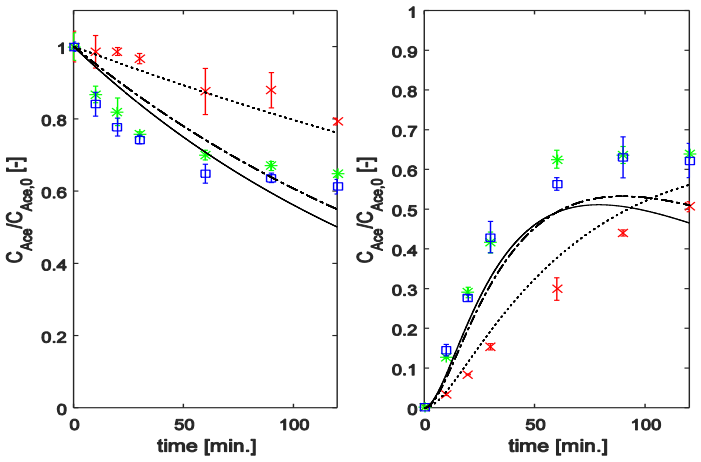

Figure 7.11: Comparison of model predictions relative to experimental results of Ace in the pH 9.5 (Left) and pH 3 (Right) reservoirs, with undecane (x), Xylene (×), and Toluene (□) as solvents. The dotted, full and dash-dotted lines indicate the model predictions of IPA in undecane, xylene and toluene, respectively. The model applies $PC_{Ace,1} = [0.1; 0.3; 0.25]$ and $PC_{Ace,2} = [0.1; 0.3; 0.25]$ for undecane, xylene and toluene, respectively.

In general, the model results show a good correlation with experimentally determined MPPA and BA results. However, experimental results for IPA and Ace do not correspond to the model predictions. In order to get better predictions of the dynamic behavior of IPA and Ace it may be required to improve the sensitivity of the HPLC method, minimize the headspace in the vials and at the same time consider implementation of a GC method to analyze the solvent phase and thereby close the mass balance. In addition, it may be beneficial to implement a continuous splitter in the microfluidic LLE characterization setup to improve the throughput and minimize external effects occurring during the extraction experiments.

7.4.2 Combined system: ATA-82 in PVA particles

Experiments with reactor modules, with various loadings of ATA-82 entrapped in PVA particles, were conducted. The experiments were performed solely with undecane as the solvent, with 1 M BA dissolved. These experiments serve the purpose of understanding the operational dynamics of the ISPR concept. For example, these experiments are useful for identifying potential issues of MPPA build-up in the reactor module and the high pH aqueous reservoir.

The applied PBR modules for these tests deviated from the applied modules described in chapter 5, due to the application of larger PVA particles (3-4 mm diameter). This fact, in combination with an over-simplified forward reaction kinetic model derived for ATA-82 in chapter 5 limited the use of the developed model to predict the dynamic behavior of the experiments.

7.4.2.1: Residence time

Firstly, the influence of residence time in the reactor modules is tested by varying the feed flow rate into the system. Figure 7.12 presents, the results of these tests, which are highlighted as the change in MPPA and BA concentrations at various residence times.

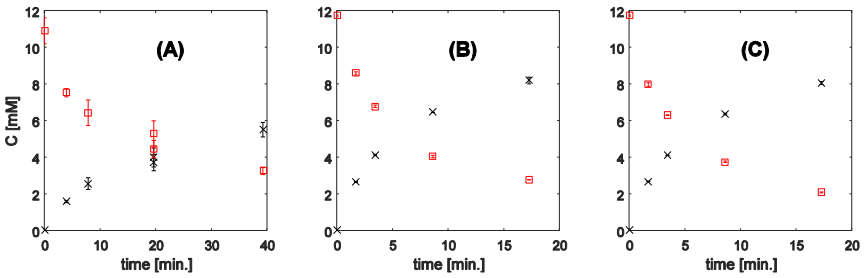

Figure 7.12: Identifying the impact of PBR residence time (X-axis) on the degree of BA (□) conversion and MPPA (x) formation at three different loadings of ATA-82 in PVA particles. A) 0.44 g_{PVA} (0.02 g_{ATA-82}), B) 0.54 g_{PVA} (0.03 g_{ATA-82}), and C) 0.68 g_{PVA}(0.03 g_{ATA-82}).

According to the above results, a flow rate of 250 µL/min results in MPPA yields in the range of 25-35% for all the tested reactor modules (residence times of 3.5 minutes, 7.9 min for experiment (A)). The specific flow rate was chosen to minimize the MPPA presence in the reactor modules and thereby minimize its inhibitory effects. The longer residence times achieved for the low loading experiment (A), are due to the presence of a larger dead volume in the reactor module (the dead end filters expanded when the experiment was initiated). The length of the reactor module for that experiment was approximately 2.5 cm, which gives an approximate dead volume of 1.96 mL.

7.4.2.2: Benzylacetone (BA)

In Figure 7.13, the measured concentrations of BA over time in the high and low pH aqueous reservoirs are highlighted for the three loadings. The given results do not indicate any difference in the BA concentrations in the two reservoirs over time for any of the loadings. This is as expected as the aqueous streams are saturated with BA in the LLE modules. Notably the measured BA concentrations exceed the maximum solubility limit of BA (10.8 mM). This can partly be caused by the sampling procedure, where small quantities of the solvent with high BA content in the samples will greatly influence the measured BA concentration. However, if that is indeed the case then there should have been larger deviations on the measured concentrations. Another cause of this increased solubility can be related to the presence of the other reaction species, which can improve the BA solubility.

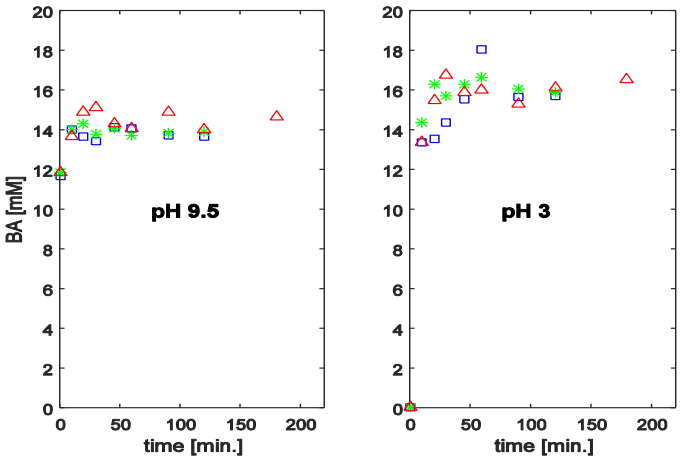

Figure 7.13: Experimental results of the time dependent BA concentrations in the pH 9.5 (Left) and pH 3 (Right) aqueous reservoirs, with three different reactor loadings: 0.44 g_{PVA} (0.02 g_{ATA-82}) (□), 0.54 g_{PVA} (0.03 g_{ATA-82}) (×), and 0.68 g_{PVA}(0.03 g_{ATA-82}) (Δ).

7.4.2.3: Isopropylamine (IPA)

In Figure 7.14, the measured concentrations of IPA over time in the two reservoirs are highlighted for the three loadings. Similarly to the experimental results without the reactor module (section 7.4.1.2), it appears that there is minimal IPA extraction in the system. The uncertainty of the analytical method makes it difficult to follow the conversion of IPA in the system, and also difficult to measure the extraction of small quantities of IPA. Notably, the IPA concentrations do not decrease significantly over time, which means that the impact of IPA evaporating from the system is minimal. Notably Rehn et al. [143] experienced significant extraction of IPA in their SLM system. The main difference between the two systems is related to the applied solvent volumes and system response times, which may cause this system to have a lower driving force for extracting IPA during operation, i.e. increased IPA concentration in the solvent over time causes lower partitioning from the pH 9.5 reservoir.

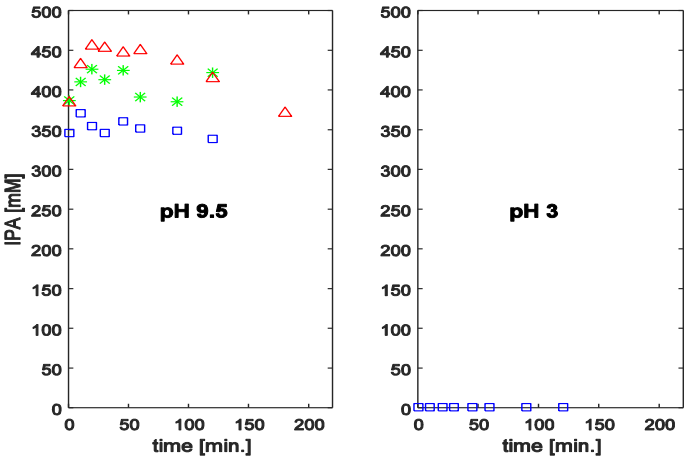

Figure 7.14: Experimental results of the time dependent IPA concentrations in the pH 9.5 (Left) and pH 3 (Right) aqueous reservoirs, with three different reactor loadings: 0.44 g_{PVA} (0.02 g_{ATA-82}) (□), 0.54 g_{PVA} (0.03 g_{ATA-82}) (×), and 0.68 g_{PVA}(0.03 g_{ATA-82}) (Δ).

7.4.2.4: 1-methyl-3-phenylpropylamine (MPPA)

In Figure 7.15, the measured concentrations of MPPA over time in the two reservoirs are highlighted for the three loadings. The results indicate that the extraction concept works as intended and the MPPA concentration in the low pH reservoir increases significantly over time. However, over time the MPPA concentration also increases slightly in the high pH reservoir, which will cause increased inhibition of the biocatalyst. In addition, the increased MPPA concentration in the high pH reservoir may also explain why there are only minor differences in the MPPA concentration profiles achieved with the various loadings, i.e. for each of the tested loadings the system is limited by the extraction. The LLE modules do not directly cause this limitation of the extraction, and it is believed that the limitation is a consequence of the applied solvent reservoir volumes, which cause the system to have a low response time compared to the achieved reaction rates in the PBR modules. This can be overcome by adjusting the applied solvent volumes and/or increasing the flow rate of the solvent in the system. Alternatively, applying a solvent with better MPPA partitioning can also be considered.

To better understand the capacity of the system, some of the tests were performed with longer operating times (Figure 7.16). In one of these experiments, a final product titer of ~180 mM (~26.5 g/L) was achieved. This is a strong indication that the given ISPR setup enables the possibility of achieving high product titers despite operating the biocatalyst at dilute conditions. Please note that a slight decrease in the MPPA concentration was observed after 120 min for one of the performed experiments. However, this is believed to be an experimental outlier that is occurring either as a consequence of the exceedance of the buffer capacity in the low pH reservoir, and/or caused by transfer of aqueous droplets in between the aqueous reservoirs. Both effects will disrupt the driving force for the separation.

Some of the specific limitations of achieving high product concentrations and good space-time-yields (STY) [g_P/L/h] in the tested system are is related to the activity of ATA-82 and the system response times. Additionally, the volumes of the solvent reservoirs and the low pH aqueous reservoir were larger than required (larger reservoirs are easier to operate). For example, if the pH 3 reservoir volumes were half the size compared to the ones used in these experiments, then the outlet product titer would have been doubled, as long as the pH is maintained. Based on the achieved concentrations in the low pH reservoir in the first 120 minutes it is found that a STY of 3.0 $g_P/L_{pH\ 3}$/h is achieved based on the low pH reservoir volume. If the STY is based on the total system volume the value will be approximately 4 times lower (0.7 g_P/L/h). Hence, the STY and achievable product titer in the pH 3 reservoir can be significantly improved by reducing the volumes of all the reservoirs in the system.

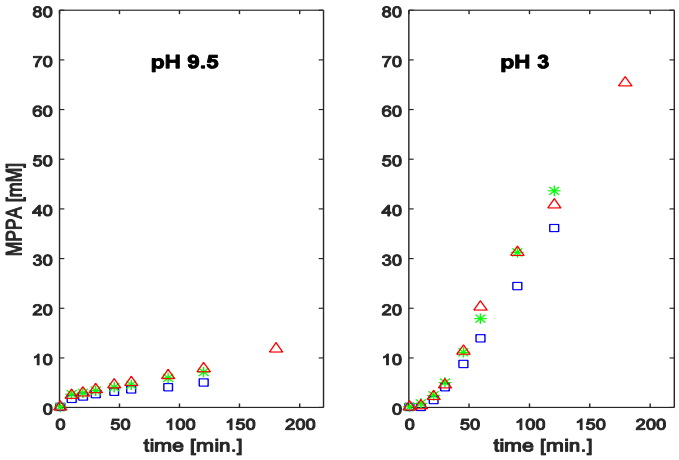

Figure 7.15: Experimental results of the time dependent MPPA concentrations in the pH 9.5 (Left) and pH 3 (Right) aqueous reservoirs, with three different reactor loadings: 0.44 g_{PVA} (0.02 g_{ATA-82}) (□), 0.54 g_{PVA} (0.03 g_{ATA-82}) (×), and 0.68 g_{PVA}(0.03 g_{ATA-82}) (Δ).

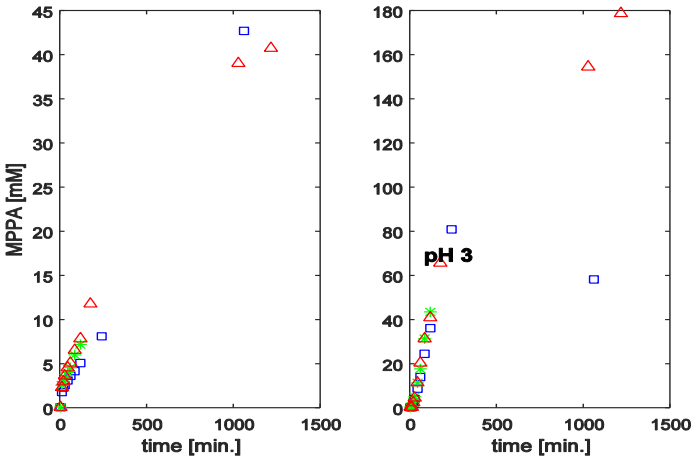

Figure 7.16: Experimental results of the time dependent MPPA concentrations in the pH 9.5 (Left) and pH 3 (Right) aqueous reservoirs, with three different reactor loadings: 0.44 g_{PVA} (0.02 g_{ATA-82}) (□), 0.54 g_{PVA} (0.03 g_{ATA-82}) (×), and 0.68 g_{PVA}(0.03 g_{ATA-82}) (Δ). For (Δ), 37% (w/w) HCl was applied after 120 min. to ensure the buffer concentration was not exceeded while operating for longer times.

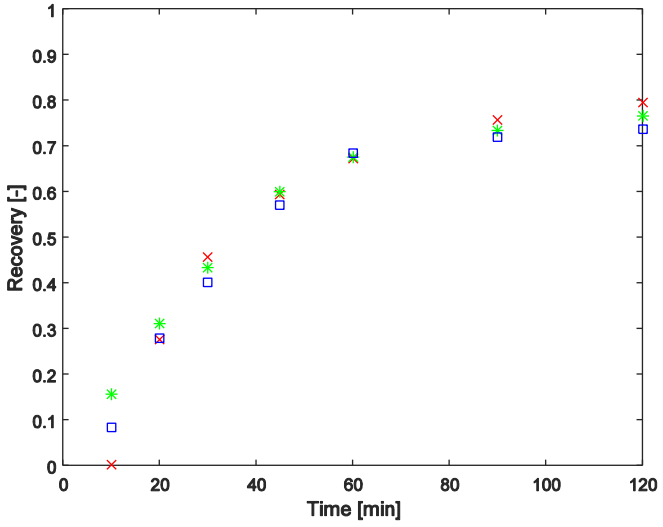

Figure 7.17: Degree of recovery with three different reactor loadings: 0.44 g_{PVA} (0.02 g_{ATA-82}) (×), 0.54 g_{PVA} (0.03 g_{ATA-82}) (×), and 0.68 g_{PVA}(0.03 g_{ATA-82}) (□). The degree of conversion is determined as the remaining MPPA in the high pH reservoir relative to the MPPA in the low pH reservoir, and excluding losses in the solvent (undecane).

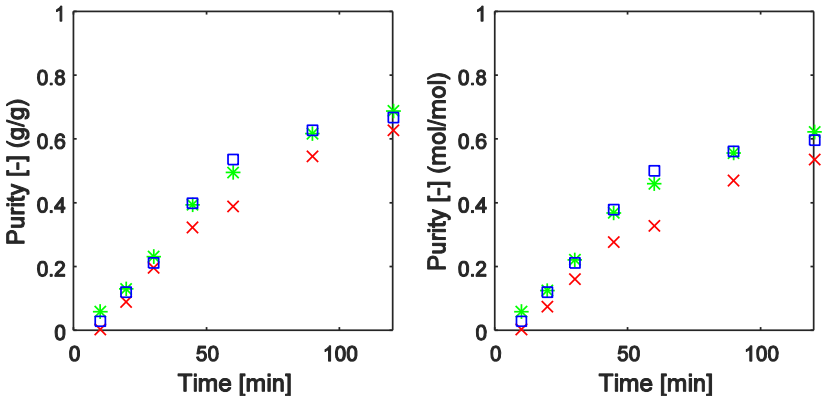

Figure 7.18: Estimated purity, on weight and mole basis, of MPPA in the final reservoir achieved with three different reactor loadings: 0.44 g_{PVA} (0.02 g_{ATA-82}) (x), 0.54 g_{PVA} (0.03 g_{ATA-82}) (x), and 0.68 g_{PVA}(0.03 g_{ATA-82}) (□).

Another interesting feature of the system is the degree of recovery and the achieved final product purity (the degree of recovery can be calculated based on equation 7.1 and the purity as shown in equation 7.2). The estimated degree of recovery is shown in Figure 7.17. These estimates indicate that approximately 80% is recovered, which is an improvement compared to the preliminary tests without reactor modules (~65% recovery for undecane). However, the preliminary tests also indicated that there were losses to the solvent, which is not considered in the estimates provided here, i.e. the solvent composition was not analyzed. In Figure 7.18, the achieved purities are presented. The purity of the final product is in the range of 60-70% (w/w), which is mainly caused by the quantity of acetone extracted into the low pH reservoir. Higher purity can be achieved by extracting BA and by acetone stripping. Furthermore, the purity can be slightly improved by reducing the size of the low pH reservoir, as the BA content relative to MPPA content will be minimized.

7.4.2.5: Acetone (Ace)

In Figure 7.19, the measured concentrations of Ace over time in the high and low pH aqueous reservoirs are highlighted for the three loadings. It can be seen that Ace builds up in both aqueous reservoirs, which to some extent will compromise the product purity. However, as mentioned, Ace is volatile and it is easy to strip off large quantities and thereby achieve improved product purity. An advantageous feature of the simultaneous extraction of Ace is that inhibitory effects on the biocatalyst caused by Ace are reduced simultaneously.

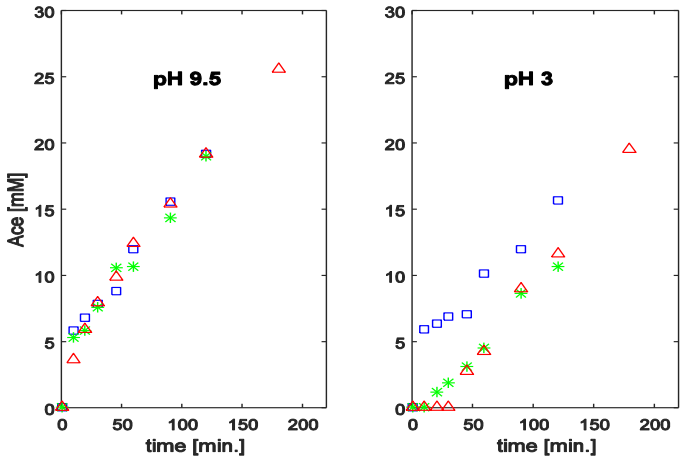

Figure 7.19: Experimental results of the time dependent Ace concentrations in the pH 9.5 (Left) and pH 3 (Right) aqueous reservoirs, with three different reactor loadings: 0.44 g_{PVA} (0.02 g_{ATA-82}) (□), 0.54 g_{PVA} (0.03 g_{ATA-82}) (×), and 0.68 g_{PVA}(0.03 g_{ATA-82}) (Δ)..

7.4.3 Combined system: flexibility

An important aspect for the application of microfluidic modules in combination to test ISPR concepts is the flexibility and the general applicability. Hence, it is important that changes to the setup and operational conditions can be implemented easily.

Therefore, to highlight the flexibility of applying microfluidic modules for biocatalytic process screening, the reactor module was tested with an alternative immobilization method and biocatalyst (ATA-50 in lyophilized cells). The immobilization method is based on performing flocculation, with chitosan, of the lyophilized cells. This was done based on the procedure as published by Rehn et al. [27]. The results from these tests are highlighted in Figure 7.20.

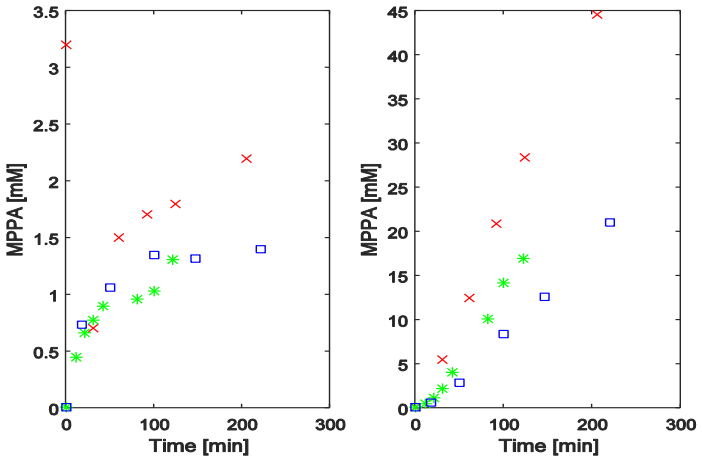

Figure 7.20: Experimental results of the time dependent MPPA concentrations in the pH 9.5 (Left) and pH 3 (Right) aqueous reservoirs, with three different reactor loadings: 1) 150 $mg_{ATA-50\ cells}$, 5 $mg_{chitosan}$ and 50 $mg_{perlite}$(x). 2) 100 $mg_{ATA-50\ cells}$, 3.3 $mg_{chitosan}$ and 50 $mg_{perlite}$(x). 3) 50 $mg_{ATA-50\ cells}$, 5 $mg_{chitosan}$ and 50 $mg_{perlite}$(□).

The results follow the same trends as experienced with ATA-82 in PVA particles. The main difference, compared to using ATA-82 in PVA particles, is that the achieved MPPA concentrations in the two reservoirs are lower relative to the loading, which can be associated with the lower measured activity of ATA-50 compared to ATA-82 (see chapter 5). It is important to note that the lower activity of ATA-50 and the given immobilization method causes the reaction rate to be the rate-limiting step and, thereby, not the response time of the LLE modules and reservoirs as seen with ATA-82 in PVA particles.

Therefore, specifically for this system, it is required to either minimize the solvent volume and/or increase the solvent flow rate in the system to ensure sufficient extraction performance, especially if applying biocatalysts with higher activities than ATA-82. Changing operational conditions, e.g. reactor temperature and/or flow rates, can easily be performed for the tested system.

Despite this work being committed to the application of microfluidic PBRs, with immobilized biocatalysts, and LLE modules in combination, to test a two-step LLE ISPR concept, it is still considered generally applicable. For example, in cases where the biocatalyst is not influenced significantly by the interface of the separation method it is possible to apply free solubilized biocatalysts. Alternatively, microfluidic membrane reactor modules can be applied to avoid the interface. Furthermore, for reactor systems where other separation methods are required, it is a matter of replacing the applied LLE separation modules with alternative unit operations. For example, resins can be implemented in the same manner as the applied PBR reactors. Gas-liquid applications, e.g. stripping or evaporation, would require implementation of backpressure regulators, but technically, it should not be any problem to implement such separation methods as well.

7.5 Monitoring and control

It is recognized that there are many potential advantages associated with the application of microfluidics for testing complex biocatalytic processes. However, limitations to this approach in general are the required volumes for analysis, and the handling of small volumes. Hence, implementation of on-line and in-line analytical methods will greatly improve the experimental throughput and handling.

The on-line HPLC system implemented for biocatalyst characterization can also be implemented in the applied two-step LLE ISPR setup. However, it would require sampling from both reservoirs, which would make the implementation complex. Furthermore, it would be advantageous to implement a sample point after the reactor module to follow the reactor performance over time. Alternatively, pH sensors can be implemented in the two aqueous reservoirs to monitor deviations in the pH caused by the extraction of the amine product. Additionally, this can be coupled with additional pumps that can add acid and base to maintain the pH in the two reservoirs and thereby indicate the product concentration and formation as a function of acid and base addition, i.e. titration. The implementation of this pH monitoring and control strategy is illustrated for the given two-step LLE ISPR concept in Figure 7.21.

In addition, it will be beneficial to analyze the solvent composition in the two solvent reservoirs, since such implementation will for example make it possible to evaluate product losses in the solvent. In view of this, it would be suitable and easy to implement in-line NIR spectroscopy, if the water saturating the solvent does not saturate the NIR spectra in the region where the reaction species absorb. The implementation of NIR spectroscopy in the solvent cycle is also illustrated in Figure 7.21.

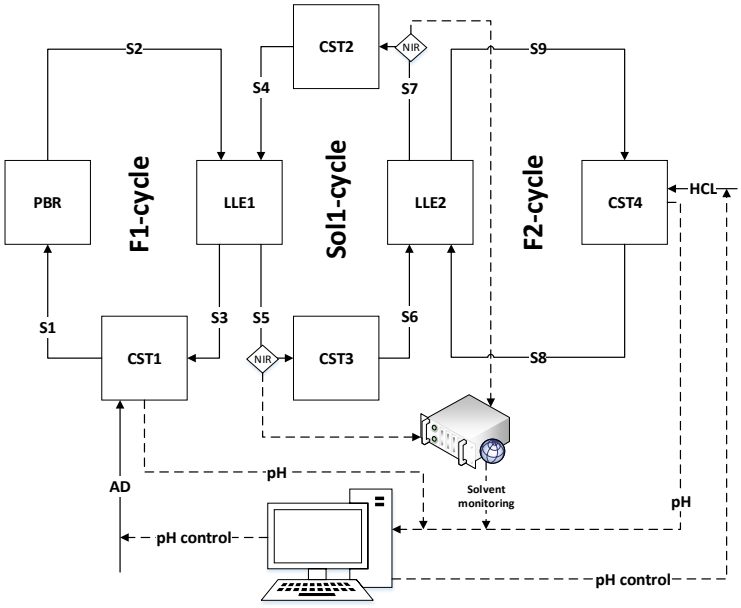

Figure 7.21: Proposed scheme for implementation of NIR monitoring of the solvent cycle and pH sensors for monitoring and control of the two-step LLE ISPR concept.

7.6 Conclusion

In this chapter the potential of applying microfluidic modules, combined in a plug-and-play manner, was highlighted as a novel technology enabling easy testing of complex biocatalytic process concepts. This was emphasized through a case study, where a two-step LLE ISPR concept was tested by combining a microfluidic reactor module with two microfluidic LLE modules.

In addition, the tested ISPR concept showed good potential for extracting hydrophobic amine products from hydrophilic amines in amine transaminase (ATA) processes to overcome severe inhibitory effects. Furthermore, the tested concept showed other advantages in the form high product purity in the stream leaving the system and high overall product recovery. The advantage of the tested system is that the biocatalyst can be operated at mild conditions, where it is stable and works efficient, without compromising the need for high product titers and purity in the outlet stream.

Chapter 8

General discussion

In this thesis, the role of microfluidics in the development of biocatalytic processes was investigated. Emphasis was given to identifying and testing ISPR concepts for ATA applications that are difficult to test in traditional batch process based methods. It is the intention of this chapter to discuss some of the aspects, which were not covered in detail elsewhere in this thesis. These aspects cover discussions on: 1) when to focus on process engineering strategies and when to focus on protein engineering strategies. 2) How to apply the knowledge obtained in microfluidics across scales. 3) The need for implementing analytics into microfluidics.

8.1 Protein engineering vs. process engineering

Biocatalysis has matured greatly in the past decades and thereby become a feasible and important option in the chemical industry for the synthesis of a broad range of chemicals [5]. The increasing application of biocatalysis in the chemical industry is a direct consequence of the tremendous advances made in protein engineering strategies, which have made it possible in many cases to modify biocatalysts to fit the process requirements [7]. Despite the major advances, it is still time consuming and labor intensive to go through iterative rounds of modifying applicable biocatalysts to fit the process requirements. Additionally, the application of protein engineering strategies is not predictable, in the sense that there is no guarantee that a biocatalyst that fits specific requirements will be developed as a consequence of applying protein engineering strategies. For example, only in a few cases it has been possible to overcome product inhibition by protein engineering [7]. Perhaps future advances in protein engineering strategies will make it possible to develop novel biocatalysts that fulfill the needed process requirements in a fast and predictable manner.

However, there are still some process challenges that cannot be addressed directly by protein engineering strategies, e.g. unstable products. Therefore, independent of the advances in protein engineering, there will always remain applications of biocatalysis whose successful implementation will depend on implementation of process engineering strategies such as ISPR. Furthermore, it should once again be emphasized that ISPR and IScPR strategies are many times based on well-known and developed conventional separation methods, making it relatively fast and easy to implement such a strategy. For example, this is very beneficial if the apparently biggest bottleneck for the usage of a given biocatalyst consists of severe inhibitory effects from the (co-)product. Low biocatalyst activity at high concentrations, e.g. due to inhibition, can also be addressed by applying additional biocatalyst, but it will increase the synthesis costs exponentially with decreasing activity. In cases where ISPR/IScPR based on conventional separation methods is considered, emphasis should be given to aim the development towards concepts and implementation strategies that are not dedicated to a single application purpose. Hence, the investment risk in ISPR/IScPR options is not based on the success of a single product. Furthermore, independent on whether or not ISPR/IScPR concepts will be implemented in the final biocatalytic process, considering such options early on in the process development will certainly facilitate the development of the primary product recovery for the final process.

8.2 Scale-up or scale-out

As highlighted in this thesis there are many benefits associated with the application of microfluidics for process development. However, the process knowledge obtained by applying microfluidics has to be transferable across scales in order to enable transition to industrial scale production in a fast, reliable and easy manner. In other words, one should always keep in mind that process development, even in microscale reactors, is performed with the goal of achieving economically viable commercial scale production. This is especially important in industries with a need for fast transition from discovery to market implementation, such as the pharmaceutical industry [1]. However, it has proven quite challenging to efficiently transfer knowledge across scales, and this is also an issue for process development performed in conventional lab scale (mL scale). It is therefore the intention here to discuss some of these challenges and introduce approaches, which are potentially applicable for scaling-up starting with process-related information obtained from microfluidics.

Generally, the scientific literature identifies two main strategies applicable to increase process throughput, starting from the microfluidic scale into pilot and commercial scale production. These two strategies are numbering-up, sometimes referred to as scaling-out, and conventional scale-up [197]. The basic concept of both strategies is illustrated in figure 8.1. Alternatively, a combination of the two scaling strategies can be applied, i.e. scale-up/scale-out, which enables the possibility to maintain important features from both scaling strategies. For example, the good mass and heat transfer properties from the microfluidic modules combined with increased throughput from the larger scale.

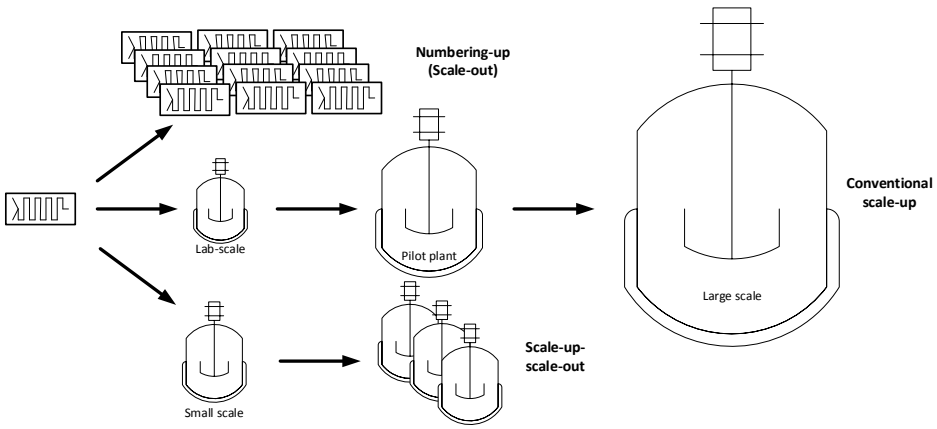

Figure 8.1: Illustration of the basic concept of numbering-up (scale-out), stepwise scale-up and scale-up/scale-out. The scale-up is performed stepwise to ensure reliable reaction performance across scales.

Numbering-up is based on operating microfluidic modules in parallel in order to reach the required process throughput, i.e. the microfluidic modules used for the process development are simply copied a number of times and operated in parallel. The advantage of this strategy is that microfluidic modules operated in parallel

should ideally ensure similar operating conditions in each module [197–199]. However, monitoring and controlling multiple modules simultaneously can become quite complex as the number of parallelized modules increases, making it challenging to ensure optimal reaction conditions in all reactor modules [197,199,200]. For example, it will be close to impossible to have individual control of each parallelized module, as it would be extremely expensive in terms of equipment and take up a lot of space. It is therefore necessary to operate parallelized microfluidic modules in a network, potentially causing variations of operating conditions in the individual reactors, e.g. due to flow maldistributions, which will influence the overall reaction performance [199]. From a Good Manufacturing Practice (GMP) point of view, such flow maldistributions can make it difficult to ensure consistent product quality over time along with sufficient periodical cleaning, making it difficult to have such a production pathway approved by regulatory authorities. These hurdles make it less attractive to apply the scaling out strategy [201,202]. On the other hand, in some cases numbering-up might be the only feasible scaling strategy. For example, the only way to ensure process safety, adequate process control and/or formation of desired product(s) [203]. This could be in cases when working with unstable compounds and/or highly exothermic reactions, where product degradation, unwanted side reactions and reaction runaway are key issues [198,203]. Additionally, in some cases only small quantities, e.g. a few grams, of a given compound are required in a fast manner, which makes it suitable to apply microfluidic devices for the actual production. For example, this is highly relevant for the production of personalized medicine and/or reactive compounds, which will greatly benefit from on-site and on-demand production that can be achieved by microscale reactors. Alternatively, the scale-up/scale-out strategy can be used where key features, such as mass and heat transfer, are maintained while the throughput can be increased with a minimum of modules in parallel.

Scale-up is the conventional strategy applied in biocatalysis to reach the required industrial scale production. Scaling-up is based on increasing reactor dimensions until a desired throughput can be ensured [102]. This strategy has the advantage that it will be possible, in principle, to retrofit new processes to pre-installed process equipment. Furthermore, it will only be required to monitor and control single reactors, i.e. reducing the complexity of the controller hardware compared to the numbering-up strategy. However, scaling-up is not straightforward as a consequence of the different physical phenomena which are dominating across scales [204], and causing altered process behavior across scales. For example, microfluidic modules are operating in the laminar flow regime, where wall effects, viscous effects and capillary effects are dominating, and where mixing is caused by diffusion. Larger scale reactors, e.g. with a volume ranging from L to m^3, are operating in the turbulent flow regime, where convective mixing, viscous effects and gravitational effects are dominating. These dominating effects cause altered process behavior compared to the microscale, e.g. because mass and heat transfer limitations vary across scales (the larger the scale, the lower the surface to volume ratio). Scale-up can be performed by trial and error or base on systematic approaches, such as scale-up based on dimensional similitude or model-based.

Dimensional similitude for scale-up is based on keeping the values of specific dimensionless numbers constant across scales, ensuring preservation of the laws of conservation of mass, momentum and heat [205]. It has however shown very difficult to replicate the unique operating conditions achievable in microfluidics at larger scale, i.e. achieving identical dimensionless numbers at large scale is often not possible. Furthermore, dimensional similitude will not take into account varying mass and heat transfer distances and thereby limitations that occur across scales. Even though the true reaction rate is independent of reactor size and structure, the observed reaction rate in any given system is influenced by the experienced mass and heat

transfer limitations. The mass and heat transfer limitations are then again influenced by the size and structure of the given reactor [71,206]. Hence, this approach is not suited for scale-up of microfluidics.

Another scale-up approach is based on mathematical modelling. Mathematical modelling is in that approach used to describe the separation method, reaction and reactor performance/behavior using mathematical equations representing physical and chemical effects in the reactor. In contrast with dimensional similitude, mathematical modelling enables the possibility to account for laws of physical and chemical rate processes to predict the reactor performance [205]. Thereby, in cases where true reaction kinetics are available, e.g. reaction kinetics which are not influenced by mass and/or heat transfer limitations, it should be possible to scale up the given system in a relatively easy manner. This also includes the possibility of taking the influence of mass and/or heat transfer limitations across scales into account. However, performing scale-up through mathematical modelling requires fast computers capable of solving very complex models in a fast routine. Computational fluid dynamics (CFD) is a powerful modelling tool for performing such advanced modelling simulations, in an attempt to describe reaction systems well enough and take rate-limiting effects across scales into account. However, even with powerful modelling tools such as CFD it is still very challenging and complex to simulate larger reactors and implement complex reaction/separation kinetics.

Independent of the applied scale-up approach, it is required to have determined the reaction/separation kinetics in advance. The use of microfluidics is thought to provide a major advantage in relation to the determination of “real” reaction/separation kinetics. This is related to the high degree of process control achievable in these reactors. This superior control will allow operating and maintaining certain mass and heat transfer limiting scenarios during operation. Furthermore, laminar flow operation can easily and with relatively high certainty be modelled using CFD simulations. Combining microfluidic experimental results with sufficient CFD models and simulations is essential to correctly interpret observations in microfluidic experiments and consequently determine reliable kinetic data from microfluidic experiments. The kinetic data can thereafter be used directly in other CFD models of larger scale systems, taking mass and heat transfer limitations across scales into account, ideally making the scale-up transition easier, faster and more reliable.

8.3 Analytics

Development of biocatalytic processes is mainly dominated by labor-intensive batch process based technologies that require extensive manual handling, which is labor intensive and imposes random experimental errors. This is also the case when performing manual sampling from microfluidic modules. For example, small deviations in the sample volume of low volume samples will cause large deviations in experimental results. Furthermore, the low flow rates commonly applied in microfluidics make it time and labor intensive to acquire sufficient sample volume manually. Therefore, a key element in the application of microfluidics is the possibility to implement in-line and on-line analytical monitoring in automated autonomously operating setups. The key benefits of such implementation is that the required sample volumes can be minimized, it can increase the experimental throughput, minimize manual labor, improve data quality, avoid and/or automate work-up procedures and methods [207]. Hence, successful implementation of such analytical monitoring options in microfluidics will facilitate the application of microfluidics as a process development and optimization tool. Furthermore, at present numerous novel and conventional analytical methods have been successfully implemented into microfluidics [207]. Thus, it is

rather a question of having the correct analytical equipment available rather than being limited by the experimental platform. Therefore, the most important limitation in this approach is the sensitivity of the available equipment, which will dictate the required operating volumes.

Chapter 9

Conclusions and future perspectives

In this thesis, *in-situ* product removal (ISPR) strategies in biocatalysis were investigated as a means to overcome challenges such as inhibitory effects from the product. The main goal of this thesis was to investigate the application of microfluidics as a novel technology for testing ISPR concepts in biocatalysis, which is difficult with conventional batch process based methods and technologies. As case study for these investigations, the application of amine transaminases (ATAs) for the asymmetric synthesis of chiral amines was chosen. The industrial and academic interest in ATAs is driven by the possibility of ATAs to enable efficient synthesis of enantiomerically active amines, which for example are important building blocks for many pharmaceuticals. However, synthesis of chiral amines by applying ATAs is commonly challenged by severe inhibitory effects, unfavorable thermodynamics and low solubility of the reaction species, to name a few of the most commonly experienced challenges, making it an excellent case study for investigation of ISPR/IScPR strategies.

9.1 Conclusions

Part of the work presented in this thesis evolved around defining a methodology for identifying and choosing proper ISPR/IScPR methods for ATAs processes (chapter 4). The methodology is based on identifying the challenges of the applied biocatalyst and the pure component physicochemical properties of the involved reaction species. Hence, the need for ISPR/IScPR and the most suitable options are identified. The methodology is focusing on challenges related to unfavorable thermodynamics, inhibitory effects from products/co-products and the product stability. Some of the key findings, which formed the basis of the proposed methodology are:

- **Unfavorable thermodynamics:** For the given methodology it was identified and proposed that in cases with unfavorable thermodynamics, $K_{eq} < 1$, it is required to either change the amine donor or implement cascade reaction systems to shift the equilibrium. The easiest and least complex option is to change the donor, but it required that the biocatalyst is compatible with this change. Furthermore, changing the donor can have a severe impact on how easy it is to recover the product after reaction. Cascade reactions were proposed as suitable ISPR/IScPR strategies because conventional separation methods are not suited for shifting the equilibrium, as they commonly do not have the same selectivity as the cascade reactions.
- **Product inhibition:** In cases where the biocatalyst performance suffers from severe inhibitory effects from the product/co-product, it is suitable to consider conventional separation methods. The advantage of conventional separation methods is that they are well-known and developed concepts, which makes it less of a risk compared to relying on protein engineering to solve the problem. Despite the tremendous progress made in protein engineering strategies, it is still not a guarantee that product inhibition will be minimized. Furthermore, in cases where the product is unstable, then it is required to consider ISPR strategies.

- **Downstream process development:** Furthermore, if inhibition is overcome, e.g. by protein engineering or changing the biocatalyst, then the methodology researched in this thesis can be applied to identify a suitable primary recovery step. Hence, the methodology motivates and addresses the aspect of considering recovery options early in the process development alongside with specifying the biocatalyst requirements.

The remaining part of this work evolved around the application of microfluidics for development, testing and evaluating of the proposed ISPR/IScPR options highlighted by the proposed methodology. This was performed by characterizing single microfluidic modules, representing the different process steps, individually and in combination in a plug-and-play manner. As a case study for these tests, the ATA catalyzed synthesis of 1-methyl-3-phenylpropylamine (MPPA) from benzylacetone (BA) was chosen using isopropylamine (IPA) as the amine donor. For this specific reaction system a two-step LLE ISPR concept was proposed, which enabled selective extraction of hydrophobic amines from hydrophilic amines. Some of the key findings and experiences made while performing this work are:

- **Biocatalyst characterization (chapter 5):** An on-line HPLC was integrated with microfluidic packed bed reactor modules as a means of ensuring high throughput characterization of biocatalysts. The main benefit from hooking up such an on-line analytical method to microfluidic systems is that it completely avoids manual sample handling and preparation, which can be challenging when operating with µL volumes. Furthermore, this setup made it possible to perform fast characterization of various process conditions influencing the biocatalyst performance. For example, testing the impact of changing substrate, amine donor, product, and co-product concentrations on the biocatalyst performance was possible. Such applications make the setup suitable for identifying optimal operating conditions and identifying potential challenges for the given biocatalyst in an easy and automated manner. A limitation to the assembled setup is the laminar flow profile in the reactor modules, which makes the measured biocatalyst performance a relative measure and thereby challenges the general applicability of the measured enzyme kinetics.
- **Separation characterization (chapter 6):** A microfluidic setup was assembled to test microfluidic liquid-liquid extraction. The given setup solely consisted of PTFE tubing connected in a Y-connector resulting in slug flow in the LLE modules. Based on varying the residence time in the LLE modules it was possible in a fast manner to determine partition coefficients and to some extent consider the mass transfer between the phases in the modules. Similar to the biocatalyst characterization, this setup will enable fast characterization of the influence of various process conditions on the extraction performance in multiple solvents.
- **Substrate supply (chapter 6):** It was identified that simultaneous extraction of the hydrophobic substrate (BA), would challenge the ISPR concept. However, since the applied substrate in the case studies had low aqueous solubility it was decided to apply the extraction as a simultaneous substrate supply strategy by dissolving BA in undecane (the extracting solvent). A big advantage of this kind of multi-functional separation method is that it avoided the need for considering an alternative reaction medium to increase the BA solubility, which could potentially compromise the biocatalyst.
- **Two-step LLE ISPR concept (chapter 7):** Based on the results from the characterization of the biocatalyst and the microfluidic LLE modules with undecane, it was found suitable to test a combined two-step LLE ISPR concept. This was done by combining a large microfluidic PBR module with two externally located microfluidic LLE modules in a plug-and-play manner. The assembled setup verified

that the ISPR concept worked as intended, and indeed made it possible to achieve high product purity and titers in the second extraction step without compromising the performance of the biocatalyst. This is a strong indication that it is indeed possible to test complex ISPR/IScPR concepts in an easy manner by applying microfluidics, which is otherwise difficult with conventional technologies.

- **Intensified biocatalyst performance (chapter 7):** Specific for the tested two-step LLE ISPR concept for ATA applications it was identified to be generally applicable for the separation of hydrophobic amines form hydrophilic amine donors. An advantage of the given system is that it is possible to maintain low product concentration and high substrate concentrations in the reaction mixture and thereby ensure intensified biocatalyst performance (delayed build-up of inhibitory product). The biggest limitation to the current system is the mixing response times, the required reservoir volumes and the activity of the tested biocatalysts (ATA-50 and ATA-82), which made it difficult to achieve high product concentrations in a relatively short time. However, the tested two-step LLE ISPR system did enable high product titers over longer periods, i.e. in the range of 26.5 g_P/L in 20 hours.

As a concluding remark, microfluidics for process development should be considered in combination with conventional biocatalytic process development technologies. That combination will make it possible to address the aspect of intensifying biocatalytic processes and thereby aid in expanding and accelerating the applicability of biocatalysis in future chemical manufacturing.

9.2 Open challenges and future perspectives

Biocatalysis is a maturing technology, which is developing faster and faster. This is caused by great improvements made to existing technologies on the one hand, and by the development of new methods and technologies that accelerate the biocatalyst and process development on the other hand. Furthermore, such progress aids in broadening the application range of biocatalysis. However, with such progress, also new challenges appear, resulting in new questions and problems that need to be resolved. During this work some apparent challenges and questions were not addressed, which could be very interesting for future work:

- **Solvent selection:** In this work, a rather limited number of solvents were tested for the extraction of hydrophobic amines. Further work should therefore be put into identifying generally applicable solvents suitable for extraction of various chiral amines from aqueous solutions. Additionally, for further screening it would be of interest to characterize the relative impact of the pH on the extraction performance. A starting point for this would be a thorough review of the scientific literature.
- **Biocatalyst formulation:** In this work only two immobilization techniques were considered, which could be broadened in the future. Therefore, for future work different biocatalyst formulations and immobilization techniques should be considered. Different formulations and immobilization techniques will have advantages and disadvantages for various applications (not necessarily only for microfluidics and ATAs). For example, in microfluidics some immobilization techniques will cause formation/application of particles that are too large to fit into the modules in an easy manner.
- **Biocompatibility:** Here the implication of applying *in-situ* LLE on the biocatalysts, i.e. the solvent and biocatalyst compatibility, was not investigated in detail. The impact of dissolved solvent in the aqueous phase on the biocatalyst should be investigated, to see if the biocatalyst performance is

compromised. Alternatively, the presence of a liquid-liquid interphase in the reactor modules could be investigated as a means to consider other ISPR/IScPR implementation strategies.

- **Two-step LLE ISPR for ATA processes:** For future work concerning the specific two-step LLE ISPR concept investigated in this work it could be interesting to identify the general applicability (other amines) and consider commercial production aspects of such ISPR concepts. A necessity before commercial production should be considered is the identification/development of ATAs with higher specific activity and/or expression than the ones applied in this work. The developed model of the ISPR concept could also be improved and combined with robust enzyme kinetics as a means to assess the actual intensification potential of the system.
- **Plug-and-play microfluidics:** There are an increasing number of commercial suppliers of microfluidic separation modules, which enable to test a broad range of ISPR/IScPR applications based on conventional separation methods. Therefore, for future work it could be interesting to consider other case studies requiring various ISPR/IScPR methods and implementation strategies. This would be crucial for evaluating the general applicability and the limitations of microfluidics for testing complex biocatalytic process concepts.
- **Analytics in microfluidics:** A big challenge in microfluidics is the handling and preparation of small volume samples. Therefore, it is ideal to integrate on-line and/or in-line analytics in the microfluidic experimental setup, which will greatly reduce manual labor and at the same time increase the knowledge throughput.
- **Microfluidics across scales:** The aim of developing biocatalysts and biocatalytic processes is commercialization. It is therefore important to address how the knowledge acquired by using the microfluidic experimental platform can be transferred into production, once suitable solutions are identified at the microscale. Various approaches to reach the desired production capacity were briefly discussed in this thesis, i.e. scale-up and scale-out. However, it would be interesting to combine that discussion with economic considerations for various production scenarios, where advantages and disadvantages of the different strategies could be identified in more detail.

References

1 Pollard, D.J. and Woodley, J.M. (2007) Biocatalysis for pharmaceutical intermediates: the future is now. *Trends Biotechnol.* 25, 66–73

2 Tufvesson, P. *et al.* (2011) Guidelines and cost analysis for catalyst production in biocatalytic processes. *Org. Process Res. Dev.* 15, 266–274

3 Straathof, A.J. *et al.* (2002) The production of fine chemicals by biotransformation. *Curr. Opin. Biotechnol.* 13, 548–556

4 Krühne, U. *et al.* (2014) Biocatalytic process development using microfluidic miniaturized systems. *Green Process Synth* 3, 23–31

5 Schmid, A. *et al.* (2001) Industrial biocatalysis today and tomorrow. *Nature* 409, 258–268

6 Schmid, A. *et al.* (2002) The use of enzymes in the chemical industry in Europe. *Curr. Opin. Biotechnol.* 13, 359–366

7 Bornscheuer, U.T. *et al.* (2012) Engineering the third wave of biocatalysis. *Nature* 485, 185–194

8 Burton, S.G. *et al.* (2002) The search for the ideal biocatalyst. *Nature* 20, 37–45

9 Hartman, R.L. and Jensen, K.F. (2009) Microchemical systems for continuous-flow synthesis. *Lab Chip* 9, 2495–2507

10 Kruhne, U. *et al.* (2014) Systematic Development of Miniaturized (Bio)Processes using Process Systems Engineering (PSE) Methods and Tools. *Chem. Biochem. Eng. Q.* 28, 203–214

11 Beilen, J.B. Van and Li, Z. (2002) Enzyme technology: An overview. *Curr. Opin. Biotechnol.* 13, 338–344

12 Kirk, O. *et al.* (2002) Industrial enzyme applications. *Curr. Opin. Biotechnol.* 13, 345–351

13 Hailes, H.H. *et al.* (2007) Perspective: Integration of biocatalytic conversion into chemical syntheses. *J. Chem. Technol. Biotechnol.* 82, 1063–1066

14 Santacoloma, P.A. *et al.* (2011) Multienzyme-Catalyzed Processes : Next-Generation Biocatalysis. *Org. Process Res. Dev.* 15, 203–212

15 Tufvesson, P. *et al.* (2010) Process considerations for the scale-up and implementation of biocatalysis. *Food Bioprod. Process.* 88, 3–11

16 Schoemaker, H.E. *et al.* (2003) Dispelling the myths--biocatalysis in industrial synthesis. *Science* 299, 1694–1697

17 Nielsen, P.H. *et al.* (2007) Cradle-to-gate environmental assessment of enzyme products produced industrially in denmark by novozymes A/S. *Int. J. Life Cycle Assess.* 12, 432–438

18 Wohlgemuth, R. (2009) The locks and keys to industrial biotechnology. *N. Biotechnol.* 25, 204–213

19 Tao, J. and Xu, J.-H. (2009) Biocatalysis in development of green pharmaceutical processes. *Curr. Opin. Chem. Biol.* 13, 43–50

20 Woodley, J.M. (2008) New opportunities for biocatalysis: making pharmaceutical processes greener. *Trends Biotechnol.* 26, 321–327

21 Hatti-Kaul, R. *et al.* (2007) Industrial biotechnology for the production of bio-based chemicals - a cradle-to-grave perspective. *Trends Biotechnol.* 25, 119–124

22 Dunn, P.J. (2012) The importance of Green Chemistry in Process Research and Development. *Chem. Soc. Rev.* 41, 1452

23 Wohlgemuth, R. (2007) Perspective Interfacing biocatalysis and organic synthesis. *J. Chem. Technol. Biotechnol.* 82, 1115–1121

24 Tufvesson, P. *et al.* (2011) Process considerations for the asymmetric synthesis of chiral amines using transaminases. *Biotechnol. Bioeng.* 108, 1479–1493

25 Datta, S. *et al.* (2013) Enzyme immobilization: an overview on techniques and support materials. *3 Biotech* 3, 1–9

26 Tufvesson, P. *et al.* (2011) Towards a cost-effective immobilized lipase for the synthesis of specialty chemicals. *J. Mol. Catal. B Enzym.* 68, 200–205

27 Rehn, G. *et al.* (2013) Chitosan flocculation: An effective method for immobilization of E. coli for biocatalytic processes. *J. Biotechnol.* 165, 138–144

28 Schmidt-Dannert, C. and Arnold, F.H. (1999) Directed evolution of industrial enzymes. *Trends Biotechnol.* 17, 135–136

29 Hibbert, E.G. and Dalby, P.A. (2005) Directed evolution strategies for improved enzymatic performance. *Microb. Cell Fact.* 4, 1–6

30 Carey, J.S. *et al.* (2006) Analysis of the reactions used for the preparation of drug candidate molecules. *Org. Biomol. Chem.* 4, 2337–2347

31 Kohls, H. *et al.* (2014) Recent achievements in developing the biocatalytic toolbox for chiral amine synthesis. *Curr. Opin. Chem. Biol.* 19, 180–192

32 Clifton, J.E. *et al.* (1982) Arylethanolamines derived from salicylamide with a- and b-adrenoceptor blocking activities. Preparation of labetalol, its enantiomers, and related salicylamides. *J. Med. Chem.* 25, 670–679

33 Savile, C.K. *et al.* (2010) Biocatalytic Asymmetric Synthesis of Chiral Amines from Ketones Applied to Sitagliptin Manufacture. *Science (80-.).* 329, 305–309

34 Turner, N.J. and Truppo, M.D. (2010) Biocatalytic routes to nonracemic chiral amines, in chiral amine synthesis. In *Chiral amine synthesis* (Nugent, T. C., ed), Wiley-VCH Verlag GmbH & Co. KGaA

35 R. Martin, A. *et al.* (2011) Characterization of a High Activity (S)-Aminotransferase for Substituted (S)-Aminotetralin Production: Properties and Kinetics. *J. Bioprocess. Biotech.* 01, 1–6

36 Breuer, M. *et al.* (2004) Industiral Methods for the Production of Optically Active Intermediates. *Angew. Chem. Int. Ed.* 43, 788–824

37 Cimarelli, C. and Palmieri, G. (2000) Asymmetric reduction of enantiopure imines with zinc borohydride: stereoselective synthesis of chiral amines. *Tetrahedron: Asymmetric* 11, 2555–2563

38 Tararov, V.I. and Börner, A. (2005) Approaching highly enantioselective reductive animation. *Synlett* 2, 203–211

39 Malik, M.S. *et al.* (2012) Features and technical applications of ω-transaminases. *Appl. Microbiol. Biotechnol.* 94, 1163–1171

40 Malik, M.S. *et al.* (2012) ω-Transaminase-catalyzed kinetic resolution of chiral amines using l-threonine as an amino acceptor precursor. *Green Chem.* 14, 2137

41 Höhne, M. and Bornscheuer, U.T. (2009) Biocatalytic routes to optically active amines.

ChemCatChem 1, 42–51

42 Ghislieri, D. and Turner, N.J. (2014) Biocatalytic Approaches to the Synthesis of Enantiomerically Pure Chiral Amines. *Top. Catal.* 57, 284–300

43 Hanson, R.L. *et al.* (2008) Preparation of (R)-amines from racemic amines with an (S)-amine transaminase from Bacillus megaterium. *Adv. Synth. Catal.* 350, 1367–1375

44 Koszelewski, D. *et al.* (2010) omega-Transaminases for the synthesis of non-racemic a-chiral primary amines. *Trends Biotechnol.* 28, 324–332

45 Steffen-Munsberg, F. *et al.* (2015) Bioinformatic analysis of a PLP-dependent enzyme superfamily suitable for biocatalytic applications. *Biotechnol. Adv.* 33, 566–604

46 Schätzle, S. *et al.* (2011) Enzymatic asymmetric synthesis of enantiomerically pure aliphatic, aromatic and arylaliphatic amines with (R)-selective amine transaminases. *Adv. Synth. Catal.* 353, 2439–2445

47 Bruunshuus, I. *et al.* (1997) , Properties and units in the clinical laboratory sciences. , *IUPAC Technical report 1997 - IFCC Recommendation 1997*. [Online]. Available: http://www.iupac.org/nc/home/about/members-and-committees/divisions/vii/ifcc-documents/iii-elements-of-properties-and-their-code-values.html?sword_list%5B%5D=aminotransferase

48 Höhne, M. *et al.* (2010) Rational assignment of key motifs for function guides in silico enzyme identification. *Nat. Chem. Biol.* 6, 807–813

49 Skalden, L. *et al.* (2015) Two Subtle Amino Acid Changes in a Transaminase Substantially Enhance or Invert Enantiopreference in Cascade Syntheses. *ChemBioChem* 16, 1041–1045

50 Al-Haque, N. *et al.* (2012) A robust methodology for kinetic model parameter estimation for biocatalytic reactions. *Biotechnol. Prog.* 28, 1186–1196

51 Cassimjee, K.E. *et al.* (2015) A quantum chemical study of the omega-transaminase reaction mechanism. *Org. Biomol. Chem.* 13, 8453–8464

52 Cassimjee, K.E. *et al.* (2011) Active site quantification of an Ω-Transaminase by performing a half transamination reaction. *ACS Catal.* 1, 1051–1055

53 Nobili, A. *et al.* (2015) Engineering the Active Site of the Amine Transaminase from Vibrio fluvialis for the Asymmetric Synthesis of Aryl-Alkyl Amines and Amino Alcohols. *ChemCatChem* 7, 757–760

54 Rausch, C. *et al.* (2013) Crystal structure of the ω-aminotransferase from Paracoccus denitrificans and its phylogenetic relationship with other class III amino- transferases that have biotechnological potential. *Proteins Struct. Funct. Bioinforma.* 81, 774–787

55 Wohlgemuth, R. *et al.* (2015) Microscale technology and biocatalytic processes: opportunities and challenges for synthesis. *Trends Biotechnol.* 33,

56 Sackmann, E.K. *et al.* (2014) The present and future role of microfluidics in biomedical research. *Nature* 507, 181–9

57 Wiles, C. and Watts, P. (2012) Continuous flow reactors: a perspective. *Green Chem.* 14, 38

58 Newman, S.G. and Jensen, K.F. (2013) The role of flow in green chemistry and engineering. *Green Chem.* 15, 1456

59 Anastas, P.T. and Kirchhoff, M.M. (2002) Origins, current status, and future challenges of green chemistry. *Acc. Chem. Res.* 35, 686–694

60 Poliakoff, M. *et al.* (2002) Green chemistry: science and politics of change. *Science* 297, 807–810

61 Wegner, J. *et al.* (2011) Ten key issues in modern flow chemistry. *Chem. Commun. (Camb).* 47, 4583–4592

62 Jensen, K.F. *et al.* (2014) Tools for chemical synthesis in microsystems. *Lab Chip* DOI: 10.1039/c4lc00330f

63 Darvas, F. *et al.* (2014) *Flow Chemistry*, (1st edn) De gruyter.

64 Jiménez-González, C. *et al.* (2011) Key green engineering research areas for sustainable manufacturing: A perspective from pharmaceutical and fine chemicals manufacturers. *Org. Process Res. Dev.* 15, 900–911

65 Nagy, K. and Jensen, K. (2011) Catalytic processes in small scale flow reactors. *Chem. Today* 29, 29–31

66 Moore, J.S. and Jensen, K.F. (2014) "Batch" kinetics in flow: online IR analysis and continuous control. *Angew. Chem. Int. Ed. Engl.* 53, 470–3

67 McMullen, J.P. and Jensen, K.F. (2010) An Automated Microfluidic System for Online Optimization in Chemical Synthesis. *Org. Process Res. Dev.* 14, 1169–1176

68 Schaber, S.D. *et al.* (2014) Design, Execution, and Analysis of Time-Varying Experiments for Model Discrimination and Parameter Estimation in Microreactors. *Org. Process Res. Dev.* 18, 1461–1467

69 Sahoo, H.R. *et al.* (2007) Multistep continuous-flow microchemical synthesis involving multiple reactions and separations. *Angew. Chemie - Int. Ed.* 46, 5704–5708

70 Fagaschewski, J. *et al.* (2012) Modular micro reaction engineering for carboligation catalyzed by benzoylformate decarboxylase. *Green Process. Synth.* 1, 337–344

71 Aota, A. *et al.* (2009) Parallel multiphase microflows: fundamental physics, stabilization methods and applications. *Lab Chip* 9, 2470–2476

72 Andrade, L.H. *et al.* (2014) Continuous Flow Synthesis of Chiral Amines in Organic Solvents: Immobilization of E. coli Cells Containing Both ω-Transaminase and PLP. *Org. Lett.* 16, 6092–6095

73 Mitic, A. *et al.* (2013) Applications, benefits and challenges of flow chemistry. *Chim. Oggi/Chemistry Today* 31, 4–8

74 Roberge, D. *et al.* (2013) Control of Hazardous Processes in Flow: Synthesis of 2-Nitroethanol. *J. Flow Chem.* 4, 1–9

75 Klais, O. *et al.* (2009) Guidance on safety/health for process intensification including MS design Pat I: Reaction hazards. *Chem. Eng. Technol.* 32, 1831–1844

76 Whitesides, G.M. (2006) The origins and the future of microfluidics. *Nature* 442, 368–373

77 Bird, R.B. *et al.* (2002) *Transport Phenomena*, (2nd edn) John Wiley and Sons inc.

78 Bruus, H. (2008) *Theoretical microfluidics*, Oxford University Press.

79 He, L. and Niemeyer, B. (2003) A novel correlation for protein diffusion coefficients based on molecular weight and radius of gyration. *Biotechnol. Prog.* 19, 544–548

80 Feigin, L.A. and Svergun, D.I. (1987) *Structure Analysis by Small-Angle X-Ray and Neutron Scattering*, Plenum Press.

81 Young, M.E. *et al.* (1980) Estimation of diffusion coefficients of proteins. *Biotechnol. Bioeng.* 22,

947–955

82 Ortega, A. *et al.* (2011) Prediction of hydrodynamic and other solution properties of rigid proteins from atomic- and residue-level models. *Biophys. J.* 101, 892–898

83 Fischer, H. *et al.* (2004) Average protein density is a molecular-weight-dependent function. *Protein Sci.* 13, 2825–2828

84 Levenspiel, O. (1999) *Chemical reaction engineering*, John Wiley and Sons inc.

85 Bolivar, J.M. and Nidetzky, B. (2013) Multiphase biotransformations in microstructured reactors: opportunities for biocatalytic process intensification and smart flow processing. *Green Process. Synth.* 2, 541–559

86 Hessel, V. *et al.* (2005) Gas - Liquid and Gas - Liquid - Solid Microstructured Reactors : Contacting Principles and Applications. *Ind. Eng. Chem. Res.* 44, 9750–9769

87 Liu, H. and Zhang, Y. (2009) Droplet formation in a T-shaped microfluidic junction. *J. Appl. Phys.* 106,

88 Day, P. *et al.* (2008) *Microdroplet Technology: Principles and Emerging Applications in Biology and Chemistry*, Springer Science+Business Media.

89 Van Der Graaf, S. *et al.* (2006) Lattice Boltzmann simulations of droplet formation in a T-shaped microchannel. *Langmuir* 22, 4144–4152

90 De Menech, M. *et al.* (2008) Transition from squeezing to dripping in a microfluidic T-shaped junction. *J. Fluid Mech.* 595, 141–161

91 Nisisako, T. *et al.* (2004) Novel microreactors for functional polymer beads. *Chem. Eng. J.* 101, 23–29

92 Kreutzer, M.T. *et al.* (2005) Multiphase monolith reactors: Chemical reaction engineering of segmented flow in microchannels. *Chem. Eng. Sci.* 60, 5895–5916

93 Günther, A. and Jensen, K.F. (2006) Multiphase microfluidics: from flow characteristics to chemical and materials synthesis. *Lab Chip* 6, 1487–1503

94 De Loos, S.R.A. *et al.* (2010) Gas-liquid dynamics at low Reynolds numbers in pillared rectangular micro channels. *Microfluid. Nanofluidics* 9, 131–144

95 Ergun, S. (1952) Fluid flow through packed columns. *Chem. Eng. Prog.* 48, 89 – 94

96 Caulkin, R. *et al.* (2012) Predictions of porosity and fluid distribution through nonspherical-packed columns. *AIChE J.* 58, 1503–1512

97 Nguyen, N.-T. and Wu, Z. Micromixers—a review. , *Journal of Micromechanics and Microengineering*, 15. (2004) , R1–R16

98 Zaiput Flow Technologies. . [Online]. Available: https://www.zaiput.com/. [Accessed: 01-Sep-2015]

99 Hartman, R.L. *et al.* (2010) Multistep microchemical synthesis enabled by microfluidic distillation. *Angew. Chemie - Int. Ed.* 49, 899–903

100 Tufvesson, P. *et al.* (2015) Economic considerations for selecting an amine donor in biocatalytic transamination. *Org. Process Res. Dev.* 19, 652–660

101 Blow, N. (2009) Microfluidics: the great divide. *Nat. Methods* 6, 683–686

102 Bieringer, T. *et al.* Future Production Concepts in the Chemical Industry: Modular - Small-Scale - Continuous. , *Chemical Engineering and Technology*, 36. (2013) , 900–910

103 Jensen, K.F. *et al.* (2014) Tools for chemical synthesis in microsystems. *Lab Chip* 14, 3206–3212

104 Ehrfeld Mikrotechnik BTS. . [Online]. Available: http://www.ehrfeld.com/home.html. [Accessed: 07-Jul-2015]

105 Syrris. . [Online]. Available: http://syrris.com/. [Accessed: 07-Jul-2015]

106 Fluidgent. . [Online]. Available: http://www.fluigent.com/. [Accessed: 07-Jul-2015]

107 Chemtrix. . [Online]. Available: http://www.chemtrix.com/. [Accessed: 07-Jul-2015]

108 Poulsen, A. *et al.* (2013) 3D-printer vejen til innovation? *Dansk Kemi* 94, 32–34

109 Hartman, R.L. *et al.* Deciding whether to go with the flow: Evaluating the merits of flow reactors for synthesis. , *Angewandte Chemie - International Edition*, 50. (2011) , 7502–7519

110 Valera, F.E. *et al.* (2010) The flow's the thing...or is it? Assessing the merits of homogeneous reactions in flask and flow. *Angew. Chem. Int. Ed. Engl.* 49, 2478–85

111 Woodley, J.M. (2013) Application of In situ Product Removal (ISPR) Technologies for Implementation and Scale-Up of Biocatalytic Reductions. In *Synthesis Methods for Biologically Active Molecules: Exploring the Potential of Bioreductions* (Brenna, E., ed), Wiley-VCH Verlag GmbH & Co. KGaA

112 Mathew, S. and Yun, H. (2012) omega-Transaminases for the Production of Optically Pure Amines and Unnatural Amino Acids. *Acs Catal.* 2, 993–1001

113 Peng, Y. *et al.* (2014) Engineering chiral porous metal-organic frameworks for enantioselective adsorption and separation. *Nat. Commun.* 5, 4406

114 Zheng, G.W. and Xu, J.H. (2011) New opportunities for biocatalysis: Driving the synthesis of chiral chemicals. *Curr. Opin. Biotechnol.* 22, 784–792

115 Drauz, K. (2012) *Enzyme catalysis in organic synthesis. Vol. 2*, Wiley-VCH Verlag.

116 Woodley, J.M. (2013) Protein engineering of enzymes for process applications. *Curr. Opin. Chem. Biol.* 17, 310–316

117 Welch, C.J. *et al.* (2005) Adsorbent Screening for Metal Impurity Removal in Pharmaceutical Process Research Adsorbent Screening for Metal Impurity Removal in Pharmaceutical Process Abstract : A microtube screening approach affords simple and convenient. *Org. Process Res. Dev.* 9, 198–205

118 Schügerl, K. and Hubbuch, J. (2005) Integrated bioprocesses. *Curr. Opin. Microbiol.* 8, 294–300

119 Bechtold, M. and Panke, S. (2009) In-situ Product Recovery Integrated with Biotransformations. *Chim. Int. J. Chem.* 63, 345–348

120 Turner, N.J. (2009) Directed evolution drives the next generation of biocatalysts. *Nat. Chem. Biol.* 5, 567–573

121 Lye, G.J. and Woodley, J.M. (1999) Application of in situ product-removal techniques to biocatalytic processes. *Trends Biotechnol.* 17, 395–402

122 Freeman, A. *et al.* (1993) In-situ product removal as a tool for bioprocessing. *Biotechnology* 11, 1007 – 1012

123 Oudshoorn, A. *et al.* (2010) Short-cut calculations for integrated product recovery options in fermentative production of bio-bulk chemicals. *Process Biochem.* 45, 1605–1615

124 Van Hecke, W. *et al.* (2014) Advances in in-situ product recovery (ISPR) in whole cell biotechnology during the last decade. *Biotechnol. Adv.* 32, 1245–1255

125 Tufvesson, P. *et al.* (2013) Advances in the process development of biocatalytic processes. *Org. Process Res. Dev.* 17, 1233–1238

126 Tufvesson, P. *et al.* (2015) Economic considerations for selecting an amine donor in biocatalytic transamination. *Org. Process Res. Dev.* 19, 652–660

127 Fesko, K. *et al.* (2013) Investigation of one-enzyme systems in the ω-transaminase-catalyzed synthesis of chiral amines. *J. Mol. Catal. B Enzym.* 96, 103–110

128 Päiviö, M. and Kanerva, L.T. (2013) Reusable ω-transaminase sol-gel catalyst for the preparation of amine enantiomers. *Process Biochem.* 48, 1488–1494

129 Stark, D. and von Stockar, U. (2003) In situ product removal (ISPR) in whole cell biotechnology during the last twenty years. *Adv. Biochem. Eng. Biotechnol.* 80, 149 – 175

130 Woodley, J.M. *et al.* (2008) Future directions for in-situ product removal (ISPR). *J. Chem. Technol. Biotechnol.* 83, 121–123

131 Wang, P. *et al.* (2012) Microbial production of propionic acid with Propionibacterium freudenreichii using an anion exchanger-based in situ product recovery (ISPR) process with direct and indirect contact of cells. *Appl. Biochem. Biotechnol.* 166, 974–986

132 Buque-Taboada, E.M. *et al.* (2006) In situ product recovery (ISPR) by crystallization: Basic principles, design, and potential applications in whole-cell biocatalysis. *Appl. Microbiol. Biotechnol.* 71, 1–12

133 Truppo, M.D. *et al.* (2010) Efficient Production of Enantiomerically Pure Chiral Amine at Conc 50 g/L Using Transaminase. *Organic* 14, 234–237

134 Halim, M. *et al.* (2014) Microscale methods to rapidly evaluate bioprocess options for increasing bioconversion yields: Application to the ω-transaminase synthesis of chiral amines. *Bioprocess Biosyst. Eng.* 37, 931–941

135 Tufvesson, P. *et al.* (2014) A model to assess the feasibility of shifting reaction equilibrium by acetone removal in the transamination of ketones using 2-propylamine. *Biotechnol. Bioeng.* 111, 309–319

136 Yun, H. *et al.* (2004) Kinetic resolution of (R,S)-sec-butylamine using omega-transaminase from Vibrio fluvialis JS17 under reduced pressure. *Biotechnol. Bioeng.* 87, 772–778

137 Meadows, R.E. *et al.* (2013) Efficient Synthesis of (S)-1- (5-Fluoropyrimidin-2-yl) ethylamine Using an ω-Transaminase Biocatalyst in a Two-Phase System. *Org. Process Res. Dev.* 17, 1117–1122

138 Bea, H.S. *et al.* (2011) Asymmetric synthesis of (R)-3-fluoroalanine from 3-fluoropyruvate using omega-transaminase. *Biotechnol. Bioprocess Eng.* 16, 291–296

139 Shin, J.S. and Kim, B.G. (1997) Kinetic resolution of alpha-methylbenzylamine with omicron-transaminase screened from soil microorganisms: application of a biphasic system to overcome product inhibition. *Biotechnol. Bioeng.* 55, 348–358

140 Seo, J.-H. *et al.* (2011) Necessary and sufficient conditions for the asymmetric synthesis of chiral amines using ω-aminotransferases. *Biotechnol. Bioeng.* 108, 253–263

141 Yun, H. and Kim, B.-G. (2008) Asymmetric Synthesis of (S)-α-Methylbenzylamine by Recombinant Escherichia coli Co-Expressing Omega-Transaminase and Acetolactate Synthase. *Biosci. Biotechnol. Biochem.* 72, 3030–3033

142 Shin, J.S. *et al.* (2001) Kinetic resolution of chiral amines with omega-transminase using an enzyme-membrane reactor. *Biotechnol. Bioeng.* 73, 179–187

143 Rehn, G. *et al.* (2014) Supported liquid membrane as a novel tool for driving the equilibrium of ??-transaminase catalyzed asymmetric synthesis. *J. Biotechnol.* 179, 50–55

144 Börner, T. *et al.* (2015) A Process Concept for High-Purity Production of Amines by Transaminase-Catalyzed Asymmetric Synthesis: Combining Enzyme Cascade and Membrane-Assisted ISPR. *Org. Process Res. Dev.* 19, 793–799

145 Simon, R.C. *et al.* (2013) Chemoenzymatic synthesis of all four diastereomers of 2,6-disubstituted piperidines through stereoselective monoamination of 1,5-diketones. *Chem. - A Eur. J.* 19, 2859–2865

146 Simon, R.C. *et al.* (2013) Concise chemoenzymatic three-step total synthesis of isosolenopsin through medium engineering. *European J. Org. Chem.*

147 Wang, B. *et al.* (2013) An efficient single-enzymatic cascade for asymmetric synthesis of chiral amines catalyzed by ω-transaminase. *Chem. Commun.* 49, 161–3

148 Simon, R.C. *et al.* (2014) Recent Developments of Cascade Reactions Involving ω - Transaminases. *ACS Catal.* 4, 129–143

149 Koszelewski, D. *et al.* (2008) Asymmetric synthesis of optically pure pharmacologically relevant amines employing ω-transaminases. *Adv. Synth. Catal.* 350, 2761–2766

150 Mutti, F.G. *et al.* (2011) Stereoselectivity of four (R)-selective transaminases for the asymmetric amination of ketones. *Adv. Synth. Catal.* 353, 3227–3233

151 Fuchs, M. *et al.* (2012) Amination of benzylic and cinnamic alcohols via a biocatalytic, aerobic, oxidation–transamination cascade. *RSC Adv.* 2, 6262–6265

152 Tufvesson, P. *et al.* (2012) Experimental determination of thermodynamic equilibrium in biocatalytic transamination. *Biotechnol. Bioeng.* 109, 2159–62

153 Chemistry, R.S. of (2015) , Chemspider: Search and share chemistry. . [Online]. Available: http://www.chemspider.com/

154 Zhao, L. *et al.* (2002) Analysis of aromatic amines in water samples by liquid-liquid-liquid microextraction with hollow fibers and high-performance liquid chromatography. *J. Chromatogr. A* 963, 239–248

155 Yan, H. and Wang, H. (2013) Recent development and applications of dispersive liquid-liquid microextraction. *J. Chromatogr. A* 1295, 1–15

156 Zhu, L. *et al.* (2002) Liquid – liquid – liquid microextraction of aromatic amines from water samples combined with high-performance liquid chromatography. *J. Chromatogr. A* 963, 231–237

157 Pedersen-Bjergaard, S. and Rasmussen, K.E. (2008) Liquid-phase microextraction with porous hollow fibers, a miniaturized and highly flexible format for liquid-liquid extraction. *J. Chromatogr. A* 1184, 132–142

158 Peng, S.X. *et al.* (2000) Automated high-throughput liquid-liquid extraction for initial purification of combinatorial libraries. *Anal. Chem.* 72, 261–266

159 Bommarius, A.S. *et al.* (2011) Status of protein engineering for biocatalysts: How to design an industrially useful biocatalyst. *Curr. Opin. Chem. Biol.* 15, 194–200

160 Reetz, M.T. (2011) Laboratory evolution of stereoselective enzymes: A prolific source of catalysts for asymmetric reactions. *Angew. Chemie - Int. Ed.* 50, 138–174

161 Liu, Y. *et al.* (2001) On-line monitoring and controlling system for fermentation processes. *Biochem. Eng. J.* 7, 17–25

162 Zumbusch, P. V. *et al.* (1994) On-line monitoring of organic substances with high-pressure liquid chromatography (HPLC) during the anaerobic fermentation of waste-water. *Appl. Microbiol. Biotechnol.* 42, 140–146

163 Wu, C.-H. and Wee, S. (2015) Micro sequential injection system as the interfacing device for process analytical applications. *Biotechnol. Prog.* 31, 607–613

164 Welch, C.J. *et al.* (2009) Online analysis of flowing streams using microflow HPLC. *Org. Process Res. Dev.* 13, 1022–1025

165 Zhu, L. *et al.* (2007) On-line HPLC combined with multivariate statistical process control for the monitoring of reactions. *Anal. Chim. Acta* 584, 370–378

166 Doyle, M.J. and Newton, B.J. (2002) Chromatography with On-line HPLC and Ion Chromatography For Process Control. *Cast*

167 Kohls, H. *et al.* (2015) Selective Access to All Four Diastereomers of a 1,3-Amino Alcohol by Combination of a Keto Reductase- and an Amine Transaminase-Catalysed Reaction. *Adv. Synth. Catal.* 357, 1808–1814

168 Mallin, H. *et al.* (2014) Immobilization of (R)- and (S)-amine transaminases on chitosan support and their application for amine synthesis using isopropylamine as donor. *J. Biotechnol.* 191, 32–37

169 Scott Fogler, H. (2014) *Elements of chemical reaction engineering*, Pearson Education Limited.

170 Zajkoska, P. *et al.* (2014) Immobilised whole-cell recombinant monoamine oxidase biocatalysis. *Appl. Microbiol. Biotechnol.* 99, 1229–1236

171 Grosová, Z. *et al.* (2009) Production of d-galactose using β-galactosidase and Saccharomyces cerevisiae entrapped in poly(vinylalcohol) hydrogel. *Food Chem.* 116, 96–100

172 Stloukal, R. *et al.* (2014) Dye decolorisation by laccase immobilised in lens-shaped poly(vinyl alcohol) hydrogel capsules. *Chem. Pap.* 68, 1514–1520

173 Rodríguez-Nogales, J.M. *et al.* (2013) Immobilization of Oenococcus oeni in lentikats® to develop malolactic fermentation in wines. *Biotechnol. Prog.* 29, 60–65

174 Rebroš, M. *et al.* (2013) Recombinant α-L-rhamnosidase of Aspergillus terreus immobilization in polyvinylalcohol hydrogel and its application in rutin derhamnosylation. *Biocatal. Biotransformation* 31, 329–334

175 LentiKat's Biotechnologies. . [Online]. Available: http://www.lentikats.eu/cs/. [Accessed: 01-Sep-2015]

176 Durieux, A. *et al.* (2000) Continuous malolactic fermentation by Oenococcus oeni entrapped in Lentikats. *Biotechnol. Lett.* 22, 1679–1684

177 Zhou, Q. *et al.* (2009) Ultrasound-assisted ionic liquid dispersive liquid-phase micro-extraction: A novel approach for the sensitive determination of aromatic amines in water samples. *J. Chromatogr. A* 1216, 4361–4365

178 Saraji, M. and Boroujeni, M.K. (2014) Recent developments in dispersive liquid-liquid microextraction. *Anal. Bioanal. Chem.* 406, 2027–2066

179 Seader, J.D. (2006) *Separation process principles*, Wiley.

180 Dessimoz, A.L. *et al.* (2008) Liquid-liquid two-phase flow patterns and mass transfer characteristics in rectangular glass microreactors. *Chem. Eng. Sci.* 63, 4035–4044

181 Burns, J.R. and Ramshaw, C. (2001) The intensification of rapid reactions in multiphase systems using slug flow in capillaries. *Lab Chip* 1, 10–15

182 Logtenberg, H. *et al.* (2011) Multiple flow profiles for two-phase flow in single microfluidic channels through site-selective channel coating. *Lab Chip* 11, 2030–2034

183 Atencia, J. and Beebe, D.J. (2005) Controlled microfluidic interfaces. *Nature* 437, 648–655

184 Guillot, P. *et al.* (2006) Viscosimeter on a Microfluidic Chip Viscosimeter on a Microfluidic Chip. *Society* DOI: 10.1021/la060131z

185 Assael, M.J. *et al.* (1991) Measurements of the viscosity of n-heptane + n-undecane mixtures at pressures up to 75 MPa. *Int. J. Thermophys.* 12, 811–820

186 Gani, R. *et al.* (2005) Method for selection of solvents for promotion of organic reactions. *Comput. Chem. Eng.* 29, 1661–1676

187 Henderson, R.K. *et al.* (2011) Expanding GSK's solvent selection guide – embedding sustainability into solvent selection starting at medicinal chemistry. *Green Chem.* 13, 854

188 Curzons, a. D. *et al.* (1999) Solvent selection guide: a guide to the integration of environmental, health and safety criteria into the selection of solvents. *Clean Technol. Environ. Policy* 1, 82–90

189 Clark, J.H. and Tavener, S.J. (2007) Alternative solvents: Shades of green. *Org. Process Res. Dev.* 11, 149–155

190 Straathof, A.J.J. (2003) Auxiliary phase guidelines for microbial biotransformations of toxic substrate into toxic product. *Biotechnol. Prog.* 19, 755–762

191 Halling, P.J. (1994) Thermodynamic predictions for biocatalysis in nonconventional media: Theory, tests, and recommendations for experimental design and analysis. *Enzyme Microb. Technol.* 16, 178–206

192 Zhao, Y. *et al.* (2007) liquid-liquid two-phase mass transfer in the T-junction microchannels. *AIChE J.* 53, 3042–3053

193 Shin, J.S. and Kim, B.G. (1999) Modeling of the kinetic resolution of alpha-methylbenzylamine with omega-transaminase in a two-liquid-phase system. *Enzyme Microb. Technol.* 25, 426–432

194 McMurry, J. (2007) *Organic chemistry : a biological approach*, Thomson Brooks/Cole.

195 Efron, B. (1979) the 1977 Rietz Lecture - bootstrap methods: another look at the jackknife. *Ann. Stat.* 7, 1–26

196 Wohlgemuth, R. *et al.* (2015) Microscale technology and biocatalytic processes: opportunities and challenges for synthesis. *Trends Biotechnol.* 33, 302–314

197 Jensen, K.F. (2001) Microreaction engineering — is small better? *Chem. Eng. Sci.* 56, 293–303

198 Elvira, K.S. *et al.* (2013) The past, present and potential for microfluidic reactor technology in chemical synthesis. *Nat. Chem.* 5, 905–15

199 Saber, M. *et al.* (2010) Microreactor numbering-up in multi-scale networks for industrial-scale applications: Impact of flow maldistribution on the reactor performances. *Chem. Eng. Sci.* 65, 372–379

200 Tonkovich, a. *et al.* (2005) Microchannel Technology Scale-up to Commercial Capacity. *Chem. Eng. Res. Des.* 83, 634–639

201 Roberge, D.M. *et al.* (2009) Industrial design, scale-up, and use of microreactors. *Chim. Oggi* 27, 8–11

202 Wegner, J. *et al.* (2011) Ten key issues in modern flow chemistry. *Chem. Commun.* 47, 4583–4592

203 Zhang, X. *et al.* (2004) Application of Microreactor Technology in Process Development. *Org. Process Res. Dev.* 8, 455–460

204 Losey, M.W. *et al.* (2001) Microfabricated multiphase packed-bed reactors: characterization of mass transfer and reactions. *Ind. Eng. Chem. Res.* 40, 2555–2562

205 Perry, R.H. (1997) *Perry's chemical engineers' handbook*, McGraw-Hill.

206 Kockmann, N. and Roberge, D.M. (2011) Scale-up concept for modular microstructured reactors based on mixing, heat transfer, and reactor safety. *Chem. Eng. Process. Process Intensif.* 50, 1017–1026

207 McMullen, J.P. and Jensen, K.F. (2010) Integrated microreactors for reaction automation: new approaches to reaction development. *Annu. Rev. Anal. Chem.* 3, 19–42

Appendix A

Publications

Appendix A.1: Biocatalytic process development using microfluidic miniaturized systems

Review

Ulrich Krühne, Søren Heintz, Rolf Ringborg, Inês P. Rosinha, Pär Tufvesson, Krist V. Gernaey and John M. Woodley*

Biocatalytic process development using microfluidic miniaturized systems

Abstract: The increasing interest in biocatalytic processes means there is a clear need for a new systematic development paradigm which encompasses both protein engineering and process engineering. This paper argues that through the use of a new microfluidic platform, data can be collected more rapidly and integrated with process modeling, can provide the basis for validating a reduced number of potential processes. The miniaturized platform should use a smaller reagent inventory and make better use of precious biocatalysts. The EC funded BIOINTENSE project will use ω-transaminase based synthesis of chiral amines as a test-bed for assessing the viability of such a high throughput biocatalytic process development, and in this paper, such a vision for the future is presented.

Keywords: biocatalysis; microfluidics; process development; transaminase.

***Corresponding author: John M. Woodley,** Center for Process Engineering and Technology, Department of Chemical and Biochemical Engineering, Technical University of Denmark, 2800 Lyngby, Denmark, e-mail: jw@kt.dtu.dk
Ulrich Krühne, Søren Heintz, Rolf Ringborg, Inês P. Rosinha, Pär Tufvesson and Krist V. Gernaey: Center for Process Engineering and Technology, Department of Chemical and Biochemical Engineering, Technical University of Denmark, 2800 Lyngby, Denmark

1 Introduction

The increasing academic and industrial interest in biocatalytic processes (chemical reactions catalyzed by an isolated enzyme, immobilized enzyme, or whole cell containing one or more enzymes) is to a large extent driven by the need for selective chemistry [1]. Even more remarkable is that such selectivity is achieved with enzymes under mild reaction conditions. While high selectivity may be easily achievable using biocatalysis, for implementation in industry, it is also necessary to develop a process that is sufficiently efficient that it can be economically feasible. For example, for a pharmaceutical intermediate, a product concentration over 50 g/l must leave the reactor and a high yield of product on biocatalyst (termed biocatalyst yield) must also be achieved [2, 3]. The exact threshold values depend on the type of catalyst and the industry sector (or more accurately the selling price of the product relative to the cost of the substrate). However, almost without exception, a new biocatalytic process studied in the laboratory will not fulfill these requirements, since enzymes are usually evolved to convert natural substrates at low concentrations. This presents an interesting challenge for process chemists and engineers, since the wish to implement a new (non-natural) substrate at high concentrations can only be addressed by a concerted development effort with a combination of biocatalyst modification and process modification. The driver for such process development is economic and while targets can be evaluated in a given case, there remains a further problem, because there are many options to choose from and different routes to solve a given problem [4]. While some solutions are more effective than others, and some are easier to implement than others, there remain many choices to be made. One consequence of such complexity is that to date such an analysis has inevitably been carried out on a case-by-case basis, meaning that often the final scale-up and implementation does not even take place, because it takes too long and is too difficult. Furthermore, in many cases, at an early stage it is not clear which way to develop the process and where to put the research effort. In order to overcome this, one potential vision for the future could be a systematic procedure for automated data collection, followed by testing of a more limited number of alternatives at a miniature scale, such that operations can be carried out with a reduced reagent inventory and potentially even in parallel. Indeed, such schemes already exist for chemical synthetic systems and while the level of complexity with biocatalysis is frequently greater, it is also the case that their value might be the greater. At the very least, it would enable more process options to be evaluated in a shorter time (see Figure 1 for a schematic representation of the philosophy).

Combined with process modeling techniques (Krühne et al., 2013, submitted for publication), this could provide

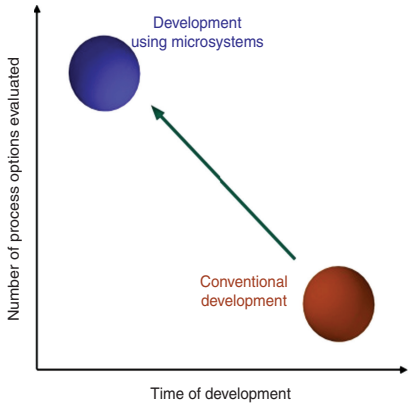

Figure 1 Philosophy underlying miniaturization in the context of process development for biocatalytic processes.

a way to map the solution space and enable design decisions to be made more rapidly and with greater confidence. This is one of the main objectives of the EC-funded BIOINTENSE project. In this brief article, the rationale behind high throughput biocatalytic process development will be discussed, together with the challenges and opportunities such an approach can bring. One of the most important application areas of biocatalytic processes is in the synthesis of pharmaceutical intermediates, where speed of development (and integration with the neighboring catalytic steps) is of the utmost importance.

2 Biocatalytic process development in the pharmaceutical sector

In the pharmaceutical industry, process development time is critical (both for chemical as well as biocatalytic synthetic steps) and therefore it is essential to evaluate and screen process options rapidly. For biocatalytic processes, in order that resources spent on development are used in the most efficient manner possible, a systematic method is necessary to help identify the process constraints (reaction related constraints as well as biocatalyst related constraints). The constraints form the basis of a methodology to identify suitable improvement strategies.

For biocatalytic processes, several strategies are available to improve the process from the initial laboratory reaction, so that it is suitable for industrial application. Strategies focused on reducing the cost contribution of the biocatalyst include fermentation technology (e.g., optimization of the production host platform, carbon feeding strategy, oxygen supply and media composition) to reduce the cost of producing the biocatalyst, as well as protein engineering and biocatalyst immobilization to ensure that the biocatalyst (irrespective of its cost) is subsequently used in the most effective way possible (maximum biocatalyst yield: kg product/kg biocatalyst). Strategies focused on reducing the other cost contributions include reaction engineering (e.g., addition of an organic solvent or use of substrate excess), reactor engineering (e.g., substrate feeding), or process engineering (e.g., *in situ* product removal), to enable the process to run as effectively as possible (maximum reaction yield, biocatalyst yield and product concentration). Additionally, it is important to recognize the interaction between the strategies.

Interestingly, several recent reviews about the application of protein engineering strategies to solve biocatalytic process challenges have argued that the advances in protein engineering now make it possible to 'fit' the biocatalyst to the process [5, 6], as originally proposed by Burton and coworkers [7]. Therefore, once initial activity for the desired reaction has been detected, the enzyme performance can indeed be enhanced by protein engineering, to improve the desired properties, such as substrate repertoire and selectivity, as well as activity and stability [8]. Today, there are many examples where new biocatalytic routes have been established through significant improvement of an existing enzyme, via iterative rounds of mutagenesis and screening [5, 6, 9, 10]. However, despite the remarkable advances in protein engineering, we are yet to be convinced that it is possible to fit the biocatalyst to all process conditions. For example, while optimal operating conditions for a biocatalyst can be expanded significantly from pH 7 and ambient temperature, enzymes still have limitations when compared to chemical catalysts (which in general operate at high concentrations of substrates and products, as well as elevated temperatures [11]), meaning that operation under extreme conditions may not be possible. However, of even greater importance is the fact that the thermodynamic constraints of the process cannot be addressed by biocatalyst modifications directly. While in nature, enzymes usually catalyze thermodynamically favorable reactions, for non-natural substrates as well as reactions run in synthetic mode, this is frequently not the case. Thus, the design of any process needs to also consider the likely operating space for the biocatalyst and the implication of changing key parameters on the process feasibility and cost [4].

3 Process development using microfluidic miniaturized systems

Microfluidic technologies concern the use of fluids in small compartments (e.g., with a size in the order of µl

volumes and with dynamic flow driven by pressure gradients or other methods). Such technologies are sometimes referred to as micro unit operations (MUOs), where the basic concept is to have conventional large scale equipment mimicked at a micro scale (e.g., reactors and separators [12]). However, microfluidic devices also enable novel process development methods [13–15]. At small scale, different physical effects dominate the flow compared to larger scale technologies. Microfluidic technologies exploit these effects in a way that simply cannot be achieved at a larger scale. Often these dominant effects are described by dimensionless numbers [16]:

- In microfluidic devices, the Reynolds number (*Re*), the ratio of convective to viscous forces, is low (*Re*<100 and usually around 1) indicating that viscous forces are dominating and thereby laminar flows are obtained:

$$Re=\frac{\rho v d_h}{\mu}$$

  where ρ is the fluid density, v is the fluid velocity, d_h is the hydraulic diameter (4A/P, where A is the cross sectional area and P the wetted perimeter) and μ is the fluid viscosity.
- The Péclet (*Pe*) number, the ratio of mass transfer rate due to convection compared to that of diffusion, becomes small in microfluidic devices, indicating that the rate of mass transport is dominated by diffusion:

$$Pe=\frac{va}{D}$$

  where D is the diffusion coefficient and a is the radial length scale.
- The bond number (*Bo*), the ratio of gravitational forces to those caused by surface tension, is small in microfluidic devices, as a consequence of dominant surface tension forces, i.e., *Bo*<<1:

$$Bo=\frac{\rho g a^2}{\gamma}$$

  where g is the gravitational acceleration ($9.81\ \frac{m}{s^2}$) and γ is the surface tension.
- The Damköhler number (*Da*) is another important dimensionless number for the characterization of microfluidic systems. This number is used to relate the chemical or biochemical reaction timescale to other phenomena that occur in miniaturized systems. This can, for instance, be the material transport due to diffusion, interphase transport and fluid dynamic convective driving forces. The mathematical description is omitted here due to the dependency on the specific case considered.

At a larger scale these effects do not have such a significant impact, which may result in problems when transferring processes from micro to large scale and *vice-versa*. However, it is quite common with conventional technologies to experience problems when transferring knowledge obtained at the lab scale to the industrial scale. Alternatively, rather than scaling-up by increasing dimensions, microfluidic systems can be numbered-up/parallelized in order to obtain the desired process throughput (although clearly there is a cost penalty since 'economies of scale' are lost). Indeed, this scaling strategy is, in many cases, not straightforward due to operating and handling issues of many systems in parallel [17].

Nevertheless, for screening of reactions, biocatalysts and processes, many possibilities exist and therefore, even with the potential limitations for scale-up of processes developed in microfluidic systems, there are many motivators for using microfluidic systems for process development. Indeed, in our opinion it seems most likely that process development will benefit most from the application of miniaturized systems. There is a growing group of bioprocess practitioners that share this view, working not only on development problems related to applied biocatalysis [18–20], but also fermentation [21] and protein recovery for biopharmaceutical applications [22]. Some of the key motivators are reduced development costs and accelerated process development, compared to conventional technologies in the ml scale. In many cases, microfluidic technologies have been applied for chemical synthesis, for example, where otherwise difficult syntheses have been operated and controlled under new and in some cases extreme conditions [23, 24]. However, there is an increasing interest in applying microfluidic technologies for the development of biocatalytic processes, due to the many general benefits and advantages highlighted in the scientific literature [25]. Examples of potential, advantages and benefits for process development based on microfluidic devices are discussed below, where special attention is given to how this will influence the development of new biocatalytic processes.

The first obvious benefit of performing process development in microfluidic systems is the reduced consumption of valuable and scarce resources. The reduced consumption of resources makes it possible to obtain greater process knowledge with the available resources and at the same time reduce the development costs. For biocatalytic processes, this is especially important, since the availability of a generally expensive biocatalyst is initially limited and will continue to be so until the process has been validated. For example, when improving the performance of biocatalysts through protein engineering,

only small quantities of different putative mutants need to be tested for their performance before larger scale production is initiated. The reduced consumption is in general, especially for the fine chemicals and pharmaceutical industries, a major driver for using microfluidic systems. Development costs can therefore be reduced since resources are so valuable.

Process development requires the testing and optimization of different biocatalyst and process options [e.g., reactors and downstream unit operations (separations)], which can in principle be performed relatively easily in microfluidic systems. For example, scientific literature can be found on membrane based microfluidic separation units [26]. Furthermore the liquid-liquid extraction in microsystems has also been proven to be successful [27], especially operated in a continuous way. The extraction in microsystems in two phase systems is also being investigated more [28]. Furthermore, the most promising microfluidic unit operations can easily be tested in combination, to get an indication of how they influence one another. It should though be mentioned that individual reaction systems or processes benefit differently from miniaturization and in some cases it will not be advantageous to use microsystems. In the scientific literature, it has been argued, with good justification, that micro-reactors benefit faster reactions [29]. However, there are also examples where slower reaction systems, e.g., biocatalytic reaction systems, have proven to greatly benefit from being operated at a micro scale [30]. The easy testing and optimization of process options in microfluidic systems opens the possibility of greatly accelerating the development of new processes, which is especially important in intellectual property (IP)-dominated industry sectors, such as pharmaceuticals. Assuming that miniaturized microfluidic systems contribute to easy testing and optimization of processes, such systems open the possibility of greatly accelerated process development, realized through parallelization and automation of the microfluidic systems. Operating the systems in parallel potentially increases screening and testing throughput. This potentially makes it possible to test different process conditions and options relatively quickly, thus generating knowledge that can be used to select and focus on feasible process options, eliminating infeasible processes. The information collected could also serve well the regulatory needs for Quality-by-Design (QbD) of the US Food and Drug Administration [31]. However, a certain degree of automation will be required in order to run the systems in parallel and ensure high throughput, and certainly there is still a major effort in software development required in order to reach automated and parallelized experimental microfluidic platforms [32]. Nevertheless, in principle at least, microfluidic systems already require a certain degree of automation in order to be operated. For example, it is not possible to achieve controlled flows through the devices without automated pumps. Automated systems will also aid in increasing the throughput of the parallel systems, since they in principle are able to operate continuously, with minimum downtime. Automated systems also have the advantage of having consistent systematic errors, making results comparable, unlike manual sample handling which may vary from operator to operator and from day to day.

Furthermore, microfluidic systems can be manufactured in a modular way, thus allowing the user to combine the different fluidic modules to test the influence of different process steps on the process efficiency [33–35]. It will therefore be possible to test the entire miniaturized process before making any efforts to scale-up the best process option.

Microfluidic systems have the advantage of enhanced process control (e.g., controlled flow scenarios and with rapid heat and mass transfer). The characteristic high surface-to-volume ratio in microfluidic systems enables fast and highly controlled heat and mass transfer. This opens up possibilities for dynamic process scenarios (e.g., fast transition between hot and cold regions for reactions operated in cascades). Likewise, laminar flows in microfluidic systems make it possible to operate with different flow scenarios (e.g., parallel, plug flow, slug flow). This can be very useful in order to precisely control mass transfer in these systems and enables the possibility of obtaining valuable mass transfer knowledge for the processes of interest. Also, it makes it much easier to simulate and model the processes in a microfluidic device.

Having laminar flows also enables easy liquid separation in the systems, based on capillary forces or controlled phase (or flow) splitting. This is very useful for extractive purposes and provides an option to operate biocatalytic processes in new ways. For example, this could enable the possibility of having substrate(s) continuously fed to the reaction stream. Other possibilities are *in situ* product removal or *in situ* co-product removal operating scenarios, where an auxiliary phase is used to continuously remove products or co-products from the reaction stream. For biocatalytic processes, these scenarios could potentially be useful in order to improve process feasibility by shifting unfavorable reaction equilibria and overcoming the inhibitory effects of substrates and products on the biocatalyst.

The laminar flows correspond to having a membrane free separation or supply system. It is also possible to inject an auxiliary phase between two reacting phases (i.e., liquid membrane operation using hydrodynamic

focusing, and thereby control the reaction rate). It is, however, also possible to implement ordinary membranes into these systems, as for example demonstrated by Cervera-Padrell and co-workers [36]. The driving force for the laminar flow and membrane operations is the concentration gradient between the different fluids.

Biocatalytic processes are operated in different ways dependent on the formulation of the biocatalyst, i.e., free, surface immobilized, immobilized in/on support particles, or in whole cell form. In relation to microfluidic systems, the different immobilization scenarios can be exploited in order to perform controlled sequential cascade reactions, or actually replicate metabolic pathways. For example, in Figure 2A, a micro packed bed reactor performing a cascade reaction is illustrated and in Figure 2B, an illustration of a packed bed reactor can be seen, where laminar side-by-side flow is used to perform continuous adsorption and desorption of products.

4 Transaminases

One of the most important functionalities in pharmaceutical molecules is the amine group and in recent years, therefore, routes to optically pure chiral amines have attracted considerable academic and industrial interest. Of the possible routes for synthesis of such molecules, which include selective crystallization and chemical catalytic methods, biocatalysis is particularly attractive. Biocatalytic methods offer high selectivity, under mild conditions with a renewable and tunable catalyst. In principle, several biocatalytic options exist, but the use of ω-transaminases (EC 2.6.1.X) in synthetic mode has driven significant research to find not only S-selective, but also R-selective enzymes for specific applications, and process routes to effectively implement the technology. Despite the excellent selectivity of this reaction and its unique ability to create a chiral center, in principle with 100% yield, in reality the ω-transaminase is one of the more challenging of the biocatalytic reactions; the substrates and products are often poorly water-soluble, the equilibrium is frequently unfavorable [37] and the substrate(s) and product(s) are more often than not inhibitory to the reaction (see Table 1) [38, 39]. This means that at first glance such a process is not only economically infeasible, but indeed far away from the targets which would be required for economic industrial exploitation [3]. Interestingly, in common with many other biocatalytic reactions, via a combination of protein engineering and clever use of reaction, reactor and process engineering, a cost effective process can be established (see Figure 3), and excellent precedent has already been set with the synthesis of sitagliptin by Merck and Co (USA) [42, 43], and other examples by Cellgene/Cambrex (USA and Sweden) [44] and Astra Zeneca (UK and Sweden)[45].

However, there are many other potential molecules to be synthesized using ω-transaminases, where the challenges have not yet been overcome and in general no standardized procedure exists to design an appropriate reaction, reactor and process for a given transaminase conversion. For this reason, we decided to use this reaction as a test system for the microfluidic development platform in the BIOINTENSE project.

Transaminases catalyze the transfer of an amine (-NH2) group from a donor molecule, usually an amino acid or a simple non-chiral amine such as 2-propylamine, to a pro-chiral ketone acceptor, yielding a chiral amine as well as a co-product ketone (or alpha-keto acid) (Figure 4). The enzyme requires the cofactor pyridoxal phosphate

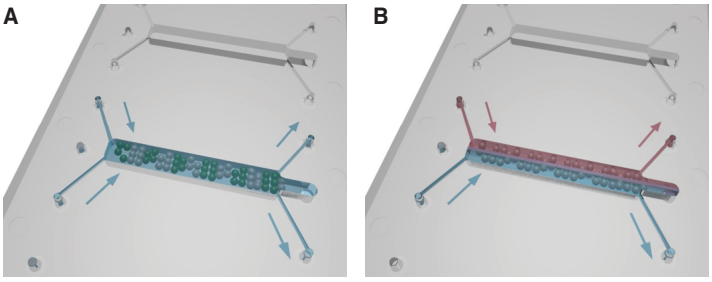

Figure 2 (A) Example of a micro packed bed reactor operated with a cascade reaction performed by immobilized enzyme on particles arranged in a sequential order. Green and gray particles represent different immobilized biocatalysts; (B) example of a novel way to operate micro packed bed reactors in which a simultaneous adsorption (blue stream) and desorption (red stream) flow is established with the help of a side by side laminar flow. This flow concept is currently under investigation and can be achieved by an appropriate design of the length and depth ratio of the Micro Packed Bed Reactor (μ-PBR). The channeling effects which also occur in miniaturized systems should in this way be limited to each side of the separated flow.

Table 1 Overview of challenges, solutions and implementation issues for ω-transaminase based reactions. The table is read by identifying a potential 'solution' (from the list on the left hand side of the table) to address a given reaction or biocatalyst 'challenge' (listed at the top of the table). In order to decide between solutions, the list of 'issues' (on the right hand side of the table) should be consulted.

Solutions	Reaction challenges			Biocatalyst challenges				Implementation issues
	Low thermodynamic equilibrium	Low substrate solubility	Substrate and product degradation	Inhibition by substrates or products	Stability of biocatalyst	Low catalyst activity or specificity	Separation of biocatalyst	
Excess amine donor	✓							Inhibition of catalyst; insufficient equilibrium shift; stability; costs; separation
Whole-cell biocatalyst	✓				✓			Selectivity; separation (foaming); Genetically Modified Organism
Degradation or recycling of co-product (cascade)	✓			✓				Compatibility of biocatalysts; added cost of biocatalysts; co-factor recycling
Distillation of (co-)product	✓							Co-distillation of water and/or solvent
Extraction of (co-)product, Resin/membrane/solvent	✓	✓		✓				Selectivity between substrates, co-products and products
Co-solvent/2-phase system		✓		✓				Enzyme stability; compatibility with free enzymes/cells; separation down-stream
In situ substrate supply/fed batch		✓	✓	✓				Capacity; compatibility with free enzymes/cells
Alter catalyst (Directed evolution, etc.)					✓	✓		Development time and cost
Immobilization					✓		✓	Deactivation; development costs; higher catalyst costs

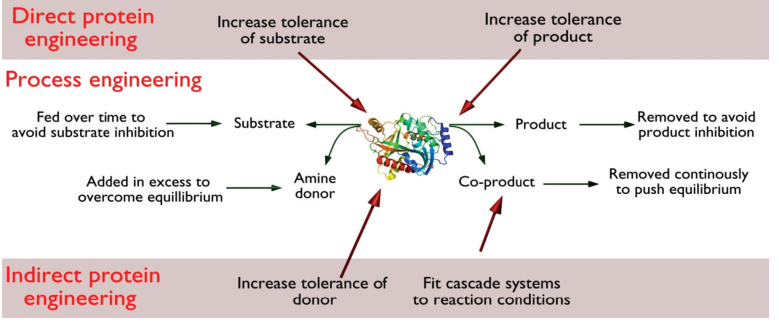

Figure 3 Illustrative presentation of different strategies which can be applied to improve transaminase based biocatalytic technology for chiral amine synthesis. Protein engineering can be used to improve the biocatalyst to withstand harsh process relevant conditions (e.g., overcome inhibition), while process engineering strategies can be applied to shift the equilibrium in a favorable direction (e.g., by *in situ* product removal (ISPR) and/or *in situ* co-product removal (IScPR) [40, 41].

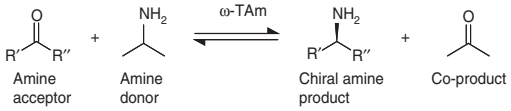

Figure 4 Asymmetric synthesis of chiral amines by ω-transaminase.

(PLP) to act as a shuttle to transfer the amine group. The cofactor is tightly bound to the enzyme and therefore does not pose the cofactor regeneration problems so often encountered in biocatalytic oxidation and reduction reactions [46, 47].

The asymmetric synthesis of chiral amines by ω-transaminase consists of three major steps (Figure 5); fermentation, biocatalytic reaction and product recovery. In order to avoid unnecessary costs, the biocatalyst is used in the crudest possible form (either as whole cells or cell free extract). Immobilization of the enzymes can be used to facilitate recovery and recycle, thereby improving the biocatalyst yield (g products/g biocatalyst).

After the reaction is complete, the biocatalyst is removed (biocatalyst separation) and the product is isolated from the substrate (which may also be recycled dependent upon the cost contribution to the process) prior to purification.

There are many challenges inherent to transaminase processes that need to be dealt with and numerous reports have been published that address one or more of these challenges. Frequently, the suggested strategies solve more than one problem, for instance the use of an auxiliary phase may solve issues related to substrate and product inhibition as well as low water solubility; by contrast, the solution might pose other problems, such as lower biocatalyst stability. An overview of transaminase process challenges has been compiled in Table 1, along with the suggested technologies and strategies used to overcome these, as well as the further implications of using a specific technology.

5 Discussion

Although there is a great potential for the application of microfluidic miniaturized systems in process development, there are also several challenges related to their operation.

One of the main challenges is the large number of samples required for analysis due to the sensitivity of the measurements and manual sample handling for off-line measurements. The implementation of on-line measurements could be a possible solution. However, the standard on-line measurement methods [e.g., near-infrared (NIR) and ultraviolet (UV)] can be quite problematic. The compounds involved in the processes studied by BIOINTENSE, amines and ketones, have peaks appearing in critical regions of the NIR and UV spectra. For instance, the amines are shadowed by water in the NIR spectrum, and in the UV spectrum, the peaks appear in the lower region, where common materials used for fabrication of microfluidic devices will have shadowing effects.

The integration of the hardware such as pumps, valves, analytical equipment and the heating/cooling zone can be quite challenging when working at the micro scale. For this reason, it is necessary to standardize connections to simplify their application. There is a similar constraint related to the available technology that can be applied to process development. Here, there is a need for readily and commercially available platforms, modules and methodologies. For instance, for biocatalytic processes, there is no guidance and there has been a trend towards starting from the very beginning each time. For that matter, methodologies should also cover development and scale-up procedures and/or strategies. This is one of the tasks that will be undertaken in BIOINTENSE.

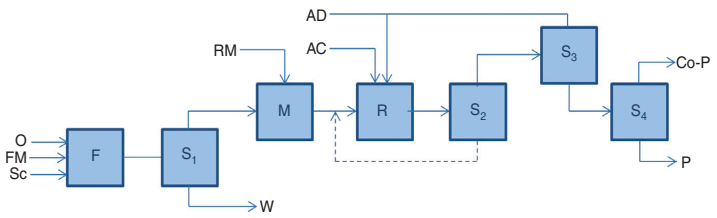

Figure 5 Generalized process flow sheet for transaminase-catalyzed reactions. Unit operations: fermenter (F), mixer (M), reactor (R), cell/fermentation broth separator (S_1), biocatalyst/reaction medium separator (S_2), amine donor/acceptor separator (S3) and chiral amine product/co-product separator (S4). Process streams: amine acceptor (AC), amine donor (AD), product (P), co-product (Co-P), fermentation media (FM), oxygen (O), reaction media (RM), starter culture (SC), waste fermentation broth (W).

Likewise, the formation (or use) of solids in microsystems can cause severe channel clogging due to surface adhesion. The large surface to volume ratio supports adhesion and it is difficult to prevent [48]. This is a great bottleneck, since the biocatalyst formulation can vary, e.g., free solubilized enzymes, immobilized enzymes on solid support, or whole cells. Biocatalysts are usually expensive and it is intended to use them in as crude as possible a state, or at least for as many cycles as possible [3]. Another challenge that should be considered is the catalyst immobilization in strategic locations of the micro-reactor surface for topology studies. These studies can involve complex biocatalyst distribution patterns determined by simulations using biocatalyst immobilization and can be difficult to replicate experimentally.

6 Future outlook

In the BIOINTENSE project, we are developing entirely new tools and only time will tell if the results and the performance of the microsystem based platform will reveal a new 'high throughput' paradigm. However, based on the preliminary results obtained, it can already now be seen that the developed 'microtools' contribute to entirely new results, including deepening the understanding and knowledge of mass transfer parameters (like diffusion velocities of the substrates and products). With the help of this information, it will become possible to understand the complex interactions of the biocatalytic system better and hence it can also be expected that in the long run, this information can contribute to the rapid development of the identified processes. Indeed, we are convinced that it will be necessary to develop a miniaturized toolbox for the investigation and screening of process options. Nevertheless, the exact composition of that toolbox is today unknown. The project will show, in the end, if the full advantages of microsystems can be applied for rapid process development and if this is, from an economic point of view, worthwhile. However, the highest expectations are at the moment to prove if the miniaturized process toolbox will contribute to the acceleration of the process development and thereby to the reduction of development time.

Acknowledgements: Financial support by the European Union FP7 Project BIOINTENSE – Mastering Bioprocess integration and intensification across scales (KBBE 2012.3.3-03 Grant Agreement Number 312148) is gratefully acknowledged.

Received October 2, 2013; accepted November 2, 2013; previously published online December 6, 2013

References

[1] Pollard DJ, Woodley JM. *Trends Biotechnol.* 2007, 25, 66–73.
[2] Straathof AJJ, Panke S, Schmid A. *Curr. Opin. Biotech.* 2002, 13, 548–556.
[3] Tufvesson P, Lima-Ramos J, Nordblad M, Woodley JM. *Org. Proc. Res. Dev.* 2011b, 15, 255–274.
[4] Tufvesson P, Lima-Ramos J, A-Haque N, Gernaey KV, Woodley JM. *Org. Proc. Res. Dev.* 2013, 17, 1233–1238.
[5] Bornscheuer UT, Huisman GW, Kazlauskas RJ, Lutz S, Moore JC, Robins K. *Nature* 2012, 485, 185–194.
[6] Woodley JM. *Curr. Opin. Chem. Biol.* 2013, 17, 310–316.
[7] Burton SG, Cowan DA, Woodley JM. *Nat. Biotech.* 2002, 20, 35–46.
[8] Turner NJ. *Nat. Chem. Bio.* 2009, 8, 567–573.
[9] Bommarius AS, Blum JK, Abrahamson MJ. *Curr. Opin. Chem. Biol.* 2011, 2, 194–200.
[10] Reetz MT. *Angew. Chem. Int. Ed.* 2011, 50, 138–174.
[11] Vennestrøm PNR, Christensen CH, Pedersen S, Grunwaldt J-D, Woodley JM. *ChemCatChem* 2010, 2, 249–258.
[12] Aota A, Mawatari K, Kitamori T. *Lab Chip* 2009, 9, 2470–2476.
[13] Whitesides GM. *Nature* 2006, 442, 368–373.
[14] Baraldi PT, Hessel V. *Green Proc. Synth.* 2012, 1, 149–167.
[15] Wirth T. *Microreactors in Organic Chemistry and Catalysis*, 2nd ed., Wiley-VCH Verlag GmbH & Co KGaA: Weinheim, Germany, 2013.
[16] Bruus H. *Theoretical Microfluidics*, Oxford University Press: Oxford, 2008.
[17] Roberge DM, Gottsponer M, Eyholzer M, Kockmann N. *Chem. Today* 2009, 27, 8–11.
[18] Cull S, Lovick J, Lye G, Angeli P. *Bioprocess Biosyst. Eng.* 2002, 3, 143–153.
[19] O'Sullivan B, Al-Bahrani H, Lawrence J, Campos M, Cázares A, Baganz F, Wohlgemuth R, Hailes HC, Szita N. *J. Mol. Catal. B* 2012, 77, 1–8.
[20] Dencic I, de Vaan S, Noël T, Meuldijk J, de Croon M, Hessel V. *Ind. Eng. Chem. Res.* 2013, 52, 10951–10960.
[21] Betts J, Baganz F. *Microb. Cell Fact.* 2006, 1, 21.
[22] Nfor BK, Verhaert PDEM, van der Wielen LAM, Hubbuch J, Ottens M. *Trends Biotechnol.* 2009, 27, 673–679.
[23] Jensen KF. *Chem. Eng. Sci.* 2001, 56, 293–303.
[24] Hartman RL, Jensen KF. *Lab-on-a-Chip* 2009, 9, 2495–2507.
[25] McMullen JP, Jensen KF. *Annu. Rev. Anal. Chem.* 2010, 3, 19–42.
[26] De Jong J, Lammertink R, Wessling M. *Lab Chip* 2006, 6, 1125–1139.
[27] Kralj JG, Sahoo HR, Jensen KF. *Lab Chip* 2007, 7, 256–263.
[28] Žnidaršič-Plazl P, Plazl I. *Lab Chip* 2007, 7, 883–889.
[29] Roberge DM, Ducry L, Bieler N, Cretton P, Zimmermann B. *Chem. Eng. Technol.* 2005, 28, 318–323.

[30] Bodla VK, Seerup R, Krühne U, Woodley JM, Gernaey KV. *Chem. Eng. Technol.* 2013, 36, 1017–1026.
[31] U.S. Food and Drug Administration, Department of Health and Human Services. Pharmaceutical CGMPs for the 21st Century - a Risk-Based Approach: Progress Report. U.S. Food and Drug Administration, Department of Health and Human Services: 2007: http://www.fda.gov/AboutFDA/CentersOffices/Officeof-MedicalProductsandTobacco/CDER/ucm128080.htm#mission.
[32] Gernaey KV, Baganz F, Franco-Lara E, Kesny F, Krühne U. Luebberstedt M, Marx U, Palmqvist E, Schmid A, Schubert F, Mandenious C-F. *Biotechnol. J.* 2012, 7, 1308–1314.
[33] Perozziello G, Simone G, Candeloro P, Gentile F, Malara N, Larocca R, Coluccio M, Pullano SA, Tirinato L, Geschke O. *Micro Nanosyst.* 2010, 2, 227–238.
[34] Shaikh KA, Ryu KS, Goluch ED, Nam J, Liu J, Thaxton CS, Chiesl TN, Barron AE, Lu Y, Mirkin CA. *Proc. Natl. Acad. Sci.* 2005, 102, 9745–9750.
[35] Yuen PK. *Lab Chip* 2008, 8, 1374–1378.
[36] Cervera-Padrell AE, Morthensen ST, Lewandowski DJ, Skovby T, Kiil S, Gernaey KV. *Org. Proc. Res. Dev.* 2012, 16, 888–900.
[37] Tufvesson P, Jensen JS, Kroutil W, Woodley JM. *Biotech. Bioeng.* 2012, 109, 2159–2162.
[38] Ward JM, Wohlgemuth R. *Curr. Org. Chem.* 2010, 14, 1914–1927.
[39] Tufvesson P, Lima-Ramos J, Jensen JS, Al-Haque N, Neto W, Woodley JM. *Biotech. Bioeng.* 2011a, 108, 1479–1493.
[40] Goldberg K, Edegger K, Kroutil W, Liese A. *Biotech. Bioeng.* 2006, 95, 192–198.
[41] Lima-Ramos J, Neto W, Woodley JM. *Top. Catal.* 2013, DOI 10.1007/s11244-013-0185-0.
[42] Savile CK, Janey JM, Mundorff EC, Moore JM, Tam S, Jarvis WR, Colbeck JC, Krebber A, Fleitz FJ, Brands J, Devine PN, Huisman GW, Hughes GJ. *Science* 2010, 329, 305–309.
[43] Truppo MD, Strotman H, Hughes G. *ChemCatChem* 2012, 4, 1071–1074.
[44] Martin A, DiSanto R, Plotnikov I, Kamat S, Shonnard D, Pannuri S. *Biochem. Eng. J.* 2007, 37, 246–255.
[45] Frodsham L, Golden MD, Hard S, Kenworthy MN, Klauber DJ, Leslie K, MacLeod C, Meadows RE, Mulholland KR, Reilly J, Squire C, Tomasi S, Watt D, Wells AS. *Org. Proc. Res. Dev.* 2013, 17, 1123–1130.
[46] Pannuri S, DiSanto R, Kamat S. Biocatalysis. In *Kirk-Othmer Encyclopedia of Chemical Technology*, Wiley: Hoboken, NJ, USA, 2003.
[47] Hwang BY, Cho BK, Yun H, Koteshwar K, Kim B-G. *J. Mol. Catal.* B. 2005, 37, 47–55.
[48] Hartman RL. *Org. Proc. Res. Dev.* 2012, 16, 870–887.

Appendix A.2: Systematic development of miniaturized (bio)processes using Process Systems Engineering (PSE) methods and tools

Systematic Development of Miniaturized (Bio)Processes using Process Systems Engineering (PSE) Methods and Tools

U. Krühne,* H. Larsson, S. Heintz, R. H. Ringborg, I. P. Rosinha, V. K. Bodla, P. A. Santacoloma, P. Tufvesson, J. M. Woodley, and K. V. Gernaey

Center for Process Engineering and Technology, Department of Chemical and Biochemical Engineering, Technical University of Denmark (DTU), Building 229, DK-2800 Lyngby, Denmark

doi: 10.15255/CABEQ.2014.1940

Original scientific paper
Received: February 14, 2014
Accepted: March 3, 2014

The focus of this work is on process systems engineering (PSE) methods and tools, and especially on how such PSE methods and tools can be used to accelerate and support systematic bioprocess development at a miniature scale. After a short presentation of the PSE methods and the bioprocess development drivers, three case studies are presented. In the first example it is demonstrated how experimental investigations of the bi-enzymatic production of lactobionic acid can be modeled with help of a new mechanistic mathematical model. The reaction was performed at lab scale and the prediction quality analyzed. In the second example a computational fluid dynamic (CFD) model is used to study mass transfer phenomena in a microreactor. In this example the model is not only used to predict the transient dynamics of the reactor system but also to extract material properties like the diffusion velocities of substrate and product, which is otherwise difficult to access. In the last example, a new approach to the design of microbioreactor layouts using topology optimization is presented and discussed. Finally, the PSE methods are carefully discussed with respect to the complexity of the presented approaches, the applicability with respect to practical considerations and the opportunity to analyze experimental results and transfer the knowledge between different scales.

Key words:

Computational Fluid Dynamics (CFD), modeling, Process Systems Engineering (PSE), (bio)processes

Introduction

The development of new chemical engineering design tools is essential for the implementation of the latest technology in the manufacture of chemical and other products. The focus of this paper is on process systems engineering (PSE) methods and tools, and especially on how such PSE methods and tools can be applied to speed up or support systematic bioprocess development at miniature scale. In this context, the term bioprocess is interpreted broadly, and includes both biocatalysis (enzyme or resting cell conversion) as well as fermentation (growing cell conversion). In the following section, we first provide a brief introduction to the main drivers of biocatalysis and fermentation process development. The paper also contains a short overview of PSE methods and tools. The use of such tools is illustrated on the basis of three examples, which summarize some of our recent experiences in the area. The paper ends with a discussion on future perspectives with respect to the use of PSE methods and tools in miniaturized bioprocess systems and for extrapolation of results across reactor scales (scaling up).

*Corresponding author: ulkr@kt.dtu.dk

Bioprocess development drivers – biocatalysis

The need for selective chemistry is the main driver behind the increasing academic and industrial interest in biocatalytic processes (chemical reactions catalyzed by an isolated enzyme, immobilized enzyme or whole cell containing one or more enzymes).[1] While biocatalysis may easily hold the promise of high selectivity, economic process feasibility is also necessary for implementation in industry. Economic feasibility translates into a minimum required product concentration that must leave the reactor, as well as a yield of product on biocatalyst that is to be achieved, as has been illustrated by Tufvesson and coworkers for a number of different scenarios.[2] The exact threshold values for minimum product concentration and yield of product on biocatalyst will indeed depend on the particular industry sector as well as the selling cost of the product relative to the cost of the substrate. In fact, most new biocatalytic processes studied in the laboratory do not fulfill these requirements, mainly because enzymes are usually evolved to operate under mild conditions converting natural substrates at low concentrations. Hence, achieving an economically feasible biocatalytic process in terms of minimum re-

quired product concentration and yield of product on biocatalyst is therefore often challenging, and can only be addressed by a combination of process modifications as well as biocatalyst modifications. Indeed, in many cases it is not clear at an early stage how to develop the process. In order to overcome this, one potential vision for the future could be automated data collection and systematic testing of alternatives at a miniature scale such that operations can be carried out in parallel and with a reduced reagent inventory. This is the main aim of the EC-funded BIOINTENSE project, and the experimental and practical challenges of such an approach have recently been discussed by Krühne and co-workers (2014).[3]

When considering the list of potential process and biocatalyst modifications, analyzing all potential options is a combinatorial problem that is too difficult and time-consuming to be addressed by evaluating options one-by-one in the laboratory, even at miniature scale. However, specifically at this point, mathematical models can be used to supplement biocatalytic process development, and to support the rapid identification of the most promising biocatalytic process options among many. This also matches the above-mentioned ideas on automated data collection and systematic testing of alternatives at a miniature scale. Automated data collection can indeed be combined with automated model structure selection and parameter estimation, as recently illustrated for a conventionally-catalyzed Diels-Alder reaction with complex kinetics in a microreactor.[4]

Bioprocess development drivers – fermentation

Fermentation processes have been used for hundreds of years in the production of food, including beer and wine. However, partly due to the scarcity of fossil fuels, fermentation processes have become increasingly attractive during the past decades to produce proteins (including enzymes), fine and bulk chemicals as well on the basis of renewable raw materials. The essential difference between a biocatalytic process and a fermentation process is that the catalyst in the fermentation process is a living microorganism – most often a genetically modified organism overexpressing the genes required to produce the product of interest – that grows on a carbon substrate which usually also forms the substrate for the formation of the product of interest. As a consequence, successful implementation of an economically feasible fermentation process relies on achieving a high enough product yield on substrate (especially for lower value products) as well as maintaining a delicate balance between using substrate for biomass growth on the one hand and product formation on the other hand. If biomass growth is not sufficiently prioritized, the product formation rate will be too low, resulting in suboptimal exploitation of the available reactor volume. On the other hand, if biomass growth is promoted too much, the final yield of product on substrate achieved in the fermentation process and the product concentration will be suboptimal. Thus, the main economic drivers of an industrial fermentation process are the yield of product on substrate and the final product concentration that can be achieved – the higher the better, since less water needs to be removed from the product in the downstream processing. Furthermore, for aerobic fermentations the energy cost for oxygen supply is also an important cost.

Mathematical models are often used to study laboratory scale fermentation processes. However, their use in industry is rather limited, and fermentation process development has traditionally relied on an extended series of experiments at lab-scale and pilot-scale in order to find the operating conditions that result in an economically feasible fermentation process. In recent years, microliter and milliliter scale devices capable of performing fermentations have been developed as well,[5] and have been promoted for use in fermentation process development. However, it is quite clear that additional research work is needed before the use of microscale or milliliter scale devices will be the generally accepted process development strategy or support tool. Mechanistic models could, according to us, be helpful in realizing that future vision.

PSE methods and tools

Process systems engineering (PSE) is an interdisciplinary field within chemical engineering that focuses on the design, operation, control, and optimization of chemical, physical, and biological processes through the aid of systematic computer-based methods. A systems approach is generally model-based, i.e. different types and forms of mathematical models play a prominent role in process design/operation, evaluation and analysis as they have the potential to provide the necessary process understanding, supplement the available knowledge with new data, and reduce time and cost for process-product development.[6,7] PSE methods and tools have been applied successfully to many industries, such as the chemical and petrochemical, the pharmaceutical[8] and biotechnological industries.

While working on a process development task, independent of scale, mathematical models are often used to summarize the available process knowledge and to describe the dynamics of the most important process variables. Such ‘dynamic models’ are usually mechanistic models of a process or a

unit operation, for example consisting of a set of ordinary differential equations (ODEs) which represent the input-output dynamics. Once available, such a model can be supplemented by a set of well-established model analysis tools,[9–11] for example also including uncertainty and sensitivity analysis to assess the statistical quality (reliability) of the simulated scenarios.[12] Perhaps most importantly from a process development point of view, the calibrated dynamic models can be used for *in-silico* testing of a set of potential process operating strategies, e.g. by comparing different control strategies in a series of dynamic simulations, without disturbing process operation. The latter is a major advantage, but requires a dynamic model which has been calibrated on the basis of available process data.

Case study examples

Example 1: Bi-enzyme production of lactobionic acid (Santacoloma, 2012)[3]

The main goal of this first example was to analyze the reliability of a mechanistic mathematical model describing a biocatalytic reaction in a lab-scale reactor in terms of its prediction quality. During the process the temperature was controlled at 30 °C and pH was maintained at 3.9. Furthermore, concentrations of lactose, lactobionic acid and oxygen were measured for 6 hours. After that time, the lactose was completely consumed. The sampling interval for lactose and lactobionic acid was 1 hour and the samples were measured by High-performance liquid chromatography (HPLC). The dissolved oxygen measurements were recorded every 10 seconds.

Production of lactobionic acid (4-O-β-D-galactopyranosyl-D-gluconic acid), a compound used in the production of high-value products, pharmaceutical and food applications, is primarily achieved by the oxidation of lactose. The general scheme for the biocatalytic production of lactobionic acid is shown in Fig. 1. A first enzyme, cellobiose dehydrogenase (CDH), catalyzes the dehydrogenation of lactose to lactobiono-lactone, which is spontaneously hydrolyzed to lactobionic acid. In this case, the double action of the redox mediator 2,2'-azinobis(3-ethylbenzothiazoline-6-sulfonic acid) (ABTS) is exploited. In the first reaction, ABTS acts as an electron acceptor regenerating the initial oxidation state of the first enzyme (CDH). In the second reaction, ABTS serves as electron donor to obtain the reduction by laccase (lacc), which is the second enzyme added to the system. The reduced state of laccase catalyzes the second reaction where oxygen (the co-substrate) is fully reduced to water.[14,15]

The mathematical model for this system was obtained from the literature, including the kinetic parameters of the multi-enzyme process.[16] and was implemented in MATLAB. Both enzymes involved in the process (CDH and lacc) follow the substituted enzyme mechanism. Kinetic parameters for each enzyme were obtained from the literature.[14,15,17] Interaction due to the combination of enzymes was not taken into account in these studies. In this case study, the bi-enzyme process was carried out in batch mode, in a membrane bioreactor. The main purpose of this reactor was to provide bubble-free oxygenation. Furthermore, the mass transfer of oxygen from the gas to the liquid phase was included in the mathematical model.[16]

The following assumptions were made for the mathematical model: (1) Substrate and product inhibition are neglected in the process; (2) pH and temperature are maintained constant during the operation; (3) Perfect mixing in the reactor.

The model for the system consists of six differential equations, and can be written down in a compact matrix notation,[18] as shown in Table 1. An example of how the matrix in Table 1 should be read is shown in Eq. 1 with the oxygen balance:

$$\frac{\mathrm{d}C_{o_2}}{\mathrm{d}t} = r_{omt} - \frac{1}{2} r_2 \tag{1}$$

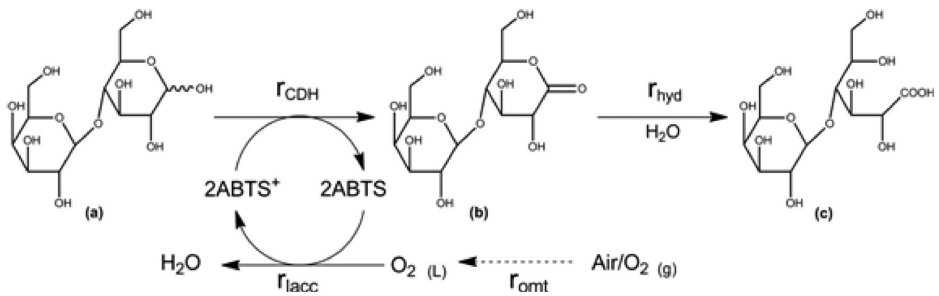

Fig. 1 – *General reaction scheme for bi-enzyme production of lactobionic acid: (a) lactose, (b) lactobiono-lactone and (c) lactobionic acid*

Table 1 – *Mass balances of the batch process for lactobionic acid production represented by the stoichiometric matrix notation*

Component / Process	C_{lact} (mM)	C_{LBL} (mM)	C_{LBA} (mM)	C_{O_2} (mM)	C_{ABTS} (mM)	C_{ABTS+} (mM)	Process rates
Enzyme 1- CDH	–1	1			2	–2	r_{CDH}
Enzyme 2- Lacc.				–1/2	–2	2	r_{lacc}
Hydrolysis		–1	1				r_{hyd}
Aeration				1			r_{omt}

Table 2 – *Reaction rate expressions for lactobionic acid production*

Reaction rate (symbol)	Reaction rate expression
r_{CDH}	$r_{CDH} = V_{max\_1} \frac{C_{Lact} \cdot C_{ABTS+}}{K_{M_{Lact}} \cdot C_{ABTS+} + K_{M_{ABTS+}} \cdot C_{Lact} + C_{Lact} \cdot C_{ABTS+}}$
r_{lacc}	$r_{lacc} = V_{max\_2} \frac{C_{O_2} \cdot C_{ABTS}}{K_{M_{O_2}} \cdot C_{ABTS} + K_{M_{ABTS}} \cdot C_{O_2} + C_{O_2} \cdot C_{ABTS}}$
r_{hyd}	$r_{hyd} = K_{hyd} \cdot C_{LBL}$
r_{omt}	$r_{omt} = K_L a \cdot (C_{O_2}^{sat} - C_{O_2})$

The enzymatic reactions follow the bi-bi ping-pong (or substituted-enzyme[19,20]) kinetics. In this case study, both enzymes follow the same type of mechanism. Hence, two coupled substituted-enzyme mechanisms are suggested to describe both enzymatic reactions. The process rates are summarized in Table 2.

Progress curves for lactic acid, dissolved oxygen and lactobionic acid formed the basis of a parameter estimation. Details of the parameter estimation procedure can be found in Santacoloma (2012).[13] The resulting model fit is illustrated in Fig. 2. The parameter estimates, including confidence intervals, are provided in Table 3.

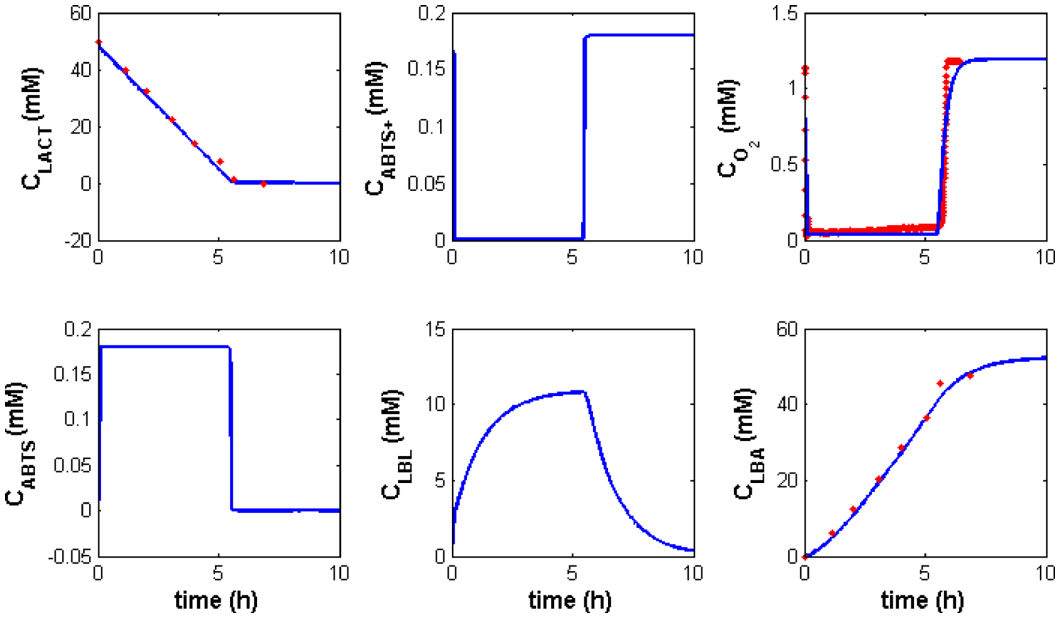

Fig. 2 – *Comparison between experimental data and simulation of the system using the estimated parameters (line – simulation, dots – measurement)*

Table 3 – *Lactobionic acid example: parameter estimates with 95 % confidence intervals and correlation matrix of the estimated parameters*

Parameter	Estimates with 95 % C. intervals		Units	Correlation matrix						
				θ_1	θ_2	θ_3	θ_4	θ_5	θ_6	θ_7
$V_{max\ 1}$	23.33	± 16.4	mM h^{-1}	1						
$K_{M\ lact}$	1.27	± 3.06	mM	–0.47	1					
$K_{M\ ABTS+}$	4.10 e–5	± 0.09	mM	0.85	–0.71	1				
$V_{max\ 2}$	58.48	± 34.7	mM h^{-1}	0.29	0.13	–0.08	1			
$K_{M\ ABTS}$	8.74 e–3	± 0.51	mM	0.42	0.18	–0.06	0.83	1		
K_La	3.84	± 0.10	h^{-1}	0.13	0.13	0.23	–0.07	–0.22	1	
K_{hyd}	0.655	± 0.44	mM h^{-1}	–0.00	0.00	–0.00	–0.00	–0.00	0.00	1

Despite the assumptions, the suggested mathematical model can in general describe the process dynamics. Seven parameters were found to be identifiable based on the given dataset, but the kinetic parameters (K_M) for both oxidation states of the intermediate redox mediator ABTS are very small which physically means fast dynamics in the system as the lactic acid approaches depletion. That effect could probably also explain – at least to some extent – the uncertainty in those parameters, observable in Table 2 as a large confidence interval. Several other parameters show rather large confidence intervals as well. This means[12] that the absolute values of the parameters should be interpreted with care, i.e. the model can describe the process dynamics but the physical meaning of the parameters is limited. Improved quality of the parameter estimation (reduced confidence intervals) could be achieved by collecting measured data on other model variables as well.

Example 2: CFD to study mass transfer phenomena in microreactors (Bodla *et al.*, 2013)[21]

The second case study demonstrates the combination of microreactor technology and computational fluid dynamics (CFD) to contribute towards understanding of the diffusional properties of substrate and product in a biocatalytic reaction. Such knowledge can then be applied to design new reactor configurations.

As a case study, an ω-transaminase catalyzed transamination for the synthesis of chiral amines was selected. Biocatalytic transamination is studied intensively nowadays, mainly because the transamination reaction is attractive for synthesis of optically pure chiral amines (which are valuable building blocks for pharmaceuticals and precursors). However, in the synthetic direction the reaction is often limited by unfavourable thermodynamics, as well as substrate and product inhibition of the enzyme activity.[22] The reaction is catalysed by ω-transaminase, in the presence of a co-factor, pyridoxal-5'-phosphate (PLP), by transferring the amine group from the amine donor to a pro-chiral acceptor ketone, yielding a chiral amine along with a co-product ketone. The reaction follows the bi-bi ping pong mechanism where the substrate is first bound to the enzyme while co-product is released before the second substrate is bound and the final product leaves the enzyme.[23] Thus diffusion of the substrate to the enzyme binding site and the product diffusion potentially have a significant effect on the reaction performance. Hence, it was specifically intended here to study the diffusion characteristics of the substrate and the product under operating conditions.

Transient experiments were performed in a microchannel under continuous flow conditions. Following a step input of the diffusing species at the inlet at time $t = 0$, the phenomenon of species transport in uniform poiseuille flow is explained by the convection-diffusion equation.[24] A species that is diffusing relatively fast creates a more radial mixing profile, while a species diffusing more slowly has less effect. Under laminar flow conditions, residence time distribution (RTD) experiments were performed by inducing a step input at the inlet of the channel after reaching steady-state, while the concentration over time is subsequently measured at the outlet in order to obtain the response curves, $E(t)$ as shown in Eq. 2. These distribution profiles are helpful in understanding the diffusional properties of each species. Slowly diffusing species have more lag time, and thus it takes more time to reach the normalized concentration at the outlet. The first molecules of the species will also break through sooner at the end of the channel compared to relatively faster diffusing species (Fig. 3).

$$E(t) = \frac{C(t)}{C_o} \tag{2}$$

Where C_o is the species concentration at the inlet for a step input, and $C(t)$ is the concentration measured at the outlet at time t. The RTD experiments were performed in the microchannel at a flow rate of 7.5 μL min^{-1} for the amine acceptor substrate (acetophenone), for the amine product (methylbenzylamine), and for glucose, as shown in Fig. 3. The channel dimensions (width $0.5 \cdot 10^{-3}$ m, height $1 \cdot 10^{-3}$ m, length 0.1 m) are sufficiently small and the flow rate is sufficiently low to maintain a laminar flow (Reynolds number is 0.2). Glucose is a compound with a known aqueous diffusion coefficient of $0.67 \cdot 10^{-9}$ m^2 s^{-1} and was therefore used as a reference.

Computational fluid dynamics (CFD) models of the flow behaviour were also constructed for a range of diffusion coefficients with the intention of distinguishing between fast and slowly diffusing compounds (i.e. compounds with orders of magnitude differences of their diffusion coefficients). ANSYS CFX version 12.5 was used as software package for this purpose. Response curves were obtained from the simulations, after inducing a step input at the inlet, and by measuring the area average of the species concentration at the outlet of the channel and are also plotted in Fig. 3.

The results in Fig. 3 provide a comparison of the experimental data obtained from transient experiments with the RTD curves resulting from CFD simulations. The simulation result, with a diffusion coefficient of $0.67 \cdot 10^{-9}$ m^2 s^{-1}, fits well with the data for the product, indicating that the diffusion coefficient of the product is close to that of glucose. With respect to acetophenone, the results indicate an increased lag time to reach the normalized concentration at the outlet compared to the product implying that the substrate is diffusing slower than the product. Compared to the simulations, the experimental data does not fit exactly, although the behaviour of the response curve is closer to that of the simulation with a diffusion coefficient of $0.67 \cdot 10^{-12}$ m^2 s^{-1}. Hence it can be interpreted that the diffusion coefficient is in the order of magnitude of 10^{-12}. Thus it can be concluded that the substrate is diffusing considerably slower than the product (around 10^3 fold slower).

For experimental values, a standard deviation of about 10 % from the mean has been observed. This could account for an error of 10 % in determining the value of the diffusion coefficients. Further errors in numerical simulations will have a combined effect on determining the value of the diffusion coefficients. CFD simulations for solving the Navier -Stokes equations for fluid dynamics are well established in various applications. It is important to replicate the exact geometry including the wall effects and boundary conditions in the simulation since the response curve is a function of these variables. Appropriate meshing of the geometry is also crucial to minimize the numerical error. The finer the mesh size or the higher the number of mesh elements, the more precise will the numerical calculations be. For transient simulations, the time-step is also important when the error has to be minimized. However, there is a tradeoff between the mesh size, the time-step and the required computational time and effort. Thus a compound (such as glucose in this case study) with a known diffusion coefficient can be used to confirm if the simulations are able to predict the experimental data. Assuming about 5 % error in the numerical simulations, the combined error could be in the order of 5 % – 30 %.

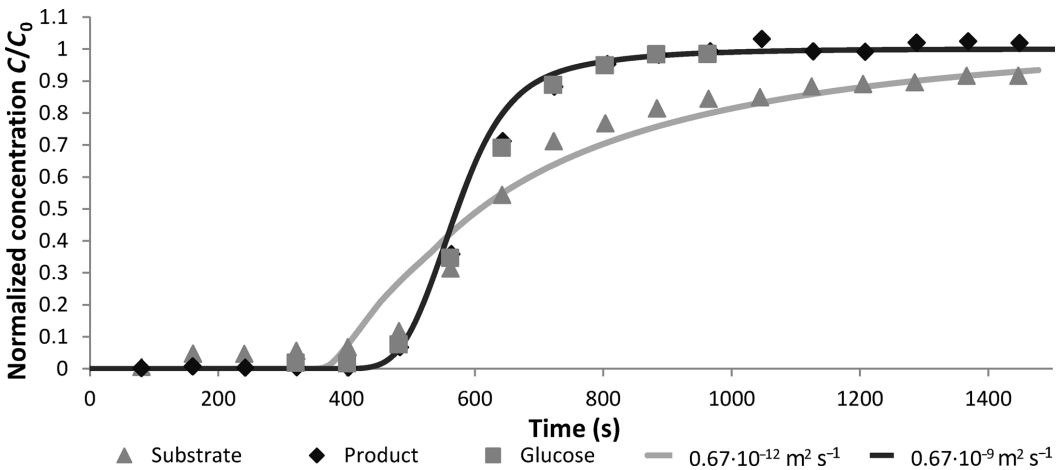

Fig. 3 – *CFD simulations with induced diffusion coefficients of $0.67 \cdot 10^{-9}$ m^2 s^{-1} and $0.67 \cdot 10^{-12}$ m^2 s^{-1} plotted as continuous lines; Experimental results are plotted as markers. Figure adapted from (Bodla et al., 2013)*[25]

In this case, the substrate is estimated to be diffusing 1000 fold slower compared to the product, where the real value could thus be about 700–1300 times slower compared to the product (assuming maximum 30 % error). So when comparing the numerical response curves with the experimental data, errors in both numerical simulation and experimental data can result in incorrect estimation of the diffusion coefficients.

The knowledge of substrate and product diffusion coefficients is crucial for the choice and design of reactors for biocatalytic reactions. Different reactor configurations can be achieved based on the flow and species transport characteristics. It has been demonstrated that the reactor configurations built from this knowledge perform better than the traditional well mixed batch reactor.[21] In order to build reactor configurations for industrial purposes, it is furthermore also crucial to be able to extrapolate the results from microscale to larger industrial scale. Although it is challenging to obtain the selectivity of a microreactor configuration in a conventional reactor, the data acquired at microscale can be used as a guide to understanding the process limitations during scale-up.

Example 3: Topology optimization (Schäpper *et al.*, 2011)[25]

The third case study (Schäpper *et al.*, 2011),[25] presents a new approach to the design of microbioreactor layouts using topology optimization, a method which had previously been successfully applied in the design of optimal catalytic microreactors.[26] Topology optimization is an iterative mathematical optimization technique which can optimize a design according to the value of a pre-defined objective function. In this case the design was the spatial distribution of immobilized yeast cells and their carrier material inside a small bioreactor, which was optimized based on the yeast cells' total production of a given protein as the objective function.

The yeast *Saccharomyces cerevisiae* was chosen for this study for several reasons: it is one of the best known model systems, and *S. cerevisiae* is furthermore one of the microorganisms most commonly used in the biotechnology industry.

Simulations were carried out using the software COMSOL coupled to MATLAB and the optimized reactor was a rectangular microbioreactor with a length of 1.2 mm and a width of 1.2 mm. A constant pressure difference between inlet and outlet provided a continuous flow of glucose containing medium inside the reactor.

Inside the reactor, the distribution of a carrier material with immobilized yeast cells was then optimized. The carrier was modeled as a porous, sponge-like material which gave rise to an additional so called Darcy friction anti-parallel to the flow medium. For the volumes inside the reactor with no carrier present, i.e. those regions only containing culture medium, the Darcy friction was set to zero.

For a given distribution of carrier material in the reactor, the flow velocities of the medium were calculated from the steady state Navier-Stokes equation, taking the Darcy friction of the carrier material into consideration. These flow velocities were then used in the second part of the calculations, where kinetic models were applied to model the protein production in the reactor.

Topology optimization was then applied in order to find a better reactor design with a more beneficial distribution of carrier material, and each candidate was evaluated based on how high a protein production the configuration could achieve.

The kinetic model in this study was based on the work of Bránýik *et al*. (2004)[27] and Zhang *et al*. (1997),[28] and describes the yeast metabolism through the three metabolic events described in Fig. 4.

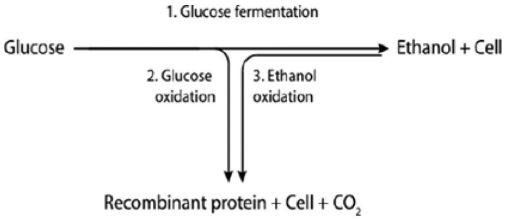

Fig. 4 – *The three pathway model for yeast metabolism suggested by Zhang et al. (1997).[28] (Figure adapted from (Schäpper et al., 2011)[25])*

According to the model, glucose may be oxidized to carbon dioxide along the respiratory metabolic pathway 2. However, if the glucose flow becomes too large for the respiratory capacity of the cell, excess glucose is fermented to ethanol according to pathway 1, and the activity of the enzymes in the glucose oxidation pathway is reduced. When glucose approaches depletion, ethanol begins to be metabolized by pathway 3. The cells grow exclusively on ethanol when glucose is exhausted.

In this model, the production of the desired protein is assumed to be associated with growth and is exclusively associated to the oxidative metabolism (pathways 2 and 3) in the yeast cells. This means that the production of the protein will be negatively affected by, for example, too high glucose concentrations.

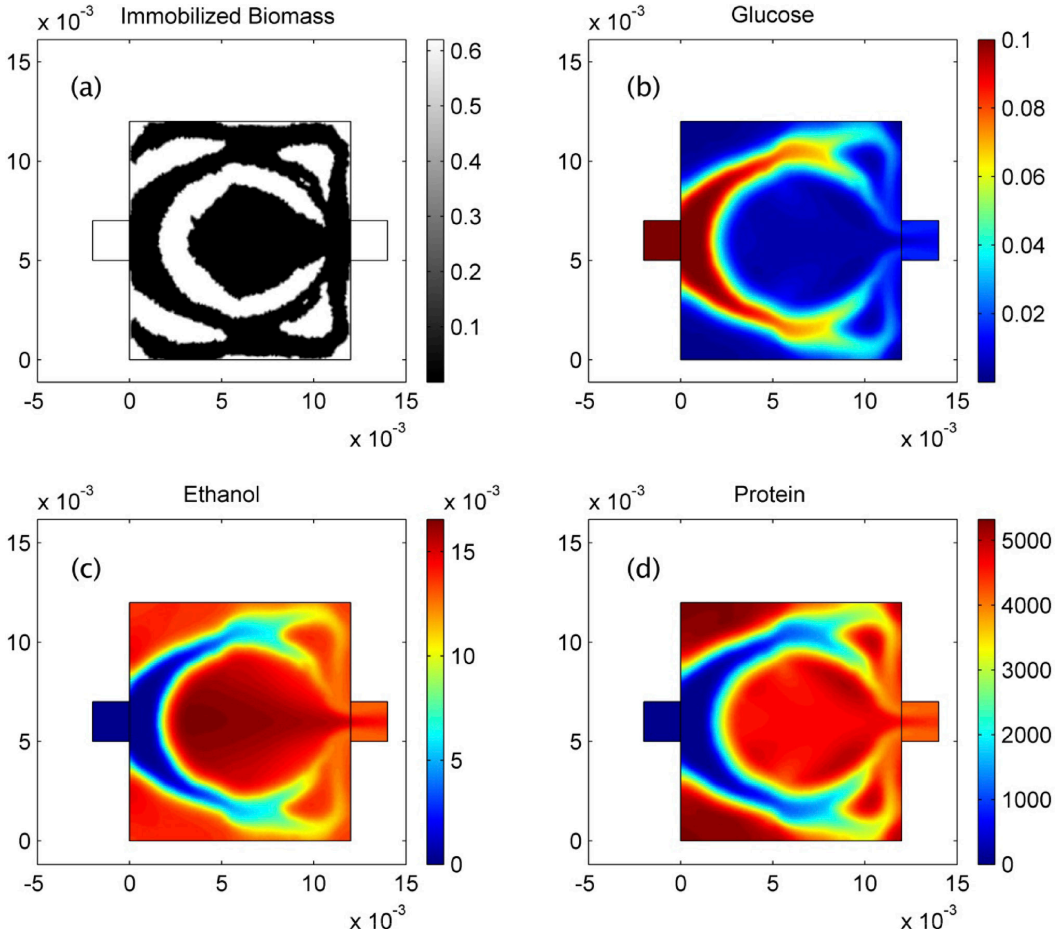

Fig. 5 – *Resulting structure and concentrations for a glucose inflow concentration of 0.1 g L^{-1}. (a) Distribution of biomass where white = cells and black = fluid, (b) glucose concentration [g L^{-1}], (c) ethanol concentration [g L^{-1}] and (d) protein concentration [units L^{-1}]. From Schäpper et al. (2011).*[26]

With this as a basis, a set of equations describing glucose consumption, ethanol production and consumption, protein production as well as both immobilized and suspended biomass was implemented as a kinetic model. The concentrations of glucose, ethanol, protein and biomass were then calculated at steady state based on the kinetic models coupled to their diffusion in the medium as well as their convection, based on the previously calculated flow velocities. From this the objective function, which was the total production of protein in the system, was calculated and the carrier distribution re-organized in order to try to find a more optimal distribution, by repeating the flow and kinetic calculations.

The total protein production in the optimized bioreactors (i.e. in the reactors with an optimized distribution of carrier) was then compared to the calculated performance of non-optimized reactors (i.e. in reactors where the carrier material was homogeneously distributed).

This comparison was made for different glucose concentrations in the feed and the results can be seen in Table 4, which shows that the protein mass flow rate at the outlet increased at least five-fold for all the simulated glucose concentrations when topology optimization was applied. The resulting structure for the case with a glucose concentration of 0.1 g L^{-1} in the feed can be seen in Fig. 5, together with its resulting glucose, ethanol and protein concentrations at steady state.

The significant gain in protein concentration can be explained by the fact that a structurally optimized distribution, where flow is distributed and islands of biomass are surrounded by streams of liq-

Table 4 – *Comparison of the total protein outputs for the homogeneous and the optimized reactor at different glucose feed concentrations*

Glucose feed conc. (mg L^{-1})	Protein flow at the reactor outlet (U sec^{-1})		
	homogeneous reactor	structurally optimized reactor	increase (fold)
1	0.3	2.7	5.8
5	1.4	12.9	9.1
10	2.7	23.1	8.4
30	7.2	57.4	8.0
50	10.7	91.7	8.5
100	17.6	170.3	9.7
200	25.2	229.5	9.1
500	39.0	325.2	8.3
1000	63.8	380.4	6.0

uid flow, allows for a more balanced distribution of glucose across the reactor leading to higher local protein production rates.

This first theoretical investigation of the potential of topology optimization for improvement of microbial cultivation processes at micro scale has clearly shown that the use of this methodology can potentially lead to microbioreactors with a significantly higher productivity than conventional reactor designs where immobilized biomass is homogeneously distributed.

Discussion

The presented case studies have different levels of complexity, and address different experimental scales as well. For the first case a lab-scale biocatalytic reaction is described by a system of coupled algebraic and ordinary differential equations that have been solved for a number of state variables, while for the second case, a microreactor, the Navier-Stokes equation has been solved with a mass balance for two different slow diffusing species. Finally in the last case study the partial differential equation systems for momentum and mass transport have been coupled with the kinetic rate laws of a relatively simple biological model, and this model of a microbioreactor was then linked with an optimization routine.

In the case studies, different types of information can be gathered from the calculations. In the first example, a model is confirmed with respect to the prediction quality, which by calibration may be further improved. In the second example a CFD model is applied in order to gain a better understanding of existing experimental data collected in a microscale reactor. Here new insight is quickly gained from a rapidly performed experiment, and this new information – the diffusion coefficient – can subsequently be used for the prediction of later experiments. Finally, the third example is completely theoretical and describes how an advanced model is used with the intention of generating new design configurations of an otherwise relatively well known fermentation system. The future challenge here is to verify experimentally whether new and intensified reaction systems can be generated. An evolutionary algorithm is furthermore implemented in order to achieve this goal.

Such examples are interesting from a scientific point of view, but also the more practical oriented scientist or engineer should consider the more systematic use of PSE methods and tools, since these methods and tools offer a range of convincing opportunities, as well as saving considerable resources. Indeed guiding experimentalists to the most valuable experiments is a key role of PSE methods and tools in general, and modeling in particular.

In most cases it is impossible to investigate all potential process configurations experimentally. Indeed, there is often not enough material (substrate, enzymes and other reactants) available, and if so the time/manpower for the experiments is limited. PSE methods can assist here as well. A broad range of theoretical configurations can be tested in relatively simple simulations and hence the impact of product inhibition, substrate inhibition, co-factor inhibitions and especially also mass transfer limitations due to reactor designs can be tested. A sensitivity analysis[12] is helpful for planning of experiments which can be used for the Design of Experiments (DoE) or Optimal Experimental Design (OED). The sensitivity analysis – local or global – will for example give an indication of which variables to measure in order to allow estimation of specific parameters. New process options can be investigated as well, before they are experimentally tested. In this way, PSE methods and tools can support process development. Even more importantly, PSE methods and tools can support process development in a structured way, meaning that the tools can be used over and over again each time a new process development task is started up.

Another area of application is the direct coupling of experimental data and mathematical simulations. Here well-established models will help to access requested but not available information. For example in case study 2 the diffusion characteristics of acetophenone and methylbenzylamine were not known and could not be found in literature. A surprising result was that by an appropriate experimental design (again planned with help of a model) it was discovered that one of the species diffuses sub-

stantially slower than the other. This was unexpected, since the molecular weight and the chemical structure are very similar. The acquired material properties are fundamentally important for the mass transfer limitations in the reaction and hence this information can also be used for scale up and scale out of reactors and processes.

From an intellectual point of view most interesting is the application of models for testing of concepts and even generation of entirely new ideas. It is not important, that the model predicts correctly from a quantitative point of view. As long as the qualitative prediction capacity is sufficient, the models can be used for the generation of understanding, insight and evaluation of new ideas. The user can visit the virtual laboratory in order to test simple relationships, complex interactions between different kinetic formulations and material transport limitations or simply to obtain a different view of a problem which the user is assumed to have been working with already for a long time. The more exact and experimentally validated the models are, the user might even omit the experimental validation of the simulation. This is classically done in engineering areas like turbine design or ship design, where the fabrication of prototypes is too demanding with respect to the costs.

The impact of the PSE tools can be substantial when the interdisciplinary nature of the project is guaranteed by a proper collaboration of different experts, such as protein scientists, chemists, process engineers, mathematicians and physicists. Then today futuristic appearing models can be used for advanced optimization routines, where under the assumption that the model is right, complex configurations can be automatically produced and hence reactors can be optimized with respect to topology and shape.

A last important potential application area for PSE methods is the transfer of experimentally established knowledge across scales. Miniaturized reactor technology is receiving increased attention due to the economic potential with respect to reduced time and costs in process development. But even though more and more companies are using or experimenting with such technology it is still unknown to what extent the experimental results can be used for the comparison with setups at another scale.

As presented in Table 5, the experimental setup of micro-scale experiments is dominated by laminar flow conditions and hence the mixing is poor and often diffusion limited. This results in considerable material transfer limitations and hence partial differential equations (PDE) have to be solved, for instance by use of CFD models, in order to predict the conditions in such systems. When changing to bench or pilot scale experiments it can be assumed that the systems are relatively well mixed and the mathematical description can be reduced to ordinary differential equations (ODEs), which simplifies the mathematical description of those systems. At full scale the situation is again such that there are mixing limitations due to the physical reactor design and a limited transfer of kinetic energy in comparison to bench/pilot scale setups. The fluid dynamic conditions are here highly turbulent and hence more complex PDE systems (CFD models) have to be applied which also consider turbulence modeling. Under the assumption that

1. The kinetics can be transferred across scales and
2. The model analysis tools can be used at all scales

it will be possible to answer many open questions with respect to the varying performances of systems at different scales, which is a research area in biochemical process technology which receives considerable attention nowadays.

Table 5 – *Summary of the variation of reactor characteristics and model tools across reactor scales*

Scale	Characteristics	Models
Micro-scale	Not well mixed, laminar flow, material transport limitations	PDEs (CFD)
Lab scale	Well-mixed	ODEs
Pilot scale	Usually well-mixed	ODEs
Full scale	Often not well mixed, gradients	PDEs (CFD), ODEs (compartment model)

According to the complexity of the presented case studies also the requested mathematical skills, knowledge and experience of the user has to be appropriately matching the task. For the first case study an experienced student, working for instance on a master project, might be the appropriate person to perform the task. As here presented, the system is modelled with help of MATLAB and mass balances which are coupled with the governing kinetic reaction rate expressions. In the second case study a commercial CFD software (ANSYS CFX 12.5) has been used, which made the numerical investigation simple with respect to the CFD work (days). But it should be considered that a commercial license of such software might not be available at all companies or research institutions. This would then demand either an investment into a license or the use of open software, where the latter then would need considerable training for the person involved. Finally in the third case, again a commercial CFD software (COMSOL) has been used and coupled with an evolutionary algorithm written in MATLAB. Clearly this is the most advanced PSE example that is presented here and a considerable experience

with this software tool has been a requirement. Consequently, the user of this software has been an advanced user and has nevertheless spent a considerable amount of time (month) on this task.

Conclusions and perspectives

This article has briefly presented an overview about how Process System Engineering (PSE) methods can be used for the systematic development of (bio) reactor systems. Three case studies have been presented with different applications, reactions and scales. The intention of the studies is to present different applications of PSE tools. One important focus area is the use of PSE methods for the development of miniaturized reactor systems. It was demonstrated, how models can assist in achieving a better understanding of the process conditions, the prediction of process performance and the theoretical investigation of reaction conditions with computer based algorithms for reactor improvement. The manuscript gives the reader a motivation for the use of PSE models and tools at different scales and level of detail of applications. This included practical aspects like determination of material constants or reaction performance as well as more academic use like in optimization routines. The future and experimental studies will show if such *in silico* investigations will contribute to the reduction of process development costs and improved understanding of processes across scales.

ACKNOWLEDGEMENTS

Financial support by the European Union FP7 Project BIOINTENSE – Mastering Bioprocess integration and intensification across scales (Grant Agreement Number 312148) is gratefully acknowledged. The research work furthermore received financial support from the Danish Council for Independent Research | Technology and Production Sciences (project number: 10-082388), and from the Novo Nordisk Foundation (project: Exploring biochemical process performance limits through topology optimization).

List of symbols and nomenclature

Abbreviations

CDH – Cellobiose dehydrogenase
ABTS – 2,2'-azino-bis(3-ethylbenzothiazoline-6--sulfonic acid) diammonium salt
$ABTS^+$ – 2,2'-azino-bis(3-ethylbenzothiazoline-6--sulfonic acid) diammonium salt cation radical
HPLC – High-performance liquid chromatography

Nomenclature

V_{max} – Maximum initial velocity of an enzyme, mM h^{-1}
K_M – Michaelis-Menten constant, mM
K_La – Volumetric mass transfer coefficient, h^{-1}
K_{hyd} – Hydrolysis constant, h^{-1}
C_0 – Initial concentration of any species, mM
C – Concentration of any species, mM
r – Reaction rate, mM h^{-1}

Subscripts

lact – Lactose
LBL – Lactobiono-lactone
LBA – Lactobionic acid
O_2 – Oxygen
ABTS – Reduced redox intermediate
$ABTS^+$ – Oxidized redox intermediate
omt – Oxygen mass transfer

Superscripts

CDH – Cellobiose dehydrogenase
lacc –Laccase
$ABTS^+$ – Oxidized redox mediator
ABTS – Reduced redox mediator
sat – Saturation

References

1. *Pollard, D. J., Woodley, J. M.*, Trends Biotechnol. **25** (2007) 66. doi: dx.doi.org/10.1016/j.tibtech.2006.12.005
2. *Tufvesson, P., Lima-Ramos, J., Nordblad, M., Woodley, J. M.*, Org. Process Res. Dev. **15** (2011) 266. doi: dx.doi.org/10.1021/op1002165
3. *Krühne, U., Heintz, S., Ringborg, R., Rosinha, I. P., Tufvesson, P., Gernaey, K. V., Woodley, J. M.*, Green Processing Synth. **3**, 1, (2014) 23.
4. *McMullen, J. P., Jensen, K. F.*, Org. Process Res. Dev. **15** (2011) 398. doi: dx.doi.org/10.1021/op100300p
5. *Schäpper, D., Zainal Alam, M. N. H., Szita, N., Eliasson Lantz, A., Gernaey, K. V.*, Anal. Bioanal. Chem. **395** (2009) 679. doi: dx.doi.org/10.1007/s00216-009-2955-x
6. *Klatt, K., Marquardt, W.*, Comput. Chem. Eng. **33** (2009) 536. doi: dx.doi.org/10.1016/j.compchemeng.2008.09.002
7. *Stephanopoulos, G., Reklaitis, G. V.*, Chem. Eng. Sci. **66** (2011) 4272. doi: dx.doi.org/10.1016/j.ces.2011.05.049
8. *Gernaey, K. V., Cervera-Padrell, A. E., Woodley, J. M.*, Comput. Chem. Eng. **42** (2012) 15. doi: dx.doi.org/10.1016/j.compchemeng.2012.02.022
9. *Asprey, S. P., Macchietto, S.*, Comput. Chem. Eng. **24** (2000) 1261. doi: dx.doi.org/10.1016/S0098-1354(00)00328-8

10. *Sales-Cruz, M., Gani, R.*, Comp. Aid. Chem. Eng. **16** (2003) 209.
doi: dx.doi.org/10.1016/S1570-7946(03)80076-7
11. *Marquardt, W.*, Chem. Eng. Res. Design **83** (2005) 561.
doi: dx.doi.org/10.1205/cherd.05086
12. *Sin, G., Gernaey, K. V., Eliasson Lantz, A.*, Biotechnol. Progr. **25** (2009) 1043.
doi: dx.doi.org/10.1002/btpr.166
13. *Santacoloma* (2012) Multi-enzyme process modelling. PhD thesis, Technical University of Denmark, Kgs. Lyngby, Denmark. p 197.
14. *Van Hecke, W., Bhagwat, A., Ludwig, R., Dewulf, J., Haltrich, D., Van Langenhove, H.*, Biotechnol. Bioeng. **102** (2009) 1475.
doi: dx.doi.org/10.1002/bit.22165
15. *Ludwig, R., Ozga, M., Zámocky, M., Peterbauer, C., Kulbe, K. D., Haltrich, D.*, Biocatal. Biotranfor. **22** (2004) 97.
16. *Van Hecke, W., Ludwig, R., Dewulf, J., Auly, M., Messiaen, T., Haltrich, D., Van Langenhove, H.*, Biotechnol. Bioeng. **102** (2009) 122.
doi: dx.doi.org/10.1002/bit.22165
17. *Galhaup, C., Goller, S., Peterbauer, C. K., Strauss, J., Haltrich, D.*, Microbiol. **148** (2002) 2159.
18. *Sin, G., Ödman, P., Petersen, N., Eliasson Lantz, A., Gernaey, K. V.*, Biotechnol. Bioeng. **101** (2008) 153.
doi: dx.doi.org/10.1002/bit.21869
19. *Cornish-Bowden, A.*, Fundamental of enzyme kinetics, Third Edition, Portland Press Ltd., London, 2004.
20. *Leskovac, V.*, Comprehensive Enzyme Kinetics, Kluwer Academic/Plenum Publishers, New York, 2003.
21. *Bodla, V. K., Seerup, R., Krühne, U., Woodley, J. M., Gernaey, K. V.*, Chem. Eng. Technol. **36** (2013) 1017.
doi: dx.doi.org/10.1002/ceat.201200667
22. *Tufvesson, P., Lima-Ramos, J., Jensen, J. S., Al-Haque, N., Neto, W., Woodley, J. M.*, Biotechnol. Bioeng. **108** (2011) 1479.
doi: dx.doi.org/10.1002/bit.23154
23. *Al-Haque, N., Santacoloma, P. A., Neto, W., Tufvesson, P., Gani, R., Woodley, J. M.*, Biotechnol. Progr. **28** (2012) 1186.
doi: dx.doi.org/10.1002/btpr.1588
24. *Bruus, H.*, Theoretical Microfluidics, First Edition, Oxford University Press, Oxford, 2008.
25. *Schäpper, D., Lencastre Fernandes, R., Lantz, A. E., Okkels, F., Bruus, H., Gernaey, K. V.*, Biotechnol. Bioeng. **108** (2011) 786.
doi: dx.doi.org/10.1002/bit.23001
26. *Okkels, F., Bruus, H.*, Physical Review E. **75** (2007) 16301.
doi: dx.doi.org/10.1103/PhysRevE.75.016301
27. *Bránýik, T., Vicente, A. A., Kuncová, G., Podrazký, O., Dostálek, P., Teixeira, J. A.*, Biotechnol. Progr. **20** (2004) 1733.
doi: dx.doi.org/10.1021/bp049766j
28. *Zhang, Z., Scharer, J. M., Moo-Young, M.*, Bioprocess Eng. **17** (1997) 235.
doi: dx.doi.org/10.1007/s004490050380

Appendix A.3: Applications, benefits and challenges of flow chemistry

Krist V. Gernaey

Applications, benefits and challenges of flow chemistry

PEER REVIEWED

ALEKSANDAR MITIC, SØREN HEINTZ, ROLF H. RINGBORG, VIJAYA BODLA, JOHN M WOODLEY, KRIST V. GERNAEY*

*Corresponding author

1. Technical University of Denmark (DTU), Department of Chemical and Biochemical Engineering, Søltofts Plads, Building 229, 2800 Kgs. Lyngby, Denmark

KEYWORDS

Flow chemistry; Organic Synthesis; Biocatalysis; Process Analytical Technology (PAT); Microreactor Technology.

ABSTRACT

Organic synthesis (incorporating both chemo-catalysis and biocatalysis) is essential for the production of a wide range of small-molecule pharmaceuticals. However, traditional production processes are mainly based on batch and semi-batch operating modes, which have disadvantages from an economic, environmental and manufacturing perspective. A potential solution to resolve these issues is to use flow chemistry in such processes, preferably with applications of micro- and mini-sized equipment. In addition, Process Analytical Technology (PAT) may be implemented in a very efficient way in such equipment due to the high degree of automation and process controllability that can be achieved in small scale continuous equipment.

INTRODUCTION

Continuous production is often cited as both eco-friendly and economic, mainly due to the higher energy efficiency and reduced consumption of resources that can be achieved in comparison with traditional batch production (1-4). Furthermore, continuous production fulfills very well the requirements defined by the regulatory bodies, such as the Food and Drug Administration (FDA). More particularly, the FDA has clearly indicated that it favors such processes – including on-line measurement and control – with the publication of the Process Analytical Technology (PAT) guidance in 2004 (5). PAT defines the key Initiative of cGMP (6) and is incorporated into the International Conference on Harmonization (ICH) Q8 guidance (7). The Initiative has shown many advantages in modern organic synthesis and biotechnology, and has consequently been applied in other industry sectors, such as food, chemical and life sciences (8). The objective of this manuscript is to briefly review applications of flow chemistry in modern organic synthesis. Furthermore, the focus will be on emphasizing the benefits of such processes and additionally on identifying the remaining challenges for further improvement.

MICRO-CHEMICAL PROCESSING IN ORGANIC SYNTHESIS

Organic synthesis can be performed in continuous mode by using mini- and micro-structured flow devices. Small scale continuous flow technology has many potential advantages, such as: rapid heat and mass transfer, increased safety, easy scale-up/scale-out, fast process characterization, potential for real-time release, operation with unstable reaction species, and so on (9, 10). Due to such advantages integration of these small scale devices in plant architectures has become more common in the last two decades (11). It is important to note here that not all chemical reactions are suited to such small-scale equipment. For example, according to Roberge et al. (12), chemical reactions with a half-life higher than 10 min should preferably be operated in batch manufacturing mode. However, it has been demonstrated that some of these reactions too could be drastically accelerated by downsizing the equipment to a micro-scale level (13). Furthermore, chemical reactions with very reactive substrates, such as Grignard exchange reactions and reactions with chloride, bromide and amine species are all very suitable for flow chemistry applications. These reactions, with typical half-lives below 1 s, can therefore be completed in the mixing zone alone (12, 14, 15). Finally, chemical reactions with half-lives from 1 s up to 10 min could also benefit from the micro-scale devices (16). Better control of heat flow and temperature are the main advantages of operating such reactions at micro-scale (12).

The kinetics of biocatalytic processes (mixed order, obeying Michelis-Menten) will always be best exploited in a batch or continuous plug flow mode, especially for reactions requiring a high conversion. For this reason, continuously stirred tank reactors are rarely used for biocatalytic reactions in industry. However, at reasonable concentrations for industrial implementation most biocatalytic reactions are limited by substrate inhibition, meaning that a fed-batch system becomes favorable. Often the product too is inhibitory which is most normally dealt with, by *in-situ* product removal (ISPR) (1, 3, 17-19). Such a combination of 'feed and bleed' combined with the mixed order kinetics, characteristic of an enzyme catalyzed reaction, implies that a batch with feed and ISPR, or alternatively a plug flow with multiple feed and product removal points down the column, would be attractive. Hence, we believe that flow chemistry also can be attractive to biocatalysis. Performing synthesis at micro-scale is even more attractive when one considers

the small amounts of material (both substrates and products) available at an early stage of biocatalytic process development. Operating in plug flow enables the effective testing of immobilized enzyme formats as well, and simplifies integration with the neighboring chemical operations (20). Besides the limiting effects of inhibitions at industrially relevant process conditions, there are also situations where the reaction equilibrium of the biocatalytic processes is unfavorable. In those situations it is necessary to use different methodologies to shift the equilibrium towards the desired products. For example *in-Situ* co-Product Removal (IScPR) is a potential solution enabling higher yields and productivities (21, 22).

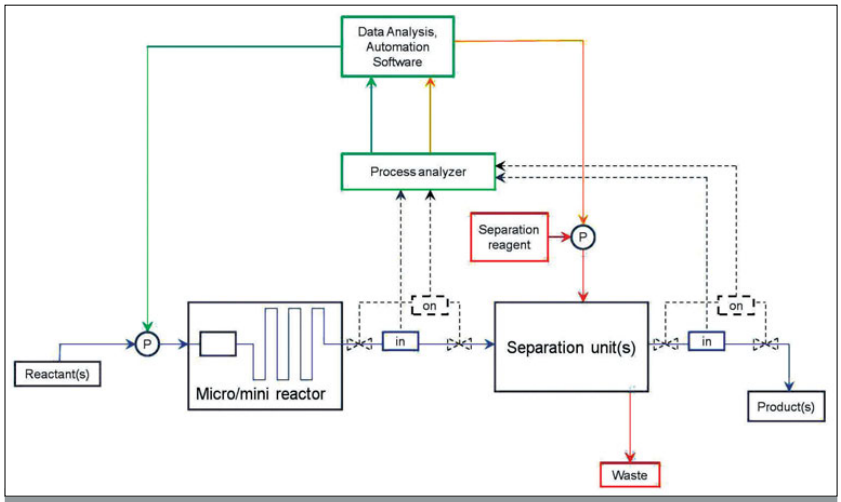

Figure 1. Simplified scheme of the Lab-on-a-chip system with implemented PAT requirements. Blue solid line – main flow; blue dashed line – process signal obtained by in-line process monitoring; black dashed line – on-line process monitoring and resulting process signal; green solid line – data from a process analyzer to data analysis section intended to establish process control and automation of the pumps for the reactor section; yellow solid lines – data from a process analyzer to data analysis section intended to establish process control and automation of the pumps for the separation section; red solid line – separation agent and waste material flow.

The benefits of flow systems have been reported to some extent in the scientific literature, for both simple and more complex systems. One example of relatively simple biocatalytic systems is using lipase (EC. 3.1.1.3). The enzyme is particularly robust in non-natural environments, e.g. high concentrations, organic solvents, etc. (3, 23, 24). An example of more complex biocatalytic systems is the use of ω-transaminase (ω-TA – EC. 2.6.1.1) to transfer an amine to a prochiral ketone. Transaminase based biocatalytic processes typically experience severe substrate and product inhibition, along with unfavorable reaction equilibrium depending on the choice of amine donor (21, 25). In preliminary work Bodla et al. (26) showed improved productivity in micro-scale systems compared to conventional batch methods for such a reaction.

INTEGRATION OF MICROREACTORS IN THE PLANT ARCHITECTURE

Even though they are only suited for micro-chemical processing, miniaturized total analysis systems (μ-TAS) or lab-on-a-chip systems are receiving increasing attention in the process industries. This approach integrates all analytical steps on the same platform (27), and could thereby successfully avoid unnecessary storage of intermediate products. In this way, faster manufacturing of a desired compound could be obtained, as well as circumventing significant losses in processes with very reactive substrates and intermediates. A simplified process flow scheme of such lab-on-a-chip system is shown in Figure 1, together with integrated process in-/on-line monitoring, process control and automation.

The previous section was entirely focused on the reaction step in continuous flow. However, incorporation of multi-step chemical synthesis in micro-scaled devices usually necessitates coupling the reaction step(s) with a subsequent continuous separation step. Traditional separation approaches for two immiscible liquids at macro-scale levels are mainly based on gravitational forces. However, if downsizing is applied, surface forces become dominant (9).

A recent lab-scale example with the use of a hydrophobic membrane separator (Figure 2) showed great efficiency for separating two immiscible liquids (28). However, it requires long-term tests at industrial scale before such membrane separators will be accepted by industry. While waiting for the results of such trials, development of separators without membranes is preferred (29). Furthermore, effective separation of two miscible liquids has been achieved by applying micro-evaporation principles (30), as well.

Solid particles form a major issue in meso- and especially in micro-scaled equipment. One successful approach for handling solids is to use acoustic irradiation, which is often applied in modern organic synthesis with the main purpose to avoid bridging inside the channels. Another phenomenon called constriction could also cause potential problems in small scale flow devices, and it is usually avoided by using different fluid velocities, or more precisely by applying periodical flushing actions. Assuming constant concentrations of starting materials or formed particles present inside micro-channels, the extent of such constriction phenomena could be predicted. Indeed, assuming constant inflow conditions, quantification of the constriction rates is possible on the basis of simple measurements of pressure drops along the microchannels (31).

For biocatalytic applications it will often be a necessity to operate these systems in the presence of solids, e.g. as a consequence of the biocatalyst formulation (see below), or in some cases due to reaction species with low solubilities (21, 24). Operating biocatalytic processes in these miniaturized modules can therefore, for many applications, be expected to give some precipitation and clogging problems, which have to be overcome (33, 34). Use of unconventional reaction media, e.g. organic solvents, can result in avoiding high concentrations of insoluble compounds. However, unconventional reaction media can have severe effects on the biocatalyst performance, e.g. toxic and denaturizing effects (34). Protein engineering here provides the means to modify the biocatalyst in a manner so it becomes more resistant to operation in non-conventional media (1, 2). Protein engineering is generally used for biocatalyst modifications to improve performance in process relevant conditions (22).

The formulation of the biocatalyst can also cause clogging.

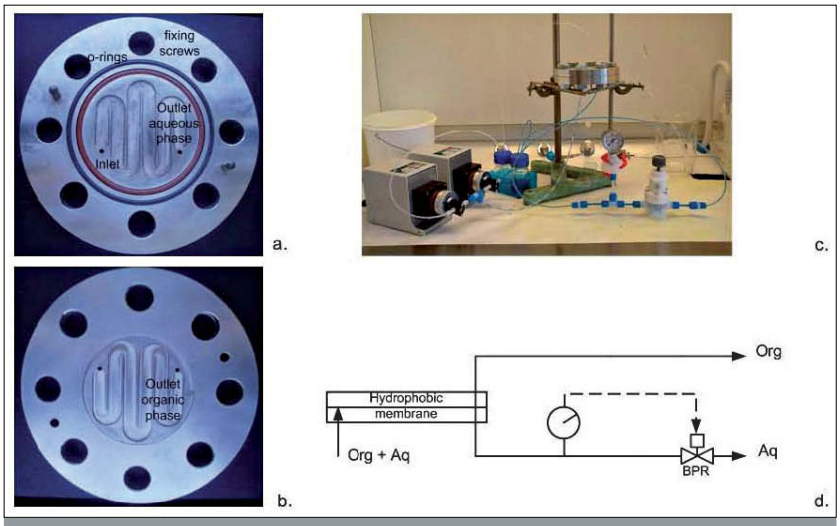

Figure 2. A PTFE membrane separator applicable for splitting two immiscible liquids. a. Part of the separator intended for the aqueous phase. b. Part of the separator intended for the organic phase. c. Image of the PTFE membrane separator with aqueous phase coloured in blue and uncoloured toluene phase. d. Scheme of the PTFE membrane separator setup (28).

The formulation of the biocatalyst is highly dependent on the process economics, e.g. the feasibility of a biocatalytic process can be greatly improved by applying the biocatalyst in the crudest possible form (35), as a consequence of reduced purification costs. It can therefore for some applications be necessary to use solutions potentially containing precipitate, polymers, cells, etc. resulting in clogging issues caused by adhesion of compounds or cells to surfaces (36). Also, for some applications the biocatalysts are immobilized onto solid supports with the purpose of improving the catalyst stability along with simplification of catalyst recirculation (37). For some biocatalytic applications, we expect that it will be ideal to use the biocatalyst directly from the fermentation, without any major purification steps beforehand. This could greatly improve process feasibility, but at the same time result in potential issues with regards to high solid concentrations in flow systems.

The majority of new synthetic pathways in organic chemistry involve chemical catalysts and in some cases biocatalysis as one step in the otherwise chemical synthetic sequence. Hence, removal of transition metals is still receiving considerable attention in pharmaceutical production. Due to the high toxicity of these chemical elements, the allowed concentrations in final products are usually very low (38) and thereby very efficient metal removal procedures are required. Currently, most procedures are based on batch processing (39), however, examples with packed-bed columns showed promising performance in flow, as described by Wiles et al. (40).

DOWNSTREAM PROCESSING

Besides developing efficient synthesis pathways in miniaturized systems, there is also a demand for efficient inline downstream methods in order to recover and purify products. The high surface-to-volume ratios attainable at micro-scale result in faster mass transfer suggesting improved effectiveness of such systems compared to macro-scale. Combining upstream with downstream unit operations in micro-chemical or biochemical processing enables testing entire processes on a bench – e.g. factory-on-a-bench. In some situations it might even be desired to run the actual process on a bench. However, there is a clear need for miniaturized equivalents of large scale downstream unit operations before this factory-on-a-bench concept can be fully realized. There has been some focus already on providing such miniaturized unit operations (41, 42). Here the main focus will be on continuous extraction in flow systems.

Liquid-liquid extraction (LLE) is a well-established product recovery method in the pharmaceutical industry. Laminar flow conditions experienced in micro-scale extraction units give the possibility to operate with both segmented and side-by-side flows. Side-by-side flow operation allows easy laminar flow splitting in a continuous manner, and both extraction in concurrent and counter current flow modes can be established. Segmented flow operation improves the mass transfer by diffusion, due to an even higher surface area than side-by-side flow. However, it is not possible to separate the segments by gravitational forces as in conventional methods, because surface tension forces are dominant in micro-scale. LLE with segmented flows requires other separation methods, e.g. membrane separation units have shown great potential for continuous separation in such flow systems (43). For biocatalytic applications there can be issues concerning biocompatibility and phase toxicity if streams are recycled, and specifically for such applications it would be necessary to modify biocatalysts to operate efficiently in the presence of organic solvents (protein engineering, see previous section).

Solid-liquid extraction using particles (resins etc) is an attractive alternative option to processes where organic solvents exhibit operational challenges, e.g. biocompatibility, phase toxicity, emulsification, etc. Porous resins, in general, are inert, easy to handle and simplify product isolation (filtration). In biocatalysis, resins can additionally be used to enhance the reaction performance for reactions with kinetic limitations. This is achieved by using them as an auxiliary phase for substrate supply and product removal (ISPR) by integrating the reaction and extraction steps. However, at micro-scale and more specifically in flow systems, one important limitation is that solid reagents are difficult to handle as they may clog micro-channels.

High surface-to-volume ratios attainable at microscale result in faster mass transfer suggesting the improved effectiveness of such systems compared to macro-scale. However, the increase in pressure drop needs to be addressed with a suitable reactor design solution. Losey et al. (44), for example, reported an increase in mass transfer by more than 2 orders of magnitude for cyclohexene hydrogenation in a micro packed bed reactor, using activated carbon catalyst,

compared to a macro scale counterpart. The increase in pressure drop was in that case addressed by splitting the flow into multiple channels and thus reducing the overall pressure drop while retaining the effective cross-sectional area and obtaining higher reactor throughput.

PROCESS MONITORING, CONTROL AND AUTOMATION

Efficient production of the desired compounds is the main goal in organic synthesis. Operating the processes in an efficient manner does however require a high degree of process understanding to enable improved monitoring and control. It is though very challenging to implement in-line monitoring in micro-scale systems because of the small dimensions required for the sensors, as well as the fact that analysis of very complex process signatures is needed. Traditional applications based on in- and on-line spectroscopic methods are desired even though they are difficult to obtain. A recent example of process monitoring and control in flow was published by Cervera-Padrell et al. (45).

Fulfilment of the PAT requirements involves automation of the established processes. Several successful case studies have been reported using different kinds of commercially available software (46). The most desired way is to perform in/on-line process monitoring and control due to the very fast response that can be obtained. Consequently, faster data analysis is achieved and, for example, corrective actions to avoid or reduce side reactions are performed easily, which is essential for fast reactions.

Besides using miniaturized systems for operation of complex biocatalytic processes, there is also the possibility of using these miniaturized systems for process development and research purposes. The micro-scale flow systems indeed have the potential of being powerful tools which can aid in detailed process screenings and biocatalyst characterization under realistic process conditions. Early, in the development of new biocatalytic processes, there is limited availability of resources, e.g. biocatalyst to be tested. The limited availability of resources puts some constraints on how many experiments can be performed. The level of system detail is therefore also determined by the available quantity of the biocatalyst to be tested, and this should be enough to evaluate the potential of a given process. The use of miniaturized systems for process investigations enables more detailed characterization with lower sample volumes and could be used to set up sophisticated models describing the systems. There are however limitations with regard to how low the sampling volumes can become before analytical limitations become a hindrance, as illustrated in Figure 3.

CONCLUSIONS AND FUTURE PERSPECTIVES

Flow chemistry in meso- and micro-scale devices has found many useful applications in modern organic synthesis and increasingly also in biocatalytic processes. Increased selectivity and yields, increased safety, and additional benefits lead to higher applicability of these processes in the modern pharmaceutical industry, especially in relation to complex processes. Furthermore, easier implementation of the requirements defined by the PAT Initiative has made flow chemistry into a key focus point.

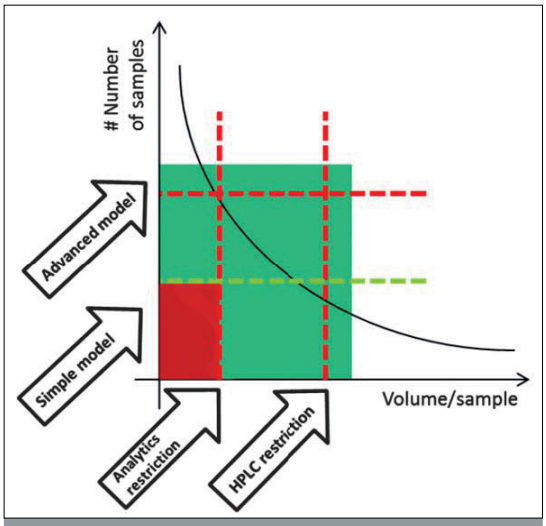

Figure 3. Illustration of the correlation between analytical limitations and model complexity, when availability of resources is scarce during process development. E.g. multiple data points are required for more sophisticated models, but the volume per sample for analytical measurements gives restrictions to the number of samples which can be obtained when having scarce resources.

However, obstacles in performing process monitoring and consequently process controls in micro-scaled devices are still a major challenge. Hence, further focus is on the development of better data analysis tools in order to facilitate efficient process control actions on the basis of the collected data.
Extrapolating from these miniaturized systems to larger production volumes can mainly be done in two ways, by means of scale-up or scale-out (numbering-up). When considering scale-up, this can introduce additional obstacles as a consequence of altered reaction and flow conditions. It is therefore essential to develop tools that can help to predict the cost to scale-up and scale-out, respectively, and to use such tools to support decision making when designing the production process.

ACKNOWLEDGEMENTS

The authors acknowledge the support of: (1) project BIOINTENSE, financed through the European Union 7th Framework Programme (Grant agreement no.: 312148); (2) the Danish Council for Independent Research | Technology and Production Sciences (project number: 10-082388).

REFERENCES AND NOTES

1. Pollard, D.J., Woodley, J.M., *Trends Biotechnol.*, **25(2)**, 66-73 (2006).
2. Bornscheuer, U.T., Huisman, G.W., et al., *Nature*, **485**, 185-194 (2012).
3. Schmid, A., Dordick, J., et al., *Nature*, **409**, 258-268 (2001).
4. Baughman E., *Process Analytical Chemistry: Introduction and Historical Perspectives*, Chapter 1, in *Process Analytical Technology-Spectroscopic Tools and Implementation Strategies for the Chemical and Pharmaceutical Industries*, Edited by Bakeev, K.E., Ed. Blackwell Publishing Ltd, Oxford, Iowa, USA (2005).
5. FDA, *Guidance for Industry. PAT - A framework for innovative pharmaceutical manufacturing and quality assurance*, U.S. Food and Drug Administration, U.S. Department of Health and Human Services, Rockville, USA (2004).
6. FDA, *Drug Applications and Current Good Manufacturing Practice (CGMP) Regulations*, U.S. Food and Drug Administration, U.S. Department of Health and Human Services, Rockville, USA (2004).
7. FDA, *Guidance for Industry. Q8 Pharmaceutical Development*. U.S. Food and Drug Administration, U.S. Department of Health and Human Services, Center for Drug Evaluation and Research (CDER), Center for Biologics Evaluation and Research (CBER), International Conference of on Harmonization (2006).
8. Workman, J., Koch, M., et. al., *Anal. Chem.*, **81(12)**, 4623-4643 (2009).
9. Hartman, R.L., Jensen, K.F., *Lab Chip*, **9(17)**, 2495-2507 (2009).
10. Hessel, V., Löb, P., et al., *Microstructured Reactors for Development and Production in Pharmaceutical and Fine Chemistry*, in *New Avenues to Efficient Chemical Synthesis: Emerging Technologies*. Edited by Seeberger, P.H., Blume, T., Ed. Springer-Verlag, Berlin, Heidelberg, Germany (2007).
11. Ehrfeld, W., Hessel, V., et al., *Microreactors*, Chapter 22, in *Ullmann's Encyclopedia of Industrial Chemistry*, Edited by Bohnet, M., Ullman, F., Ed. Wiley Online Library, Weinheim, Germany (2003).
12. Roberge, D.M., Ducry, L., et al., *Chem. Eng. Technol.*, **28(3)**, 318-323 (2005).
13. Damm, M., Glasnov, T.N., et al., *Org. Process Res. Dev.*, **14(1)**, 215-224 (2009).
14. Riva, E., Gagliardi, S., et al., *Tetrahedron*, **66(17)**, 3242-3247 (2010).
15. Wakami, H., Yoshida, J-I., *Org. Process Res. Dev.*, **9(6)**, 787-791 (2005).
16. Wiles, C., Watts, P., *Expert Opin. Drug Discovery*, **2(11)**, 1487-1503 (2007).
17. Carstensen, F., Apel, A., et al., *J. Membr. Sci.*, **394-395**, 1-36 (2012).
18. Truppo, M.D., Turner, N.J., *Org. Biomol. Chem.*, **8**, 1280-1293 (2010).
19. Truppo, M.D., Rozzell, J.D., et al., *Org. Process Res. Dev.*, **14**, 234-237 (2010).
20. Hailes, H.C., Dalby, P.A., et al., *J. Chem. Technol. Biotechnol.*, **82**, 1063-106 (2007).
21. Tufvesson, P., Lima-Ramos, J., et al., *Biotechnol. Bioeng.*, **108(7)**, 1479-1493 (2011).
22. Woodley, J.M., *Curr. Opin. Chem. Biol.*, **17(2)**, 1-7 (2013).
23. Itabaiana Jr., I., Miranda, L.S., et al., *J. Mol. Catal. B: Enzym.*, **85-86**, 1-9 (2013).
24. Tufvesson, P., Fu, W., et al., *Food and Bioprod, Process.*, **88(1)**, 3-11 (2010).
25. Malik, M.S., Park, E.S., et al., *Appl. Microbiol. Biotechnol.*, **94(5)**, 1163-1171 (2012).
26. Bodla, V.K., Seerup, R., et al., *Chem. Eng. Technol.*, **36(00)**, 1–11 (2013).
27. Manz, A., Graber, N., et al., *Sens. Actuators, B*, **1-6**, 244-248 (1990).
28. Cervera-Padrell, A.E., Morthensen, S.T., et al., *Org. Process Res. Dev.*, **16(5)**, 888-900 (2012).
29. Burns, J., R., Ramshaw, C., *Chem. Eng. Res. Des.*, **77(3)**, 206-211 (1999).
30. Wootton, R.C.R., deMello, A.J., *Chem. Commun.*, 266-267 (2004).
31. Hartman, R.L., Naber, J.R., et al., *Org. Process Res. Dev.*, **14(6)**, 1347-1357 (2010).
32. Jensen, K.F., *Microchemical systems for Discovery and Development, in New Avenues to Efficient Chemical Synthesis: Emerging Technologies*. Edited by Seeberger, P.H., Blume, T., Ed. Springer-Verlag, Berlin, Heidelberg, Germany (2007).
33. Hartman, R.L., *Org. Process Res. Dev.*, **16(5)**, 870-887 (2012).
34. Klianov, A.M., *Trends in Biotechnol.*, **15(3)**, 97-101 (1997).
35. Tufvesson, P., Lima-Ramos, J., et al., *Org. Process Res. Dev.*, **15(1)**, 266-274 (2011).
36. Lu, H., Koo, L.Y., et al., *Anal. Chem.*, **76(18)**, 5257-5264 (2004).
37. Mateo, C., Palomo, J.M., et al., *Enzyme Microb. Technol.*, **40(6)**, 1451-1463 (2007).
38. Garrett, C.E., Prasad, K., *Adv. Synth. Catal.*, **346(8)**, 889-900 (2004).
39. Corbet, J-P., Mignani, G., *Chem. Rev.*, **106(7)**, 2651-2710 (2006).
40. Wiles, C., Watts, P., *Review*, **2(11)**, 1487-1503 (2007).
41. Aota, A., Mawatari, K., Kitamori, T., Lab Chip, 9(17), 2470-2476 (2009).
42. Hartman, R.L., Sahoo, H.R., Yen, B.C., Jensen, K.F., *Lab Chip*, **9(13)**, 1843-1849 (2009).
43. Kralj, J.G., Sahoo, H.R., Jensen, K.F., *Lab Chip*, **7(2)**, 256-263 (2007).
44. Losey, M.W., Schmidt, M.A., et al., *Ind. Eng. Chem. Res.*, **40**, 2555-2563 (2001)
45. Cervera-Padrell, A.E., Nielsen, J.P., et al., *Org. Process Res. Dev.*, **16(5)**, 901-914 (2012).
46. Chew, W., Sharratt, P., *Anal. Methods*, **2(10)**, 1412-1438 (2010).

Appendix B

Chapter 4: supplementary material

Calculation of the required [P] or [cP] concentrations at various initial substrate concentrations:

The initial concentration of BA in the reaction mixture gives some restrictions with respect to how low a concentration the desired ISPR/IScPR strategy should operate with in order to be efficient. In figure B.1, some apparent values are calculated indicating how low product or co-product concentrations are required to achieve various degrees of conversion, where B.1A is at low initial concentration (10 mM) and B.1B is at high initial concentration (337 mM), using equivalent amounts of the amine donor.

From these calculations it becomes clear that operating with low substrate concentrations and slightly unfavorable thermodynamics, will require the separation process to be extremely selective and capable of removing very low quantities of the product and/or co-product. It is therefore very important to characterize how selective ISPR/IScPR options are, and at which concentrations they can potentially operate in a feasible way. Enzymatically based cascade reactions for IScPR are known to be very selective and capable of operating with very low concentrations. However, cascade reactions add significant complexity to the process and are partly for that reason not always a feasible choice. In many cases, it can be useful to consider the implementation of conventional separation methods as the preferred ISPR strategies in combination with a donor excess in order to loosen the requirements for the separation and maintain a high degree of conversion. The benefit of implementing ISPR strategies based on conventional separation processes is that it will ultimately result in an outlet product stream with potentially high product titer, from which it should be significantly easier and cheaper to recover the product.

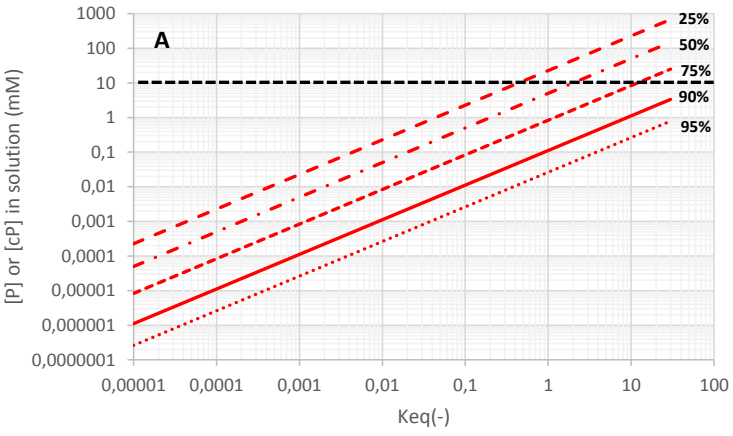

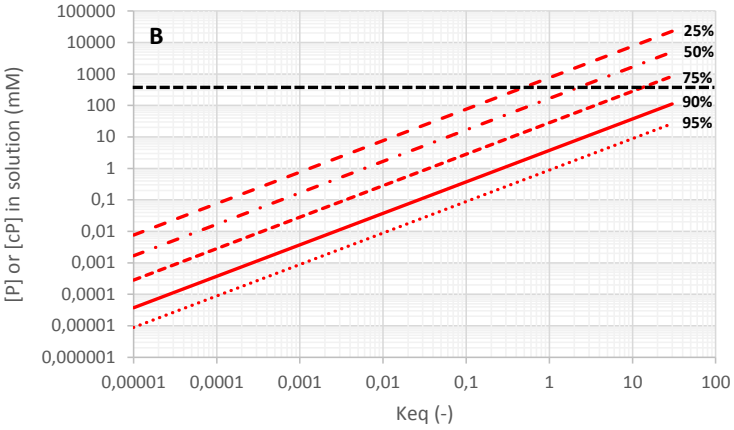

Figure B.1: Overview of required product and/or co-product concentrations in order to achieve various degrees of conversion for different thermodynamic scenarios. The plots are based upon having equivalent amounts of substrate and amine donor. A) Illustration of the requirements when operating with low initial BA concentration, i.e. 10 mM, which is close to the indicated solubility limitation. B) Illustration of the requirements when operating with higher concentrations, i.e. 337 mM (~50 g/L). The horizontal dashed line in both plots corresponds to the initial BA and amine donor concentration.

Case study 2 plots and calculations:

In figure B.2, it is shown how the application of an excess of the amine donor will influence the requirements for minimum allowable product and/or co-product concentration as a complement to the excess to shift the reaction equilibrium. The calculations are based upon equation 4 and assuming $K_{eq} = 0.74$ and an initial BA concentration of 10 mM (close to the solubility limit).

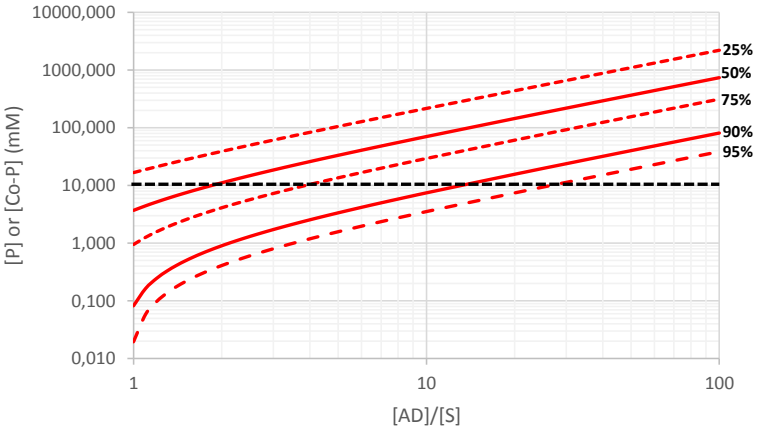

Figure B.2: Degrees of conversion expressed by the relation between minimum product and/or co-product concentrations and various amine donor excess ratios, for an initial substrate concentation of 10 mM BA.

A suplementary alternative to applying an amine donor excess, in order to loosen the requirements for product and co-product separation is to increase the solubility of the main substrate. In figure B.3, it is shown how increasing the solubility of the main substrate will reduce the minimum allowable product/co-product concentration in order to achieve the desired yield. The degree of conversion values are calculated assuming an amine donor excess of 10.

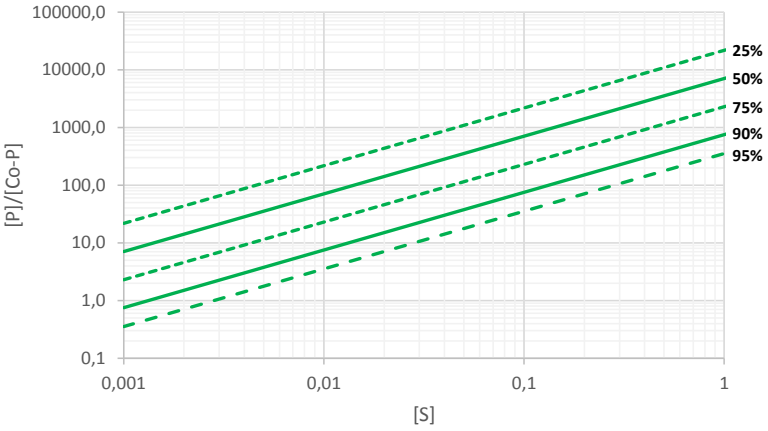

Figure B.3: Degrees of conversion expressed by the relation between minimum product and/or co-product concentrations and various initial substrate concentrations, using an amine donor excess of 10.

Plot of uncharged IPA vs. uncharged MPPA:

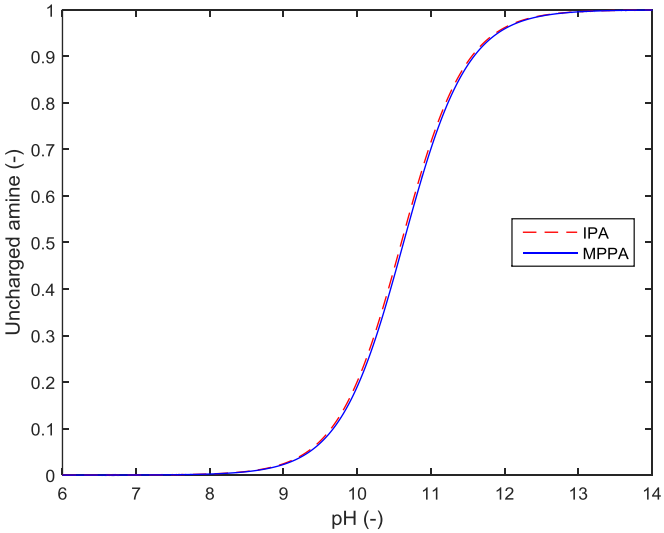

Figure B.4: Fractions of charged and uncharged molecules at various pH values for the two amines MPPA and IPA.

Plot of uncharged Alanine vs. uncharged MPPA:

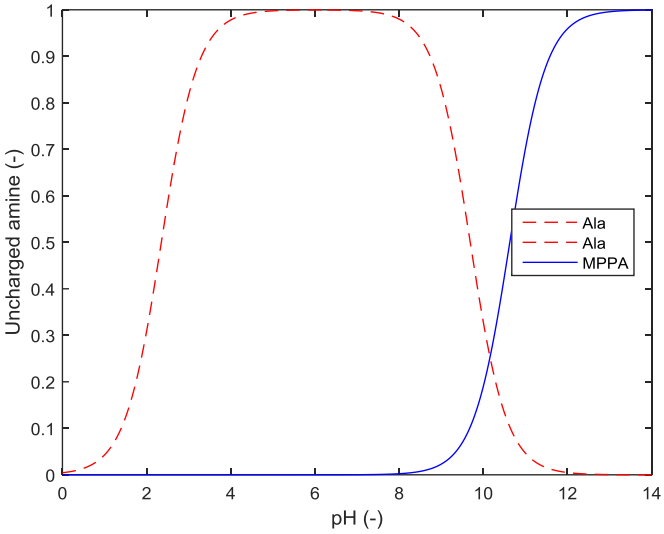

Figure B.5:Fractions of charged and uncharged molecules at various pH values for the two amines MPPA and Ala.

Appendix C

Off-line HPLC analytical methods

Two HPLC methods on a Dionex Ultimate 3000 HPLC (Dionex, Sunnyvale, CA, USA), with an UV photodiode array detector, were applied to determine the concentrations of the main reaction species involved in this project. The compounds were separated using a Gemini-NX 3µ C18 110Å (100 x 2 mm) column (Phenomenex, Torrance, CA, USA). The two methods are as follows:

Method 1:

This method was applied to determine concentrations of the two main reaction species for all case studies, 1-methyl-3-phenylpropylamine (MPPA) and benzylacetone (BA). Additionally, the method can be used to quantify the amine donor and ketone co-product from one of the reaction systems, i.e. phenylethylamine (PEA) and acetophenone (ACP). The details on how the method was operated are listed in Table C.1.

Table C.1: HPLC method for determination of racemic 1-methyl-3-phenylpropylamine (MPPA), benzylacetone (BA), phenylethylamine (PEA) and acetophenone (ACP).

Method settings	
Mode	Isocratic
Flow	0.450 mL/min
Mobile phase	35 % Acetonitrile 65% H_2O pH-11 (adj. by NaOH)
Column	Gemini-NX 3µ C18 110Å (100 x 2mm)
T_{oven}	30 °C
Detection	X min (210 nm) - PEA X min (210 nm) - ACP 2.67 min (210 nm) - MPPA 3.63 min (210 nm) - BA
Time of analysis	5 min
Std. Inj. Vol.	1 µL

Note: it may be beneficial to determine low ACP concentrations at a wavelength of ~244 nm, due to stronger absorbance at this wavelength.

An example of a spectrum of a sample containing both MPPA and BA is shown in Figure C.1.

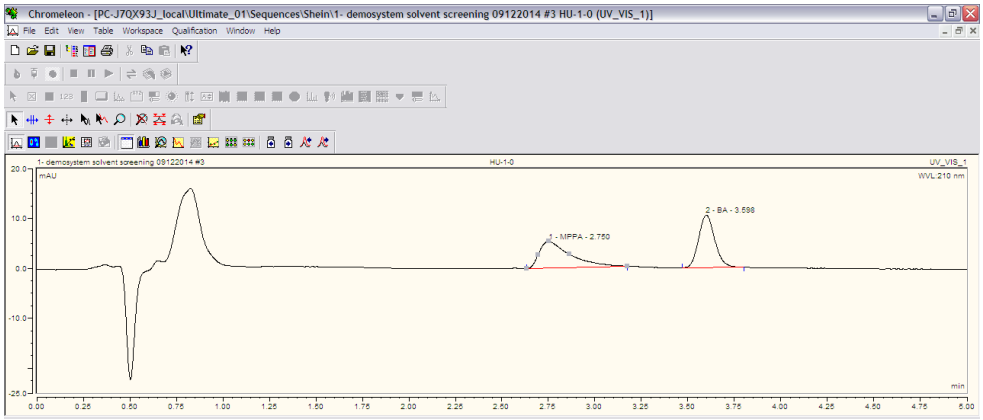

Figure C.1: Spectrum obtained from a solution of MPPA, BA, IPA and Ace on 09-12-2014.

The quantitative analysis was performed from peak areas by external standards. The generated standards are highlighted below in Figure C.2 and Figure C.3 for BA and MPPA, respectively (column: 00D-4453-b0).

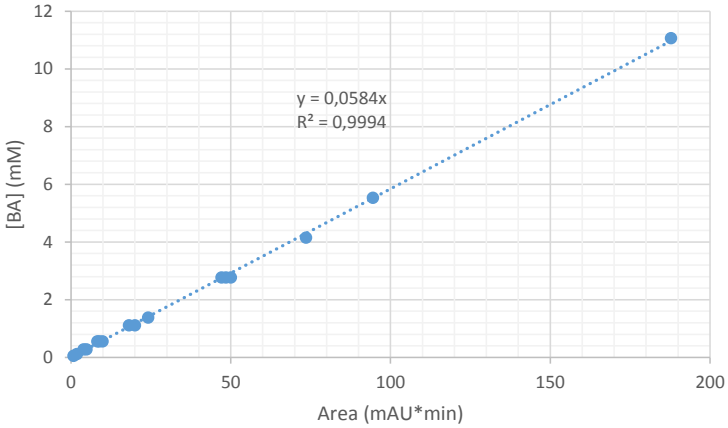

Figure C.2: Standard curve for benzylacetone (BA) at 210 nm (column: 00D-4453-b0).

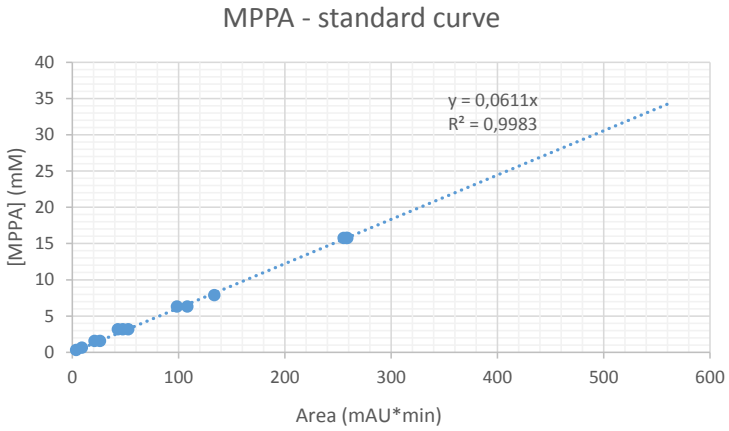

Figure C.3: Standard curve for 1-methyl-3-phenylpropylamine (MPPA) at 210 nm (column: 00D-4453-b0).

Additionally the continuous performance of the column and the standards was validated by independent external standards. The validation results are highlighted below in Figure C.4 and Figure C.5 for BA and MPPA, respectively. The dashed lines surrounding the full line in the middle of the figures corresponds to ±5% errors.

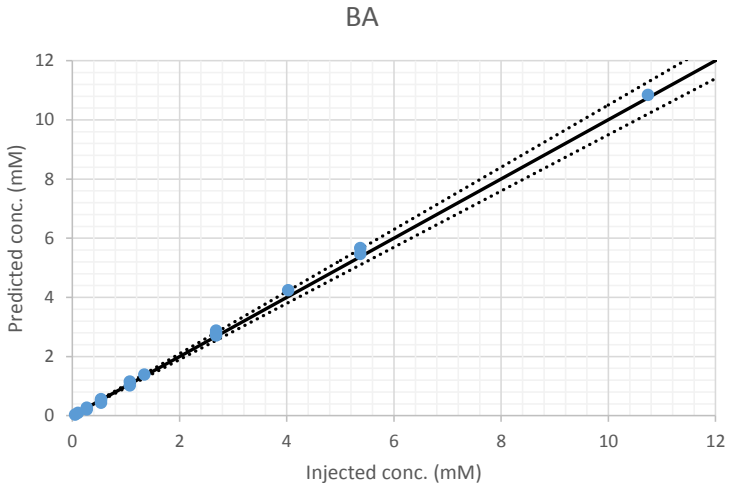

Figure C.4: Validation of BA analytical method over time (column: 00D-4453-b0), i.e. performed to ensure that the standard was still valid over time.

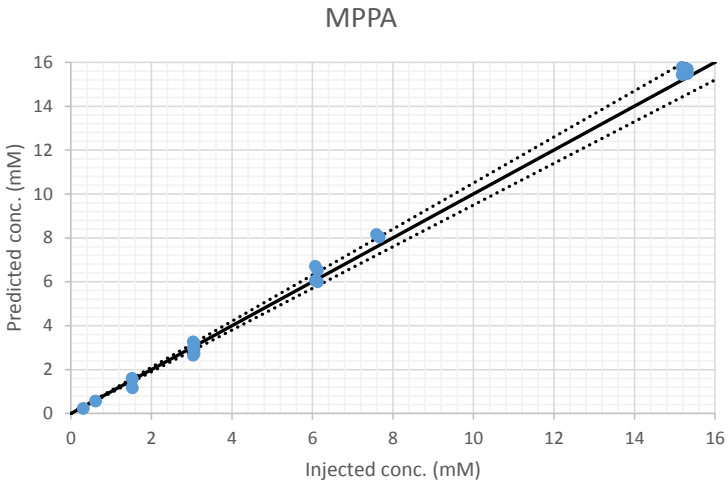

Figure C.5: Validation of MPPA analytical method over time (column: 00D-4453-b0), i.e. performed to ensure that the standard was still valid over time.

Method 2:

This method was applied to determine concentrations of the amine donor isopropylamine (IPA) and the co-product acetone (Ace) from the main case study. The details on how the method was operated are listed in Table C.2.

Table C.2: HPLC method for determination of isopropylamine (IPA) and acetone (Ace).

Method settings	
Mode	Isocratic
Flow	0.300 mL/min
Mobile phase	5 % Acetonitrile 95% H_2O pH-11 (adj. by NaOH)
Column	Gemini-NX 3µ C18 110Å (100 x 2mm)
$\boldsymbol{T_{oven}}$	30 °C
Detection	1.7 min (270 nm) - Ace 3.0 min (200 nm) - IPA
Time of analysis	5 min
Std. Inj. Vol.	1 µL

An example of spectra of IPA and Ace is shown in Figure C.6 and Figure C.7, respectively.

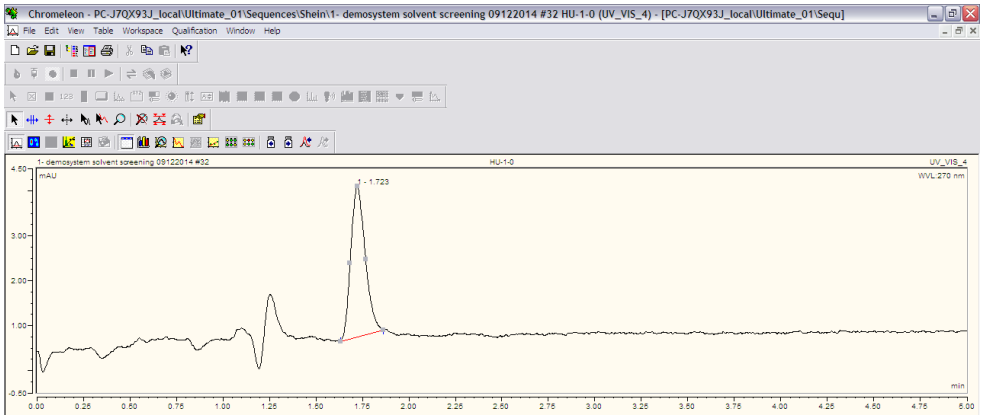

Figure C.6: Acetone (ace) peak for a spectrum obtained from a solution of 1-methyl-3-phenylpropylamine (MPPA), benzylacetone (BA), isopropylamine (IPA) and Ace on 09-12-2014.

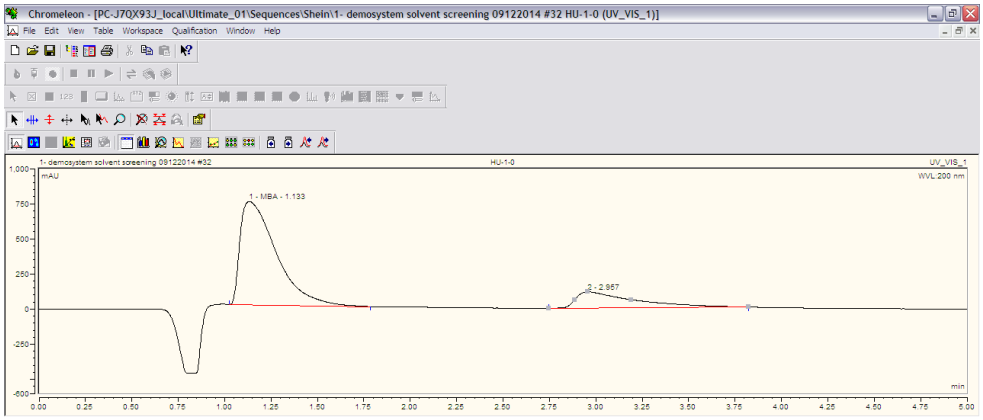

Figure C.7: Impurity peak and an isopropylamine (IPA) peak for a spectrum obtained from a solution of 1-methyl-3-phenylpropylamine (MPPA), benzylacetone (BA), IPA and acetone (Ace) on 09-12-2014.

The quantitative analysis was performed from peak areas by external standards. The generated standards are highlighted below in Figure C.8 and Figure C.9 (column: 00D-4453-b0).

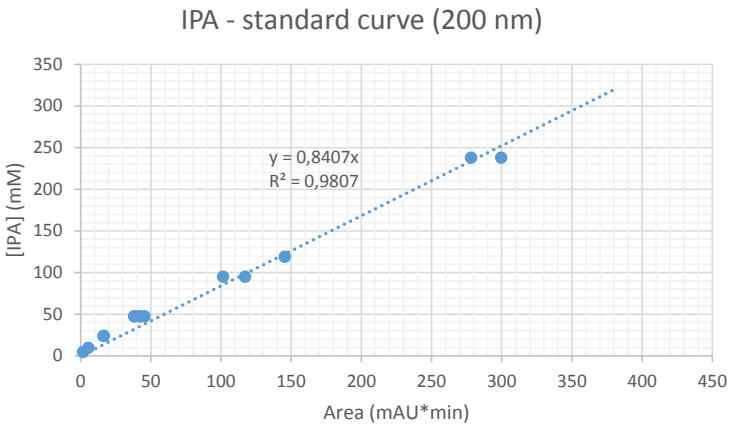

Figure C.8: Standard curve for isopropylamine (IPA) at 200 nm (column: 00D-4453-b0).

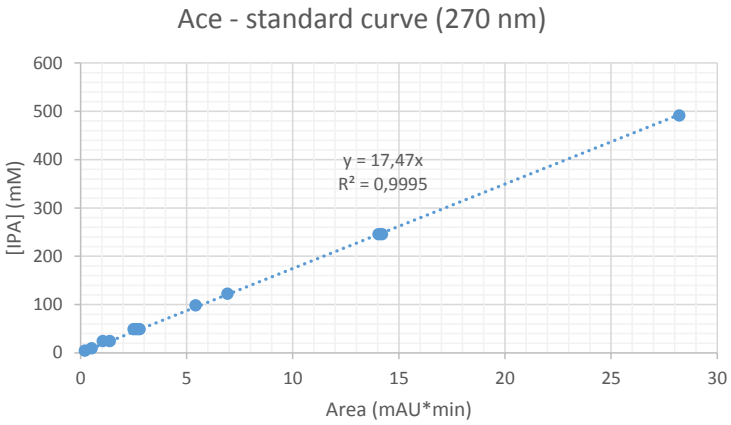

Figure C.9: Standard curve for acetone (Ace) at 270 nm (column: 00D-4453-b0).

Additionally the continuous performance of the column and the standard was validated by independent external standards; the results are highlighted below in Figure C.10 and Figure C.11 for IPA and Ace, respectively. The dashed lines surrounding the dashed line in the middle correspond to ±5% errors.

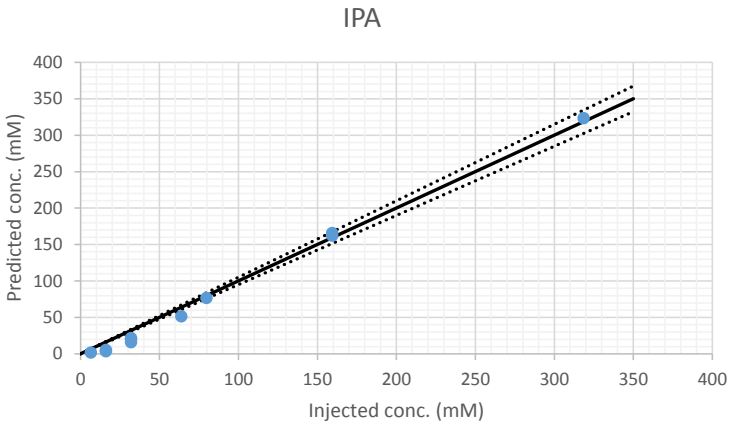

Figure C.10: Validation of IPA analytical method over time (column: 00D-4453-b0), i.e. performed to ensure that the standard was still valid over time.

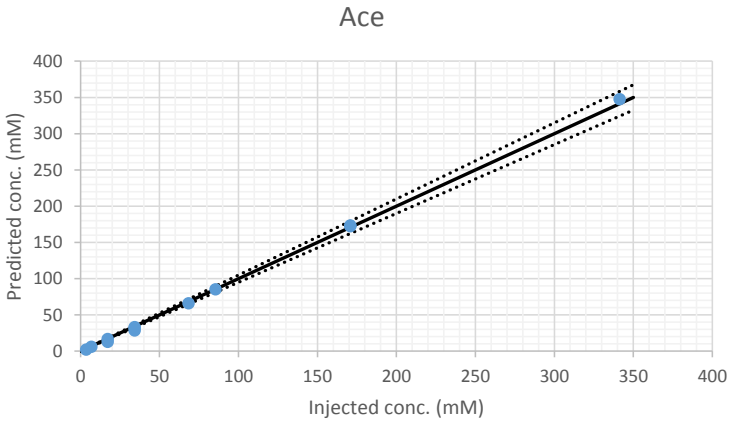

Figure C.11: Validation of Ace analytical method over time (column: 00D-4453-b0), i.e. performed to ensure that the standard was still valid over time.

The reason for performing frequent calibrations and validations for each used column is to ensure that the predictions are reliable over time. Furthermore, the operational conditions with high pH are extremely tough on the columns. Hence, their performance is significantly decreasing over time and tailing effects become an increasing issue for the amine compounds. Furthermore, the UV lamps break and/or lose intensity over time, which can also influence the spectra significantly.

CAPEC-PROCESS Research Center
Department of Chemical and Biochemical Engineering
Technical University of Denmark
Søltofts Plads, Building 227
Dk-2800 Kgs. Lyngby
Denmark

Phone: +45 45252800
Web: www.capec-process.kt.dtu.dk